Imperial College London - Department of Epidemiology and Biostatistics, School of Public Health

THE USE OF SATELLITE DATA, METEOROLOGY AND LAND USE DATA TO DEFINE HIGH RESOLUTION TEMPERATURE EXPOSURE FOR THE ESTIMATION OF HEALTH EFFECTS IN ITALY.

Francesca Katherine de'Donato

A thesis submitted in fulfilment of the requirements for the degree of Doctor in Philosophy of Imperial College London

February 2018

ABSTRACT

Introduction. Despite the mounting evidence on heat-related health risks, there is limited evidence in suburban and rural areas. The limited spatial resolution of temperature data also hinders the evidence of the differential heat effect within cities due to individual and area-based characteristics.

Methods. Satellite land surface temperature (LST), observed meteorological and spatial and spatio-temporal land use data were combined in mixed-effects regression models to estimate daily mean air temperature with a 1x1km resolution for the period 2000-2010. For each day, random intercepts and slopes for LST were estimated to capture the day-to-day temporal variability of the Ta–LST relationship. The models were also nested by climate zones to better capture local climates and daily weather patterns across Italy. The daily exposure data was used to estimate the effects and impacts of heat on cause-specific mortality and hospital admissions in the Lazio region at municipal level in a time series framework. Furthermore, to address the differential effect of heat within an urban area and account for potential effect modifiers a case cross-over study was conducted in Rome. Mean temperature was attributed at the individual level to the Rome Population Cohort and the urban heat island (UHI) intensity using air temperature data was calculated for Rome.

Results. Exposure model performance was very good: in the stage 1 model (only on grid cells with both LST and observed data) a mean R^2 value of 0.96 and RMSPE of 1.1°C and R^2 of 0.89 and 0.97 for the spatial and temporal domains respectively. The model was also validated with regional weather forecasting model data and gave excellent results (R^2=0.95 RMSPE=1.8°C. The time series study showed significant effects and impacts on cause-specific mortality in suburban and rural areas of the Lazio region, with risk estimates comparable to those found in urban areas. High temperatures also had an effect on respiratory hospital admissions. Age, gender, pre-existing cardiovascular disease, marital status, education and occupation were found to be effect modifiers of the temperature-mortality association. No risk

gradient was found by socio-economic position (SEP) in Rome. Considering the urban heat island (UHI) and SEP combined, differential effects of heat were observed by UHI among same SEP groupings. Impervious surfaces and high urban development were also effect modifiers of the heat-related mortality risk. Finally, the study found that high resolution gridded data provided more accurate effect estimates especially for extreme temperature intervals.

Conclusions. Results will help improve heat adaptation and response measures and can be used predict the future heat-related burden under different climate change scenarios.

Declaration of originality

I declare that this thesis is my own work and that the work conducted by others is presented, it is fully references and acknowledged as appropriate. The temperature exposure methodology was a development of the Kloog et al. model including a wider number of land use predictor (spatial and spatio-temporal) variables and nesting by climate zone to account for different climates, weather patterns and geographical characteristics that vary across Italy over small spatial domains. Furthermore, air temperature data from various meteorological networks was also incorporated.

Copyright declaration 

Acknowledgments

I am very grateful to my supervisors Paolo Vineis and Itai Kloog for the guidance and advice they have given me throughout my PhD at Imperial College and for the learning experience overall.

I am very obliged to the Department for Epidemiology Lazio Regional Health Service ASL Roma 1 for funding my Phd, to Dr. Marina Davoli for giving me this opportunity and especially to Dr.Paola Michelozzi for supporting me and giving me the opportunity to carry out the research and challenging my choices.

Thanks to the "girlies": Clare, Laura, Sarah and Tori, who made my PhD even more special and made me feel at home, as always. Paoletta for her professional and friendly advice and to her lovely family for the time spent together. Thanks to my colleagues at DEPLAZIO and Phd fellows for the sharing of experiences.

Last but not least my parents and family for being there, always. A super special thanks to my husband Max, for his precious help, advice and stimulating discussions, sharing work and family with you is the greatest achievement in my life. My amazing daughters, Flami and Giuli, who have supported me along the way and encouraged me to achieve this special goal. I couldn't have done it without your smiles, patience and love.

In the loving memory of my granny Ethel and grandad Bernard, you will both greatly be missed.

TABLE OF CONTENTS

List of Tables

Table 5.10A Analysis excluding 2003. Relative risk in natural mortality and hospital admissions for increases in mean temperature between the 50th – 75th , 50th – 90th and 50th-99th percentile of the Lazio regional distribution (mean temperature distribution with 2003).

Table 5.10B Analysis excluding 2003. Relative risk in natural mortality and hospital admissions for increases in mean temperature between the 50th – 75th , 50th – 90th and 50th-99th percentile of the Lazio regional distribution (mean temperature distribution without 2003).

Table 5.11. Relative risk of natural, cardiovascular and respiratory mortality for increases in mean temperature considering distribution of percent urban and impervious surfaces in Rome and municipalities of the Lazio region.

Table 5.12. Statistical testing of heterogeneity among strata specific mortality and hospital admission estimates for municipality size, ISA and percent urban levels.

Table 6.1. Characteristics of the study population. Rome census 2001.

Table 6.2. Number of deaths in the cohort during summer (May- September) by age, gender, cause, marital status, education, employment and co-morbidities in the study period (2002-2010).

Table 6.3. Number of deaths in the cohort during summer (May- September) by socio-economic position, impervious surface, percent urban development and urban heat island intensity in the study period (2002-2010).

Table 6.4a. Mean Temperature distribution for Rome during summer (May- September), by month and by year in the study period (2002-2010).

Table 6.4b. Mean Temperature distribution for cohort grid cells during summer (May- September), by month and by year in the study period (2002-2010).

Table 6.5 Heat-related effects on total mortality. Risks for increases in mean temperature between the 50^{th} and 75^{th}, 50^{th} to 99^{th} of the summer distribution in Rome by age groups, gender, age and age combined and co-morbidities.

Table 6.6 Heat-related effects on cardiovascular mortality. Risks for increases in mean temperature between the 50^{th} and 75^{th}, 50^{th} to 99^{th} of the summer distribution in Rome by age groups, gender, age and age combined and co-morbidities.

Table 6.7 Heat-related effects on respiratory mortality. Risks for increases in mean temperature between the 50^{th} and 75^{th}, 50^{th} to 99^{th} of the summer distribution in Rome by age groups, gender, age and age combined and co-morbidities.

Table 6.8 Heat-related effects on total mortality. Risks for increases in mean temperature between the 50^{th} and 75^{th}, 50 to 95^{th}, 50^{th} to 99^{th} of the summer distribution in Rome by SEP, UHI and SEP and UHI combined.

Table 6.9 Heat-related effects on cardiovascular mortality. Risks for increases in mean temperature between the 50^{th} and 75^{th}, 50 to 95^{th}, 50^{th} to 99^{th} of the summer distribution in Rome by SEP, UHI and SEP and UHI combined.

Table 6.10 Heat-related effects on respiratory mortality. Risks for increases in mean temperature between the 50^{th} and 75^{th}, 50^{th} to 95^{th} ,50^{th} to 99^{th} of the summer distribution in Rome by SEP, UHI and SEP and UHI combined.

Table 6.11 Statistical testing of heterogeneity among strata specific total mortality estimates by levels of age groups, gender, age and gender combined, marital status, education, occupation, co-morbidities, SEP, UHI, ISA and level of urbanization.

Table 6.12 Statistical testing of heterogeneity among strata specific cardiovascular mortality estimates by levels of age groups, gender, age and gender combined, marital status, education, occupation, co-morbidities, SEP, UHI, ISA and level of urbanization.

Table 6.13 Statistical testing of heterogeneity among strata specific respiratory mortality estimates by levels of age groups, gender, age and gender combined, marital status, education, occupation, co-morbidities, SEP, UHI, ISA and level of urbanization.

Table 6.14 Heat-related effects on respiratory mortality. Risks for increases in mean temperature between the 50^{th} and 75^{th}, 50^{th} to 95^{th}, 50^{th} to 99^{th} of the summer distribution in Rome by impervious surface and % urban development.

Table 6.15 Heat-related effects on total mortality considering 3 temperature exposures. Risks for increases in mean temperature between the 50^{th} and 75^{th}, 50^{th} to 95^{th}, 50^{th} to 99^{th} in Rome considering monitoring site temperature, urbanistic zone average temperature and high resolution gridded temperature.

Table 6.16 Heat Attributable deaths for mean temperature increases between the 50^{th} – 75^{th} and 50^{th}-99^{th} percentile considering three temperature exposures. Summers 2002-2010.

List of Figures

List of Abbreviations

AATSR . - Advanced Along-Track Scanning Radiomete

AD – Attributable deaths

AQUA - NASA circular sun-synchronous polar orbit satellite which orbits the earth from south to north,with afternoon equatorial crossing.

ARPA – *Agenzia Regionale per la Protezione dell'Ambiente* – Italian regional environment protection agencies

ASTER - Advanced Spaceborne Thermal Emission and Reflection Radiometer

AVHHR - Advanced very-high-resolution radiometer

BMI- Body mass index

CI – Confidence interval

CLC – Corine land cover

CNMCA – Centro Nazionale meteorologia e Climatologia Aeronautica Militare

CV – cross validation

CVD – cardiovascular

Dlnm – distributed lag nonlinear models

ENAV - Ente Nazionale Assistenti al Volo

ENVISAT – ESA polar orbiting Environmental Satellite

e0 - surface water vapour pressure

ESA – European Space Agency

ETM+ - Enhanced Thematic Mapper Plus;

EUMETSAT- European Organisation for the Exploitation of Meteorological Satellites

GHG- greenhouse gases

HUMIDEX – humidity index

IDW - inverse distance weighted

IPCC – Intergovernmental Panel for Climate change

ISA – Impervious surface

ISPRA- *Istituto Superiore per la Protezione e la Ricerca Ambientale, Italy*

ISTAT – Italian national institute of statistics

LAADS - NASA Level 1 Atmosphere Archive & Distribution System

LANDSAT – polar- orbiting earth observation satellites owned by USGS and NASA

LST – Land Surface Temperature

MCMC –Multi city multi country time series study on temperature effects

MERRA - Modern-Era Retrospective Analysis for Research and Applications

MESH – Medical Subject Index

METEOSAT – Geostationary orbiting meteorological satellites EUMETSAT

MODIS – Moderate Resolution Imaging Spectroradiometer

NASA – National Aeronautics and Space Administration

NDVI - Normalized Difference Vegetation Index

NIR - Near infra-red

NOAA – US National Oceanic and Atmospheric Administration

OLI - Operational Land Imager

PET- Physiologically Equivalent Temperature

POES - Polar Orbiting Environmental Satellites

RAMS - Regional Atmospheric Modelling System

RCP – Representative Concentration Pathways

RENCAM - Rome cause specific mortality registry

RMSPE - root mean squared prediction error

ROLS – Rome Longitudinal Study Population Cohort

RQ – research query

SEP – Socio economic position

SEVIRI - Spinning Enhanced Visible and Infrared Imager

SIO – Lazio regional hospital admissions registry

SVF - sky view factor

SVF - sky view factor factor

SZA - solar zenith angle

Ta – air temperature

TERRA – NASA circular sun-synchronous polar orbit satellite which orbits the earth from north to south, with morning equatorial crossing.

TIR – Thermal infrared radiation

TIRS - Thermal Infrared Sensor;

Tkin – kinetic surface temperature

TM -Thematic Mapper

Trad – radiant temperature

Ts – surface temperature

TVX – temperature vegetation index

UHI – Urban heat Island

USGS - U.S. Geological Survey

VCF - Vegetation continuous fields

YLL – years of life lost

WHO – World health Organization

WMO- World Meteorological Organization

CHAPTER 1 - INTRODUCTION

1.1 RATIONALE

The World Meteorological Organization (WMO) has estimated that heat and extreme weather events are among the 10 worst reported natural disasters in terms of human lives lost globally [1]. Europe and the Mediterranean have been identified as one of the areas most at risk in terms of temperature increases, precipitation decline and drought considering climate change scenarios according to the Vth IPCC Assessment Report[2]. According to the climate change models and different Representative Concentration Pathway (RCP) scenarios, temperatures are predicted to rise globally between 1.0°C and 3.7°C and will continue to rise beyond 2100 under all scenarios except RCP2.6. RCPs represent greenhouse gas concentration pathways adopted by the IPCC in the Vth Report and represent possible climate futures, depending on how much greenhouse gases are emitted. They are identified by their total radiative forcing by year 2100 compared to year 1750, so RCP2.6 will have declining concentrations and the lowest radiative forcing (2.6 W m-2) while RCP8.5 is the high concentrations pathway with emissions rising till the end of the century thus having the highest radiative forcing (8.5 W m-2)[2]. A recent study conducted by WHO estimated that the future heat-related burden for Europe is expected to be between 30,867 and 45,930 attributable deaths per year by 2030-2060 considering the RCP 4.5 and RCP 8.5 scenarios respectively[3]. The heatwave events across Europe in 2003, 2010 and more recently 2015 and 2017 have had a significant impact on health, thus making heat-related health effects a hot topic on the public health agenda over the past ten years. In Italy alone, the estimated excess deaths attributable to future climate change for the same time frame are of 4454 and 6099 deaths respectively under the RCP 4.5 and RCP 8.5 scenarios[3].

The short-term effects of temperatures and extreme events have been extensively studied throughout the literature[4–6]. In particular heat has been related to an increase in total and cause-

specific mortality[5,7–10] as well as non-fatal outcomes such as hospital admissions, emergency room visits and ambulance calls[11–15]. The vulnerability of human populations to extreme weather events is a function of their sensitivity to the exposure, of the character, magnitude and rate of the climate extreme, and of the adaptation measures and actions in place[16]. In healthy individuals, an efficient thermoregulatory system enables the body to cope effectively with thermal stress. Body thermal comfort can be maintained by appropriate thermoregulatory responses, however if these responses are compromised, health status is at risk and may lead to death.[17]

Times series studies have been carried out to define the shape of the relationship and estimate the acute effects of temperatures on health outcomes. The association between temperature and mortality has been identified and described as a non-linear U-, J- or V-shaped function, with the lowest mortality rates recorded at moderate temperatures, rising progressively as temperatures increase or decrease[7,8,10,18,19]. Effects of heat vary geographically[5,20,21] and depend on local climatic conditions and population characteristics (demography, socioeconomic conditions, health status)[6].

Despite the mounting evidence showing the acute effects of heat on health outcomes, especially mortality and morbidity, there is limited evidence of the effects in suburban and rural areas primarily due to data limitations. Most research has been carried out in urban areas primarily due to data availability in terms of exposure and the number of outcome counts, large enough to ensure statistical power in the modelling of the effects. Studies evaluating the effects of air temperature on health outcomes have used data from traditional weather stations, located outside the urban area, usually in proximity to airports. These stations have standardized WMO criteria for weather data collection and have long–time series of data. Epidemiological studies thus consider a point source of exposure which is used in an ecological approach to estimate

the mean effect at population level for the whole city. Although weather monitoring networks are better in terms of temporal data retrieval and quality of the data, as they are retrieved with standardized instruments and procedures, they are however, often lacking in terms of the spatial scale as they are rarely designed to capture the spatial variability of temperatures and local climatic conditions. Inevitably this causes substantial exposure misclassification as well a bias in the estimates related to the exposure considered[22]. Primarily due to the fact that intra-urban variations in temperature are ignored, and secondly because the point source may not be representative of the exposure for a large part of the population. Exposure from one monitoring point is attributed to the population of an entire city or area. In large urban areas, the urban heat island (UHI) plays an important role in the intra-urban thermal differences populations are exposed to and together with individual socio-economic and health status population status characteristics within the urban domain may influence the effects of heat on health outcomes[23–25].

Moreover, as monitoring networks are expensive and require constant maintenance, they are limited across space, with few stations in rural and suburban settings. For epidemiological studies this poses a relevant limitation, as studies can only be conducted in areas where data is available. However, it is worth noting that suburban and rural areas are exposed to heat and to date we have limited evidence as to what the acute health effects may be.

Satellite data can be a valid alternative to overcome this issue as they offer temperature data with a much higher spatial resolution. Since the 1980s the quality and resolution of satellite data products has exponentially improved, both in terms of spatial and temporal resolution but also in terms of products available, really providing a very interesting source of data for a wide range of research fields related to the environment. Satellite derived land surface temperature data (LST) have been used to derive air temperature[26–29] and identify urban heat islands [23,30].

Satellite derived temperature can be a solution to obtain high resolution air temperature data even in remote areas currently not covered by traditional monitoring networks as well as providing a better resolution within large urban areas that capture the spatial differentials. The use of satellite data to derive air temperature, will provide useful information on daily temperature distributions across space and time with a high resolution and help identify hotspots. More importantly, light can be shed on the short-term effects of heat in urban, suburban and rural settings providing a more accurate quantification of the heat risks also taking into account individual vulnerability factors and effect modifiers that may influence the spatial distribution of heat-related risks.

CHAPTER 2- AIMS AND OBJECTIVES

2.1 AIMS AND OBJECTIVES

The aim of my research was to use satellite-derived air temperature data with a 1x1km spatial resolution to estimate the short-term health effects of heat on mortality and hospital admissions in Italy.

In order to achieve my research aim, the following specific objectives were carried out:

1. define spatio-temporal exposure to air temperature derived from satellite land surface temperature (LST) data, meteorological and land use data for Italy with a 1x1km resolution over the period 2000-2010.

2. estimate the acute effect of heat on health outcomes (mortality and morbidity) in the Lazio region at municipal level using satellite-derived daily air temperature with a 1x1km resolution over the period 2000-2010.

3. estimate the short-term effect of heat on mortality within urban areas taking into account the differential effect of heat due to the urban heat island effect and socio-economic factors in Rome using the Rome Longitudinal Study Population Cohort (ROLS).

2.2 THESIS OUTLINE

The first chapter gives a brief overview of the study rationale and what my research entails. Chapter 2 defines the aim and objectives of the study. Chapter 3 presents a literature review of the two key aspects in my research: the definition of daily air temperature exposure derived from satellite data and then using this data to estimate health effects of heat. When reviewing the evidence on exposure a focus was given on studies estimating air temperatures using and

satellite derived- LST. Studies defining urban heat islands using satellite data were reviewed, to identify key factors that influence urban heat island intensities and may modify thermal conditions within urban areas. In terms of heat-related health effects, the literature review focused on studies conducted on mortality and hospital admissions for total, cardiovascular and respiratory causes in adults. Key aspects considered were effect estimates, statistical methodologies employed, exposure, and the potential effect modifiers of the dose-response relationship. Regarding the latter, this was of particular relevance in urban areas when considering socio-economic factors and the urban heat island effect (UHI), defined as urban areas being warmer than surrounding rural areas, especially at night due to the greater heat absorption by building materials and impervious surfaces in cities compared to natural vegetative surfaces.

Chapter 4 presents the study carried out to estimate daily air temperature with a 1x1km spatial resolution using satellite LST data from Moderate Resolution Imaging Spectroradiometer (MODIS) sensor on board NASA satellites TERRA and AQUA, observed meteorological data and land use variables from a multitude of sources.

Chapter 5 presents the time series study conducted in the Lazio region to estimate the short-term health effects of heat, in terms of cause-specific mortality and hospital admissions by municipality considering both moderate and extreme heat.

Chapter 6 describes the case cross-over study conducted in Rome using the Rome Population Cohort to estimate the effect of heat exposure on mortality considering individual socio-demographic and health status characteristics as well as area based socio-economic, land use factors and the UHI effect. In this study, each individual in the cohort was geo-coded and exposure was attributed at address level using the 1x1km resolution daily mean temperature exposure defined in chapter 4.

Chapter 7 will briefly summarize main findings and provide an overall discussion of research findings and chapter 8 present conclusions.

CHAPTER 3 – BACKGROUND AND LITERATURE REVIEW

This chapter provides a brief background to the different aspects in study and results of the literature review carried out. The aim of the review was to summarise and critically examine the current evidence base on the following key topics:

1. methodologies for deriving air temperature from land surface temperature (LST) satellite data (research query 1 –RQ1).
2. urban heat island (UHI) phenomenon (research query 2 –RQ2).
3. association between heat and health outcomes (mortality and hospital admissions) (research query 3 –RQ3).
4. health effects of heat in urban areas and the differential effect considering the UHI, with specific focus on UHI defined using satellite data (research query 4 –RQ4).

The search was conducted in PubMed and Scopus using free text terms and medical subject index (MESH) such as "land surface temperature" and "air temperature", "satellite data", "land surface temperature", "urban heat island" "mortality", "morbidity", "hospital admissions" "heat stress". The full search strategy for PubMed and Scopus can be found in Appendix 1. All papers published in peer-reviewed journals in the period 1990-april 2017 were included and only papers written in English language were considered. Results of the search strategy and the number articles selected for each aspect are shown in figure 3.1. Out of the papers screened in the first stage of the literature review 870 were excluded as title and/or abstract did not fit one of the 4 research questions. Full test papers were read and only those fitting each research question were retained for a total of 238 papers.

Figure 3.1. PRISMA Flow Diagram of the Literature search.

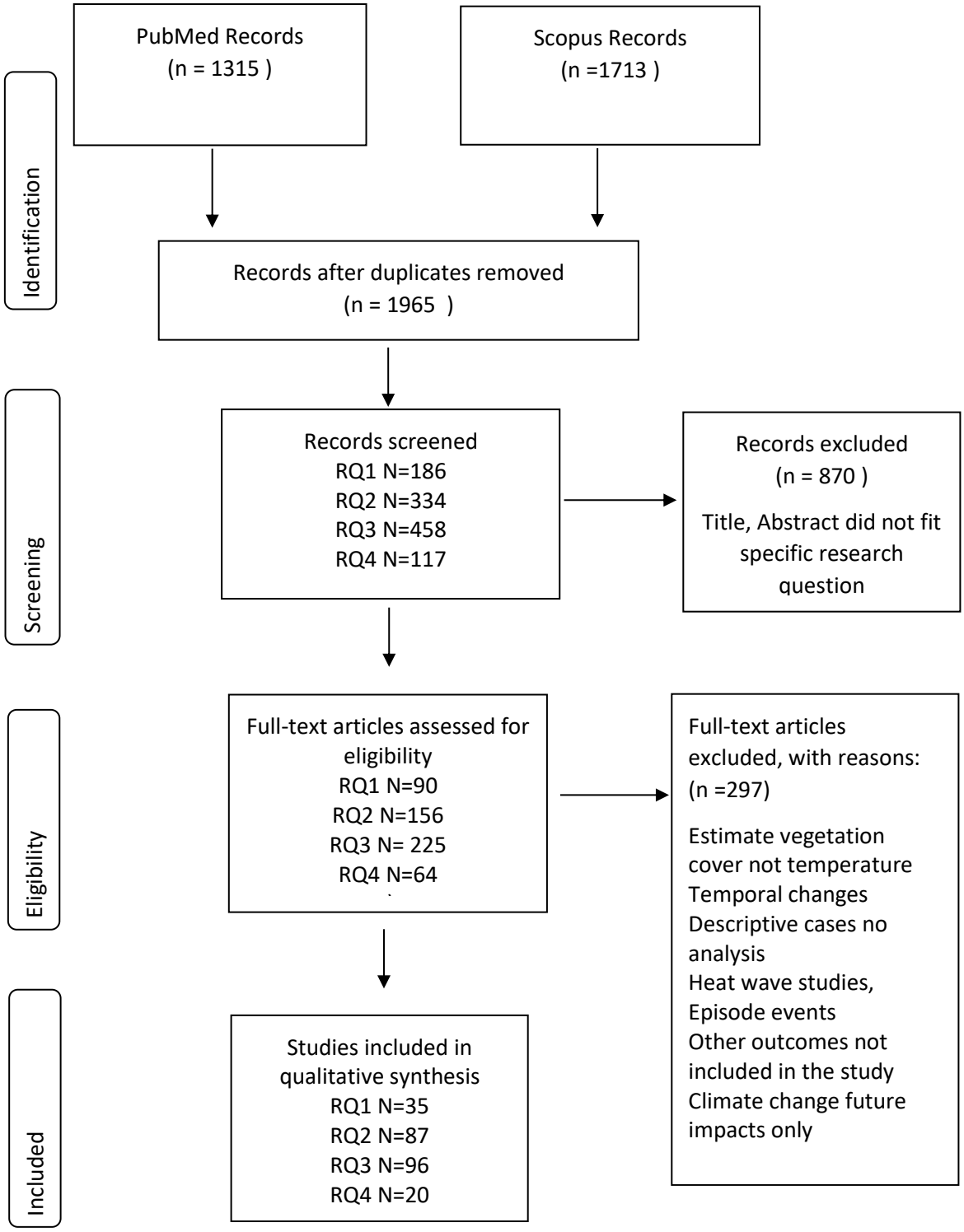

3.1 LITERATURE REVIEW ON METHODOLOGIES FOR DERIVING AIR TEMPERATURE FROM LAND SURFACE TEMPERATURE (LST) SATELLITE DATA.

3.1.1 Background to satellite data and Land surface temperature (LST)

Satellite data have been used to monitor different environmental factors and identify areas at risk to different health hazards[31,32] as well as an alternative source of data to derive environmental exposures such are temperatures and air pollution [33–37].

Land surface temperature (LST)

The satellite derived parameter considered in my research was land surface temperature (LST). The signal acquired by satellite sensors is comprised of energy emitted from the Earth's surface, energy absorbed by the atmosphere, mostly by water vapour, or re-emitted from the atmosphere [26,38,39]. LST combines all surface-atmosphere interactions and energy fluxes between the atmosphere and the ground. Thus making it one of the key parameters in the physics of land surface processes at different spatial scales [40–42]. LST is an indicative variable of the net surface energy balance driven by long-wave radiation surface emission. The surface energy balance is governed by downward and upward radiation fluxes, and, latent and sensible heat loss fluxes (Figure 3.2). The downward flux is determined by the factors mentioned above and by the surface's albedo which determines the fraction of total radiation reflected and absorbed by the surface. The upward flux, on the other hand, follows the Stefan–Boltzmann law and is determined by the surface's temperature and emissivity. The latent and sensible heat fluxes are strongly influenced by surface temperature and the apportionment of energy between them is governed by moisture content, surface type, wind velocity and emissivity [26].

Figure 3.2. Energy budget of Earth's atmosphere.

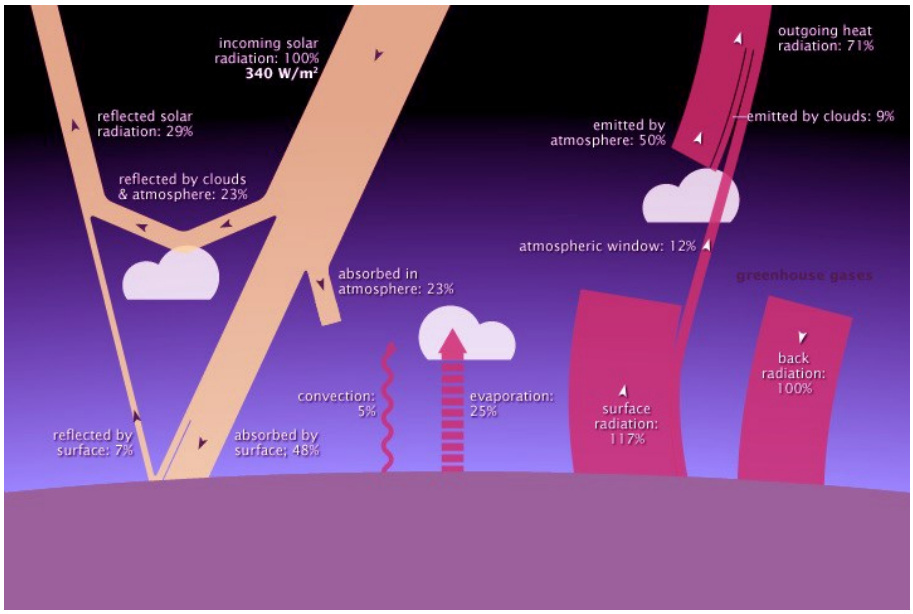

Source: Adapted from NASA earth observatory

The quality of LST retrievals is influenced by sensor characteristics, atmospheric conditions, variations in spectral emissivity, surface type heterogeneity, soil moisture, visualization geometry, and assumptions related to the split-window method[26,39,43]. Many algorithms for estimating LST from satellite data are based upon the assumption that the ground surface acts as a blackbody, with emissivity equal to one. On the contrary, most Earth's surfaces emit only a fraction of the energy emitted by a blackbody at the same temperature. The emission capacity of a land surface, compared to that of a blackbody, is typically referred to as surface emissivity[44]. Radiance emitted by land surfaces is affected by the composition of surface constituents, especially spectral emissivity, thus emitting radiance differently across the thermal spectrum[45].

Due to the difficulties in correcting for atmospheric absorption, atmospheric emission, and surface emissivity, the development of accurate LST algorithms is a far from simple process[40,46,47]. To estimate LST from space two techniques have been developed and refined throughout the years. Firstly, the single infrared channel method that requires a good radiative transfer model and atmospheric profiles was developed[48]. Following, split-window methods

that correct for atmospheric effects based on the differential absorption in adjacent infrared bands were then developed and refined[41,48–52]. The accuracy of these methods depends on the emissivity difference in the two bands, even small differences can cause significant errors in the LST retrieval as mentioned by several studies[26,41,44].

Although satellites do not measure air temperature, which is the parameter typically used to evaluate the effects on health, land surface temperature (LST) from satellite sensor measurements can be used to derive air temperature through complex methodologies[27,29]. LST data is available at different temporal and spatial scales, in my research LST MODIS -*Moderate Resolution Imaging Spectrometer* data, from NASA TERRA and AQUA satellites, with a daily temporal resolution and a spatial resolution of 1km was used, mainly driven by the fact that health effect time series studies typically use daily outcome counts. Hence, to have a daily temporal resolution, spatial resolution of 1 km was the best compromise considering data availability. Details of the methodology developed will be further explained in chapter 4.

Satellite data

Moderate Resolution Imaging Spectrometer -MODIS data

LST data is derived from the Moderate Resolution Imaging Spectrometers (MODIS) on board TERRA and AQUA NASA satellites launched in 1999 and 2002 respectively. TERRA and AQUA have a near-polar, sun-synchronous orbit at an altitude of around 700km. TERRA's orbit is from north to south and is timed to cross the equator in the morning, while AQUA orbits in the opposite direction, from south to north, crossing the equator in the afternoon. These two satellites cover the entire Earth's surface every 1 to 2 days, acquiring data in 36 spectral bands. Satellite sensors on board MODIS measure thermal infrared (TIR) signals, or bands, that are a combination of the radiant temperature of the land surface and the intervening atmosphere. The split-window algorithm used for MODIS data also corrects for emissivity

effects and provides more accurate results[41,47,51,52]. Using both TERRA and AQUA MODIS data for LST retrieval improves the quality of the LST product and the diurnal feature in the product due to better temporal, spatial and angular coverage of clear-sky observations[53].

Another valuable source of LST data is from the LANDSAT earth observation satellites, managed by NASA and the US geological survey (USGS) which were firstly launched in 1972 and provides land surface images for a wide range of uses from forestry, agriculture, geology, regional planning, and education[54]. Thermal data from LANDSAT sensors (OLI -Operational Land Imager; TIRS-Thermal Infrared Sensor; ETM+, Enhanced Thematic Mapper Plus; TM, Thematic Mapper) have also been used to retrieve LST data[55–58]. The most recent satellite, LANDSAT 8 was launched in 2013. LANDSAT data has the advantage of having a better spatial resolution (up to 30meters) but lacks the daily temporal resolution required for epidemiological studies.

Another important source of surface satellite data imagery is provided by Polar Orbiting Environmental Satellites (POES) of the US National Oceanic and Atmospheric Administration (NOAA) which have been operational since 1981. Data from the Advanced Very High Resolution Radiometer (AVHRR) multi-spectral sensor encompasses meteorological, climatological, and land use applications. In particular AVHRR data is used to monitor sea surface temperature, ice cover and vegetation cover, such as the NDVI product. AVHRR is active on two satellites orbiting the Earth in opposite directions, similarly to MODIS, allowing for total global coverage twice daily with a global coverage at 4km resolution and high resolution over local regions of 1km[59]. AVHRR is the predecessor of MODIS and used less for LST in recent years. Since 1998 Europe and the USA have set up the Joint polar system for the collaboration and sharing of instruments and data from polar orbiting satellites. The European based European Organization for the Exploitation of Meteorological Satellites (EUMETSAT)

has a series of polar orbiting satellites with similar characteristics to NOAA's which have been used mostly for meteorological, climate and land use taking advantage of the lower orbit and the possibility of using microwave instruments[60]

Geostationary satellites also provide valuable data, especially for weather applications, with very high temporal resolutions (15minutes for global coverage and every 5 minutes over continents) but lower spatial resolutions. The European-led METEOSAT satellites, managed by EUMETSAT have a geostationary orbit, 36,000 km above the equator and cover Europe, Africa and the Indian Ocean. The Spinning Enhanced Visible and Infrared Imager (SEVIRI) instrument on board METEOSAT provides data with a 3km resolution in 12 spectral bands and 1 band with a 1km resolution and is mostly used for numerical weather forecasting, nowcasting and meteorological applications[61].

The difficulty and limited use of remotely sensed imagery among non-technical users, such as the epidemiological and public health community, is the complex methodologies and the time-consuming processes necessary for atmospheric correction, geo-registering, compositing and processing satellite imagery to produce accurate environmental variables.

3.1.2 Definition of air temperature using land surface temperature (LST).

Out of the 90 articles identified in the literature search only 35 were kept and considered as relevant to the first research question (Figure 3.1 and Table 2 Appendix). The derivation of air temperature (Ta), from satellite based land surface temperature (LST) is far from simple and different methods have been proposed in the literature. Although LST and Ta are correlated, they have different physical meanings, magnitudes, methodologies of measurement and response to atmospheric conditions and diurnal phases[26,42]. During the diurnal cycle, the temperature lapse rate varies considerably, and these patterns also vary throughout the year due to lengths of day and night in the seasons. During the day LST is higher than Ta, while during

the night the opposite occurs as land surfaces loose thermal energy at a higher rate. This often leads to over and underestimation of Ta respectively[38]. During the night, as solar radiation does not affect the thermal infrared signal, the retrieval of minimum temperature is easier. Conversely, during the day a large fraction of energy is due to re-emitted long-wave radiation driven by solar radiation and defining Ta from LST is more complex.

The lapse rate between LST and Ta is controlled by the surface energy balance which in turn depends on a series of factors not necessarily provided by satellite data[26,45]. Soil emissivity, moisture content, cloud cover, vegetation, elevation, topography, surface roughness and wind velocity are important factors in defining the land-atmosphere relationship[26]. Furthermore, advection, adiabatic processes, turbulence and thermodynamic phase transformation all influence Ta variation.

The methodologies commonly used to estimate Ta based on LST, are summarized below and divided in three distinct groups as described by Zaksek et al. and Benali et al.[26,62]:

1) Statistical approaches based on regression models between LST and Ta. These techniques can be simple if based solely on LST and Ta [43,63] or more advanced, when a series of independent variable are taken into account[27,28,38,43,55,56,64–70]. The methodologies were applied to very different geographical settings, climates and land cover characteristics of the terrain. Covariates included in the regression models were very diverse and of different complexities. Some were simply spatial and others spatio-temporal. Statistical methods generally perform well, within the spatial and time frame they were derived, but require large amounts of data to train the algorithms and results are not generalizable[71,72].

2) The temperature–vegetation index (TVX) is typically used in vegetated rural areas, and is based on the assumption that the top-of-canopy temperature is the same as within the canopy, assuming an infinitely thick canopy[39,72–76] and uses the Normalized Difference

Vegetation Index (NDVI) as a key input variable. Wloczyk et al. used a multi-spectral approach using LANDSAT data to derive Ta across Germany[76]. Zhu et al. applied it to derive maximum and minimum temperatures around a river basin in the Tibetan Plateau incorporating both LANDSAT and MODIS data[75]. Stisen et al derived temperature maps over western Africa to be then used in the development of hydrological models[72]. However, it is worth mentioning that the assumption by which the relationship between LST and NDVI is linear and negative is not always applicable and is highly influenced by seasonality, ecosystem type and soil moisture variability[27,45,77]. Furthermore, this method is limited to homogeneous vegetated areas thus making it inapplicable to complex terrain with different land cover types, urban or built environments that have a key role in my research. Nieto et al. investigated the limitations of this method and proposed a new methodology that uses observed air temperature to calibrate maximum NDVI specifically for each vegetation type[71].

3) Energy-balance models are based on the concept that the sum of incoming net radiation and anthropogenic heat fluxes has to be equal to the sum of the surface's sensible and latent heat fluxes[78,79]. The applicability of these methods is limited primarily due to the large amount of information required to carry out these approaches, often not provided by remote sensing[26,80].

Throughout the literature, different methodologies have been proposed and refined (see table 2 Appendix). Cresswell et al. used a statistical model to derive Ta in southern Africa taking into account the solar zenith angle (SZA) data derived from sensors on board the European satellite METEOSAT as proxy of solar energy reaching the ground, METEOSAT data and screen temperature deviations[38]. The TVX method has been used in several studies; such as Czajkowski et al. that estimated weekly average Ta in Oklahoma[39] while Prihodoko et al. estimated Ta in several sites in Kansas using land surface radiation data in the near IR spectral

region from Advanced very-high-resolution radiometer (AVHRR) instrument on board NOAA satellites[73]. Zhu et al. also estimated Ta in the Tibetan Plateau using Terra MODIS data[75]. The TVX method, modified by lowering the threshold of the correlation coefficient between NDVI and LST was used to estimate both minimum and maximum temperature. This methodology again is limited to vegetated surfaces and is valid mainly during the growing season. Vancutsem et al. used high-resolution data from the MODIS night time LST over different ecosystems in Africa to estimate both minimum and maximum Ta, using both regression models and NDVI and SZA to account for seasonality, solar radiation, cloud cover and different land covers[45]. A more complex methodology, firstly to downscale the spatial resolution using a regression analysis between LST derived from SEVIRI - *Spinning Enhanced Visible and Infrared Imager* sensor on board Meteosat satellites, LST from MODIS data and NDVI also from MODIS and then based on the energy balance model was developed by Zaksek et al.[62]. Neural networks have also been used to estimate near Ta from satellite LST considering other land cover characteristics[81,82].

Fu et al. applied linear regression to LST MODIS data to estimate Ta for an alpine meadow in the Northern Tibetan Plateau[63]. Zhang et al. developed regression models between observed Ta from over 600 weather stations in China and LST MODIS data to estimate minimum and maximum temperatures for 2003. Researchers concluded that night-time LST was the optimum predictor and there was no great difference between TERRA and AQUA data[67]. Benali et al. developed specific models to estimate the minimum, maximum and mean Ta from TERRA MODIS LST data through a statistical approach in Portugal[26]. Both static and dynamic variables that influence the LST-Ta relationship were included in the models and then calibration and validation using statistical procedures were carried out and gave good results[26]. A study to estimate the daily surface water vapour pressure ($e0$), air temperature (Ta), and relative humidity using different MODIS LST algorithms and NDVI data was developed by

Recondo and colleagues in Spain[70]. Kloog et al. uses mixed models allowing the regression coefficients to define the relation between Ts and Ta to vary on a daily basis in Massachusetts and north-eastern USA[27,29]. These models also incorporate land use regression, meteorological observed parameters and spatial smoothing to predict Ta when satellite data was not present[29]. Shi et al. carried out the same approach in the hot humid south eastern states of USA, also validating the methodology by comparing it to NASA's Modern-Era Retrospective Analysis for Research and Applications (MERRA) model and obtaining very good model fits[28]. More recently, two studies were carried out in Israel applying the same methodology developed by Kloog et al. Rosenfeld et al. estimated maximum, mean and minimum temperatures using MODIS data from both TERRA and AQUA satellites for Israel[64]. The model was extended to include IDW (inverse distance weighted) interpolations and thin plate splines in the first stage calibration model for the estimation of both day time and night time temperatures with very good model performances[64]. High resolution LANDSAT brightness temperature data was also used to estimate air temperature in Tel Aviv, Israel using the same mixed regression model approach previously defined by Kloog et al. and Shi et al. to evaluate changes over time in spatial distribution of air temperature during summer[27–29,65]. This methodology was used as basis for my study, a series of other spatial and spatio-temporal parameters in the regression models were added to account for the unique geographical characteristics of Italy compared to the east coast of the US in which the study was first conducted. The fact that it has been now applied to several areas of the world with very diverse climatic zones adds value to the methodology and potential model performances.

A limited number of studies have tried to test the difference between the predictability of their models on different land surfaces within urban areas. Nichol et al. estimated Ta using LST data derived from the ASTER- Advanced Spaceborne Thermal Emission and Reflection Radiometer sensor on board TERRA in Hong Kong using spatial resampling and buffering

around air temperature points. Spatial differences observed were attributed to structural factors of land cover such as city block size, building density and percent of green areas, and secondarily to the climatic conditions[83,84].

3.2 THE DEFINITION OF THE URBAN HEAT ISLAND USING SATELLITE DATA

3.2.1 Urban Heat Island: physical principles

The heat island effect, is when urban areas have a positive thermal differential compared to rural areas[78,85]. The assumption is that this change in temperature is the result of the composition of the land surface and the atmosphere. The larger the urban area and higher the density of urban living, the higher the frequency and greater the intensity of the observed urban heat island (UHI)[78]. The introduction of artificial materials, such as concrete and asphalt, the complexity of the urban geometry, and the reduction of natural land cover, modify the surface energy balance, resulting in an increase in surface temperature that is associated to an increase in sensible heat flux and a resultant rise in air temperature[86–88]. UHI intensity is strongest during the night, when winds are weak and artificial surfaces retain heat accumulated throughout the day and slowly release it.

A systematic review conducted by Stewart in 2011 considered 190 papers published between 1950 and 2007 on the UHI to evaluate the scientific quality of work in the field and provides recommendations for better methodological developments[23]. However, the study selected only ground-based observational UHI studies, hence excluding remotely sensed derived UHI. Another recent review on UHI studies around the world provides an overview of the phenomenon quantitatively and spatially and the potential health effects[24,89]. Ngie et al. reviewed the use of satellite data and LST specifically to define UHI around the world[30]. The UHI phenomenon is a global issue and with the increasing level of urbanization and future climate change will become an even greater problem in the next century. Although studies use different methodologies to define the intensity of UHI, it is interesting to see how intensities differ between continents and cities depending on size of the city, urban geometry and characteristics, population density, surrounding land use and local climate.

A summary of the literature review on urban heat islands is reported in table 3-Appendix. Studies in which the UHI was identified using satellite data, either just in terms of surface UHI or studies which then estimate Ta within the urban canopy integrating satellite LST data and Ta from ground monitoring stations were retained. Studies on the role of land use and surface cover and the characteristics of urban areas in influencing UHI intensities were also included and reported. Out of 156 articles identified as eligible in the search strategy only 87 were retained. The interest here was to have an overview the methodologies used to define UHI, how they differ from those identified in the LST –Ta literature in terms of satellite data used, downscaling techniques for obtaining a better spatial resolution and additional factors integrated in the models to take into account the peculiarity of the urban setting. Furthermore, the review looked into key factors that contribute to the UHI intensity on the basis of land use or area characteristics. For example, land use (green areas, types of urban surfaces), building type (roof-top colouring), population density and other factors that modify the microclimate and heat\cooling conditions in cities. This aspect is crucial not only for measuring UHI intensities, but also for the comparison of urban rural gradients and temperature gradients and assessment of differential thermal characteristics based on land use structures[90]. In the review carried out by Stewart, he found that over three quarters of the studies on UHI did not provide information on land use characteristics of monitoring sites or did not assess the association between land cover and temperatures[23]. Following this, the same authors developed a standardized set of local climate zones, to classify urban and rural field sites based on surface properties[90]. In the methodology developed for my thesis this is accounted for as satellite LST data captures temperatures at surface level and the relationship with land use and land cover were used to derive air temperature as described in chapter 4. Finally, the intensity of the UHI in different cities around the world was considered for descriptive purposed.

Most studies addressing the UHI effect have used two approaches either numerical modelling of the physical processes that simulate urban energy balance fluxes through the parameterization of urban surface processes also described in the previous section[91–94], or by empirical analysis, based on Ta records from weather stations or LST derived from remote sensing. These methods attempt to define the association between the UHI intensity and the different characteristics of the cities from impervious surfaces to socio-demographic characteristics[95]. Schwarz et al. carried out a comparison of the indicators used for quantifying the surface UHI with different urban-rural definitions and reported weak correlations among the indicators[96].

High-resolution thermal infrared images, from different satellite platforms are able to match the complexity of the urban environment, and are capable of characterizing the urban land cover types required for spatial modelling of the UHI effect using a GIS approach. Thus providing a very important data source and of great interest also for epidemiological studies. MODIS daily data has been extensively used to define UHI around the world[97,98], in Europe[91,96,99–102], Asia [103–109] and North America[110–115]. Similarly, LANDSAT data has also been widely used especially to analyse the spatiotemporal patterns of UHI due to changes in land use/land cover change[108,116–126]. LANDSAT has the advantage of having very high spatial resolutions but lacks in the temporal domain, as the satellite overpass is not daily.

Urban heat islands have been identified in Rome and other Italian cities.[91,127,128] Fabrizi et al. estimated the UHI in Rome using Advanced Along-Track Scanning Radiometer (AATSR) land surface data temperature on board ENVISAT polar-orbiting satellite and observed data for the period 2003-2006[128]. Two studies estimated the UHI in Milan using MODIS data and estimated a night time canopy layer UHI intensity during summer of around 3-4°K dat.[127,129] Morabito et

al. compared LST temperatures in 11 Italian cities, including Rome using MODIS data, to map heat vulnerability but did not estimate UHI intensites.[91]

Research has been carried out to combine different satellite data or downscale data to improve both temporal and spatial resolution for defining UHI. High resolution MODIS data was used by Qiao et al. to look at the change in urbanization and the effects of this on UHI patterns in Beijing.[130] Strathpolou et al. consider four downscaling techniques in their study in order to improve the spatial scale of LST data and better identify the UHI of Athens, Greece [131]. Kourtidis et al. considered different LST data from satellites with different time passes to evaluate the diurnal pattern and change in UHI[132]. Other downscaling techniques have been used to improve the spatial resolution of fine temporal scale satellite products, for example Zaksek et al. downscaled SEVIRI data to monitor the diurnal cycle of UHI[133]. Cheval et al. used MODIS TERRA and AQUA data to estimate the UHI in Bucharest, during the day and night and considering land cover factors that might influence it [134]. Temporal changes in the UHI intensity have also been studied in recent years, and variation in the extent and intensity have been reported[118,135–137].

Findings on the relationship between land cover and UHI intensity include:

- increased UHI intensity and temperatures with a reduction of green cover[95,122,138–140], NDVI being inversely correlated to temperature[116,141,142]
- population density positively correlated to UHI intensity[116,122,143,144]
- water bodies and vegetation moisture reducing the UHI intensity[118,145,146]
- industrial zones and high constructed areas associated to higher temperatures and UHI hot spots[118,125,145,147,148]
- low albedo[120]
- the presence of impervious surfaces increase UHI intensity and temperatures[136,149,150]

- anthropogenic heating, as well as pollutant emissions could increase the intensity of UHI[151]
- roof top materials and surface temperature[152]

Zhou et al. 2013 investigate the UHI intensity in European cities using MODIS LST and Corine land cover comparing urban area size with surrounding temperatures[92]. Urban clusters are defined considering land cover characteristics and not all areas exhibit increasing UHI intensities with increasing boundary temperatures. Generally, UHI intensity is greater in larger urban areas and an inter-annual pattern is observed, with the strongest effect in summer.[30,92]

Another important issue to take into account when comparing UHI intensities is how the urban and rural areas/points are defined as well as which indicators are used. Rural areas have been defined as parts of a city region that are not influenced by the urban heat island in empirical models[78] while in remote sensing studies a priori definitions of "urban" versus "rural" areas according to land cover are defined. Researchers have used a variety of methods to identify urban and rural areas such as pixels around weather stations[153,154], areas with the highest LST versus areas with rural land cover, central districts versus rural districts and pixels with high and low imperviousness[98,100,110]. These aspects were taken into account for the selection of the rural point to define the urban heat island intensity in Rome.

3.3 LITERATURE REVIEW OF HEALTH EFFECTS OF HEAT ON HEALTH OUTCOMES

Introduction

The literature on temperature related health effects is very vast, with a multitude of aspects discussed. In order to better assess the findings in relation to my research, specific aspects were considered such as the study type and modelling methods used to estimate heat-related effects, biological mechanisms and vulnerable subgroups, characteristics of the temperature mortality-relationship and geographical differences in the effect. Furthermore, potential effect modifiers of the effect, namely individual characteristics as well as spatial and context variables were considered in the literature search.

Of the full text papers considered for eligibility in the literature review, 96 articles were retained and considered as relevant to the research question. Studies are summarized in table 4 in the Appendix.

The effect of heat on morbidity and mortality

The effect of temperature on the health of a specific population can be interpreted as the average population vulnerability to heat. Usually it is easier to understand the effect associated to extreme events such as heat waves, defined as abnormally high surface temperatures relative to those normally expected in a specific location that persist for prolonged periods of time. However there is no universal definition or consensus on a definition, especially in terms of number of consecutive days, temperature parameter or a threshold among the meteorological community. National meteorological services have adopted several different definitions. Furthermore, epidemiological studies have used a plethora of definitions, not always based on appropriate meteorological characteristics, making comparison between studies complex. Nevertheless, the literature has identified dramatic increases in mortality rates during heat wave

episodes, especially among the most vulnerable individuals living in urban areas from the 1970s[155,156] Indeed, there is also a burden related to less-extreme temperatures in summer[157]. Heat may cause death in subjects in poor health but may also exacerbate chronic diseases or trigger acute events such as stroke. For the variety of mechanisms and effects related to heat, the actual burden of heat-related deaths may be notably greater than it has been reported, since no widely accepted systematic criteria currently exist for classifying them and generally only a few deaths are directly coded as being caused by heat[158]. The most stringent definition of heat-related death is a core body temperature greater than or equal to 40.6°C at the time of death[158]. This definition precludes certifying any death as heat-related if core body temperature is not measured near the time of death, and may therefore underestimate the actual excess heat-related mortality. On the other hand, a non-specific definition of heat-related deaths may very well overestimate the attributed effect. Most excess mortality during high temperatures is related to cardiovascular, respiratory and cerebrovascular diseases, as subjects with these pre-existing conditions have a limited ability to cope with extreme heat[155,156,159–161]. The effect of high temperatures and heat waves on non-fatal outcomes[11,12,156,162–165] seems to be comparatively smaller suggesting that many heat-related deaths occur before coming to medical attention. Moreover, time series studies investigating the short-term effects of heat on health outcomes consider different thresholds or temperature ranges.

Health outcome assessment

Mortality has been always used in epidemiological studies since it is a well define outcome and mortality data are routinely collected. However, both heat- and related mortality are subject to misclassification and generally, researchers have used total mortality or cause-specific mortality as the outcome measure. Periods of intense heat also produce increases in non-fatal illnesses. The spectrum of heat-related illnesses may include milder symptoms like heat

cramps, heat syncope, heatstroke[166]. Consequently, during heat waves an increase in hospital admission rates for selected causes may also be detected[11,12,162–165,167]. The effect of high temperatures on non-fatal outcomes seems to be comparatively smaller compared to mortality outcomes. For example, a European multicity study showed a 6.71% increase in the risk of respiratory deaths for a 1°C increase in maximum apparent temperature[8] and only a 2.1% increase in respiratory admissions[12] among Mediterranean cities.

While high temperatures have an effect on mortality for both cardiovascular and respiratory causes, with comparable estimates, as shown in a recent systematic review on the elderly, (with increases in the risk of 3.44% and 3.60% for a 1°C increase in temperature above the threshold during summer, respectively for CVD and respiratory deaths). When considering morbidity heat had a significant effect on respiratory admissions but no effect on cardiovascular admissions (percent change in risk: 0.15% and 1.65% respectively for CVD and respiratory admissions)[9]. Noteworthy that the relationship between heat and non-fatal events (hospital admissions, ER visits and ambulance calls) has been less studied and has given contrasting evidence in some cases[15]. Lin et a found an increase in admissions in New York for temperature increases for chronic airways obstruction, asthma, IHD and cardiac dysrhythmias but decreased for hypertension and heart failure.[168] While Green et al. found opposite associations among the cerebrovascular disease group for temperature increases in California, specifically a protective effect of heat for hemorrhage stroke on one hand and an increase in ischemic stroke admissions on the other[163].

Study design

Several epidemiological methods have been applied to assess heat-related mortality. In the descriptive episode analysis of individual heat waves, mortality count or rates during events are generally compared with rates several days before or with rates during the same period in

the previous year to estimate the number of excess deaths attributable to the episode. In general, these studies are based on single episodes and incur in problems related to the definition of baseline mortality and the consequent quantification on mortality excess. Moreover, when the reference period contains episodes of extreme heat, baseline mortality may be influenced leading to an underestimation of the effect.

The time series approach overcomes these limitations and is well suited for modelling the short-term association between temperature and mortality. The time series approach considers sequences of data indexed by time units, specifically days being the time unit in the present analysis. For each day, counts of deaths/hospitalizations are related to average population exposure, while accounting for potential time-varying confounders. This kind of study is considered a quasi-experimental study design because the contrast (in both exposure and outcome) is performed *within the same study population* over time. Since time trends are adjusted for in the modelling phase, it follows that fixed population characteristics, or factors that vary slowly over time cannot confound the short-term association between exposure to daily temperatures and mortality/morbidity outcomes. The only putative confounders to be accounted for, in addition to time trends, are those factors which might co-vary in the short-term together with both the exposure (temperature) and the outcome (daily count of deaths/hospitalizations).

The time series approach allows to estimate the effect for different temperature ranges. The statistical modelling of the temperature-mortality dose-response function has to consider that temperature extremes (heat/cold) may have adverse health effects. Some researchers have dealt with this problem by focusing only on heat effects by season while other studies have modelled the entire temperature range and its association with health outcomes simultaneously. Different statistical approaches such as Poisson regression models,[159,169–171] autoregressive models,[172,173]

generalised linear models with parametric splines,[174,175] generalised additive models with non-parametric splines[7,10,173,176] have been implemented for estimating the effect of temperature on mortality. Distributed lag models have been used to explore the cumulative and prolonged effect of temperature on mortality, rather than focussing on the effect associated to a single lag of exposure. This method is based on the concept that environmental exposures may produce increased risk of death not only on the same day of exposure but also on subsequent days.[10,11] More recently, the distributed lag non-linear models have been developed to take into account the non-linearity of the temperature-mortality relationship and the delayed effect of temperature simultaneously.[19,177,178]

Through time series studies the association between temperature and mortality has been identified and described as a non-linear U-, J- or V-shaped function, with the lowest mortality rates recorded at moderate temperatures, rising progressively as temperatures increase or decrease.[7]

On the other hand, the case cross-over approach has been used to explore potential effect modifiers of the temperature mortality relationship.[20,169,179,180] This approach is a matched case-control design where each subject is a risk-set and the exposure on the event day (death) is compared to the average exposure on control days. It follows that each subject is the control of himself, therefore perfect adjustment for all potential confounding factors that do not vary over time or are slow-changing (age, smoking, BMI, socio-economic factors) are adjusted for by design. Other time-varying factors (e.g. seasonality) can be adjusted for by using multivariate conditional logistic regression models. This approach is highly recommended to estimate the short–term effects of environmental exposures, such as temperature, estimated at the individual level. Furthermore, the case-cross over design has been widely used to identify individual-level or address-level effect modifiers. Subgroups most vulnerable to the effects of heat might

include the fraction of the population with a greater than average adverse response either resulting from intrinsic susceptibility factors (chronic clinical conditions), individual characteristic (age, gender, socio-economic status, education, occupation) or factors that modify exposure, typically area-level characteristics (urban heat island, green space, proximity to water, impervious surfaces, building density.[9,181–183]

Seasonal pattern

In most countries, a strong seasonal pattern in mortality is observed with highest death rates in winter primarily and lower values in summer. The seasonal pattern of cardiovascular disease and other concomitant factors such as respiratory epidemics, that are more prevalent during cold weather when people usually spend more time indoor, make it difficult to disentangle the role of temperature and other meteorological variables on mortality and morbidity[184]. To try and account for these factors, most studies on the effect of temperature and weather parameters on health outcomes are controlled for season to account for the natural trend in mortality counts and other confounding factors such as influenza outbreaks.

Delayed effect and mortality displacement

A review carried out by Basu and Samet on forty-nine studies published after 1970 in peer-reviewed journals, reported that most studies on hot weather had an immediate effect on mortality, either on the same day and on the subsequent 2-3 days[4]. It has also been shown that these excess deaths are often compensated for by a fall in mortality in the following weeks, this phenomenon is known as *mortality displacement* [10,159,160,175,185]. A possible explanation is that the heat stress depletes the pool of susceptible individuals, anticipating the death event by a few weeks/months while the individuals with a less compromised health status are more able to cope with extreme temperatures and remain in the pool.

Exposure indexes

To date there is no single temperature or weather variable used to account for heat in epidemiological studies due to data availability or researcher interests. It would be useful so that results from different studies could be directly compared. In a number of epidemiological studies focusing on heat effects on health, air temperature (minimum, maximum or mean) dew point temperature or relative humidity measured at weather stations have been used as exposure measures. Other authors[165,169,186] have adopted various composite indexes of thermal discomfort such as apparent temperature and heat index[187] or Humidity index (HUMIDEX) used by the Canadian Meteorological service that combines air temperature and dew point temperature. Human thermal comfort depends on environmental and personal factors. The four environmental factors typically included are wind, air temperature, air humidity, and solar radiation. Some indicators have also incorporated personal physiology and personal factors such as clothing and level of physical activity. For example, an index that includes these factors is the Physiologically Equivalent Temperature (PET)[188]. Throughout the years, different equations have been developed to calculate these indexes which differ for complexity, the variables included (wind speed, etc) and for temperature range applicability. It is worth mentioning that these indexes are not developed explicitly for epidemiological studies and are often used inappropriately. Two studies recently conducted have shown that the effect estimates do not vary much when using different temperature measures (minimum, maximum or mean) or when different indexes are considered[189,190]. Moreover, local climate defines summer temperatures and thus heat definitions are site-specific. Epidemiological studies investigating the short-term effects of heat on health outcomes consider different thresholds or temperature ranges, based on the temperature-outcome association and by considering percentiles rather than absolute temperature values to allow comparisons between locations and studies as described in the next section.

Most studies on health effects of heat are related to single point exposure that is not entirely representative of the individual exposure or spatio-temporal exposure subjects are really exposed to as previously described. The use of satellite data and the definition of spatio-temporal temperature exposure will help bridge this gap and provide more accurate exposures not only in areas where studies have not been carried out due to lack of monitoring stations but also with a finer resolution in urban areas where temperatures differ across small distances due to the complex urban structure. Although there are limited comparative studies, recent research conducted comparing spatio-temporal and time series models for estimating the effects on mortality showed that although performance of spatio-temporal models for exposure are better the effect estimates are comparable[21], however it is worth noting that the resolution of the spatio-temporal model was far below models using temperatures derived from satellite data.

Spatial variations in heat-related effects

Time series studies performed in regions with different climates have consistently provided evidence of increased mortality in association with hot weather, showing also a geographical variability of heat-related mortality. However, comparisons between countries should be made with caution taking into account local population characteristics such as climate, baseline mortality rates, age structure of the population and health status.

Results from multi-city studies[7,10,18,191], have provided important insights into the geographical heterogeneity of the impact of heat on mortality, showing a greater effect of high temperatures in populations residing in colder regions than in those residing in warmer countries. This apparent paradox has been ascribed to the more limited adaptive capacity of the populations living in colder regions where extremely high temperatures occur infrequently[7,10,192]. Moreover, the same studies have documented that the thresholds above which mortality increases are higher in the warmest cities where populations are better acclimatized to high

temperatures during summer. These findings have recently been confirmed in several studies conducted in the Multi Country Multi City (MCMC) Consortium.[193,194] Italian cities were among the cities with the highest heat effects, with a 14% increase risk of death (pooled estimate for all Italian cities) for a rise in mean temperatures between the 90th and 99th percentile compared to a 9% in Spain and 3% in Australia[191].

In recent years studies have been published on the effect of heat in Asia mostly China,[195–198] but also in Taiwan and Korea [194,199–201] and Australia [13,202–205]. To date, there is limited evidence of the impact of high temperatures on mortality and morbidity in low or middle income countries[14,175,206–211]. However, populations residing in these countries may be particularly vulnerable due to the limited resources such as low socioeconomic status, limited access to health care services and poor health care systems[212]. The recent multi country-multicity collaboration has an added value of providing highly representative estimate from a large number of communities and countries and it includes some low- or middle-income countries (Brazil, Thailand).[193]

Studies on the spatial differences within a country are also important. Studies looking at the geographical differences in the effect on heat in the US[18,213] and European countries[8,214,215] , China[216–218], have been carried out. However, most studies are limited to urban areas where both exposure and health data is available. A recent study carried out in the UK using modelled temperature data was able to estimate the effects of heat at district level and showed a north-south gradient with the highest effect estimates in London and the south/southestern districts[219]. Similarly, a study conducted in the Czech republic identified the spatial pattern of heat-related risk at district level considering difference socio-economic risk factors[220]. While studies conducted in the US using satellite data with a 1x1km resolution were used to estimate the effect of heat on mortality in SE USA[221] and on birth outcomes in Massachusetts[222]. In

southeastern US states a 2.05% (95% CI:0.87, 3.24%) increase in mortality for every 1 °C increase in temperature above 28 °C was observed[221].

Time trends in temperature-mortality relationship

Considering climate change scenarios and possible temporal changes in the individual and community factors that determine vulnerability to extreme weather events, it is important to monitor the temporal variation of the temperature-mortality relationship to better understand a population's capacity to adapt to new climate conditions. Moreover, studies addressing inter-annual variations are to date limited. With regards to the long-term variations, some authors have observed a long-term decline in summer mortality and attributed it to changes in adaptation strategies such as the increased use of air conditioning and public health interventions.[193,213,223–225] Similar conclusions were reached in studies comparing heat wave episodes in different years, showing a decline in heat-related mortality potentially attributable to adaptation measures introduced and changes in individual behaviour and response mechanisms.[226–228] Gasparrini and colleagues showed a decrease in the effect of heat over time in several countries, namely the US, Japan, Spain and non-significantly in Canada, potentially attributable to adaptation measures such as the introduction of heat prevention programs, as also suggested. in a European city comparison between two periods.[193,215,229] On the other hand where exposures have increased and populations vulnerability might also have risen, an increment in the heat related mortality was observed.[193]

Biological mechanisms

Humans are normally capable of maintaining a constant body temperature despite wide variations in atmospheric temperature. Core body temperature usually varies between 36°C to 37.5°C and it is maintained by balancing heat gain and heat loss by physiologic and behavioural

mechanisms[230]. Under mild heat stress, acclimatization can increase the body's tolerance to heat stress, but under extreme heat the body can lose its ability to maintain temperature balance and death may occur.[166].Adverse health effects associated with an intense and prolonged exposure to high temperatures include minor illnesses such as heat cramps, heat syncope, heat exhaustion, and heatstroke[166,230,231]. Heat cramps are the mildest form of heat-related illness and occur in persons, who produce a large amount of sweat but replace it only with hypotonic fluids, probably secondary to sodium depletion. Heat syncope is caused by reduced cerebral blood flow resulting from the combination of peripheral blood pooling, reduced cardiac output and orthostatic hypotension. Heat exhaustion is the most common heat-related illness, and may develop after several days exposure to high ambient temperatures and inadequate or unbalanced replacement of fluids and electrolytes. It is characterized by fatigue, malaise, anorexia, nausea, vomiting, anxiety and confusion; potentially harmful clinical manifestations include circulatory collapse and excessive body core temperature and may be severe enough to require hospitalisation. Heatstroke is a medical emergency resulting from a failure of the thermoregulatory mechanisms that causes an accumulation of heat in the body and can be fatal[166,232]. Heat related effects on the cardiovascular system are partly mediated by the thermoregulatory responses which pose stress to the heart and circulatory system. Heat stress causes physiological changes such as increase in red blood cell counts, platelet counts and blood viscosity, or rhythm alterations via the autonomic system and blood lipid levels.[233–236] Furthermore, temperatures have also been shown to affect blood pressure[237–239], cause myocyte injury[240] or modify cholesterol levels[236]. Zanobetti et al. found that subjects with atrial fibrillation were more susceptible to extreme heat, suggestive of a greater risk of stroke events[20]. More recently, Bind et al. found that high temperatures and relative humidity were associated with DNA methylation in blood cells[241]. Mechanisms associated with heat are less clear for respiratory events, on hot days the respiratory system is under greater stress and causes

exacerbation of chronic respiratory disease among those with pre-existing respiratory conditions.[5,10,12,242] Furthermore, studies on the role of temperatures on DNA methylation suggest a plausible role in inflammatory responses due to heat[241]. Epigenetic studies will be of great use in the future to help shed light on the biological mechanisms and health risks associated to extreme heat and susceptibility factors.

Vulnerable Subgroups to Heat

Specific vulnerability factors can confer a greater risk of dying with exposure to extreme heat. These factors may be individual (gender, age, genetic factors, health status), socio-economic and environmental characteristics (living in urban areas, presence of air conditioning, building types, presence of green areas). Temperature-related effects are particularly apparent among the elderly. As age progresses, thermoregulatory responses are reduced and less sensitive thermal perception may affect the behavioural response to heat stress, facilitating the onset of heat-related illnesses and deaths. The increase in life expectancy and the ageing of populations, especially in developed countries, has mean that the pool of old (over 75 years) and very old (over 85+ year) has become larger and a greater proportion of the population is at risk[4–6,243]. However some recent studies have identified a larger risk in the "younger" elderly [244], possibly due to the fact that the greatest part of public health preventive measures are targeted to the very old subjects rather than younger ones. Other age group at risk for heat-related health effects are children but will be not addressed in the present study[164,202,245]. Compared to adults, children have a smaller body mass that warms more quickly, a smaller blood volume that limits heat transfer through peripheral blood flow and vasodilation, and a lower sweating rate. Diarrhoea or febrile illness, particularly in neonates and young infant, may increase the risk of heat-related illness because these may be associated with excessive fluid loss and dehydration[245,246].

There is still contrasting evidence on the differences in heat-related effects by gender. Several studies have documented a greater vulnerability to heat among women both in terms of mortality and morbidity [247–251] while there is limited evidence for a higher susceptibility among men[162,165]. A recent meta-analysis showed a pooled ratio relative risk for high temperatures of 0.99 (CI95% = 0.97, 1.01) for males compared to women[6]. The higher vulnerability of women is partly explained by the higher number of elderly females in the population and by physiological differences, i.e. a reduced capacity to sweat in females.[5,249]

Several studies have documented that most deaths during heat waves or high temperatures occurred in subjects with pre-existing chronic diseases like ischemic heart disease, stroke and respiratory illnesses[12,155,156,159,160,252–254] due to their limited cardiovascular adjustment needed during exposure to heat stress. Subjects with metabolic/endocrine gland disorders[161,179] or diabetes were also found to be at greater risk of heat-related deaths[179,255], probably since they have poor autonomic control and endothelial function that, in addition to the increased demand on the circulatory system, may lead to an increased risk of fatal events. Central nervous system disease and psychological illnesses have also been shown to increase the risk of death during heat waves since subjects are unable to care for themselves.[20,179,252]

Potential effect modifiers

Some studies have pointed out that vulnerability to heat is influenced by socio-economic factors. Having a low socio-economic status,[169,179,218,256] or living in low-income census tracts income or living alone and being socially isolated were found to be associated to increased mortality during high temperatures or heat episodes.[156,218,256–259] A recent study from Paris found a strong effect modification by social deprivation and this was greatest among the individuals chronically exposed to high levels of air pollution.[260]

Studies from the United States have found a differential effect of heat among different ethnic groups[20,156,169,212,256,257], probably explainable by the socio-economic differences among these groups and different access to health care services in the US. However, results are not always consistent among studies. A recent systematic review and meta-analysis showed relative risks for high temperature of 1.03 (95% CI = 1.01, 1.05) among low individual socioeconomic status (SES), and 1.01 (95% CI = 0.99, 1.02) for low area based SEP.[6] Ethnicity and different genetic factors may also modify the adaptive capacity to heat, however specific studies on this aspect are lacking. Epigenetic studies will help address this aspect.

Hot weather predominantly affects people living in urban environments, where maximum temperatures are higher and the daily thermal pattern is altered (less variable), with respect to the surrounding rural areas. This phenomenon known as the UHI and has been described in section above and a focus on the differential health effects due to urban heat is described in the next section. In metropolitan areas the effect of heat on health may be exacerbated by greater socioeconomic disparities[212,261] and by the concurrent exposure to air pollution that may interact with temperature in determining health effects.[262] Physical urban factors, such as impervious surfaces, building type and housing features, may also contribute to differences in heat-related health risk.[256,263–267] It is noteworthy that studies in rural areas are limited and further work is needed.

Finally, the role of air pollutants as effect modifiers is an important aspect. The synergistic effect of air pollutants, in particular PM10 and ozone, and temperatures on mortality outcomes during summer has been identified.[179,268–272] A recent review looking at the role of temperature as effect modifier of the pollutant-mortality association found that on days with higher temperatures the effects of ozone and particulate matter were stronger.[273] A study conducted in Italy showed a synergistic effect of heat with both ozone and PM10 during summer in Italian

cities, with higher effect estimates of temperature on days with high levels of ozone and PM10 in particular among cities in the north where air pollution levels are higher[274].

3.4 LITERATURE REVIEW OF THE HEALTH EFFECTS OF HEAT WITHIN URBAN AREAS AND THE DIFFERENTIAL EFFECT DUE TO THE URBAN HEAT ISLAND.

Very few studies have accounted for the differential effect of heat within urban areas when studying the impact of heat or heat waves; out of the 64 papers examined only 20 fit the research question (Table 5 Appendix). As shown in the previous section (section 3.3), much effort has been addressed towards modelling the relationship with complex statistical techniques or identifying vulnerable subgroups,[178,275–277] while few studies have dealt with the limitations linked to the exposure modelling.[21,189] Due to the limited spatial coverage of temperature monitoring networks, most studies consider exposure by area, from a single point measurement typically located at airports or within the city. However, temperatures are heterogeneous within cities, thus this may lead to a misclassification of individual exposure and/or bias in the estimates. Although few recent studies have accounted for the UHI as a spatial effect modifier of the temperature-mortality association, high resolution temperature data is rarely used as exposure to estimate the effects of heat in a more precise way while simultaneously dealing with the differential effect of temperatures within cities.

In the literature, the differential impact of heat on mortality within urban areas has been assessed using specific monitoring campaigns, spatio-temporal modelling of meteorological variables and socio economic factors and land use variables[278–286]. Case-cross over studies have been used in particular to identify effect modifiers of the temperature-mortality relationship within urban areas especially for socio-economic characteristics, land use factors and very few for micro-climatic conditions due to the UHI.[20,169,179,279,287,288]

The literature review identified very few studies using satellite data to assess the effects of heat on mortality and estimating the differential effects.[181,183,289–292] These studies use LST data to identify the UHI as potential modifier of the temperature mortality association[181,289,292] or

NDVI and Vegetation continuous fields (VCF) to spatially identify green areas which might mitigate the heat effect within a city.[182,183,290,291] Smargassi et al found that subjects living in postcode areas of Montreal with higher surface temperatures (greater UHI intensity) gave a higher risk of dying during hot days.[181] The analysis was also stratified by dwellings of high or low values, and an association with high LST was found in areas with dwellings of high values. This finding suggests that the health of those living in areas of lower socioeconomic status may be influenced by other risk factors more strongly than by the surface temperature at their place of death, even if a non-statistically significant trend was seen also among the latter group[181]. Laaidi et al. used NOAA AVHHR data to define land surface UHI and identify areas at higher risk to heat effects within a case-control study during the 2003 heat wave episode in Paris, France.[289] A study conducted in Hong Kong used land-use and building geometry data, NDVI and sky view factor (SVF) values to define UHI for each tertiary planning unit and then map results.[182] As for the Canadian study, when considering the potential role of socio-economic conditions differences there seemed to be an indication of a greater difference in the effect of heat among people of high SEP when stratifying by UHI.[181–183]

A study conducted in Barcelona, considered socio–demographics, green areas (VCF and perception of greenness) as factors that might modify the temperature-mortality association during summer.[183] The analysis showed the census tracts with a high percentage of old buildings, manual workers or residents perceiving little surrounding greenness had higher heat-related mortality risks. No real difference was observed for VCF defined green areas, suggesting the potential mitigating role of green areas within densely built cities remains unclear. When considering both blue and green spaces and the potential role in modifying the temperature-mortality association within the coastal city of Lisbon, Burkart et al. showed that the effects of heat were higher in areas with limited green space (NDVI lower than 0.27) and at further distances from the sea (more than 4km).[292]

Another limited number of studies have been conducted accounting for the differential effect of heat on mortality as a result of land use/land cover characteristics. A study on heat wave related mortality in Berlin, Germany, found that mortality increases during heat waves were greater in districts with a higher proportion of land area covered by sealed surfaces or inner city districts.[281]

A number of studies focused on the potential association and links between UHI and socioeconomic factors. Huang et al. used satellite LST data to define how temperature varies within urban areas and found that LST was higher in areas characterized by low income, high poverty, less education, more ethnic minorities, more elderly people and greater risk of crime.[293] These parameters need to be accounted for when studying the differential effect of heat within urban areas. A study carried out in Philadelphia, considered the role of socio-economic factors and the UHI, as well as the combination of these two aspects to identify heat vulnerability[294], thus identifying areas for each factor and a common set of at risk areas.[295] Ho et al. carried out a similar analysis considering different thermal indicators (LST, HUMIDEX, air temperature) and social vulnerability factors (deprivation index, unemployment rate, rented housing, education) as well as a combined vulnerability indicator that might cause spatial differences in heat-related mortality risk during heat waves in Vancouver. Indicators which showed the greatest spatial differences in the temperature–mortality relationship were HUMIDEX and high % unemployment\not looking for work.[291]

None of the studies actually derive air temperature from LST to use as high resolution spatio-temporal exposure in the epidemiological research carried out. These studies simply highlight differences in the effect of heat attributable to the area of residence, UHI and socio-economic factors. A recent study looked at the potential adaptation of heat within urban areas considering UHI , suggesting that for heat exposure, the areas with higher UHI were more acclimatized to

heat compared to cooler areas in the out zones[296]. This is suggestive of the need to use high resolution temperature data as exposure within case cross-over or time series models.

Finally, several studies defined heat vulnerability maps incorporating satellite data or observed meteorological data to represent the urban heat island[154,297–299], land use factors and socio economic factors, thus identifying areas most at risk within cities. Buscail et al. developed a land-use regression model to predict the LST and derive a hazard index in Rennes, France[300]. Vulnerability was assessed through census data (socio-economic status, extreme age, population density and building age) and a health risk index was derived combining land use (NDVI, vegetation and water land cover) and socioeconomic parameters. Taylor and colleagues incorporated indoor temperatures, using dynamic thermal models, and housing types as other potential factors affecting mortality risk during hot weather in London[301]. Results suggest that dwelling type caused the larger temperature anomalies across London, and had a greater influence on exposure risk, compared to the UHI. However, socio-economic factors were not taken into direct consideration in the temperature-mortality risk estimates.

Considering climate change and future projections, Heaviside and co-authors estimated the future impacts of heat waves in the West Midlands considering UKCP09 climate change simulation data also taking into account the UHI, projected population changes and a population weighted mean temperature. Findings suggest that by 2080, a heatwave could be responsible for an increase in mortality of around 3 times the rate observed in 2003 with 278 deaths compared to the 90 of 2003[302]. This aspect is very important not only for the promotion of mitigation measures to reduce GHG emissions within cities but also to raise awareness on the future heat risks and promote adaptation measures.

Overall, these studies are important for public health as they identify hot spots within cities most at risk during heat episodes to which heat prevention measures should be targeted.

Identifying the impact in terms of attributable deaths currently and under future climate change scenarios is of great importance.

The literature review helped identify main methodologies to derive air temperature from satellite data, in particular defining the source of satellite data used (satellite platform, sensors, temporal and spatial resolution) and covariate data availability required. Evidence of the urban heat island and differential effects within urban areas were specifically looked into to critically evaluate potential effect modifiers within the urban area of Rome. An overview of the evidence on the health effects of heat on mortality and morbidity and effect modifiers of the association was provided. The magnitude of the effect estimates from different geographical areas were also considered. Furthermore, the review looked at the statistical methods adopted in particular series data and case crossover studies, which will be the methodologies, used in my thesis. Finally, the literature review helped provide a broader outlook on the topic and critical perspective when discussing main findings.

CHAPTER 4 – ESTIMATION OF AIR TEMPERATURE EXPOSURE USING SATELLITE DATA.

4.1 INTRODUCTION

This chapter reports data collection, methods and results of the analysis carried out to define high spatial resolution daily air temperature over Italy for the period 2000-2010 using MODIS satellite data, meteorological and land use information.

Although meteorological stations provide accurate air temperature observations, their spatial coverage is limited and often insufficient for epidemiological studies. Satellite products have the advantage of providing better characterization across space, in terms of spatial resolution, compared to ground monitoring networks. In recent years, satellite data have become a valuable tool in epidemiology as an alternative source of temperature exposure data and specifically for the identification of at-risk areas to heat and high temperatures[128,154,303,304].

Different methodologies have been developed to estimate air temperature (Ta) using satellite derived LST[26–28,68,305]. Among these, statistical approaches based on regression models between LST and Ta and a series of independent variables (land use characteristics) have been defined[26,38,55,68,75,305]. Kloog and colleagues used mixed models allowing the regression coefficients to define the relation between LST and Ta to vary on a daily basis[27,29]. These models also included meteorological observed parameters, land use spatial covariates and spatial smoothing for the prediction of Ta when satellite data was not present[27,29]. The use of mixed models takes into account the relationship between air temperature and LST derived from satellite data and those factors that influence both the spatial and temporal differences

between the two. Temperatures derived with these methods have been used in epidemiological studies with very good results. Kloog et al. used satellite derived air temperature data to study the association between birth outcomes and temperatures in Massachusetts, USA[222], Lee et al. estimated the effect of heat and cold on mortality in three states of south-eastern USA[221], while Mehta et al. studied the association between temperatures (means and standard deviations) and QT intervals to look into the underlying mechanisms of temperature-related cardiovascular disease[306].

The aim of the study was to use MODIS land surface temperature (LST) satellite data, observed meteorological data and land use characteristics to estimate daily air temperature with a resolution of 1x1km in Italy for the period 2000-2010. The area in study is the Italian peninsula and islands of Sardinia and Sicily which overall cover an area of 301.338 km². Thanks to its unique geographical location in the Mediterranean and complex orography, comprised of the Alps in the north and Apennines stretching from north to south along the peninsula, Italy has a unique and complex climate within a relatively small spatial domain. Italy's climate ranges from Mediterranean along the coast and in central and southern regions, to a more humid subtropical climate in the inland northern areas up to the colder continental and tundra climates of the Alps.

Data derived from this methodology will be of great use not only providing exposure with a resolution of 1x1km and better spatial coverage of temperature gradients than traditional monitoring networks but will allow to make estimates of the health effects of temperature extremes in rural, suburban and urban areas with more complex and common methodologies.

4.2 METHODS - ESTIMATION OF HIGH RESOLUTION DAILY MEAN TEMPERATURE

4.2.1 Dataset

The following variables were collected for the period 2000-2010. The spatial unit is the 1x1km grid for which LST data is available. Extensive geoprocessing was carried out to attribute all spatial and spatio-temporal parameters to the fixed spatial gridded domain starting with the LST 1x1km grid for Italy.

Meteorological data

Air temperature (Ta)

Ground-level measurements of Ta were obtained from several sources. Airport standardized WMO data was retrieved for 140 monitoring stations from the National Air Force network (CNMCA – Centro Nazionale meteorologia e Climatologia Aeronautica Militare) and ENAV (Ente Nazionale Assistenti al Volo). Meteorological data for specific Italian regions was retrieved from the hydro-meteorological network of the Regional Agencies for Environmental Protection (ARPA) in Lombardia, Lazio, Emilia Romagna and Toscana (a total of 457 stations: 200 in Lombardia, 200 in Emilia Romagna, 33 in Lazio, 24 in Toscana). Additional data, mostly from 2006 onwards, from 33 personal stations included in the Weather underground network, were also included. The time period in study (2000-2010) was the overlap of all weather station data available in the time frame of the data collection phase during the first 12-18 months of my PhD. The homogenization of data collection from different sources and the definition of common parameters to define standardized dataset was a very time consuming procedure and it was the first time this was done for Italy. In future, it will allow regular updates and homogeneous data processing. The map in figure 4.1 shows the geographical distribution of the monitoring stations considered in the study. The distribution of monitors is

heterogeneous with more stations in the regions which provided data from the regional monitoring networks as well as airport stations. Better data coverage can be observed in the north of Italy compared to the south. Furthermore, there is a year-to-year difference in data availability with better coverage in the most recent years. It is by no means complete in terms of data availability, but it comprises those either available online or made available throughout the study period. Again, future updates will potentially allow the inclusion of other regional datasets if made available (online or through direct contacts).

Figure 4.1. Map of weather stations included in the study.

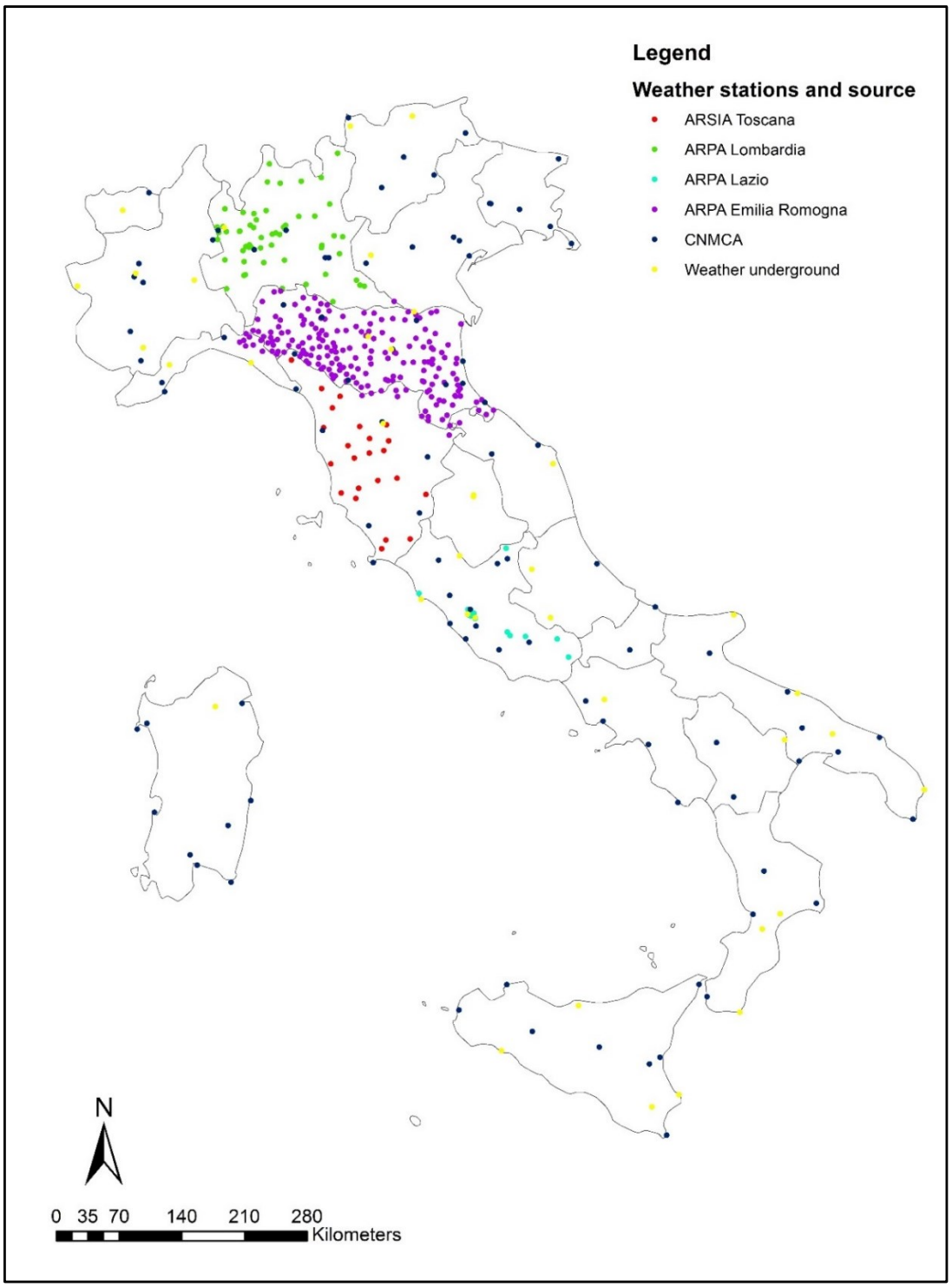

Land surface temperature (LST) and emissivity satellite data

Daily LST data was retrieved for Italy for the period 2000-2010 at a spatial resolution of 1x1 km from the Moderate Resolution Imaging Spectroradiometer (MODIS) sensors on board the TERRA satellite. TERRA LST and Emissivity (MOD11_L1) products[41,52] were used. The MODIS LST was derived from two thermal infrared band channels, 31 (10.78–11.28μm) and 32 (11.77–12.27μm) using the split-window algorithm (Wan, 2008) which corrects for atmospheric effects and emissivity using a look-up table based on global land surface emissivity in the Thermal Infra-Red (MODIS channels 31–32 or 10,000–12,500 nm) region[35,47].

Emissivity also influences LST measurements by causing a reduction of surface-emitted radiance. In addition, the anisotropy of reflectivity and emissivity may reduce or increase the total radiance from the surface[307]. Emissivity is a function of wavelength, and is not only controlled by water content, chemical composition, structure, and roughness[47], but it can also vary significantly with plant species, areal density, and growth[47]. Surface emissivity values are available in MOD11_L2 product in MODIS bands 31 and 32 and they are assigned based on land cover types[52]. The MODIS derived radiometric surface temperature corrected for atmospheric transmission has been further corrected with spectral emissivity to account for the kinetic temperature of the object based on the following equation, as suggested by Kloog et al[27]:

$$Tkin = Trad/Emissivity(\lambda)^{1/4}$$

where Tkin is related to the true kinetic surface temperature (and considered LST variable) and Trad is the radiant temperature of an object recorded by the sensor.

Four tiles of the MOD11_A1 product were downloaded from the NASA Level 1 Atmosphere Archive & Distribution System (LAADS) (https://ladsweb.modaps.eosdis.nasa.gov/search/) and clipped to retain the area of Italy, thus comprising a domain of 356,432 1x1km grid cells. For each year, daily LST data files were produced. It was decided to use night time LST as the reference satellite temperature predictor as it is more stable[45] and because solar radiation does not influence the thermal infra-red signal and the dataset was more complete. Furthermore, preliminary results and previous studies showed that differences in model performance using both night time and daytime LST were minimal [29].

Land use\Land cover data

A series of spatial indicators, retrieved from different sources, were collected to account for the different land use and land cover features which might affect the thermal properties of the land surface and air temperatures. This could contribute to improve the performance of the prediction model relating Ta to LST at the national level. The indicators are briefly described below.

Normalized difference vegetation index (NDVI): the MODIS NDVI product (MOD13A3) for every month and year in the study period was collected with a spatial resolution of 1x1 km. Data was downloaded from the NASA LP DAAC website (https://lpdaac.usgs.gov/). Monthly values were selected as NDVI values are relatively constant within a month. NDVI enables to identify vegetated areas and provides a dynamic quantification of the conditions or wellbeing of the vegetation as well as an indication of vegetation growth rate. The pigment in plant leaves, chlorophyll, strongly absorbs visible light (from 0.4 to 0.7 µm) for use in photosynthesis. The cell structure of the leaves, on the other hand, strongly reflects near-infrared light (from 0.7 to 1.1 µm). The more the foliage, the more IR and red light wavelengths are affected, respectively. NDVI is calculated considering two wavelengths: Near infra-red (NIR) due to high reflectance

of leaf structure at NIR, and red wavelengths due to the high sensitivity of leaf pigments to red light (Figure 4.2). NDVI varies between -1 and +1; densely vegetated areas will have values comprised between +0.3 and +0.8 , bare ground with values closer to zero (0.1-0.2). NDVI is important here as although it does not identify type of vegetation it accounts for the radiative properties of the vegetative cover observed by the satellite and this influences LST. The model includes both NDVI and land cover types giving a more holistic association of the LST and Ta based on land cover and radiative properties.

Elevation: data on elevation was retrieved from the European digital elevation model (EuroDEM), a pan-European height dataset in a scale of approximately 1:100 000 (Figure 4.3).

Corine Land cover data. Static land cover and land use features were retrieved from Corine land cover (CLC) database [308] and attributed to the Italian domain. CLC is a map of the European environmental landscape based on interpretation of satellite images. It provides comparable digital maps of land cover for each country for large parts of Europe, with spatial resolution of 250 × 250m. Features were selected to represent both the built environment (% low and high development) and vegetation cover (percent of crop, shrub, deciduous, evergreen, arable). For each cell the percentage of the area covered by each CLC type was considered in the study (Figure 4.4). Land use covariates in terms of vegetative land cover have never been included in these models before and data provides a valuable opportunity to test the relationship between temperatures and land cover features.

Impervious surface data was retrieved from NOAA-NGDC global inventory of the spatial distribution and density of constructed impervious surface area (ISA)[309]. Brightness of satellite observed night-time lights and population count data are included in the indicator. The reference data used in the calibration were derived from 30-meter resolution ISA estimates of

the USA from the U.S. Geological Survey. For each 1x1km grid cell the average percent of impervious surface was derived (Figure 4.5).

Population density: the number of inhabitants for each 1x1km grid cell of the Italy domain were based on the Italian census 2001 data and considered as measure of population density. Census blocks were superimposed on the 1 × 1-km Italy grid and the resident population was distributed to each cell based on cell-block intersections, under the assumption of homogeneous distribution of the population within census blocks (Figure 4.6).

Climatic zones: two classification schemes were used: 1) the Köppen climate zones[310], and 2) a local bio-climatic classification for Italy developed by ISPRA- *Istituto Superiore per la Protezione e la Ricerca Ambientale*. These classifications were attributed to each 1km grid (Figure 4.7a-b). The Köppen climatic zones classification is widely used and is based on seasonal precipitation and temperature patterns. Italy is characterized mainly by a temperate Mediterranean climate especially along the coasts and southern regions. Summers are hot and dry, due to the domination of the subtropical high pressure systems and variable rainy weather in winter due to the passing of frontal systems. Northern and Apennine regions have a more humid continental climate with less seasonal differences in precipitation and cooler winters and alpine climates at high altitudes in the Alps.

Proximity to features: the Country layers (Regions / Provinces / Municipalities, lakes, sea etc) were identified in terms of geometry and basic attributes.

A flag variable for grid cells on the coast and all major lakes was created. These cells were excluded from the analyses because satellite retrievals on water bodies are considered to be unreliable.

Dataset creation was carried out in ArcGIS 10 (ESRI. ArcGIS Desktop: Release 10. Redlands, CA: Environmental Systems Research Institute) and SAS (version 9.2). For each of the predictor variable, ArcGIS was used to attribute the features to our base grid of 1x1km MODIS LST grid.

Figure 4.2 Example map of NDVI, may 2010 Italy.

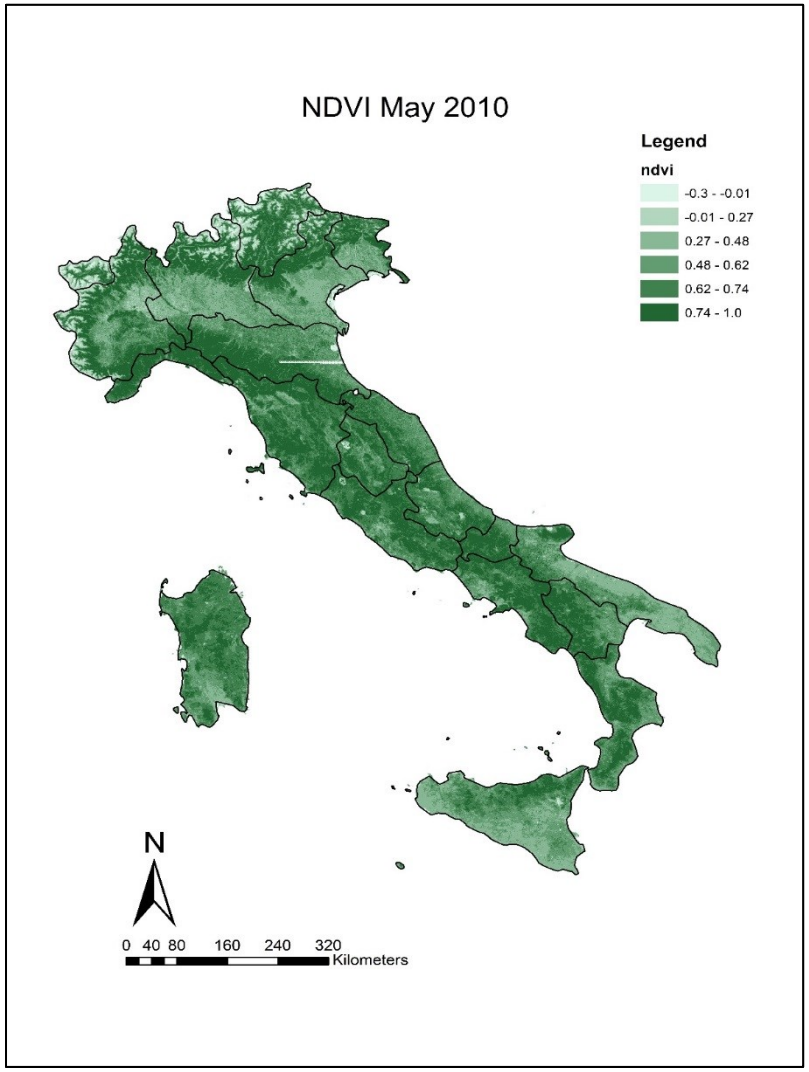

Figure 4.3 Map of elevation in meters, in Italy.

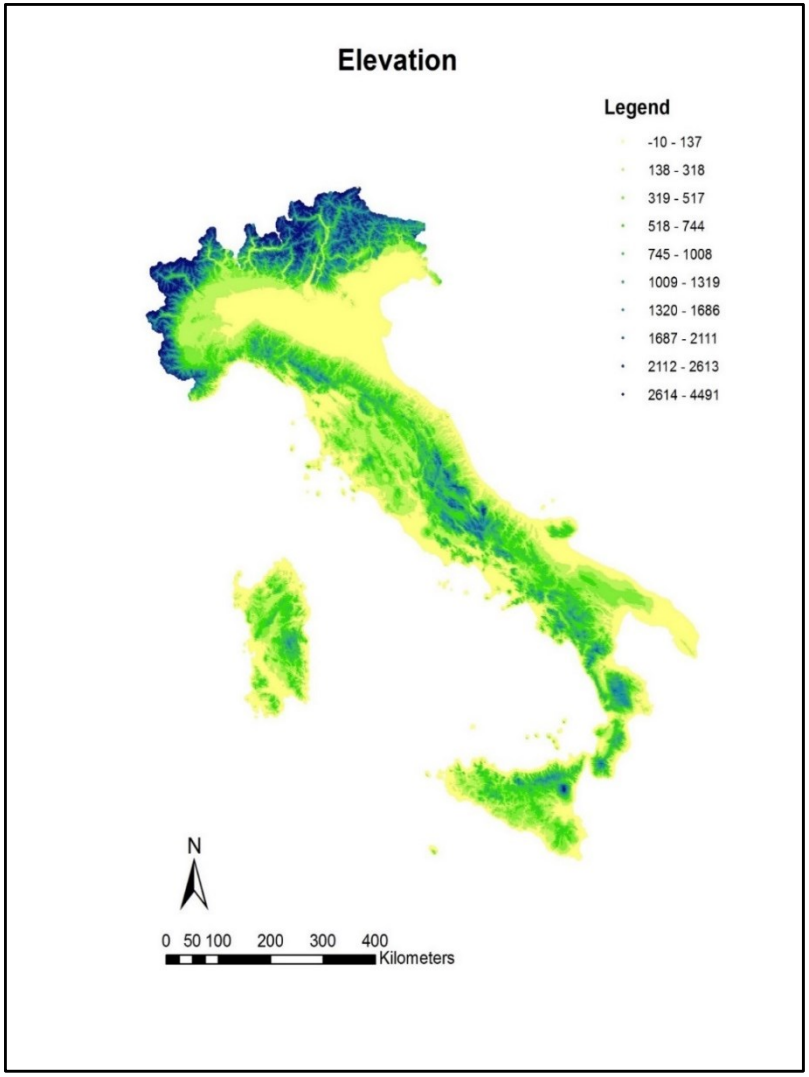

Figure 4.4. Corine land cover – vegetation in Italy.

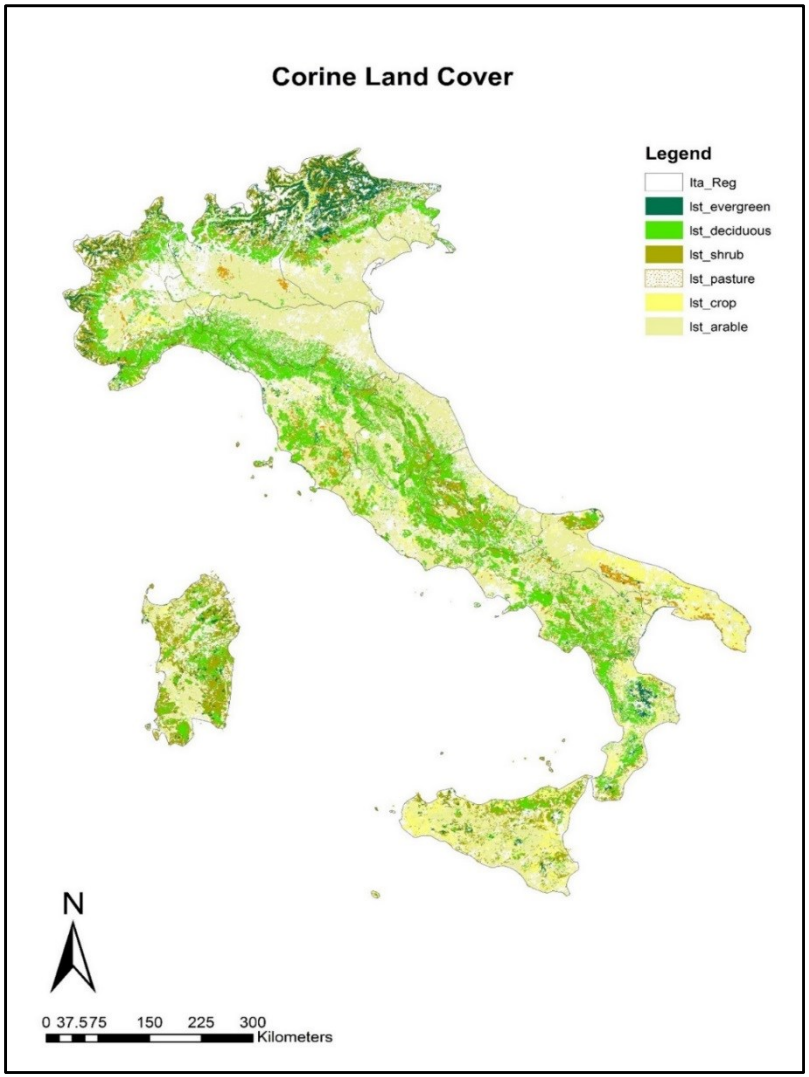

Figure 4.5. Map of impervious surfaces in Italy.

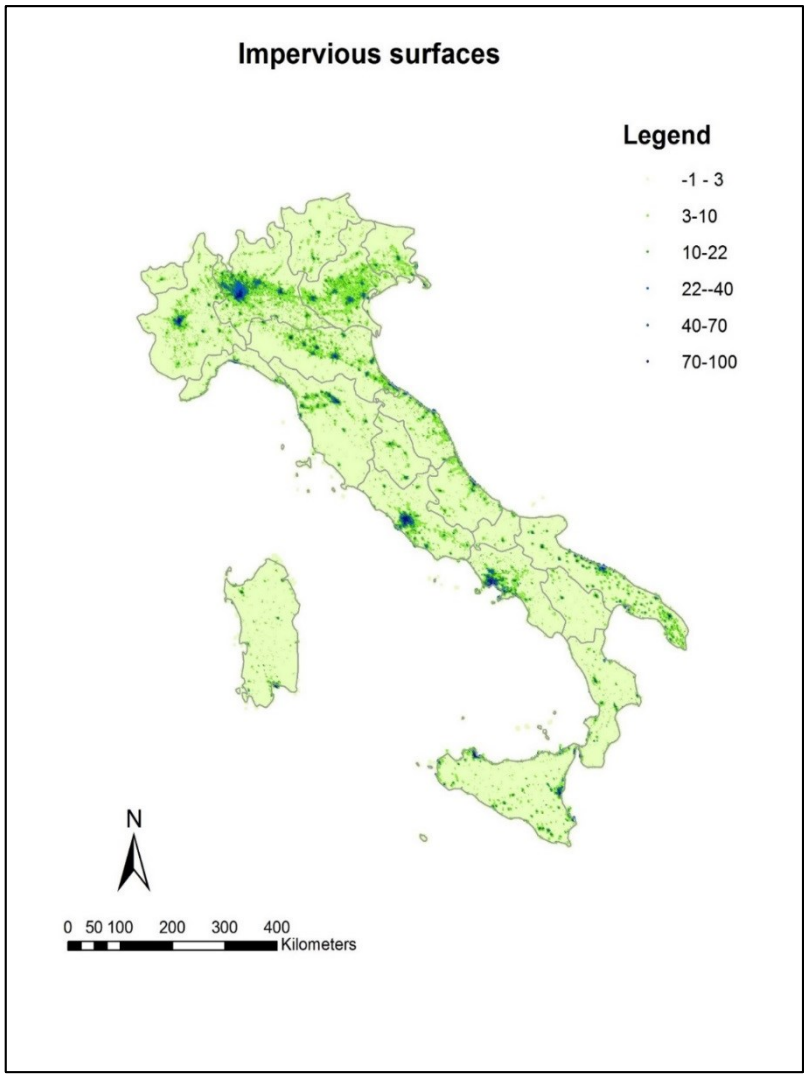

Figure 4.6. Map of population density in Italy.

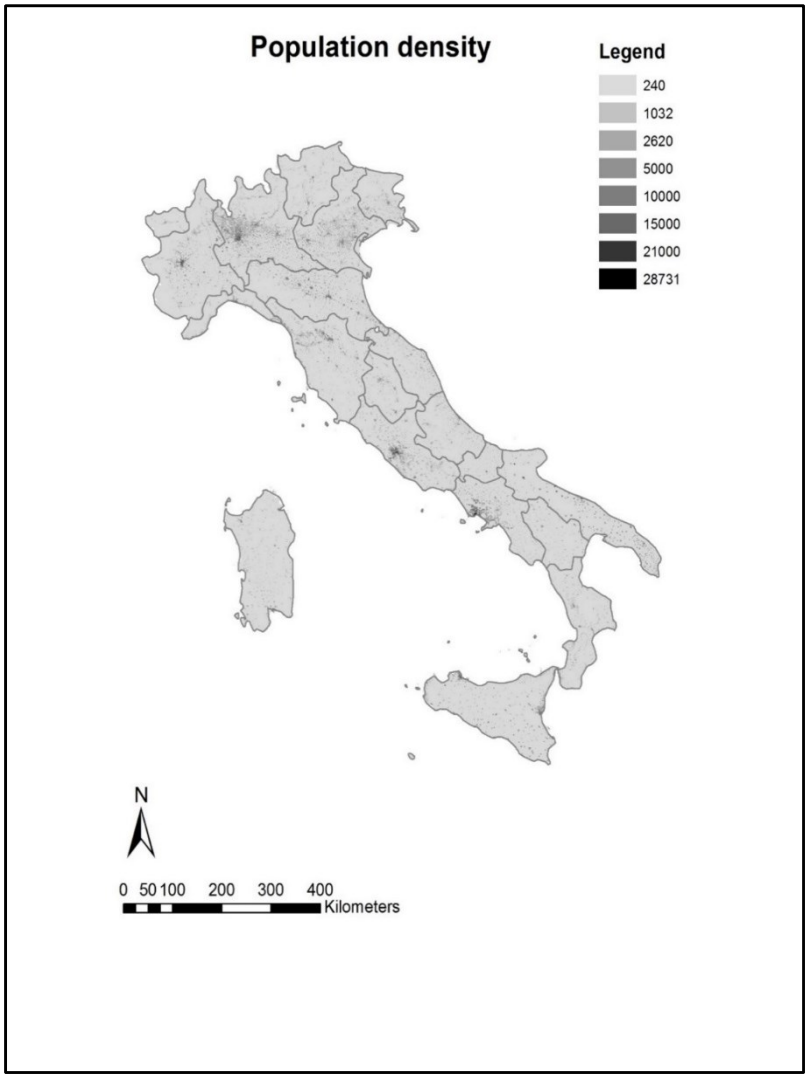

Figure 4.7a. Map of climatic zones for Italy.

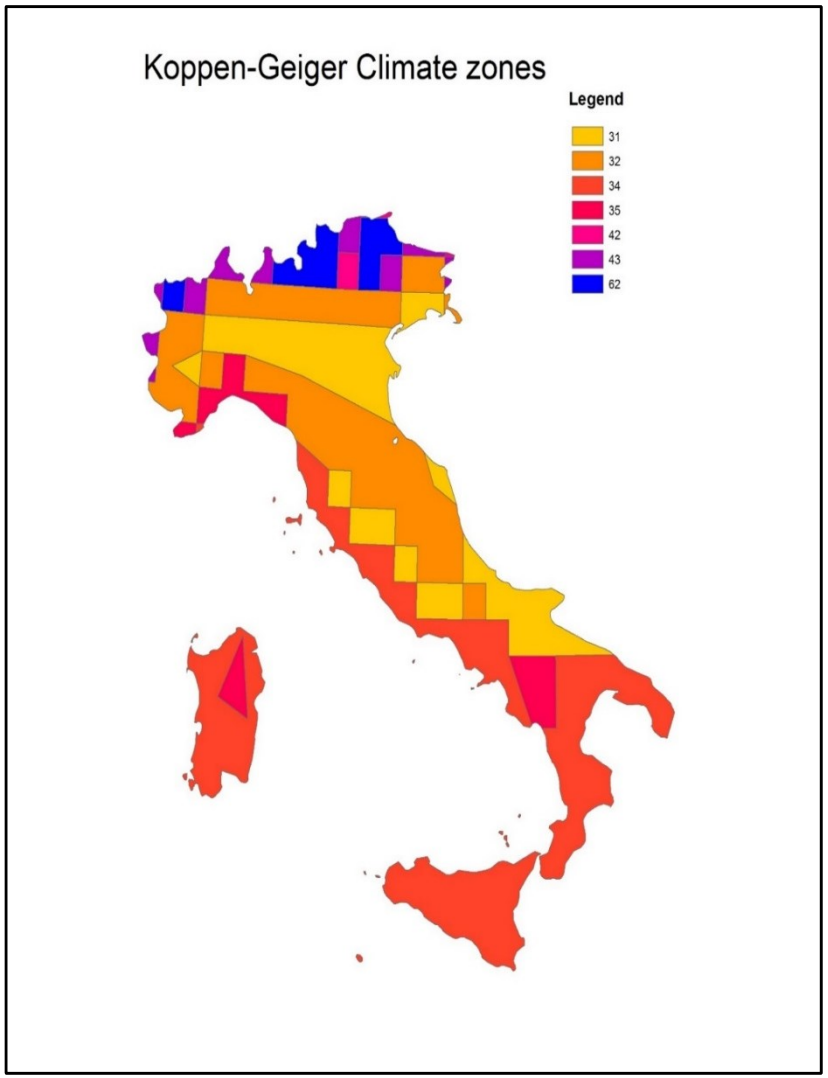

Figure 4.7b. Map of bioclimatic classification of Italy.

4.2.3 Statistical modelling

The mixed model 3-step approach developed by Kloog et al.[27,29] was applied to each year in the study period to estimate mean daily temperatures across the study domain.

In the first stage, only cells and days with data available for both Ta and LST were considered. Calibration between Ta measurements and satellite LST data was defined by fitting a mixed-effects regression model with Ta as the dependent variable and LST, spatial and temporal parameters as predictors. Furthermore, for each day, random intercepts and slopes for LST were estimated to capture the day-to-day temporal variability of the Ta–LST relationship. The model was nested by bio-climatic zones to account for the potential heterogeneities in the Ta-LST calibration across geographical areas.

The stage 1 model is the following:

$$\{Ta_{ij} = (\alpha+\mu_j) + (\beta_1+v_j)ntkin_{ij} + \beta DNVI_{ij} + \beta ISA_i + \beta Elev_i + \beta ever_i + \beta dec_i + \beta crop_i + \beta past_i + \beta shrub_i + \beta arab_i + \beta pop + \beta percurban + \mathcal{E}_{ij}(\mu_j, v_j)\}_k$$

$(\mu_j, v_j) \sim [(0,0), \Sigma]$

Where:

- Ta_{ij} is the air temperature at site i on day j
- $\alpha+\mu_j$ are the fixed and random intercepts, respectively
- $Ntkin_{ij}$ is the LST nighttime value in the grid cell corresponding to site i on a day j;
- β_1 and v_j are the fixed and day-specific random slopes, respectively
- $NDVI_{ij}$ is the monthly NDVI value in the grid cell corresponding to site i for the month in which day j falls
- ISA_i is the mean impervious surface in the grid cell corresponding to site i
- $Elev_i$ is the mean elevation in the grid cell corresponding to site i
- ever is the percent of evergreen vegetation land cover in the grid cell corresponding to site i
- dec is the percent of deciduous vegetation land cover in the grid cell corresponding to site i
- crop is the percent of land cover for crops in the grid cell corresponding to site i
- past is the percent of land cover for pasture in the grid cell corresponding to site i
- arab is the percent of arable land cover in the grid cell corresponding to site i
- shrub is the percent of shrub land cover in the grid cell corresponding to site i
- pop is the population density
- percurban is the urban fabric development
- Σ is an unstructured variance–covariance matrix for the random effects
- ε_{ij} is the error term at site i on a day j
- k is the k-th climatic zone

To validate the stage 1 model, a ten-fold out of sample cross validation (CV) was performed. Specifically, the dataset was randomly divided into 90% and 10% splits. The model was then fitted on the 90% split (training), and predictions were obtained for the remaining 10% split (testing). The procedure was iterated 10 times. The 10 testing datasets were finally pooled together and the CV-R^2 was obtained by regressing observed versus predicted Ta values. Finally, the model prediction precision was estimated by taking the root of the mean squared prediction errors (RMSPE).

In order to account for the possible geographical differences in the Ta-LST relationship due to differences in monitor characteristics and spatial coverage, the ten-fold out of sample cross validation (CV) procedure was also performed by random sampling the monitors (instead of the individual records) into 90% and 10% splits.

For each model, prediction errors were also estimated separately for the temporal and spatial components. The temporal R^2 was calculated by regressing the difference between observed Ta at site *i* and at time *j* and the annual mean Ta at the location against the predicted difference in daily site T*a* and annual predicted T*a* at the location. Spatial R^2 was calculated by regressing the annual overall mean T*a* against the mean predicted Ta at site *i* for each monitoring location.

Once the stage 1 model was defined, it was used to predict Ta in grid cells without monitors but with available LST measurements, this was denoted as the stage 2 model. Since LST values are often missing due to cloud cover or retrieval errors, the stage 2 model fails to provide predictions for many grid cell-day combinations. The final stage (Stage 3) filled in the remaining missing values and produced a full map of Ta predictions, for each day and across the spatio-temporal domain. The final stage (*Stage 3*) fills in the remaining missing values and produces a full map of Ta predictions, for each day and 1x1km grid of the spatio-temporal domain. Specifically, the third model takes advantage of the association between grid cells LST

values with Ta measurements located elsewhere, and the association with available LST values in neighboring grid cells was carried out (stage 3). Specifically, for each grid cell, Ta predictions obtained from stage 2 were regressed on the daily mean measured Ta (from the stations within different sized buffers of that grid cell), land use terms and a smooth nonparametric function of latitude and longitude of the grid cell centroid, with random cell-specific intercepts and slopes. Buffers of (5, 10, 30, 50, 100km) were calculated and the procedure was re-iterated for each distance buffer. This is similar to universal kriging, by using Ta measurements from nearby grid cells to help fill in the missing. However, it provides additional information about the Ta in the missing grid cells that simple kriging would not. Considering the spatial patterns of Ta vary temporally, a separate spatial surface was fit for each two- month period. In contrast to stage 2, the stage 3 model includes cell-specific random intercepts and slopes, which allows for temporal and spatial interpolation for each grid cell. That is, we could use the random effects for a grid cell to help impute Ta data of this cell for days when Ts measurements were unavailable. At the end of the process, daily Ta predictions will be available for all squared kilometers which provided data from stage 1, 2, and 3 in Italy and for each day and year included in the period 2000-2010.

Descriptive statistics and the performance of the model (R^2, RMSPE, spatial and temporal statistics) for each year and each stage are reported in the following section. Geographical and temporal differences were also explored.

Dataset creation was carried out in ArcGIS 10 (ESRI. ArcGIS Desktop: Release 10. Redlands, CA: Environmental Systems Research Institute) and SAS (version 9.2). Statistical modelling was performed in R (version 3.1.2) (R Development Core Team; http://R-project. org).

4.2.4 Model validation

To further validate results, weather forecast mean temperature data from the RAMS - Regional Atmospheric Modelling System model [311], with a spatial resolution of 4x4km, for central Italy for 2005 only were considered. One day RAMS air temperature forecast is shown as example in figure 4.8. This model is typically used by regional environment agencies for both numerical weather prediction and air pollutant dispersion modelling. Average daily RAMS Ta data was compared to Ta predicted from the 3 stage model. Each 1x1km grid was matched to the nearest 4x4km RAMS grid cell, all the cells falling within the RAMS grid cell were averaged and temperature values were compared with the RAMS forecast temperature.

Figure 4.8. Map of RAMS mean Temperature forecast spatial coverage, example of one day air temperature forecast, 5/7/2005

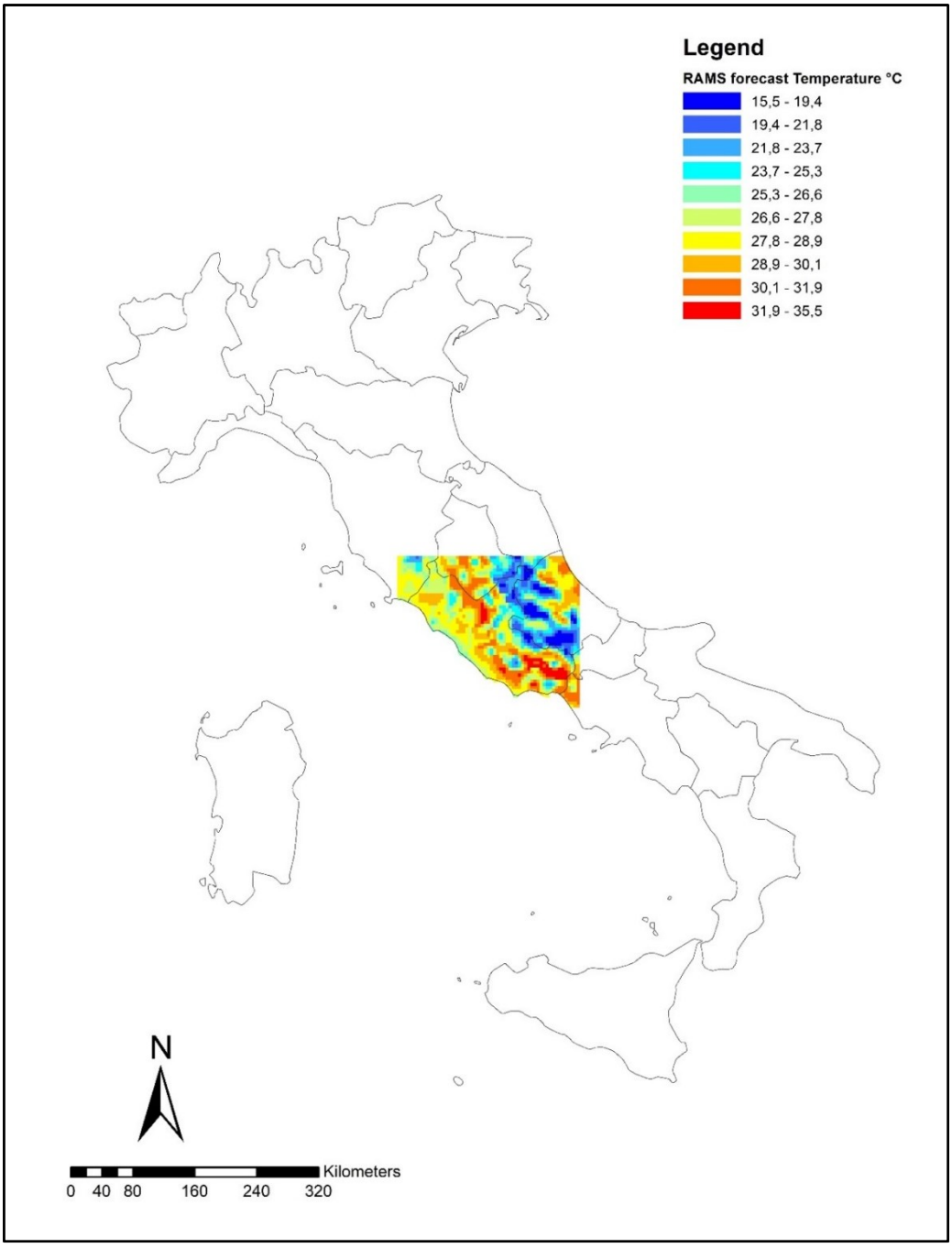

4.3 RESULTS

For each year and each stage of the analyses, datasets comprised of satellite data, observed temperature data from weather stations and land use/land cover spatial predictors. Stage 1 files include only grid cells with temperature monitors and days with available Ta and LST retrievals. Approximately, each year the file consisted of 60,000 records. Stage 2 and 3 files encompass the entire Italian domain, for a total of 356,432 grid cells. Stage 2 only included days with available LST data, for a total of around 60,000,000 records. In contrast, Stage 3 was the full spatio-temporal dataset, consisting of 356,342 x 365 (~130,000,000) records.

Considering the entire spatial domain for Italy (356,342 grid 1x1km squares) each year around 50% of the LST data was missing due to retrieval error or cloud cover (Table 4 Appendix). This varied by season and by year. Winter months had the highest number of missing values (around 60%) mainly due to cloud cover, while summer had the lowest number of missing values with around 34% (Table 4.7). No specific geographical pattern of missing data were observed.

Firstly, Pearson correlations between air temperature and the land surface data were calculated for the entire series annually and by season (Table 4.1). The correlation between air temperature and land surface temperature was very high, with values above 0.9 for the entire year. Slightly stronger correlations were observed between night-time LST and mean Ta (0.948) compared to daytime values (0.917). Correlations by season showed slightly lower values, with night time LST and air temperature correlations remaining more stable by season (winter=0.83, summer=0.81).

Table 4.1. Correlation coefficients between air temperature (Ta), Land surface temperature (LST) and Kinetic surface temperature (Tkinetic) period 2000-2010.

		Air Temperature (Ta)		
		Annual	Summer	Winter
DAY	LST	0.9172	0.7207	0.8068
	Tkinetic	0.9170	0.7206	0.8067
NIGHT	LST	0.9487	0.8207	0.8332
	Tkinetic	0.9487	0.8203	0.8332

A scatter plot of the daily recorded air temperature and night-time Kinetic temperature (LST night) for 2010 is shown in figure 4.9, in which a very good correlation between pairs is observed, especially in the higher range of temperatures.

Correlations between air temperature and spatial predictors\covariates are shown in table 4.2. Elevation and vegetated land surfaces (deciduous forest, pasture, shrub, arable and crop) were all inversely correlated with temperature, thus meaning that with altitude and in presence of more vegetated surfaces temperatures are lower. This is consistent by season as well. The only vegetation land cover covariate that gives an inverse correlation with temperature is evergreen trees, this could be associated with elevation in Alpine areas (higher temperatures below tree line compared to mountain peaks or bare ground) specifically. Studies on forest coverage and LST have observed similar patterns of warming in presence of forests with tall trees for latitudes similar to ours or cooler areas with climates comparable to the Alpine regions of Italy[312,313]. In contrast, temperatures increased in highly populated areas, over impervious surfaces and with high urban development. These spatial predictors should aid in capturing both the urban and rural thermal characteristics, as well as the differences in the Ta-LST relationship over different surfaces and land use surfaces. NDVI had a seasonal pattern with a positive association with Ta in winter and a negative association in summer. This is consistent with previous studies where the relationship between NDVI and temperature was shown to be

not linear, varied seasonally and was dependant on the type of vegetative cover, ecosystem type and soil moisture [26,27,45]. NDVI measures the health of vegetation and this has per se a seasonal pattern, in the growing season values will be higher while in winter NDVI values will be lower.

Table 4.2. Correlation between air temperature and spatial predictors, 2010.

	Air Temperature (Ta)		
	Annual	**Summer**	**Winter**
Elevation	-0.3607	-0.6701	-0.5718
Impervious surface	0.1288	0.2460	0.2499
Population density	0.1050	0.1972	0.2006
% high development	0.0566	0.1818	0.067
%low development	0.0596	0.1242	0.0514
NDVI	0.1276	-0.4401	0.1745
% deciduous	-0.1271	-0.2915	-0.2111
% evergreen	0.1173	0.1731	0.2684
% pasture	-0.3599	-0.392	-0.6484
% shrub	-0.1017	-0.1314	-0.1517
% crop	-0.0078	-0.0659	0.0494
A2 and A3 roads	0.0610	0.1246	0.1617
minor roads	0.0979	0.195	0.1872

The final stage 1 model was nested by climatic zones and included LST, NDVI, elevation, impervious surfaces and population density, different land cover vegetation types (crop, arable, shrub, deciduous, evergreen coniferous forests) as predictors. These groupings (urban development features (pop. density, impervious surfaces, high/low development), vegetation cover), were all selected a priori and model fit criteria evaluated including\excluding groupings and not single variables. This was done under the assumption that vegetation land cover across space could influence thermal properties and daily patterns hence could all give a specific contribution. The model also contained random intercepts by day and random slopes for LST each day. NDVI and elevation were included as natural spline variables with 3 degrees of freedom.

Figure 4.9b shows the scatterplot of the observed and predicted air temperature data from the final stage 1 model for 2010. As expected, the association between air temperature and the main explanatory variable (surface temperature) was highly significant. Predicted Ta from the calibration model was more similar to observed Ta compared to the original LST data (Figure 4.9a). Calibration model performances are summarized in table 3 with out-of-sample fits confirming the very good performance, with an average R^2 of 0.962 and 0.959 respectively in the 10-split Cross validation (CV) and 10-split by monitor CV. The spatial and temporal cross-validated results also showed an excellent performance, with average spatial R^2 of 0.88 and temporal R^2 of 0.97 (Table 4.3). Prediction errors were very small, with a RMSPE of 1.6°C for both CV methods (by individual records and by monitors), while the spatial RMSPE was between 1-1.2°C for both CV approaches. Prediction errors were smaller than those found in previous studies [29,45,75].

Figure 4.9a-b. Scatter plot of (a) mean air temperature and night time kinetic surface temperature and (b) observed and predicted air temperature data for all grid cells where monitors are located, Stage 1 model, 2010

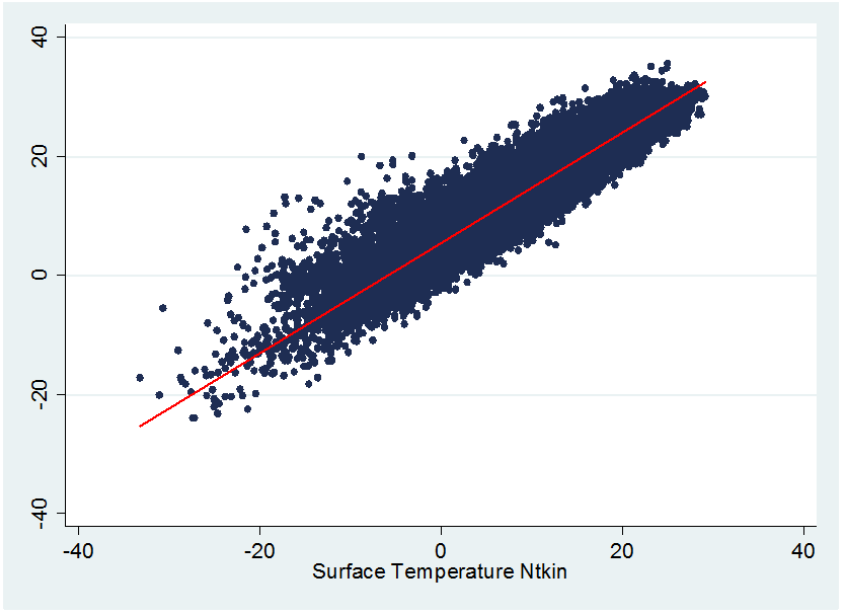

a)

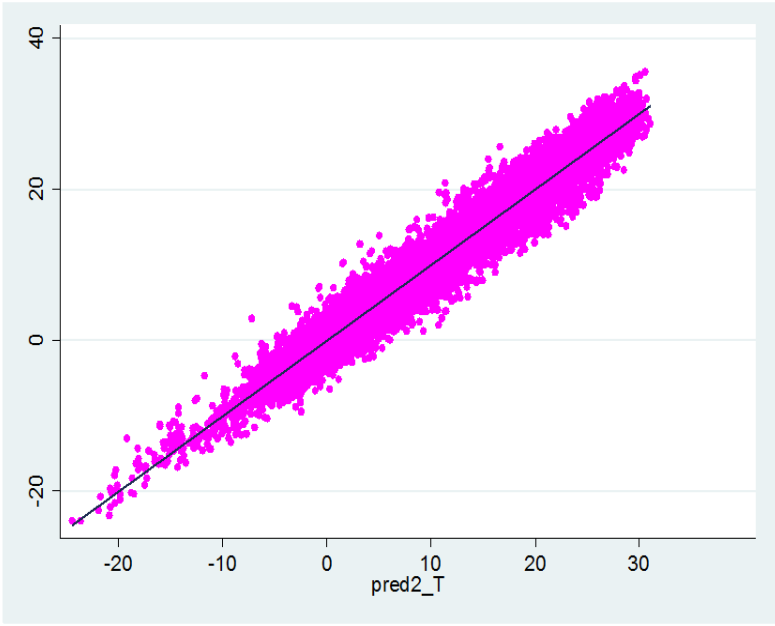

b)

Table 4.3 Stage 1 prediction accuracy. Ten fold cross-validated (CV) results with random and by-monitor cross validation.

	CV random splits					CV monitor splits				
YEAR	R^2	RMSPE	spatial R^2	spatial RMSPE	temporal R^2	R^2	RMSPE	spatial R^2	spatial RMSPE	temporal R^2
2000	0.949	1.544	0.934	1.035	0.964	0.942	1.660	0.913	1.275	0.963
2001	0.963	1.552	0.897	1.029	0.976	0.961	1.611	0.846	1.125	0.976
2002	0.956	1.622	0.903	1.105	0.971	0.956	1.641	0.885	1.263	0.971
2003	0.969	1.634	0.876	1.218	0.981	0.962	1.788	0.873	1.256	0.979
2004	0.958	1.676	0.901	1.048	0.969	0.951	1.802	0.849	1.156	0.967
2005	0.970	1.518	0.898	1.109	0.981	0.965	1.631	0.869	1.283	0.981
2006	0.966	1.563	0.898	0.990	0.977	0.966	1.569	0.886	1.035	0.978
2007	0.958	1.565	0.882	1.010	0.971	0.958	1.603	0.873	1.002	0.970
2008	0.964	1.507	0.896	0.963	0.975	0.964	1.522	0.867	1.066	0.978
2009	0.954	1.851	0.842	1.597	0.964	0.954	1.852	0.800	1.893	0.967
2010	0.972	1.416	0.908	0.945	0.981	0.972	1.388	0.910	0.947	0.981
AVERAGE	**0.962**	**1.586**	**0.894**	**1.095**	**0.974**	**0.959**	**1.642**	**0.870**	**1.209**	**0.974**

Table 4.4. Stage 3 model predictive accuracy and mean annual temperatures. Comparison between observed and predicted air temperature expressed as R^2 coefficient, RMSPE, spatial and temporal components.

			Spatial		Temporal		Temperature	
Year	R^2	RMSE	R^2	RMSE	R^2	RMSE	Mean	SD
2000	0.978	1.012	0.952	1.030	0.996	0.410	14.7*	7.2*
2001	0.984	1.031	0.905	0.970	0.997	0.415	12.8	8.3
2002	0.980	1.106	0.918	1.017	0.995	0.490	12.8	8.3
2003	0.984	1.155	0.862	1.296	0.997	0.508	13.2	9.1
2004	0.980	1.167	0.908	0.996	0.993	0.646	12.4	8.0
2005	0.985	1.065	0.917	0.985	0.996	0.511	11.9	8.5
2006	0.984	1.073	0.904	0.946	0.996	0.499	12.6	8.2
2007	0.981	1.056	0.898	0.932	0.995	0.525	13.0	7.7
2008	0.984	1.012	0.907	0.906	0.996	0.479	12.7	8.0
2009	0.978	1.292	0.910	1.194	0.988	0.882	13.0	8.4
2010	0.988	0.908	0.926	0.843	0.998	0.373	12.1	8.4
Average	**0.982**	**1.080**	**0.910**	**1.010**	**0.995**	**0.522**	**12.6**	**8.3**

The stage 1 model was then used to predict air temperature in all the grid cells where satellite data was available for each year. Stage 2 model datasets are by no means complete, but a good indication of the spatial distribution of temperatures across Italy was achieved. The stage 3 model filled the missing values to have a complete dataset. Overall the final model performance (non-cross validated) was very good, with an average R^2 of 0.982 and an average RMSPE of around 1°C, with equally good spatial and temporal model performances (table 4.4). Annual average mean temperatures were comprised between 11.9 and 13.2°C with a standard deviation (SD) of 7.7-9.1°C in the years 2001-2010. The first year in study (2000) had slightly higher values as it only comprises only data from April to December.

Maps of the average annual temperature over Italy (2000-2010) are shown in Figures 4.11-4.21 at the end of the section. Temperature varied considerably over the Italian peninsula, even across small spatial scales due to its unique location in the Mediterranean Sea and its complex orography, which influences both daily weather patterns and local climate. Considering the different climatic zones (Figure 4.8a-b), the model performance was also very good and small differences can be observed with greater model performance variation in the spatial domain compared to the temporal component (table 4.5-4.6). Average mean temperature distributions for each climatic zone were coherent with climatic characteristics; with cooler temperatures in Alpine and Apennine regions and hotter temperatures in Mediterranean climate regions (data not shown), however to evaluate climate in a coherent manner other meteorological parameters, in particular rainfall are necessary.

Major cities and urban areas can be detected, especially in the Po valley (Turin, Milan, Bologna, Florence), Rome and Naples (Figures 4.11-4.21). Considering urban-rural differences, the model had a slightly better predictive capacity in urban areas, with lower RMSPE compared to suburban and rural areas (R^2 urban = 0.971, RMSPE=1.336°C vs R^2

rural=0.961, RMSPE=1.643°C). Noteworthy that the spatial component of the model also had a better fit in urban areas (R^2 urban=0.696, RMSPE=0.839°C vs R^2 rural=0.883, RMSPE=1.064°C), reflecting the more homogeneous terrain in terms of thermal characteristics compared to rural or suburban areas. The temporal component was similar in urban and rural areas.

Temporal variation by year can also be observed in terms of model performance possibly reflecting annual climatic conditions. Model fit by season also showed slight variations with higher R^2 and smaller RMSPE in autumn (September-November) and spring (March-May), for both spatial and temporal components (Table 4.7). Figure 4.10 shows as example year of summer (June-August) and winter (December-February) mean temperatures across Italy.

Figure 4.10. Final model predicted air temperature. Summer (June-August) 2003 and winter (December-February) 2010 in Italy.

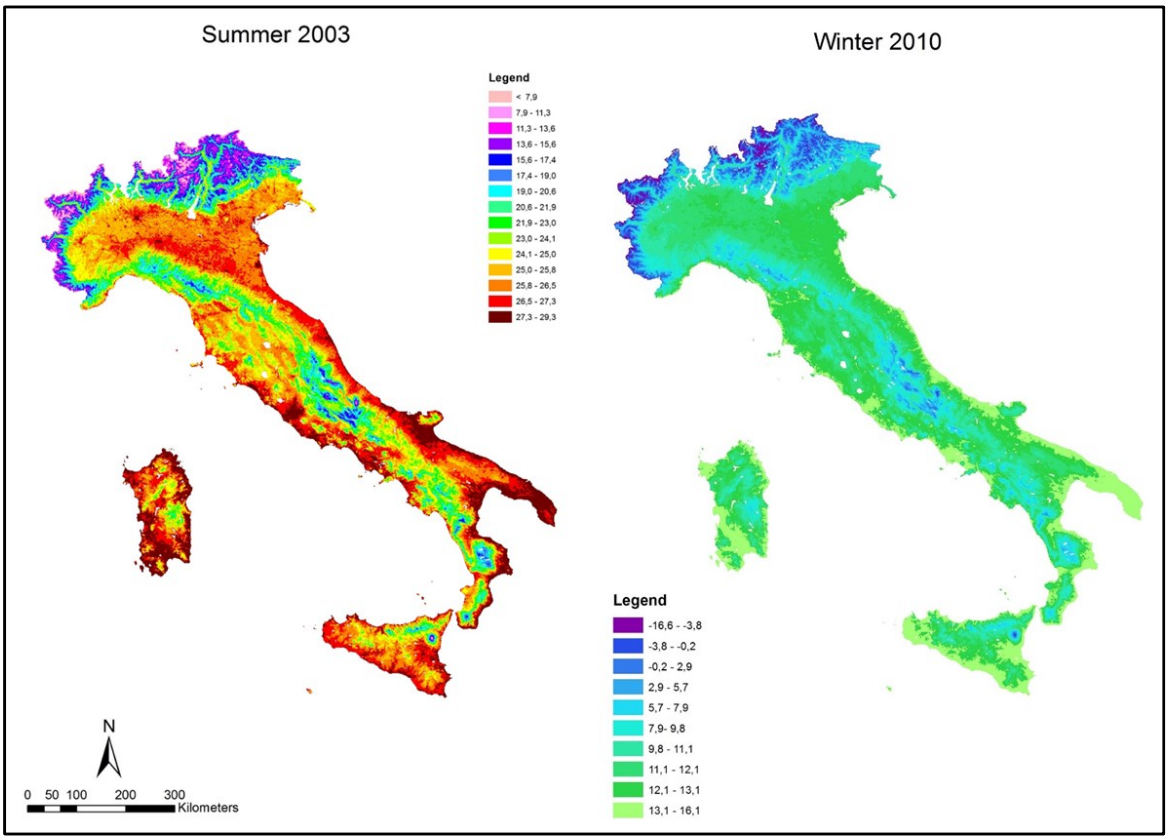

Table 4.5. Stage 3 model fit by bio-climatic zone in Italy 2001-2010.

Climate zones	R^2	Slope	Intercept	RMSPE	Spatial R2	Spatial RMSPE	Temporal R2	Temporal RMSPE
Alpine Ridge	0.917	0.982	0.079	2.934	0.900	1.715	0.927	2.262
Po Valley	0.962	1.001	0.088	1.675	0.698	0.722	0.970	1.489
High Adriaticum	0.977	1.001	-0.003	1.225	0.556	0.620	0.983	1.054
Appennine	0.964	0.997	0.024	1.504	0.818	0.968	0.977	1.174
N. Tyrrenian	0.966	1.010	-0.231	1.395	0.868	1.059	0.975	1.132
S . Tyrrenian	0.905	0.988	0.200	2.224	0.663	1.622	0.970	1.218
Low Adriaticum	0.920	0.999	0.285	2.088	0.647	1.392	0.957	1.477
S. Italy and Sicily	0.926	0.980	0.752	1.800	0.787	0.935	0.936	1.606
Sardinia	0.945	0.993	0.434	1.623	0.887	0.957	0.953	1.415

Table 4.6. Stage 3 model fit by Köppen climatic zones in Italy 2001-2010.

	R^2	Slope	Intercept	RMSPE	spatial R2	spatial RMSPE	temporal R2	temporal RMSPE
Cfa - Humid subtropical climate	0.957	1.005	-0.113	1.754	0.609	0.963	0.968	1.467
Cfb - Temperate oceanic climate	0.968	0.997	0.093	1.466	0.831	0.913	0.979	1.144
Csa - Mediterranean climate hot summer	0.935	0.989	0.418	1.809	0.735	1.173	0.962	1.340
Csb - Mediterranean climate warm summer	0.944	1.004	-0.087	1.850	0.818	1.319	0.961	1.431
Dfb - Humid continental climate warm summer	0.944	1.005	-1.390	2.358	1.000	0.073	0.931	2.235
Dfc - Subartic climate	0.929	0.938	0.287	2.811	0.990	0.714	0.882	2.685
ET - Tundra climate – Alpine	0.936	0.964	-0.467	2.307	0.895	1.036	0.937	2.094

Table 4.7. Stage 3 model predictive accuracy by season, 2001-2010.

Season	R^2	RMSPE	Spatial R2	Spatial RMSPE	Temporal R2	Temporal RMSPE	missing LST*
Winter	0.840	1.792	0.853	1.109	0.822	1.402	63%
Spring	0.921	1.623	0.865	1.024	0.939	1.250	53%
Summer	0.832	1.693	0.839	1.147	0.822	1.257	34%
Autumn	0.925	1.576	0.861	1.042	0.943	1.186	52%

*Winter (December-February), Spring (March-May, Summer (June-August), Autumn (September-November)

Figure 4.11. Annual mean predicted air temperature, 2000 Italy.

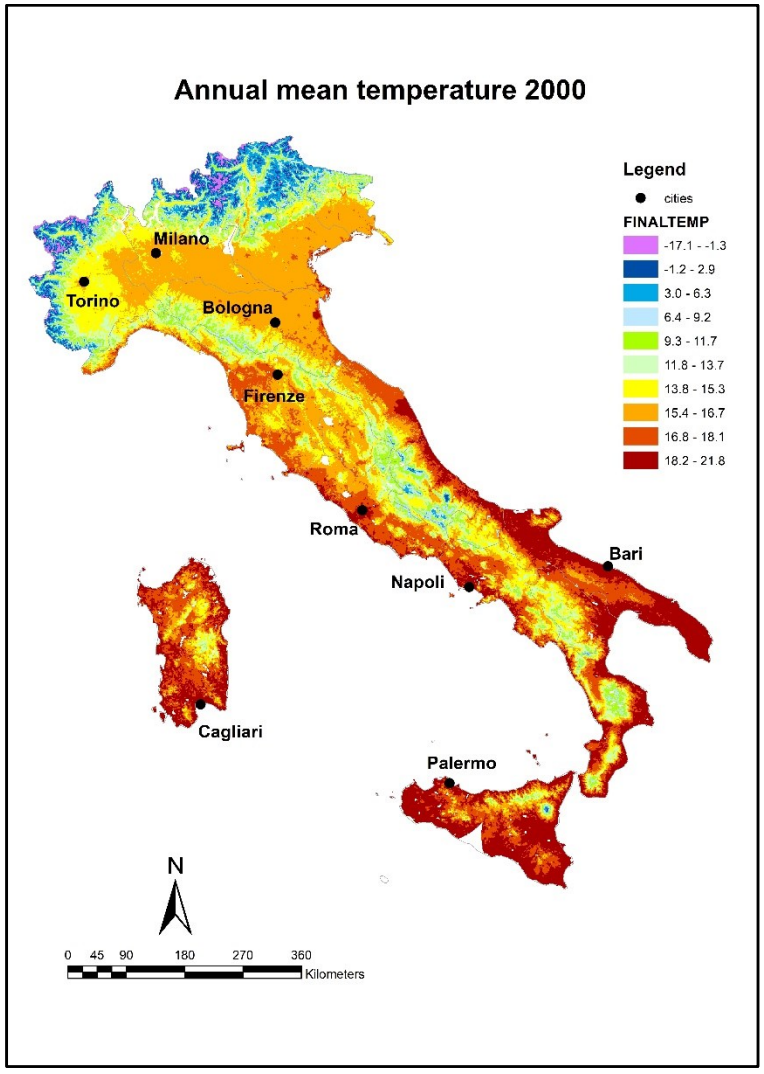

Figure 4.12. Annual mean predicted air temperature, 2001 Italy.

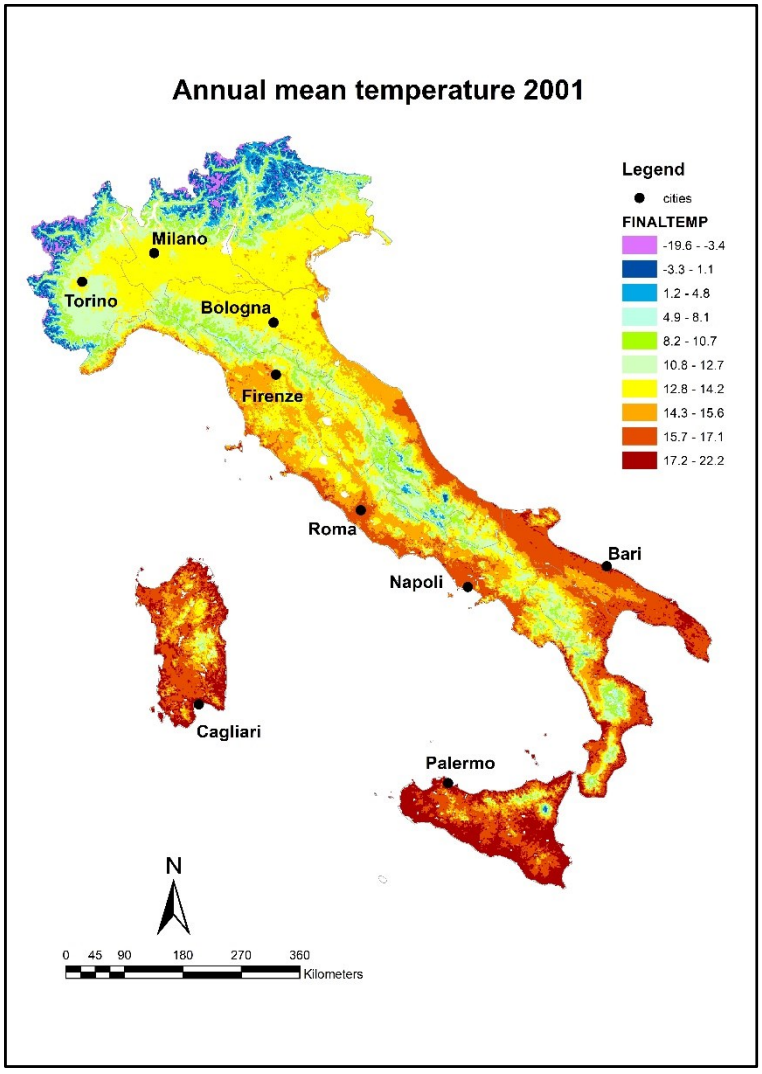

Figure 4.13. Annual mean predicted air temperature, 2002 Italy.

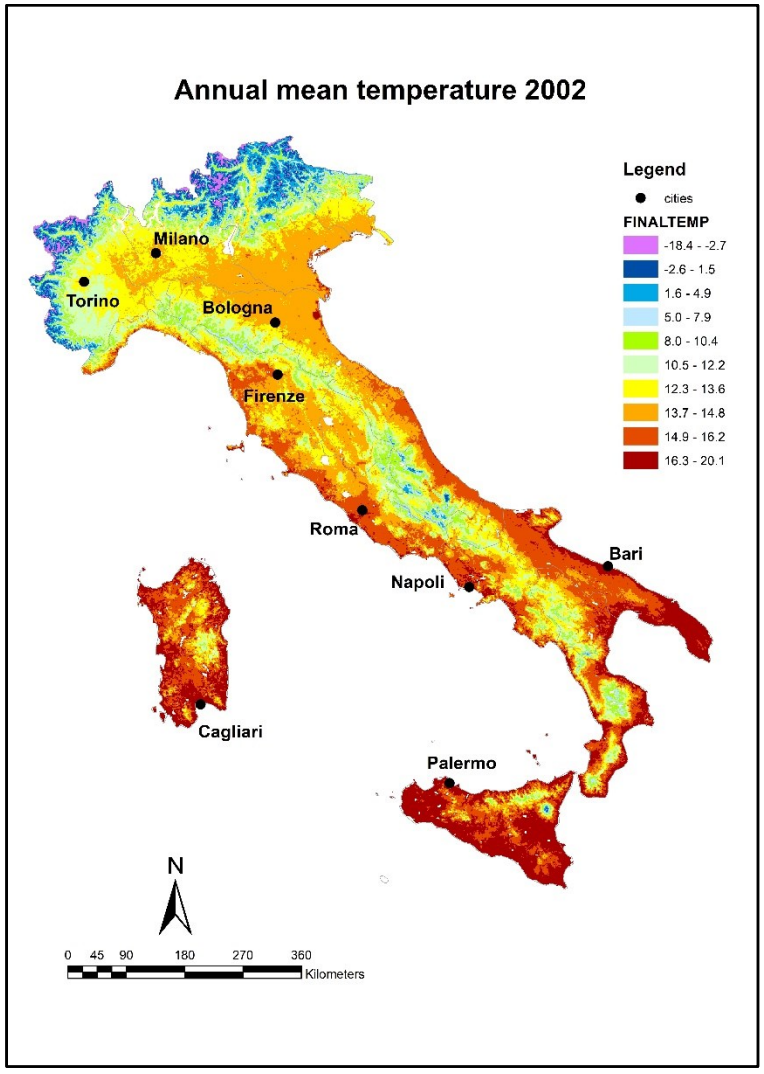

Figure 4.14. Annual mean predicted air temperature, 2003 Italy.

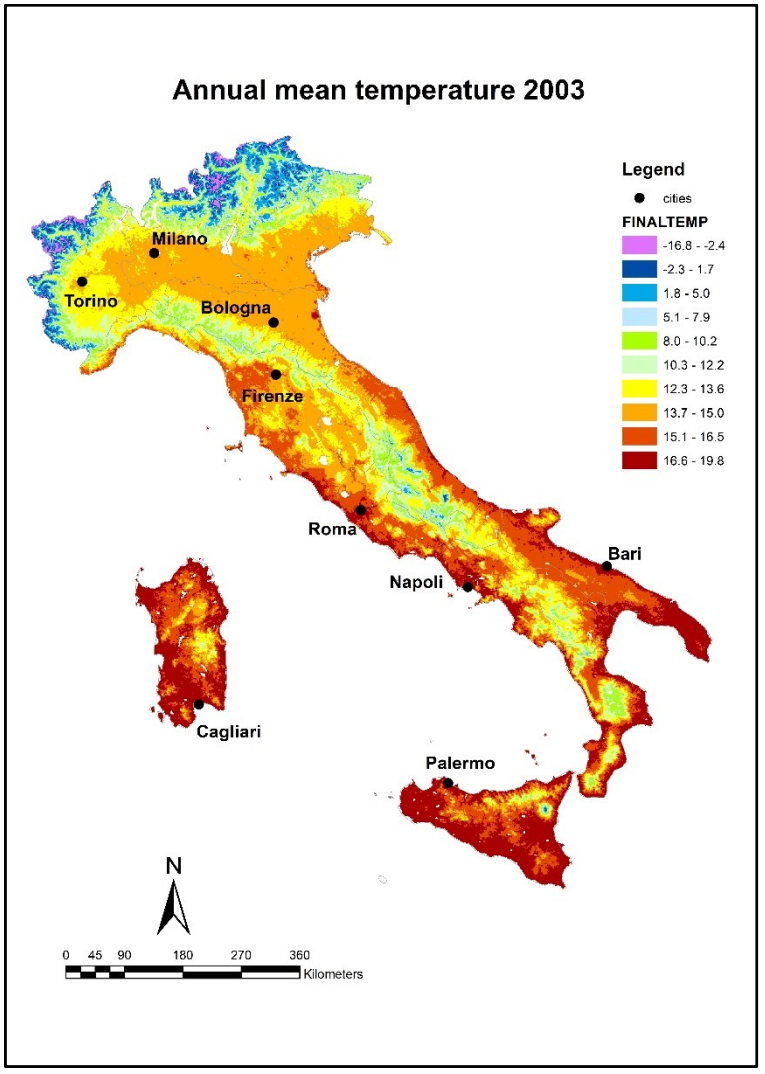

Figure 4.15. Annual mean predicted air temperature, 2004 Italy.

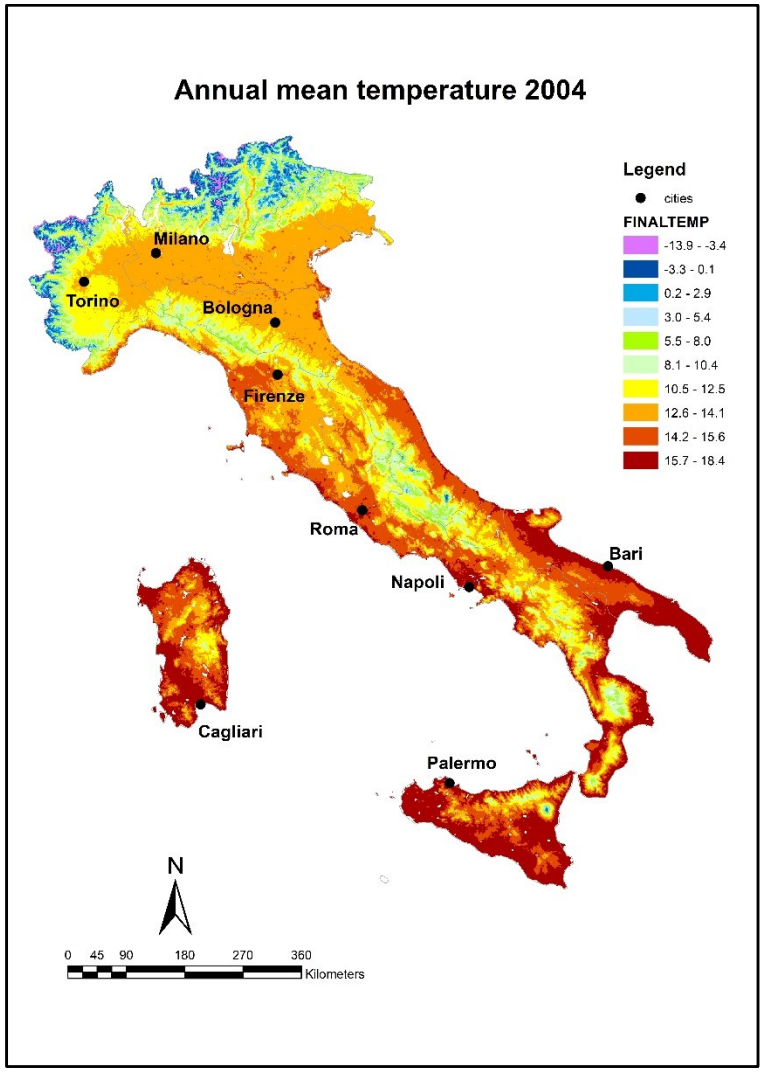

Figure 4.16. Annual mean predicted air temperature, 2005 Italy.

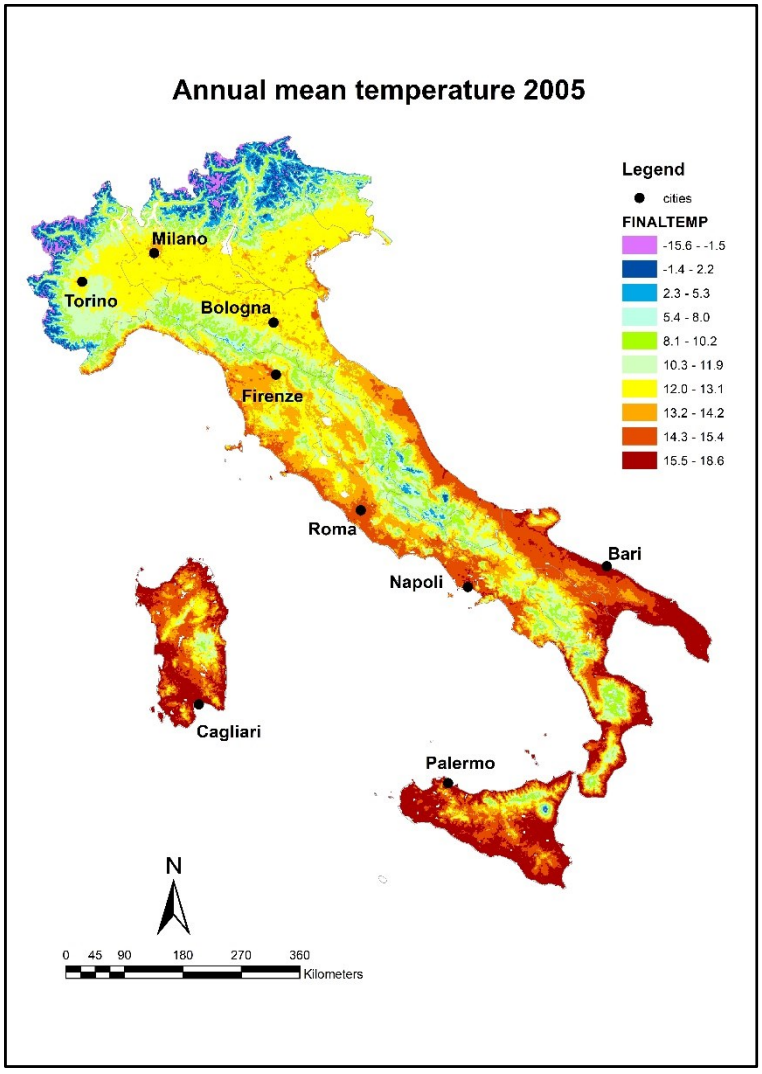

Figure 4.17. Annual mean predicted air temperature, 2006 Italy.

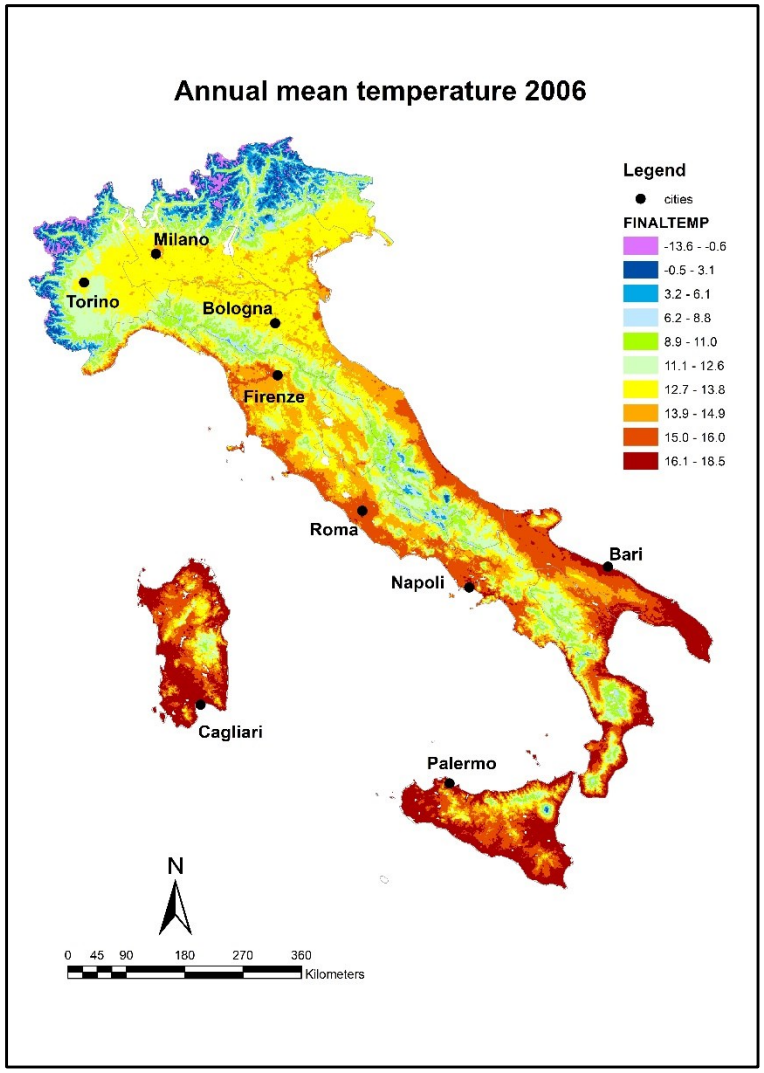

Figure 4.18. Annual mean predicted air temperature, 2007 Italy.

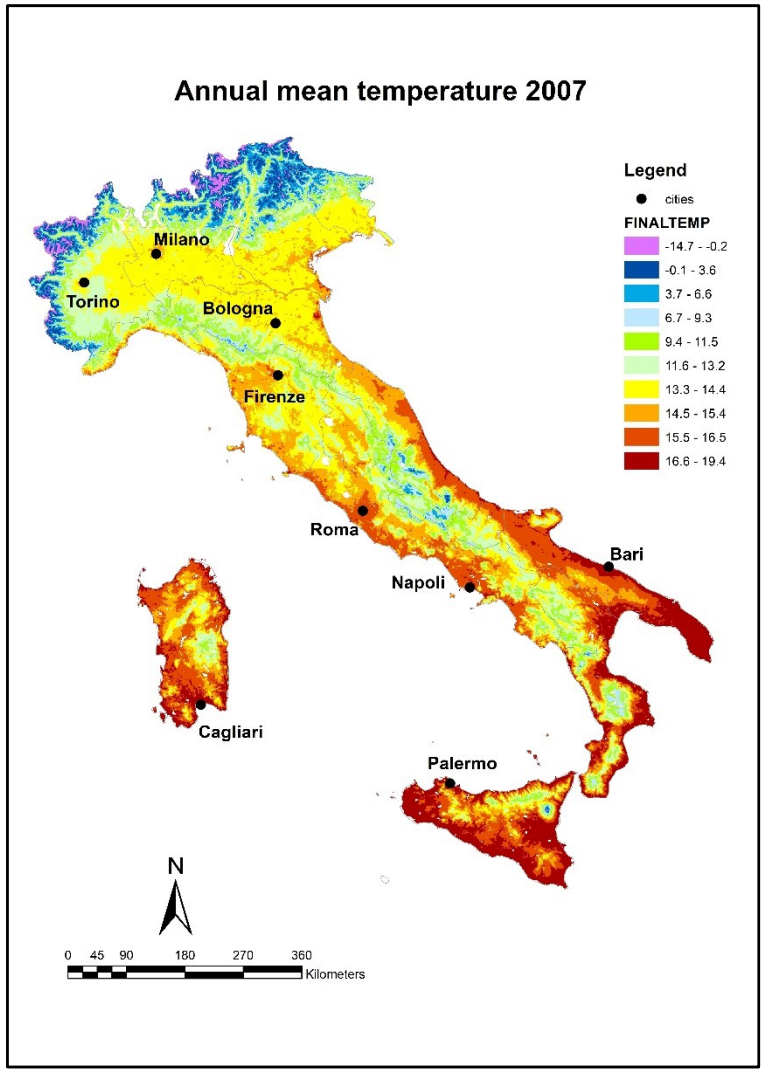

Figure 4.19. Annual mean predicted air temperature, 2008 Italy.

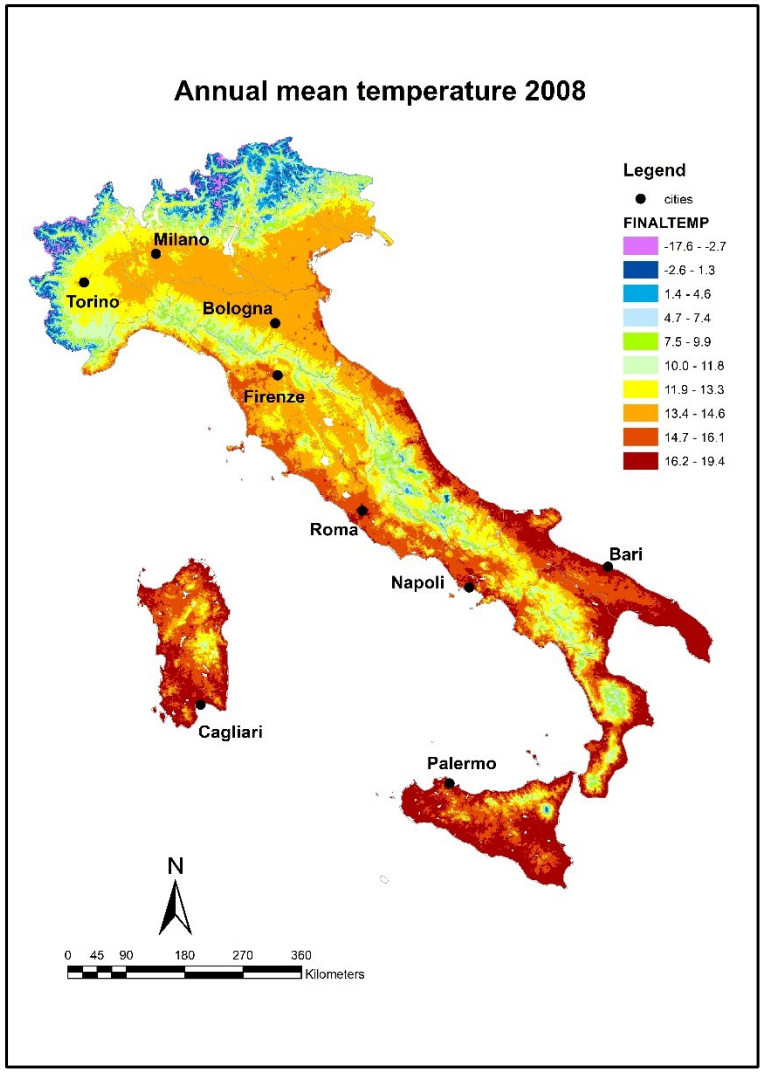

Figure 4.20. Annual mean predicted air temperature, 2009 Italy.

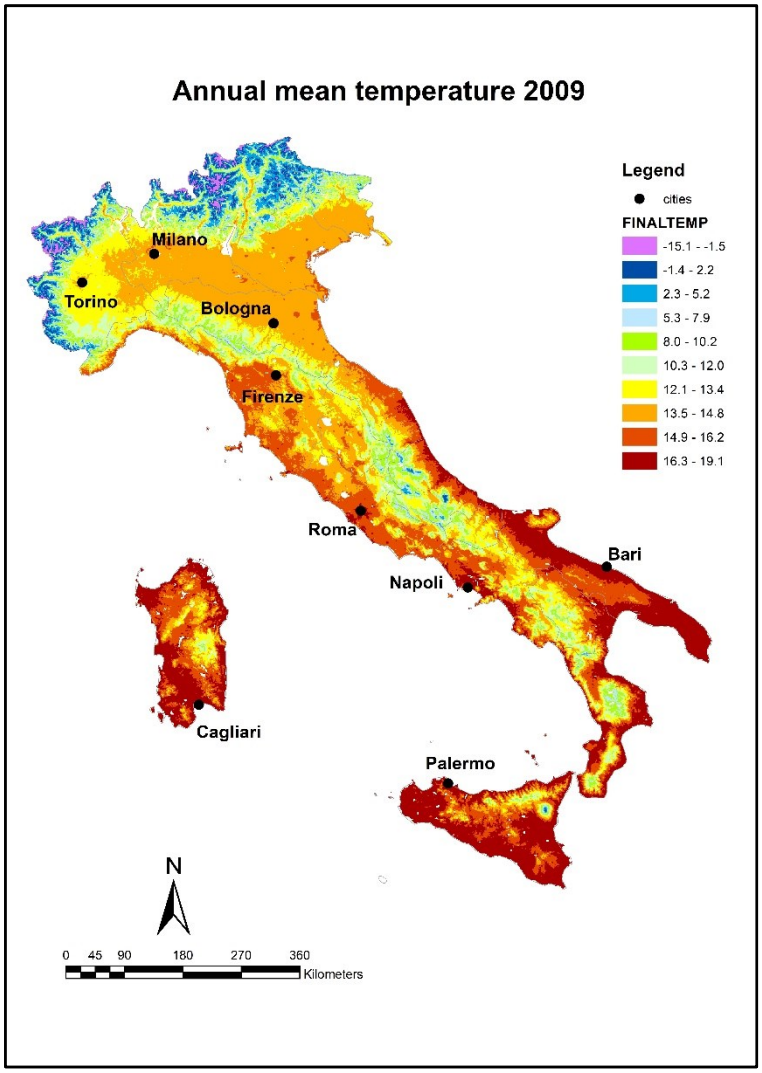

Figure 4.21. Annual mean predicted air temperature, 2010 Italy.

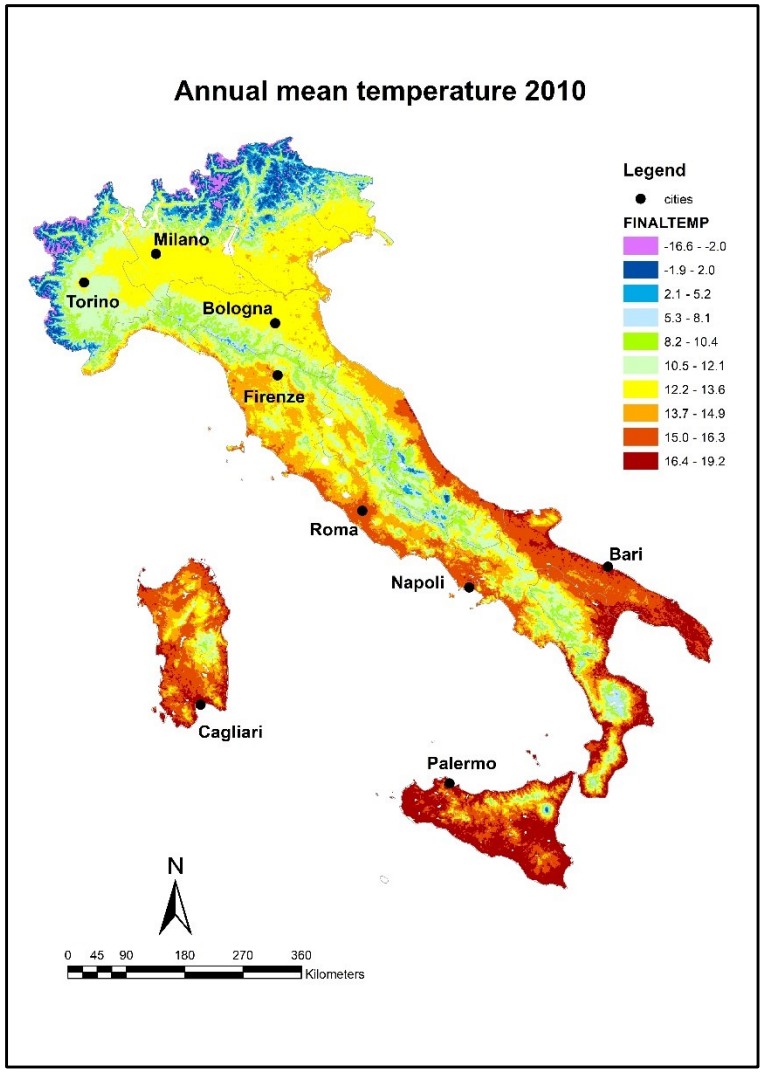

4.3.1 Model Validation

External model validation with RAMS forecast data for 2005 confirmed the very good model fitting with an overall R^2 of 0.95 and RMPSE 1.8°C. Figure 4.22 shows the correlation between RAMS forecast temperature data and satellite modelled temperature. The seasonal performance was also tested and better prediction results where observed in autumn and spring (R^2=0.92) and least in winter R^2=0.74) with RMSPE between 1.6-1.9°C. This is not surprising as winter variability and local atmospheric dynamics like thermal inversions could not be depicted by satellite data which does not take into account atmospheric dynamics. Overall, the temperature daily distribution showed an excellent fit between the two datasets (Figure 4.23).

Figure 4.22 Scatter plot of mean air temperature predicted by RAMS and stage 3 model predicted air temperature for 2005 in central Italy.

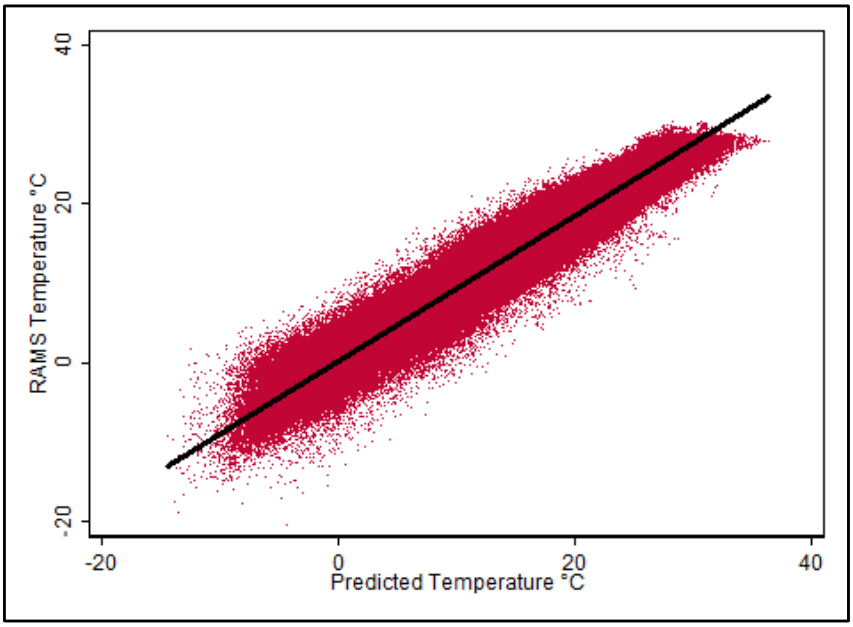

Figure 4.23. Temperature distribution for a single 1x1km grid cell, 2005.

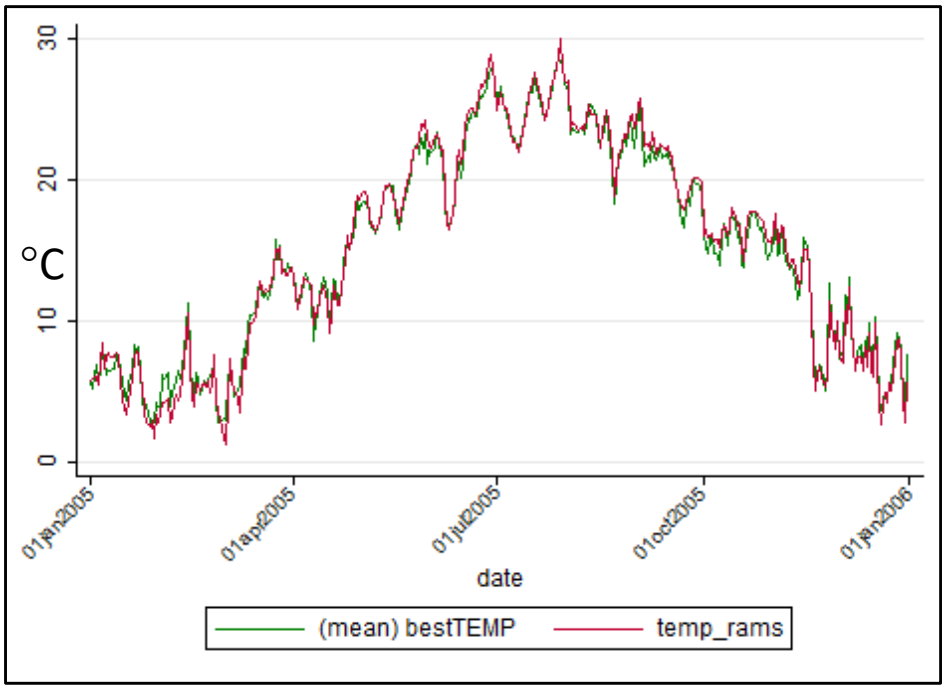

4.4 DISCUSSION

The methodology developed provides estimates of daily temperature across the whole of Italy for an 11 year period (2000-2010) with excellent model performance (mean R^2 =0.982 and mean RMSPE= 1.08°C). The model was able to estimate temperatures in the different climatic zones of Italy taking into account the complex orography and local climates as well as distinguishing between urban, suburban and rural areas and their thermal conditions. This is the first dataset with such a high spatial and temporal resolution for the whole Italian domain and will be of great importance for both environmental and epidemiological studies. The satellite derived temperature data was used to estimate the health effects of heat in the Lazio region in both urban, suburban and rural areas presented in the next section. These new estimates are very important in Italy as every year heat has a significant impact in terms of attributable deaths.[229,314] High resolution air temperature maps can provide policy makers with a more detailed spatial distribution of heat risk for both rural and suburban areas where evidence and data has been limited to date. Furthermore, within urban areas, thermal distribution maps and the UHI phenomenon can also be observed. The methodology is transferable to other regions and contexts, and conversely to previous applications it shows it can capture different climates even when land-use characteristics vary across over relatively small distances.

Furthermore, the spatio-temporal satellite temperature exposure derived from this approach can be used as a covariate in other studies in which temperature is a confounder or effect modifier of the exposure, such as air pollution [315].

However, it is worth mentioning some limitations. The methodology is far from simple and requires a great amount of input data with a good spatial and temporal resolution to derive air temperature. Satellite data availability can be an issue in some areas of the world due to missing

data (primarily due to cloud cover) or limited spatial or temporal coverage of specific satellite data products. However, considering model performance the potential benefits compared to currently available air temperatures from monitoring sites is considerable and the methodology is transferable to other contexts, accounting for local climatic and land use characteristics.

This methodology is strongly dependent on observed data from monitoring networks especially to capture daily temperature differences[28,64], without meteorological data the model performance would undoubtedly be lower. The uneven distribution of monitoring sites available in this study could have influenced the goodness of fit of the models in some zones which are under-represented (such as in the south or at high altitudes). This can be partially solved by the extension of non-conventional monitoring stations in recent years which provide a useful source of information. However, the quality of monitoring data in this case may potentially be lower compared to standard WMO or regional monitoring networks. In the future, the retrieval of additional data from regional monitoring networks might help improve model accuracy in these areas. The study shows that even using different sources of data with a heterogeneous spatial coverage estimates had a high accuracy, suggestive of an additional value of the method and use of different meteorological data.

Further analysis using finer spatial resolution satellite data can be carried out to capture the thermal differences within medium and small sized areas to better capture thermal gradients across space. The data can be fused with finer scale satellite data in order to study the complex spatial land use patterns within urban areas[137,316–318].

In conclusion, the study shows that LST satellite data can be used reliably to predict high resolution daily air temperature over complex terrain even in days with missing satellite data. Spatio–temporally resolved Ta data for an 11-year period can be used for a variety of environmental epidemiological studies in Italy. The data provide an important contribution also

for future climate change, not only for the monitoring of changes in temperature at the national level but also for the estimation of high resolution temperature-related future impacts on health.

CHAPTER 5 – SHORT-TERM EFFECTS OF HEAT ON MORTALITY AND HOSPITAL ADMISSIONS IN THE LAZIO REGION.

This chapter presents the time series analysis carried out to estimate the effects of heat on mortality and hospital admissions in the Lazio region in rural, suburban and urban areas with high resolution Ta defined in chapter 4. Datasets, methods and results are presented, followed by a brief discussion on research findings.

5.1 INTRODUCTION

The acute effects of heat and extreme temperatures on health outcomes (mortality and hospital admissions) have been studied in detail in Italian cities[8,191,193,319,320]. Multi-city national studies and international studies have shown the heterogeneous effect of heat within Italian cities due to the local climate and population characteristics[161,179,208]. A case crossover study carried out in 4 major Italian cities (Rome, Milan, Turin and Bologna) found overall OR of 1.34 (95%CI: 1.27–1.42) for a 10°C temperature increase.[179] Furthermore, a multi-country study showed that Italian cities had the highest risks , with increase in mortality ranging between 10% and 28% for increase in mean temperature between the 90th and 99th percentile[191]. However, research has been limited to urban areas and little is known on the effects of heat in suburban and rural communities. This is primarily due to the limited or non-existent monitoring stations in rural and suburban areas and the limited number of daily deaths that would be a caveat for statistical power in traditional time series analysis. Satellite derived high-resolution Ta defined in chapter 4 provided exposure data for the entire Lazio region at municipal level. The study aimed to estimate the heat effects in urban, suburban and rural settings of the Lazio region and to compare effect estimates of municipalities by size, in terms of both population, and urban

characteristics.

5.2 METHODS

5.2.1 Dataset

The study area comprises the Lazio Region located in central Italy, with an area of 17,242 km^2; it has borders with Tuscany, Umbria, and Marche to the north, Abruzzo and Molise to the east, Campania to the south, and the Tyrrhenian Sea to the west. The region is mainly flat and hilly, with small mountainous areas in the east and south east going towards the Apennines.

It's population is of almost 5.9 million inhabitants – making it the second most populated region of Italy. The capital city is Rome, which is also the capital of Italy and the largest city in the country with over 2.8 million residents. The population of Rome makes up around half of the regional population.

Study units are the 376 municipalities of the Lazio region, population (reference year 2006) of the municipalities is comprised between 117 and just over 120,000 inhabitants (Figure 5.1). Rome was considered separately due to its population size and geographical extent. It was subdivided considering the 155 urbanistic zones, reference population data for the urbanistic zones was not available (Figure 5.2).

Daily mortality data and hospital admissions data were selected as health outcomes as the evidence in the literature on the association between these outcomes and temperatures was more consistent.[5,6,12,157,243] Furthermore, the choice was driven by data availability for the entire period under study. The emergency room visit registry is comprehensive for the Lazio region from 2004 onwards, while ambulance calls are not in a standardized format at regional level and only have partial coverage.

Figure 5.1 Map of Municipalities in the Lazio region.

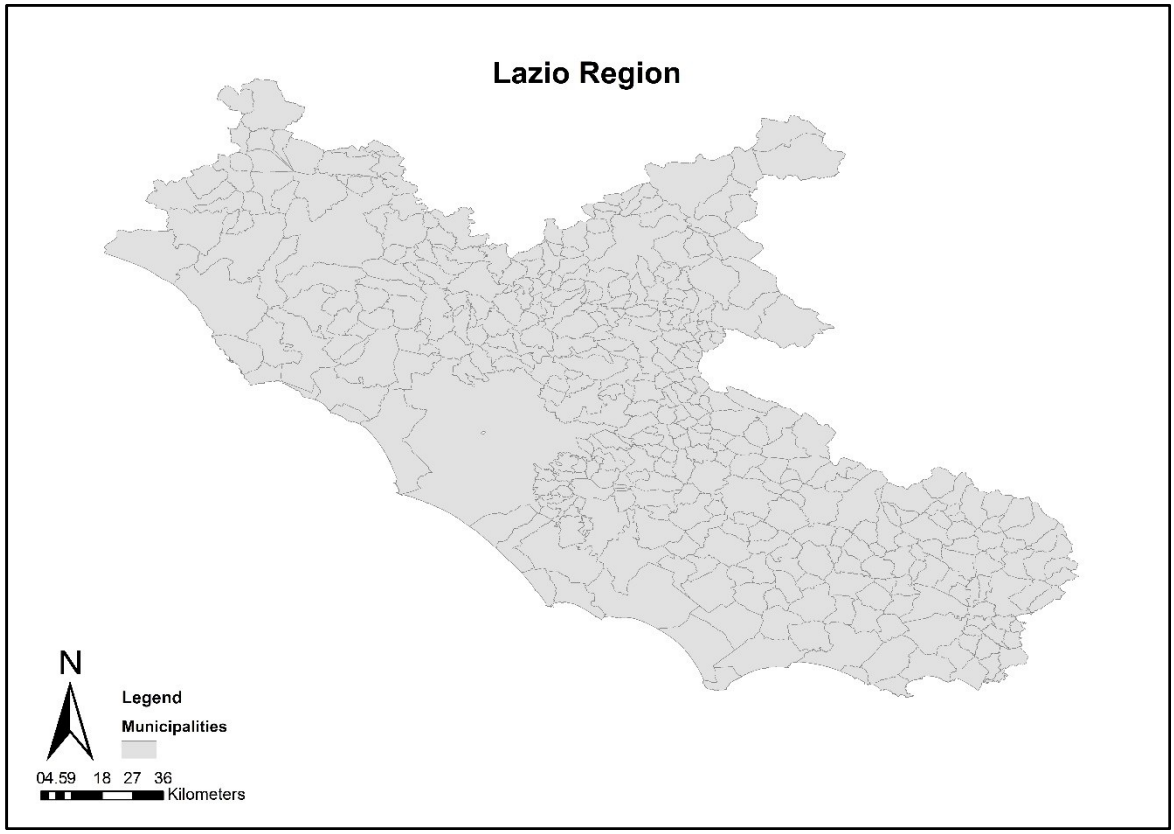

Figure 5.2 Map of urbanistic zones of Rome.

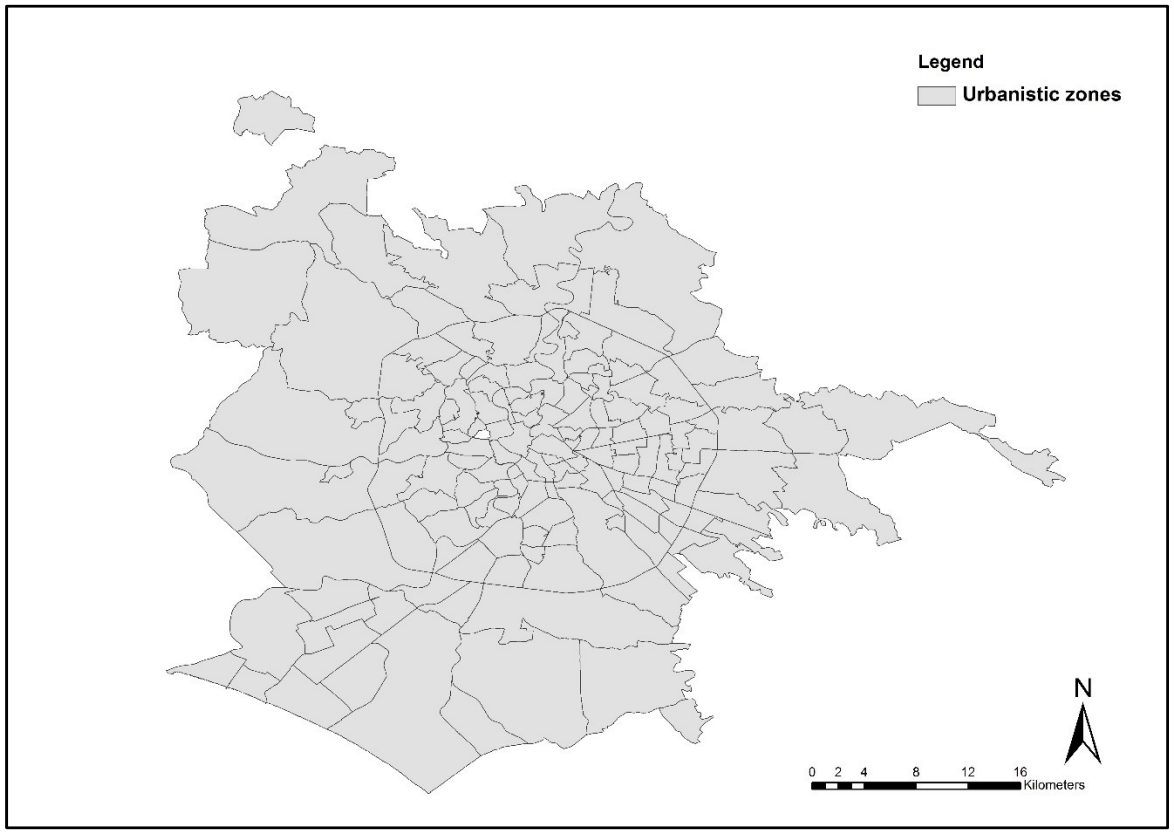

5.2.2 Exposure

From the 1x1km gridded daily mean Ta predicted for the entire Italian domain, the average temperature for each municipality in the Lazio region was calculated. Using ArcGIS the intersection of all 1x1km gridded squares were attributed to a municipality and areas in each municipality calculated. In this way, it was then possible to calculate an average temperature for each municipality weighted by the proportion of area of each grid cell. For the Municipality of Rome which occupies an area of 1287.4 km^2, a weighted average temperature would have greatly compressed the distribution of mean temperature, hence the average temperature was estimated for each of the 155 urbanistic zones of the city. The process carried out for the other municipalities in Lazio was re-iterated to calculate the average mean temperature for each of the 155 zones in Rome.

5.2.3 Mortality Dataset

Daily death counts for each municipality were extracted from the Lazio regional mortality registry (SIM) for the period 2001-2010. Total natural (International Classification of Diseases, 9th– ICD 9: 1-799), cardiovascular (ICD9 : 390-459) and respiratory causes (ICD9 : 460-519) of death for the resident population dying within the municipality were calculated for each unit in the period 2001-2010.

For Rome, daily deaths were extracted from the Rome mortality registry (RENCAM), and daily mortality counts were calculated by urbanistic zone. Again causes of death were grouped by natural (International Classification of Diseases, 9th– ICD 9: 1-799), cardiovascular (ICD9: 390-459) and respiratory causes (ICD9: 460-519) of death. Only events occurring among the resident population and dying in Rome in the period 2001-2010 were considered.

5.2.4 Hospital Admissions Dataset

Similarly, to mortality data, hospital admission data for the Lazio region was retrieved from the regional hospital admissions registry (SIO) for the period 2001-2010. Daily hospital discharge data for natural (International Classification of Diseases, 9th– ICD 9: 1-799), cardiovascular (ICD9: 390-459) and respiratory causes (ICD9: 460-519) were extracted and daily counts for each municipality in Lazio and for the urbanistic zones in Rome were computed. The hospital admissions dataset was restricted to subjects aged 35 years and over.

5.2.5 Dataset construction by spatial units

The unit of aggregation for both exposure and health outcomes are the 376 municipalities in the Lazio region and the 155 urbanistic zones in Rome. The Pontine islands were excluded as Ta was not defined. To carry out the time series analysis, municipalities were aggregated based on population size using the national institute of statistics (ISTAT) (www.demoistat.it) population data for year 2006. This year was chosen as it is the central year in the study period. The following aggregations were made based on the distribution of the population in municipalities of the Lazio Region accordingly:

- small municipalities with a population smaller than 15,000 inhabitants,
- medium size municipalities with a population between 15,000 – 40,000 inhabitants,
- large municipalities with a population size greater than 40,000 -120,000 inhabitants
- Lazio capital : Rome (2.7 million residents)

With this subdivision 326 municipalities were classed as small, 35 as medium and 14 as large. The spatial distribution is shown in figure 5.3. The Rome municipality was treated separately.

Figure 5.3. Spatial distribution of population in classes among the municipalities of the Lazio Region.

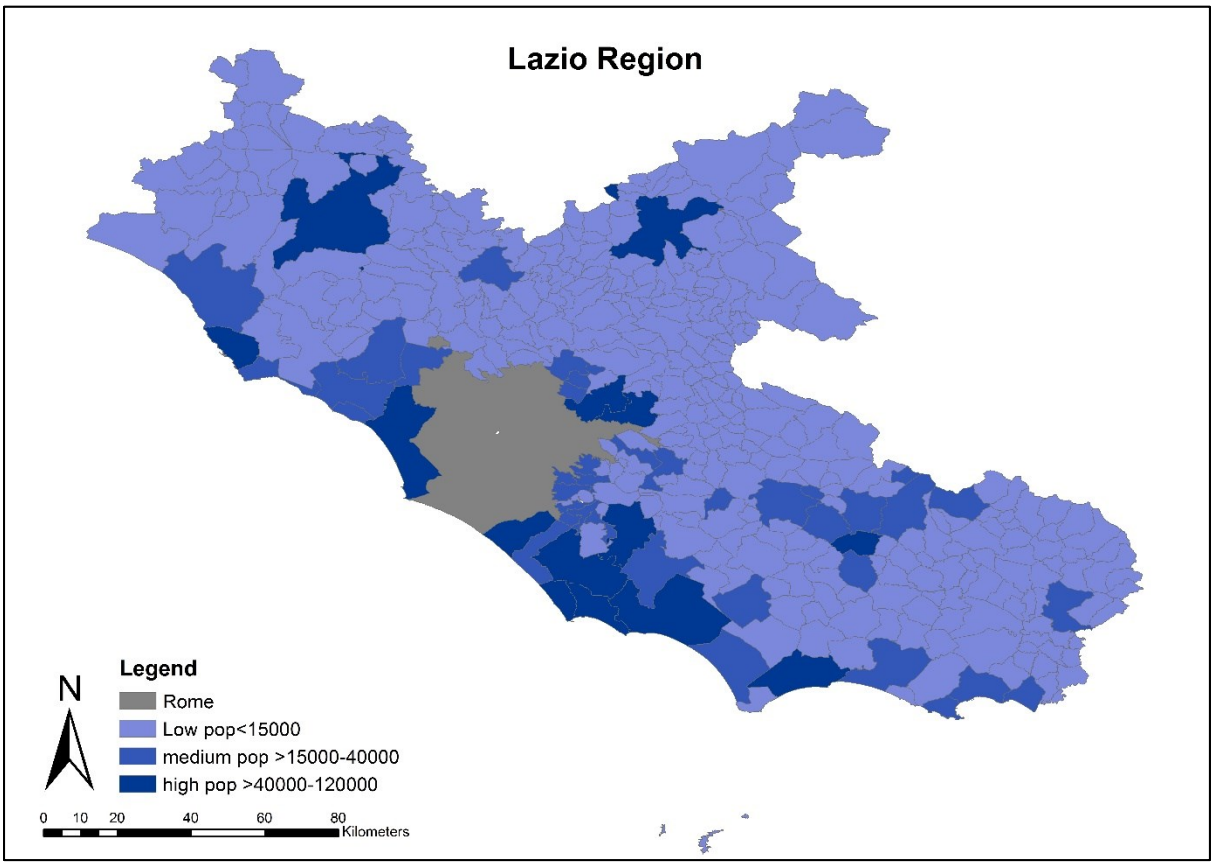

Secondly, to account for the extent of high and low development within each municipality and their role in modifying the thermal characteristics of the spatial units, Corine land cover artificial surfaces, urban fabric classes were considered. Specifically: "continuous urban fabric" (code 111) where up to 80% of the land surface is covered by impermeable features such as buildings, roads and artificially surfaced areas and "discontinuous urban fabric" (code 112), which account for continuous and discontinuous urban development, were considered in each municipality (described in section 4.2.1). These categories exclude large industrial sites, airports and ports. For each municipality the areas covered by high and low development were calculated and the sum of the area for each municipality was defined as urban and then percentage of urbanization was calculated dividing by the total area of the municipality. All

the municipalities in the Lazio region (excluding Rome) were then grouped into the following 3 classes based on the variable distribution:

- Low percent urban (below the median): % urban <1.5%
- Medium percent urban (between median and 75th percentile): >=1.5% to 3.5%
- High percent urban (above 75th percentile): >3.5%

Spatial distribution is shown in figure 5.4

For Rome the same classification, using Corine land cover continuous and discontinuous urban fabric high and low development was calculated for the 155 urbanization zones. Specifically defining the area covered by low and high development, then summing the two and finally dividing by the total area of each municipality to obtain the percentage of urbanization in each of the 155 zones of Rome. The zones were then grouped into the following 3 classes based on the variable distribution:

- Low percent urban (below the median): % urban <57%
- Medium percent urban (between median and 75th percentile) : >=57 to 82%
- High percent urban (above 75th percentile): >82%

Spatial distribution is shown in figure 5.5. The difference in distribution in urbanization in Rome and in the other municipalities justifies the choice of separating the two (table 5.1). It can be observed that the 99th percentile of the Lazio distribution corresponds to the 5th percentile for Rome.

Thirdly, to consider all anthropogenic surfaces, and not just urban development, ISA indicator of impervious surfaces (described in section 4.2.1) was also considered for each municipality, again treating Rome separately from the other municipal units in the Lazio Region. From the

original raster file, ISA was attributed as the mean of all the 1x1km grid cells included for each areal unit.

For the Lazio municipalities the zones were then grouped into the following 3 classes based on the ISA distribution:

- Low ISA (below the median): ISA <1.3
- Medium ISA (between median and 75th percentile) : >=1.3 to 2.4
- High ISA (above 75th percentile): >2.4

For Rome the same classification, using ISA was developed for the 155 urbanization zones. The zones were then grouped into the following 3 classes based on the ISA distribution for Rome municipality:

- Low ISA (below the median): ISA <50
- Medium ISA (between median and 75th percentile) : >=49.5 to 76.6
- High ISA (above 75th percentile): >76.6

Spatial distribution of impervious surface for Rome and municipalities in the Lazio region are shown in Figures 5.6 and 5.7. For ISA the median value for Lazio corresponds to the 1st percentile in Rome (table 5.1).

The table also highlights that the two variables are somewhat different and represent different land cover anthropogenic characteristics.

Table 5.1 Distribution of percentage of urbanization and impervious surfaces in the Municipalities of the Lazio Region and for the urbanistic zones in Rome.

		Percentile distribution								
		1	**5**	**10**	**25**	**50**	**75**	**90**	**95**	**99**
Percent Urban										
	Lazio	0	0	0	0	1.5	3.5	8.1	12.6	22.5
	Rome	0	22.5	4.1	17.3	57.4	82.6	94.3	97.0	100
Impervious surface (ISA)										
	Lazio	0.4	0.5	0.7	0.9	1.3	2.4	4.8	7.2	14.4
	Rome	1.3	5.8	8.9	25.5	49.5	76.6	99.6	100	100

Figure 5.4 Spatial distribution of urban development in the Lazio region.

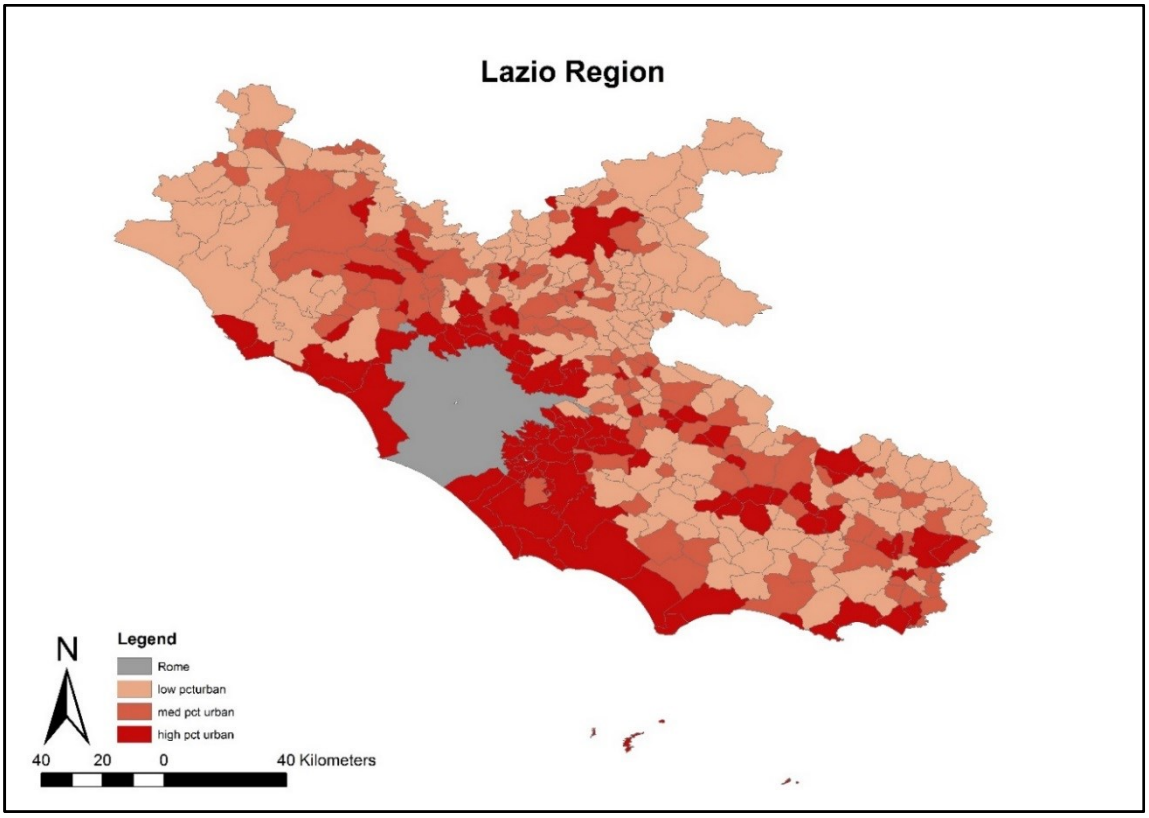

Figure 5.5 Spatial distribution of urban development in Rome.

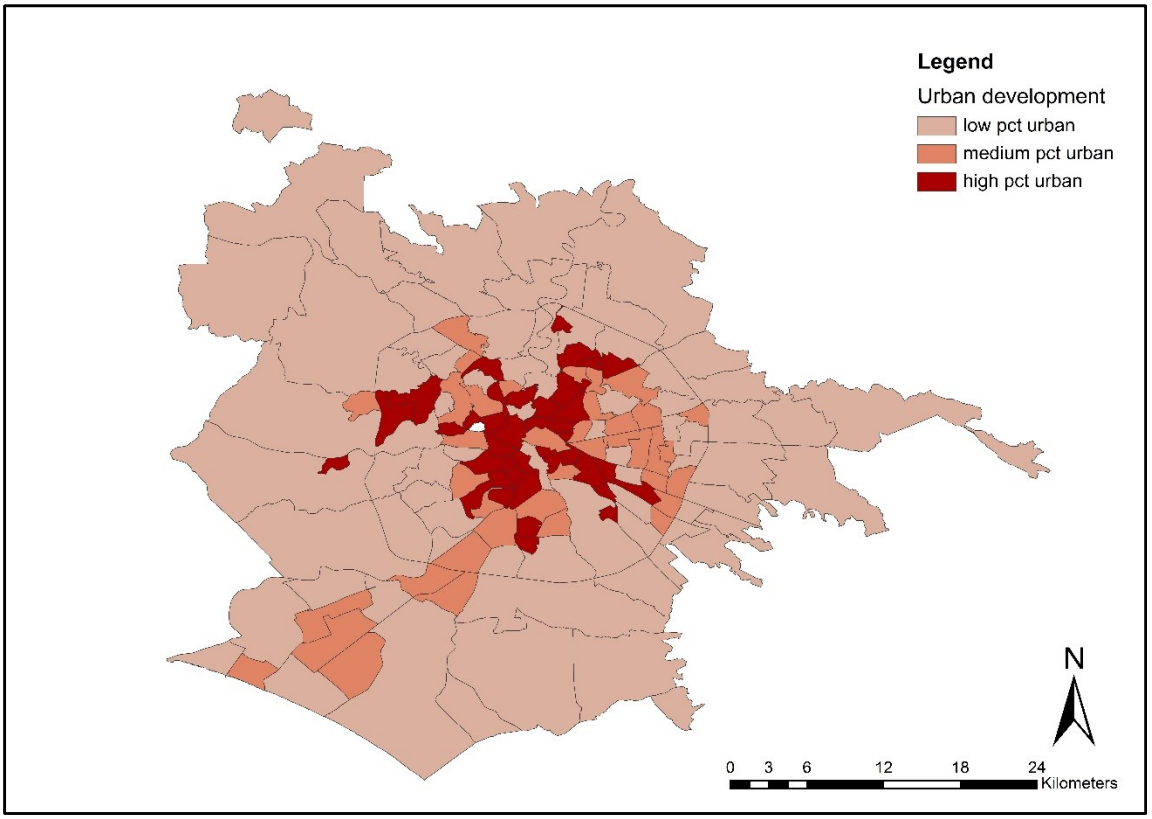

Figure 5.6 Spatial distribution of impervious surfaces in the Lazio region.

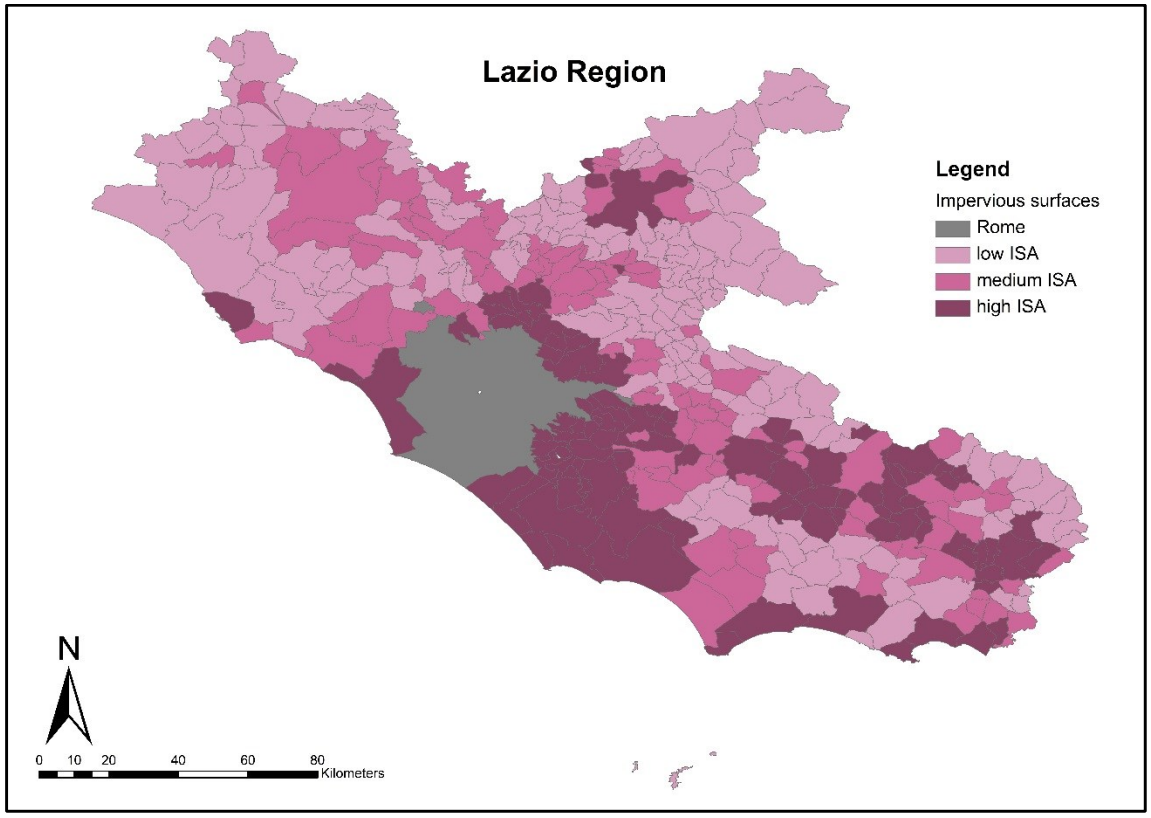

Figure 5.7 Spatial distribution of impervious surfaces in Rome.

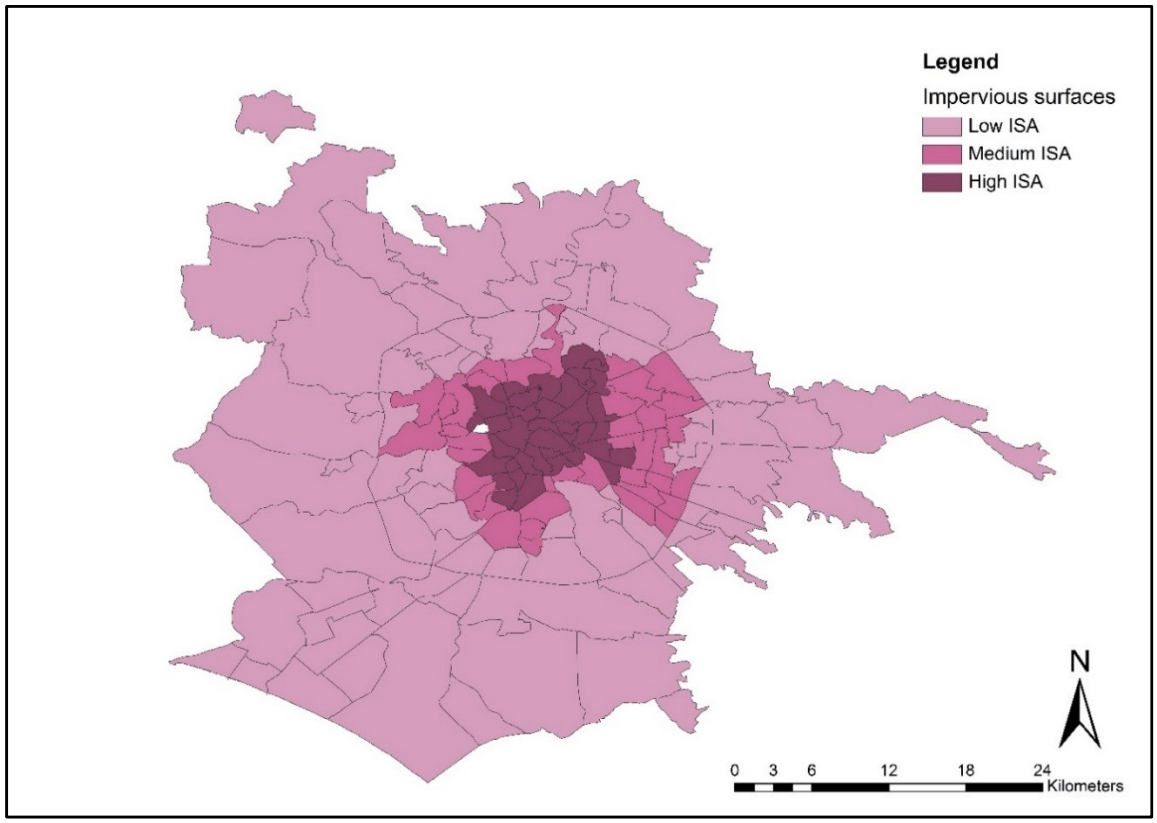

5.2.6 Statistical modelling.

Time series analysis of the short-term effect of heat

The association between cause-specific mortality/hospitalizations and daily T_a was evaluated considering a pooled time-series analysis at regional level (entire Lazio region), by combining the time series of 375 municipalities of Lazio (excluding Ponza and Ventotene) and the 155 urbanistic zones of Rome.

Study design

Time series are sequences of data indexed by time units (days in the present analysis). For each day, counts of deaths/hospitalizations were related to average population exposure, while accounting for potential time-varying confounders, first of all long-term and seasonal time trends. This kind of study is considered a quasi-experimental study design because the contrast (in both exposure and outcome) is performed *within the same study population* over time. Since time trends are adjusted for in the modelling phase, it follows that fixed population characteristics, or factors that vary slowly, over time (such as smoking rates, prevalence of cardiovascular diseases, age distribution structure, BMI, SEP etc.) cannot confound the association between (short-term) exposure to daily temperatures and mortality/morbidity outcomes. The only putative confounders to be accounted for, in addition to time trends, are those factors which might co-vary in the short-term together with both the exposure (temperature) and the outcome (daily count of deaths/hospitalizations). These will be described later under the paragraph “confounding adjustment”.

In the present study, for each spatial unit (municipality, urbanistic zone), daily T_a predictions, derived in section 4, at 1x1 km resolution, were averaged to obtain daily mean T_a exposures. Furthermore, as the focus of this study was on the effects of summer temperatures, only events

occurring between May and September were included in the analysis. An over-dispersed Poisson conditional regression model was defined [321] in which the dependent variable was the daily count of (cause-specific) deaths or hospital admissions, the exposure was the (lagged) daily mean T_a, and the model was adjusted for other time-varying confounders described later. This study will be one of the first studies to provide effect estimates of heat on health outcomes in rural, suburban and urban settings considering a high resolution T_a exposure.

Exposure modelling

In order to account for the lagged non-linear association between high temperatures and health outcomes a distributed-lag non-linear model (package *dlnm* in R) was used[276,322]. This model defines a two-dimensional function, the *cross-basis*, which incorporates both non-linear curves for the exposure-outcome relationship and lagged effects of the exposure on the outcome.[323] On the basis of the literature, a maximum lag of three days was set a priori and then allowed for non-linearity by fitting b-splines of the (lagged) temperature-outcome relationship with 3 degrees of freedom. After exploratory analyses, I chose to report results for mortality and hospital admissions outcomes at cumulative lag 0-3. Results are reported as rate ratios (RR) and 95% confidence interval, for temperature increases between the 50th to the 75th, 50th to the 99th and 50th to the 99.9th percentiles of temperature distribution by spatial aggregation to account for the response to area-specific temperatures under the assumption that local populations are acclimatized to their own specific climate. For simplicity in commenting results risks were described as relative risks.

Confounding adjustment

Confounders included in the multivariate regression model were: a) long-term and seasonal time trends specific for each spatial unit, b) holidays, and c) summer population decrease.

Specific time trends for each municipality (Lazio) and urbanistic zone (Rome) were added to the model to account for potential time-trends in the baseline rates within each spatial unit. In the conditional Poisson analysis, time trend was adjusted for by conditioning a four-way interaction term among spatial unit, year, month and day of the week [324]. This approach is analogous to a case-crossover "time-stratified" study design, nested within each area level [324]. Holidays were identified with a dummy variable assuming value 1 during national/local holidays and 0 otherwise. Summer population decrease was accounted for by use of a three-level variable assuming value 2 in the 2-week period from 1-15th August; value 1 from 16th July to 31st of August, except for the aforementioned two-week period, and 0 for all other summer days. Both terms were modelled using indicator variables.

Statistical model

The following formula, as reported in Armstrong et al. [321] summarizes the statistical model:

$$Y_{i,s}|Y_{.,s} \sim Multinomial(\{\pi_i\}), \quad \pi_i = \frac{exp\{\sum_{l=0}^{L} f * w(x_{t-l}, l) + \boldsymbol{\beta}^T x_i\}}{\sum_{j \in S} exp\{\sum_{l=0}^{L} f * w(x_{t-l}, l) + \boldsymbol{\beta}^T x_i\}}$$

where:

- $Y_{i,s}$, the count of events (cause occurring on day i belonging to stratum s, is assumed to follow a multinomial distribution with expected value π_i;
- The (lagged) exposure variable is modelled with a cross-basis defined on a number of lags equal to l, and a non-linear relationship by f;
- The strata defined by individual spatial units, years, months and days of the week are conditioned out of the likelihood;
- Other confounders (e.g. holidays and summer population decrease) are included in x_i, with their estimated regression coefficients reported in the vector $\boldsymbol{\beta}$.

As previously described, all the analyses were repeated for the whole Lazio Region, by municipality population size and by degree of urbanization (using alternatively percentage of urban areas and ISA) grouped in classes according to the distribution of the level of urbanization and ISA in the Lazio region and Rome zones. For each subset, I will report both

the non-linear curves of the temperature-outcome association (cumulative lag 0-3 for mortality and admissions), and summary estimates of relative risks of mortality from the 50th to the 75th, then from 50th to the 99th percentiles and from 50th to the 99.9th percentiles.

Sensitivity Analysis – fixed temperature effects

To compare exposure considering a set of fixed temperature values and see the response in different settings, the overall Lazio percentile distribution was considered for each spatial aggregation and estimates re-calculated.

Sensitivity Analysis – exclusion of extreme year, 2003

Sensitivity analysis was carried out excluding 2003, an extremely hot year from the analysis. Total mortality and total admissions for overall Lazio, small, medium and large municipalities and Rome (considering the urbanistic zones) effects were estimated excluding 2003 data from the analysis. Furthermore, the model was re-run considering the same temperature percentiles as the main analysis (all years) and secondly percentiles were recalculated excluding 2003 from the temperature distribution and models re-run.

Attributable deaths

Furthermore, to quantify the impact of heat on mortality and have a better idea in numerical terms of the magnitude of the issue, the attributable number of deaths for the same temperature intervals were calculated applying the methodology described by Gasparrini et al.[325]. The attributable fraction here is the fraction of deaths that would not have occurred in the absence of exposure interval considered in the exposed population of the period in study. This attributable fraction is then multiplied by the total number of deaths in the period of study considered to obtain the number of deaths due to heat. In other words the number of deaths

avoidable if the heat exposure had not have occurred. These estimates are important in terms of public health as it provides a quantification of the burden associated to heat risks.

Attributable risks were calculated within the framework of distributed lag non-linear models [325] to take into account the temporal association between exposure to heat and risk. This methodology was also implemented in a multi city study by the author and colleagues [157]. Starting from the previous model to define effect estimates centred at the same value (50th percentile) the attributable risk was calculated for the intervals in study (75^{th} vs 50^{th} and 99^{th} vs 75^{th}) as the sum of attributable deaths on days across the temperature range and included in the time series interval. Empirical CIs (eCIs) were calculated using Monte Carlo simulations, assuming a multivariate normal distribution of the best linear unbiased predictions of the reduced coefficients.

Years of Life Lost

Another measure used to measure and evaluate the impact of heat on a local population are Years of Life Lost (YLL) which quantify the burden of premature mortality as a result of heat exposure[326]. YLL take into account the age at which deaths occur by giving greater weight to deaths at younger age and smaller weight to deaths at older age[327]. The number of attributable deaths estimated for the Lazio region were related to the average life expectancy obtained from population life tables. As effect estimates were not available by age group, a simplified calculation of YLL related to heat exposure was carried out. Specifically the number of AD estimates were distributed by age on the basis of the proportion of mortality by age in the Lazio reference population (year 2006). YLL were calculated by multiplying the number of attributable deaths in the h^{th} age class (ADh) by the average life expectancy within that class (Lh) for a reference year 2006 (central year in the study):

$$YLL = \sum_{h=1}^{H} ADh\ Lh$$

As for attributable deaths, YLL for estimated for temperature increases between the 50^{th} and the 75^{th} percentile and from the 75^{th} to the 99^{th} percentile and an overall sum estimate was given.

All the statistical analyses in the study were conducted using R (version 3.1.3; Institute for Statistics and Mathematics, WU Wien, Vienna, Austria), SAS (version 9.2) and STATA (version 13; StataCorp. 2013. Stata Statistical Software: Release 13. College Station, TX: StataCorp LP).

5.3 RESULTS

5.3.1 Health data

Table 5.2 reports the mean, standard deviation, minimum and maximum number of daily total, cardiovascular and respiratory deaths for each spatial grouping in the Lazio region and in Rome. Descriptive statistics by urban development and ISA are also shown to give an idea of the numbers considered in each spatial class. Considering all the 375 municipalities of the Lazio region, the total average number of daily deaths in summer was 56.3, of these, slightly less than half were ascribable to cardiovascular causes (24.8 deaths) and only 8 to respiratory causes. Most of the municipalities in the Lazio region have a population below 15,000 inhabitants and these registered an average of 18 daily deaths during the summer months, the same number of daily deaths was observed for the 35 medium sized municipalities. Large municipalities have an average number of 19.4 daily deaths during the summer season. In terms of mortality rates, values were more homogeneous compared to counts as expected. The highest rates were observed in large municipalities for all causes of death included in the study (natural, cardiovascular and respiratory) (Table 5.3b). Mortality rates ranged from 7.92 x1000 for natural deaths to 0.46 x1000 for respiratory deaths overall in the Lazio region (excluding Rome). While for Rome, rates ranged between 9.11 to 0.53 respectively for natural and respiratory deaths (table 5.3b).

Daily deaths by ISA and urban development categories were similar with slight differences due to the attribution of individual municipalities in one or another category (Table 5.2). Generally, total daily deaths in rural areas with low development or ISA had between 6-8 events, while 13 deaths were registered in the medium category and between 36-38 daily deaths occurred in the high ISA\urban areas. In Rome, an average of 46 deaths were recorded each day in summer, with a standard deviation of 8.2, ranging between a minimum of 29 and a maximum of 73

deaths. Cardiovascular deaths comprised around 38% of total deaths and respiratory deaths comprised around 4%. ISA and urban development categories were similar in terms of average deaths in Rome compared to the Lazio region. Interesting to note that the highest number of urbanistic spatial units was classified as low ISA\development category, with 77 units (Table 5.2). Mortality rates by percent urban and ISA in the Lazio region (excluding Rome) show slightly different patterns compared to municipality population distributions, with highest mortality rates in the middle category for all causes of death rather than high percent urban or ISA. Comparing municipalities classified by population size, ISA and percent urban, mortality rates were lower for high level percent urban and ISA compared to large population municipalities (table 5.3b).

Table 5.3a provides descriptive statistics for total, cardiovascular and respiratory hospital admissions in the Lazio region and in Rome. Considering total admissions, an average of 441 admissions were observed among Lazio municipalities and 590 for Rome. Cardiovascular and respiratory admissions for Lazio and Rome were respectively 106 and 101 for the former and 39 and 27 for the latter. The proportion of cardiovascular and respiratory admissions on total admissions were greater in the Lazio region. A greater variability in daily admissions was observed in Rome with larger standard deviations for all causes.

Admission rates on the other hand, showed more variability for all natural causes (ranging from 58.95 x1000 in small municipalities to 63.67 x 1000 in large ones, while cardiovascular and respiratory admission rates were comparable by municipality size classes (15 x1000 and 6 x1000 respectively) (Table 5.3b).

Municipality categorization by ISA and urban development showed different patterns for daily hospital admissions; in the Lazio region the greatest proportion of admissions was in the more urban municipalities (high ISA, high development) ranging between 57 and 284 for total

admissions. In Rome, the number of admissions by category of ISA or urban development were similar. The only exception was between the two highest classes; for ISA the lowest number of admissions was recorded (161, SD=79) while for high urban development zones the average daily number of admissions was 227 (SD=95) suggesting very different members in each class (Table5.3a).

Mortality rates by ISA and percent urban for municipalities in the Lazio region are quite similar. Percent urban shows slightly higher values for both natural and respiratory deaths and admissions in the intermediate class of percent urban. Total (natural) death rates range between 8.74 x 1000 and 7.30 x 1000 while respiratory death rates range between 0.38 x 1000 and 0.55 x 1000. Conversely, cardiovascular death rates are highest in municipalities with the lowest percent urban (3.74 x 1000). Similar trends were observed for hospital admission rates by percent urban for all causes in study, with total admissions comprised between 59 and 63 x1000; CVD admissions rates between 14 and 16 x 1000 and respiratory admission rates between 5.98 and 6.51 x 1000 (Table 5.3b).

Mortality rates show a rising trend by ISA class, with lower death rates in the municipalities with less impervious surfaces. Respiratory and CVD admissions on the other hand, have highest rates in the low ISA category (Table 5.3b).

Table 5.2. Descriptive statistics of daily mortality counts by spatial aggregation types (municipalities by population size, % urbanization and impervious surface.

		# spatial units	Non-accidental				Cardiovascular				Respiratory			
			Mean	SD	Min	Max	Mean	SD	Min	Max	Mean	SD	Min	Max
Lazio (by municipality)		**375**	**56.3**	**9.5**	**31**	**94**	**24.8**	**5.5**	**11**	**42**	**3.2**	**1.9**	**0**	**11**
Pop. size (inhab.)	< 15,000	326	18.2	4.6	3	37	8.1	3.0	1	18	0.9	1.0	0	5
	15,000 - 40,000	35	18.8	5.1	10	28	9.1	3.4	3	14	0.9	1.1	0	4
	40,000 - 150,000	14	19.4	4.3	13	26	7.9	3.1	4	16	1.1	1.3	0	5
Urban (%)	Low	184	8.7	3.3	2	18	4.3	2.1	0	10	0.3	0.6	0	3
	Medium	97	13.2	4.1	5	25	5.4	2.4	1	13	0.7	0.9	0	3
	High	94	36.2	8.1	20	63	16.3	5.0	5	33	2.3	1.6	0	7
ISA	Low	177	6.3	2.9	0	15	2.6	1.7	0	9	0.3	0.6	0	2
	Medium	104	12.8	4.2	4	22	5.9	2.8	1	14	0.7	0.9	0	3
	High	94	38.6	7.4	24	57	17.3	4.3	9	27	2.4	1.6	0	7
Rome (by urban zone)		**155**	**46.1**	**8.2**	**29**	**73**	**17.7**	**4.8**	**6**	**27**	**2.5**	**1.7**	**0**	**10**
Urban (%)	Low	77	11.5	3.5	4	21	4.2	2.0	0	10	0.6	0.8	0	3
	Medium	38	17.1	3.8	9	25	7.1	3.1	3	17	0.9	1.1	0	3
	High	40	18.8	3.8	13	28	7.5	2.7	3	13	1.1	1.0	0	4
ISA	Low	77	13.0	4.4	3	26	4.8	2.4	0	12	0.7	0.9	0	4
	Medium	39	17.3	3.8	12	28	6.5	2.7	2	15	0.9	0.9	0	3
	High	39	15.9	4.9	8	27	6.5	2.6	2	12	1.1	1.0	0	4

Table 5.3a. Descriptive statistics of daily hospital admissions counts by spatial aggregation types (municipalities by population size, % urbanization and impervious surface.

		# spatial units	Non-accidental (35+)				Cardiovascular (35+)				Respiratory (35+)			
			Mean	SD	Min	Max	Mean	SD	Min	Max	Mean	SD	Min	Max
Lazio (by municipality)		**375**	**441**	**56**	**278**	**598**	**106**	**18**	**59**	**154**	**39**	**9**	**16**	**70**
Pop. size (inhab.)	< 15,000	326	172	24	106	227	43	9	23	66	15	5	5	32
	15,000 - 40,000	35	139	19	105	169	31	8	17	48	13	4	6	23
	40,000 - 150,000	14	127	16	99	154	30	9	16	48	9	4	3	16
Urban (%)	Low	184	72	12	38	102	19	5	8	33	6	3	1	15
	Medium	97	91	13	61	122	23	6	7	37	9	4	1	19
	High	94	279	32	208	366	63	11	36	89	23	6	10	38
ISA	Low	177	57	10	32	85	15	5	6	29	5	3	0	12
	Medium	104	101	16	59	133	24	6	6	37	8	3	2	19
	High	94	284	37	198	362	64	13	33	100	25	7	9	43
Rome (by urban zone)		**155**	**590**	**280**	**88**	**1169**	**101**	**40**	**16**	**185**	**27**	**14**	**2**	**62**
Urban (%)	Low	77	198	93	53	355	33	13	8	55	10	5	1	24
	Medium	38	236	85	67	373	40	15	10	67	10	6	2	23
	High	40	227	95	49	387	38	16	10	65	10	5	2	21
ISA	Low	77	204	95	54	395	35	14	9	74	9	5	1	23
	Medium	39	208	98	47	386	39	16	9	67	10	5	1	24
	High	39	161	79	52	351	29	11	11	54	8	5	2	23

Table 5.3b. Mortality and hospital admission rates by spatial aggregation types (municipalities by population size, % urbanization and impervious surface).

		Mortality rate (x1000)			Hospital admissions rate age35+ (x1000)		
	Population	Natural	Cardiovascular	Respiratory	Natural	Cardiovascular	Respiratory
Lazio Region (excluding Rome)	2757101	7.92	3.55	0.46	61.96	15.51	6.33
small <15000	1082347	6.46	2.92	0.33	58.95	15.64	6.11
medium>15000-40000	873455	8.04	3.84	0.48	64.13	15.09	6.67
large >40000-150000	801299	9.75	4.10	0.62	63.67	15.79	6.27
Rome	2547677	9.11	3.72	0.53	61.86	14.46	6.38
Percent urban							
low	470783	7.30	3.74	0.38	59.04	16.82	5.98
medium	555742	8.74	3.71	0.55	63.10	16.06	6.51
high	1730576	7.82	3.45	0.46	62.39	14.97	6.37
ISA							
low	360544	7.09	3.02	0.37	59.94	17.46	6.17
medium	628432	7.89	3.66	0.49	60.00	15.35	5.91
high	1768125	8.10	3.62	0.47	63.07	15.17	6.52

Percent urban and ISA rates are only for the Lazio region (excluding Rome as population data by urbanistic zones of Rome was not available)

5.3.2 Air Temperature Exposure

Figure 5.8 and 5.9 shows the average summer temperature in the study period in the Lazio region and in Rome by spatial unit.

The distribution of mean summer temperatures varied with municipality classes, with lower temperatures in small towns and an increasing trend in temperatures for each percentile as municipalities got larger (Table 5.4). The 50th percentile, stating point for the calculated effect estimates, raged between 20°C and 22.9°C while the 75th percentile of the mean temperature distribution ranged between 22.9°C and 25.5°C. Temperatures were highest in Rome throughout the distribution as expected due to the high level of urbanization and percent of impervious surfaces. Interesting to note that the small towns have more extreme maximum and minimum temperatures, with a minimum of 2.1°C and a maximum of 32.1°C, probably related to their specific geographical location in coastal areas (warmer) or in more inland high elevated zones (cooler) and being generally more rural and surrounded by vegetated areas (figure 5.8 and 5.9).

Figure 5.8 Average summer mean temperature by municipality in the Lazio region.

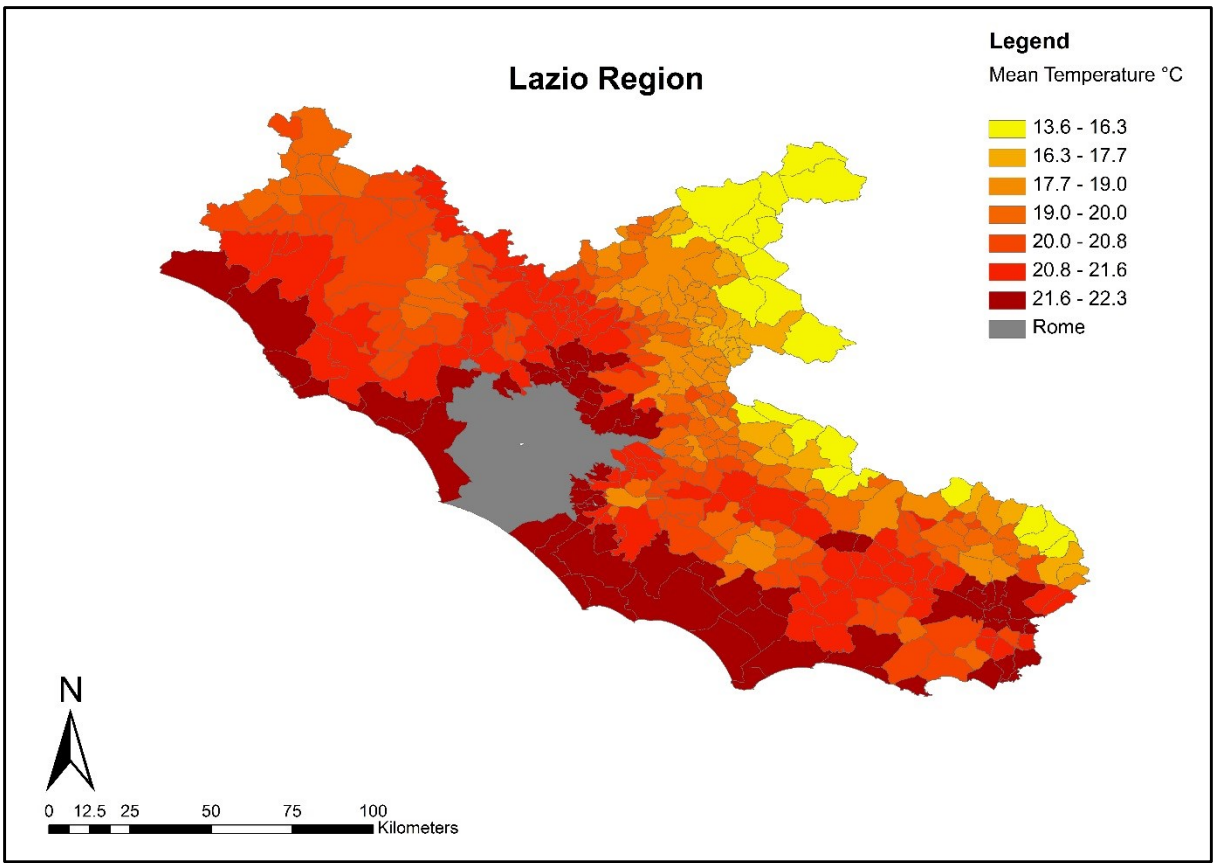

Figure 5.9 Average summer mean temperature by zone in Rome.

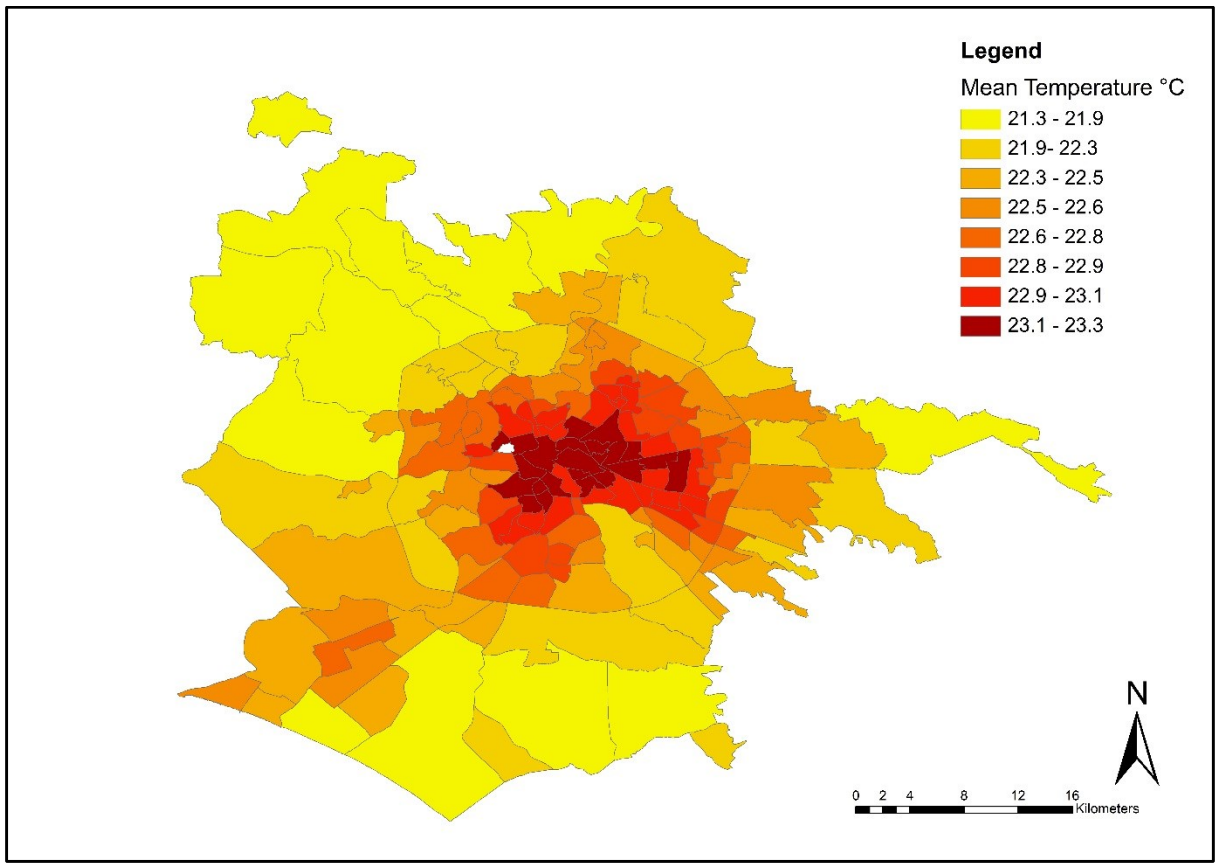

If we consider temperature distributions by percent urban and ISA, again differences between municipalities in the Lazio region and zones of Rome can be observed (table 5.5). For both ISA and percent urban an increasing trend, with higher temperature values, in municipalities with a greater percentage of area covered by anthropogenic features can be observed. Considering the two indicators by level (low, medium and high) in both Rome and Lazio the temperature distributions are similar. Interesting to note, that for Rome when comparing the two indicators the maximum temperature values are higher for the ISA classification in the more rural settings (low ISA and low percent urban), while for the medium and high development levels maximum temperature values are observed with the percent urban classification. Again Rome, was generally warmer with the temperature distribution slightly shifted to the right. Minimum values in Rome were comprised between 11.4°C and 12.6°C considering both classifications of built-up environment, while in the Lazio region minimum values were comprised between 2.1°C and 6.0°C. Among the Lazio municipalities, the median temperature value was respectively 19.5°C, 20.5°C and 21.3°C in the low, medium and high levels of the percent urban classification. While for Rome the median temperature values were higher than in the Lazio region and were respectively 22.6°C, 23.1°C and 23.3°C. Considering ISA, the median temperature value was respectively of 19.3°C, 20.7°C and 21.4°C in the low, medium and high levels of the Lazio Region. While in Rome, median values were 22.5°C, 23.1°C and 23.4°C and again higher for each level. The 75^{th} percentile ranged between 22.5°C and 24.0°C in the Lazio municipalities and between 25.3°C and 25.9°C in Rome for percent urban development. For ISA, values were similar compared to percent urban with slightly lower values for the low ISA classification and the same for medium and high ISA level.

Table 5.4 Mean summer air temperature distribution in the study period for small, medium, large municipalities of the Lazio region and in Rome.

Municipality by population size		Min	p1	p5	p10	p25	p50	mean	p75	p90	p95	p99	Max
small	<15.000	2.1	9.7	12.6	14.2	16.9	20.0	19.7	22.9	25.0	26.0	27.8	32.1
medium	15.000-40.000	7.1	12.8	15.0	16.2	18.8	21.6	21.4	24.3	26.0	27.0	28.5	31.9
large	40.000-150.000	7.0	12.8	15.2	16.4	19.0	21.9	21.6	24.6	26.3	27.2	28.6	30.8
Rome	2.700.000	11.4	14.5	16.4	17.5	20.0	22.9	22.6	25.5	27.2	28.1	29.5	33.8
Overall Lazio		**2.1**	**10.5**	**13.5**	**15.1**	**17.9**	**21.0**	**20.7**	**23.9**	**26.0**	**27.1**	**28.7**	**33.8**

Table 5.5 Mean summer air temperature distribution in the study period by percent urban and impervious surface (ISA) classes in municipalities of the Lazio region and in Rome.

		Mean Temperature distribution											
		min	**1**	**5**	**10**	**25**	**50**	**mean**	**75**	**90**	**95**	**99**	**max**
Percent Urban													
Lazio													
	low	2.1	8.9	11.9	13.6	16.3	19.5	19.3	22.5	24.7	25.8	27.6	31.5
	med	4.6	11.0	13.5	14.9	17.5	20.5	20.3	23.3	25.3	26.2	28.0	32.1
	high	5.4	12.2	14.6	15.8	18.4	21.3	21.1	24.0	25.8	26.8	28.4	31.9
Roma													
	low	11.4	14.3	16.1	17.3	19.7	22.6	22.4	25.3	26.9	27.8	29.2	33.0
	med	12.3	14.8	16.6	17.7	20.2	23.1	22.8	25.7	27.4	28.2	29.7	33.8
	high	12.5	15.0	16.8	17.9	20.4	23.3	23.0	25.9	27.5	28.4	29.8	33.3
Impervious surface (ISA)													
Lazio													
	low	2.1	8.9	11.8	13.4	16.1	19.3	19.1	22.3	24.5	25.6	27.5	31.5
	med	3.4	11.1	13.6	15.0	17.6	20.6	20.4	23.4	25.3	26.3	28.0	32.1
	high	6.0	12.3	14.6	15.9	18.5	21.4	21.1	24.1	25.9	26.8	28.4	31.9
Roma													
	low	11.4	14.2	16.1	17.2	19.7	22.5	22.3	25.2	26.8	27.7	29.1	33.8
	med	12.3	14.8	16.6	17.7	20.2	23.1	22.8	25.8	27.4	28.3	29.7	32.4
	high	12.6	15.1	16.9	18.0	20.4	23.4	23.1	26.0	27.6	28.5	29.8	32.4

5.3.3 Heat-related effects on mortality in Lazio

A non-linear association between mean temperature and mortality was identified for municipalities in the Lazio region with a steep rise in daily deaths as temperatures increased during summer. Figures 5.10-5.12 show the dose-response relationship between mean temperature and natural, cardiovascular and respiratory mortality, grouped by population size. Heat effects are shown for Rome (pink curve), for large municipalities with populations ranging from 40.000 to 150.000 inhabitants (red line), for medium sized (15.000-40.000) municipalities (blue line), for small towns with populations below 15.000 inhabitants (green line) and the overall curve for the entire region (black line) with 95% confidence interval bands in grey. Figure 5.10 shows that the effect of heat on total (natural) mortality in small and medium sized municipalities starts to increase at lower temperatures compared to Rome and large municipalities. Furthermore, the temperature distribution in Rome was slightly shifted to the right, reaching higher values and the slope in the curve seems less steep, suggesting a minor effect.

During summer, for increases in mean temperatures above the median value a statistically significant effect on mortality was observed in all groupings of municipalities in the Lazio region (Table 5.6 and figure 5.12). The effect on mortality of an increase in temperature between the 50th and 75th percentile for the entire Lazio region corresponded to a risk (RR) of 1.08 (95%CI: 1.07-1.08). The effect was lower for small rural municipalities (RR=1.06, 95%CI: 1.05-1.07) and slightly higher for medium and large municipalities (RR=1.10, 95%CI: 1.08-1.13; RR=1.13, 95%CI: 1.11-1.15). When considering more extreme temperatures, in terms of an increase between the 50th and 99th percentile, the greatest effects on mortality were observed for medium population sized municipalities with a rate ratio (RR) of 1.74 (95%CI: 1.60-1.90). Interesting to note that the effect in the extreme temperature range was the same

for the entire region, Rome and small municipalities with an increase in the risk of dying of around +50% (Table 5.6).

Furthermore, when we consider temperature increases from the 50th percentile to the maximum exposure selected (99.9th percentile) the risks were highest in small and medium sized municipalities. Estimates for very extreme values had wider confidence intervals due to the limited number of days (Figure 5.12). Finally, for natural mortality it is worth noting that compared to the entire Lazio region, higher effect-estimates were recorded in Rome for all the intervals studied. While stratifying by population size in the Lazio region, effects were greatest for small and medium sized municipalities, potentially representing rural areas.

The statistical test showed total mortality effect estimates were heterogeneous among municipality strata only for the 50th vs 75th percentile temperature intervals (Table 5.12).

Figure 5.10 Mean Temperature – all natural mortality association in the Lazio region and in Rome, summer (2001-2010).

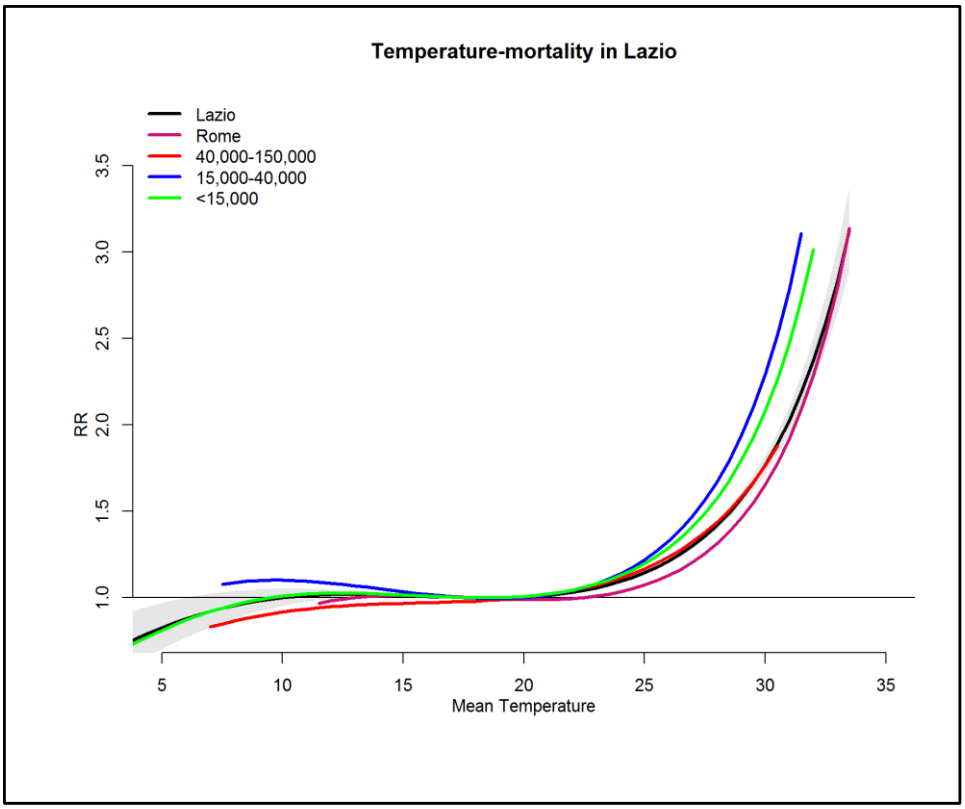

Heat-related effects on cardiovascular mortality

The dose-response relationship of cardiovascular deaths in the municipalities of the Lazio region, were very similar in shape to the overall curves, with an increase in the risk of mortality as temperatures increased but with a steeper curve, reaching higher relative risk estimates for very extreme exposures. Contrasting with total mortality, cardiovascular curves for the different sized municipality grouping were homogeneous in terms of shape thus much closer together (figure 5.11). Table 5.6 shows the risk of cardiovascular death for temperature increases during summer. The overall effect on cardiovascular mortality for an increase in temperature between the 50th and 75th percentile for the entire Lazio region corresponded to the total mortality effect, with a risk of 1.08 (95%CI: 1.07-1.08). When more extreme percentiles were considered the effect was greater for cardiovascular deaths (RR) 1.63 (95%CI: 1.58-1.67). In Rome, the heat effects were greater for cardiovascular deaths for all temperature intervals. Among the municipalities of the Lazio region, for temperatures between the 50th to 75th percentile, effects were smaller or equal to total mortality effects, while for more extreme temperature increases (50th to 99.9th) the risk of cardiovascular mortality were slightly higher (Figure 5.14). This was especially true for small and large municipalities (Table 5.6). The statistical test confirmed that effect estimates for cardiovascular mortality were heterogeneous by municipality size for all temperature intervals (Table 5.12).

Figure 5.11 Mean temperature – cardiovascular mortality association in the Lazio region and in Rome, summer (2001-2010).

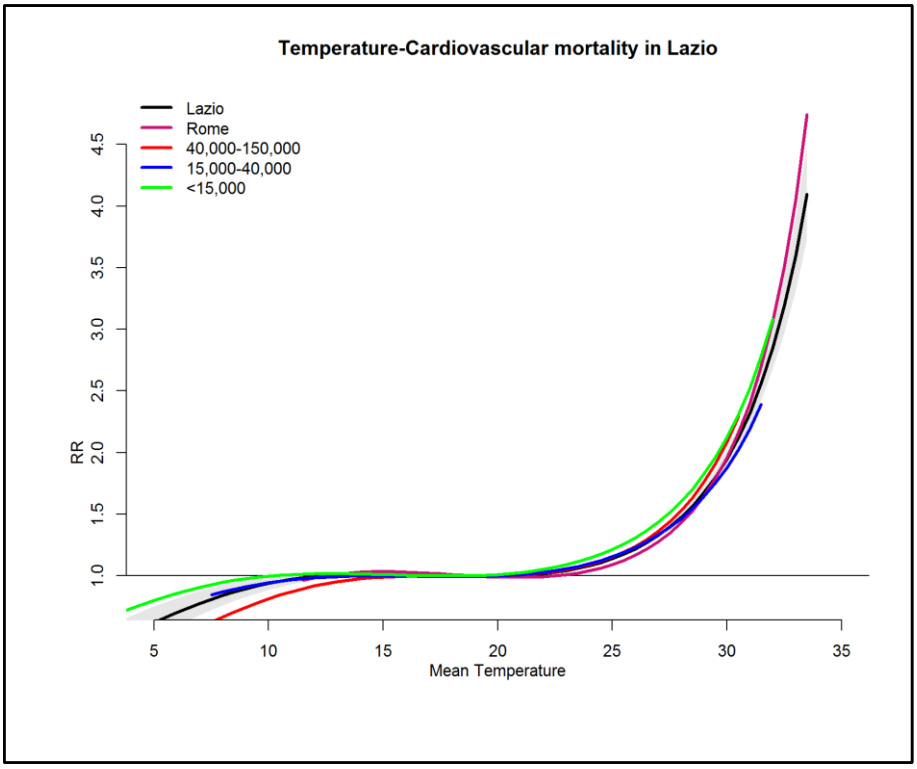

Heat-related effects on respiratory mortality

Although daily respiratory death counts were smaller in number, as mentioned before (Table 5.2) but still a significant effect of heat can be observed for respiratory causes of death (Figure 5.12 and Figure 5.15). The temperature-mortality curve for respiratory causes were somewhat diverse by municipality size, small effects were observed for municipalities with a population below 15.000 inhabitants, with very similar effects throughout the temperature distribution (Figure 5.8). While for temperature increases between the 50th and 75th percentile the greatest risk of death for respiratory causes was shown for medium and large municipalities (Figure 5.15). In Rome, the greatest risk of mortality was observed for respiratory deaths with a RR of 1.10 (95%CI: 1.09-1.11) for the 50th and 75th percentile temperature interval (table 5.6). The statistical test confirmed that effect estimates for respiratory mortality were heterogeneous by municipality size for all temperature intervals (Table 5.12).

Figure 5.12 Mean temperature – respiratory mortality association in the Lazio region and in Rome, summer (2001-2010).

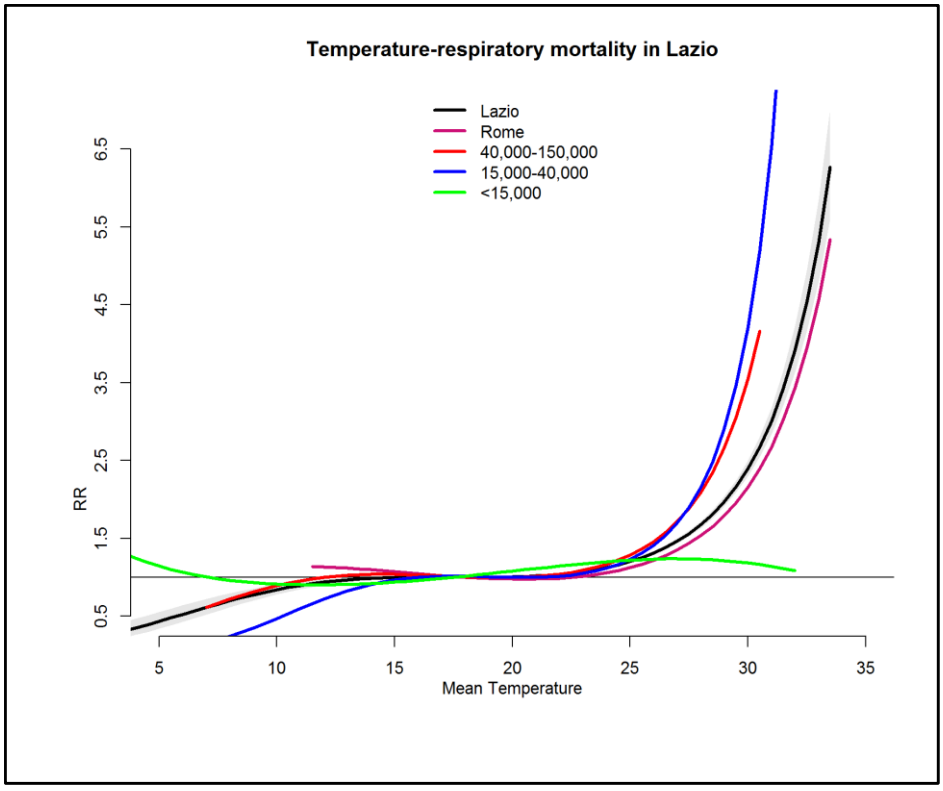

Temperature mortality effects considering a fixed temperature interval.

Considering fixed percentiles for all spatial aggregations allows for comparison municipalities and helps evaluate whether populations in urban, suburban and rural settings respond differently to a fixed set of temperatures. In some contexts, the temperature range will be higher than their own distribution and in others the same or lower. Results with fixed temperature intervals are reported in Table 5.7. The assumption here is that local populations are acclimatized to their local climate and different absolute temperatures might correspond to more or less extreme conditions. Considering the first temperature interval (p50 to p75=21.0°C-23.9°C) the effect on mortality was greater in medium sized municipalities as for the main analysis. Compared to the overall Lazio estimate (RR=1.08,95%CI: 1.07-1.08) all regional municipalities had a greater effect while Rome was below the regional overall heat risk estimate. Interesting to note that for small municipalities, the effect estimates were higher than the main analysis, as percentiles corresponded to higher temperatures (RR=1.10, 95%CI: 1.09-1.11), while for all other spatial aggregations the risks were slightly smaller (Table 5.7). Considering more extreme temperatures (p50 to p99=21°C-28.8°C) all effects estimates were higher than the regional overall estimate, except for Rome. In general, fixed interval estimates were larger for small municipalities and more contained in Rome suggesting that rural populations are less acclimatized to high temperatures as also shown by the spatial unit specific temperature distributions (Table 5.7).

Cardiovascular mortality estimates considering fixed temperature intervals again showed highest effects in the small municipalities and more contained effects in Rome. While heat continued to have a limited effect on respiratory deaths in small municipalities, also considering a fixed temperature range, while similarly to cardiovascular mortality, effects in Rome were below the Lazio overall estimate (Table 5.7).

Table 5.6 Relative risk of natural, cardiovascular and respiratory mortality for increases in mean temperature above the 50th percentile of area specific distributions.

				75th percentile		99th percentile		99.9th percentile	
		50th	75th	RR	95%CI	RR	95%CI	RR	95%CI
	Total Mortality								
Municipalities	small <15000	20.0	22.9	**1.06**	1.05 - 1.07	**1.53**	1.47 - 1.59	**1.88**	1.77 - 2.01
	medium>15000-40000	21.6	24.3	**1.13**	1.11 - 1.15	**1.74**	1.60 - 1.90	**2.15**	1.88 - 2.45
	large >40000-150000	21.9	24.6	**1.10**	1.08 - 1.13	**1.46**	1.34 - 1.60	**1.66**	1.45 - 1.91
	Rome	22.9	25.1	**1.09**	1.08 - 1.10	**1.54**	1.47 - 1.60	**1.85**	1.73 - 1.98
	Overall Lazio	*21.0*	*23.9*	***1.08***	*1.07 - 1.08*	***1.52***	*1.48 - 1.55*	***1.79***	*1.73 - 1.85*
	Cardiovascular Mortality								
Municipalities	small <15000	20.0	22.9	**1.07**	1.06 - 1.08	**1.55**	1.48 - 1.62	**1.91**	1.79 - 2.05
	medium>15000-40000	21.6	24.3	**1.09**	1.06 - 1.12	**1.52**	1.36 - 1.69	**1.79**	1.51 - 2.11
	large >40000-150000	21.9	24.6	**1.10**	1.07 - 1.14	**1.62**	1.43 - 1.85	**1.97**	1.62 - 2.39
	Rome	22.9	25.1	**1.12**	1.10 - 1.13	**1.78**	1.69 - 1.87	**2.28**	2.10 - 2.48
	Overall Lazio	*21.0*	*23.9*	***1.08***	*1.07 - 1.08*	***1.63***	*1.58 - 1.67*	***2.01***	*1.93 - 2.09*
	Respiratory Mortality								
Municipalities	small <15000	20.0	22.9	**1.08**	1.07 - 1.09	**1.14**	1.09 - 1.20	**1.11**	1.03 - 1.20
	medium>15000-40000	21.6	24.3	**1.14**	1.10 - 1.17	**2.47**	2.16 - 2.81	**3.86**	3.14 - 4.74
	large >40000-150000	21.9	24.6	**1.19**	1.14 - 1.25	**2.32**	1.89 - 2.84	**3.21**	2.37 - 4.35
	Rome	22.9	25.1	**1.15**	1.14 - 1.17	**1.94**	1.82 - 2.06	**2.53**	2.29 - 2.78
	Overall Lazio	*21.0*	*23.9*	***1.10***	*1.09 - 1.11*	***1.87***	*1.82 - 1.93*	***2.46***	*2.35 - 2.58*

Figure 5.13 Heat-related effects on total natural mortality. Relative risk for increases in mean temperature between the 50th and 75th, 50th to 99th and 50th to extreme percentile of the area specific distributions. Estimates for small, medium, large municipalities in Lazio and Rome.

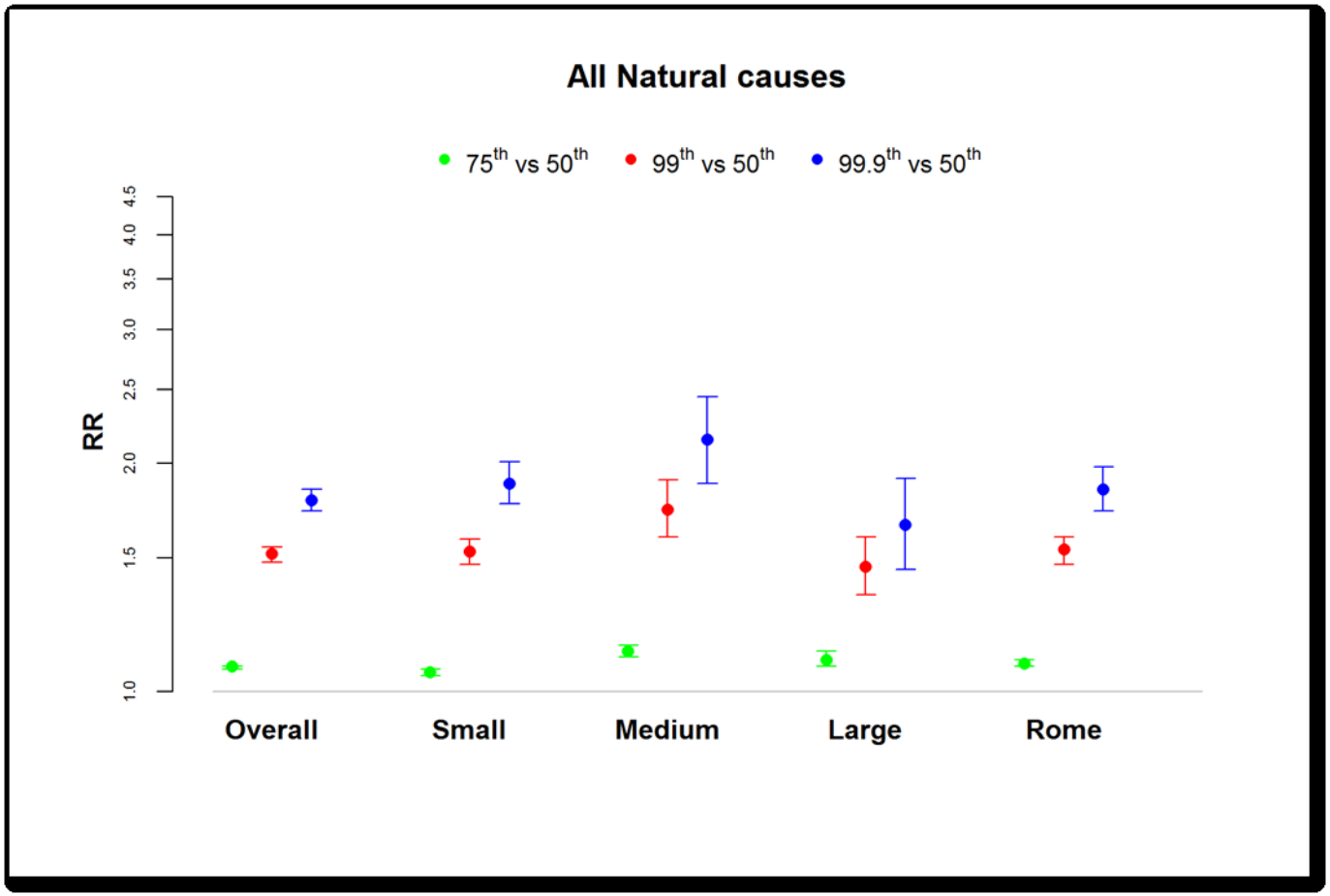

Figure 5.14 Heat-related effects on cardiovascular mortality. Relative risk for increases in mean temperature between the 50th and 75th, 50th to 99th and 50th to extreme percentile of the area specific distributions. Estimates for small, medium, large municipalities in Lazio and Rome.

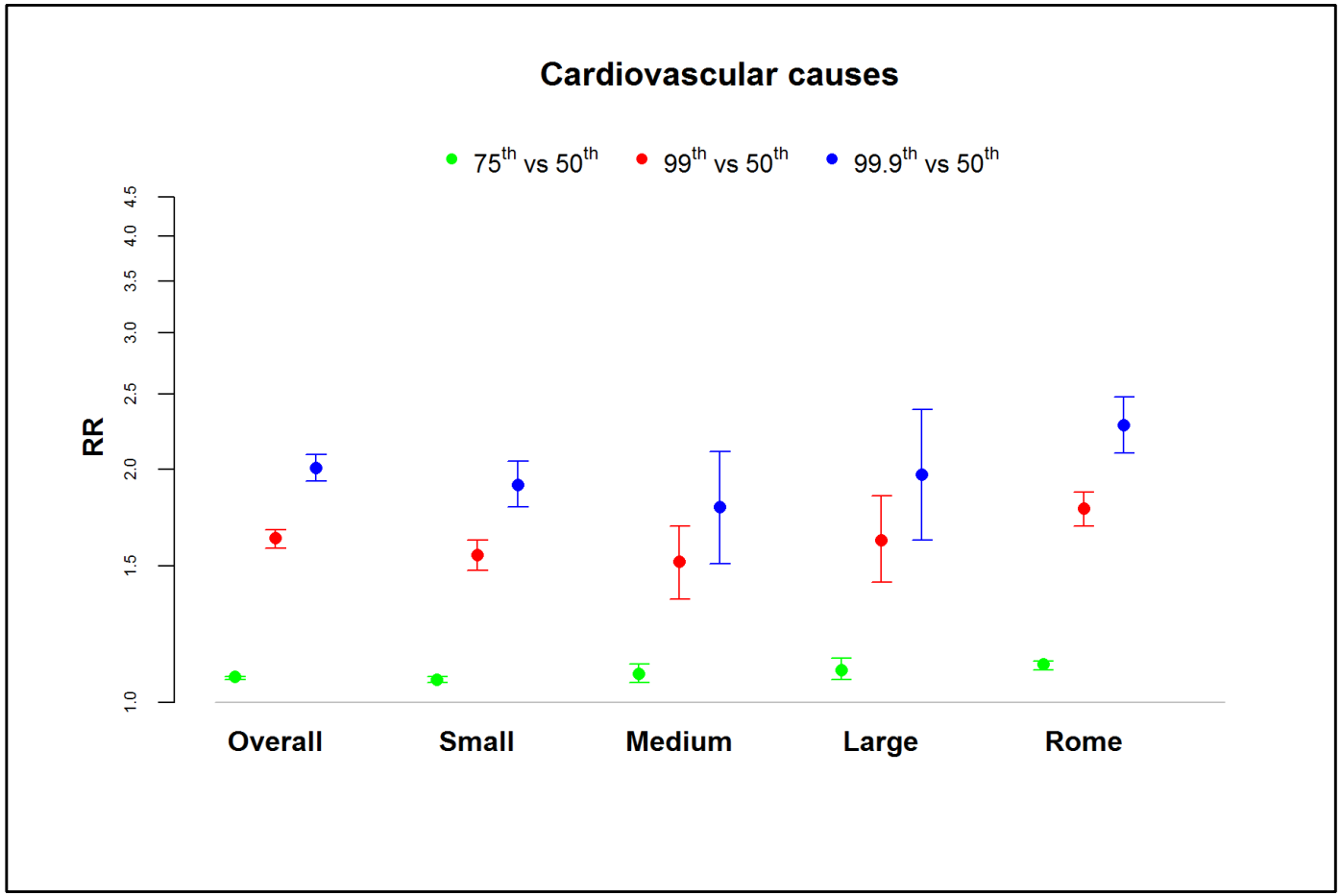

Figure 5.15 Heat-related effects on respiratory mortality. Relative risk for increases in mean temperature between the 50th and 75th, 50th to 99th and 50th to extreme percentile of the area specific distributions. Estimates for small, medium, large municipalities in Lazio and Rome.

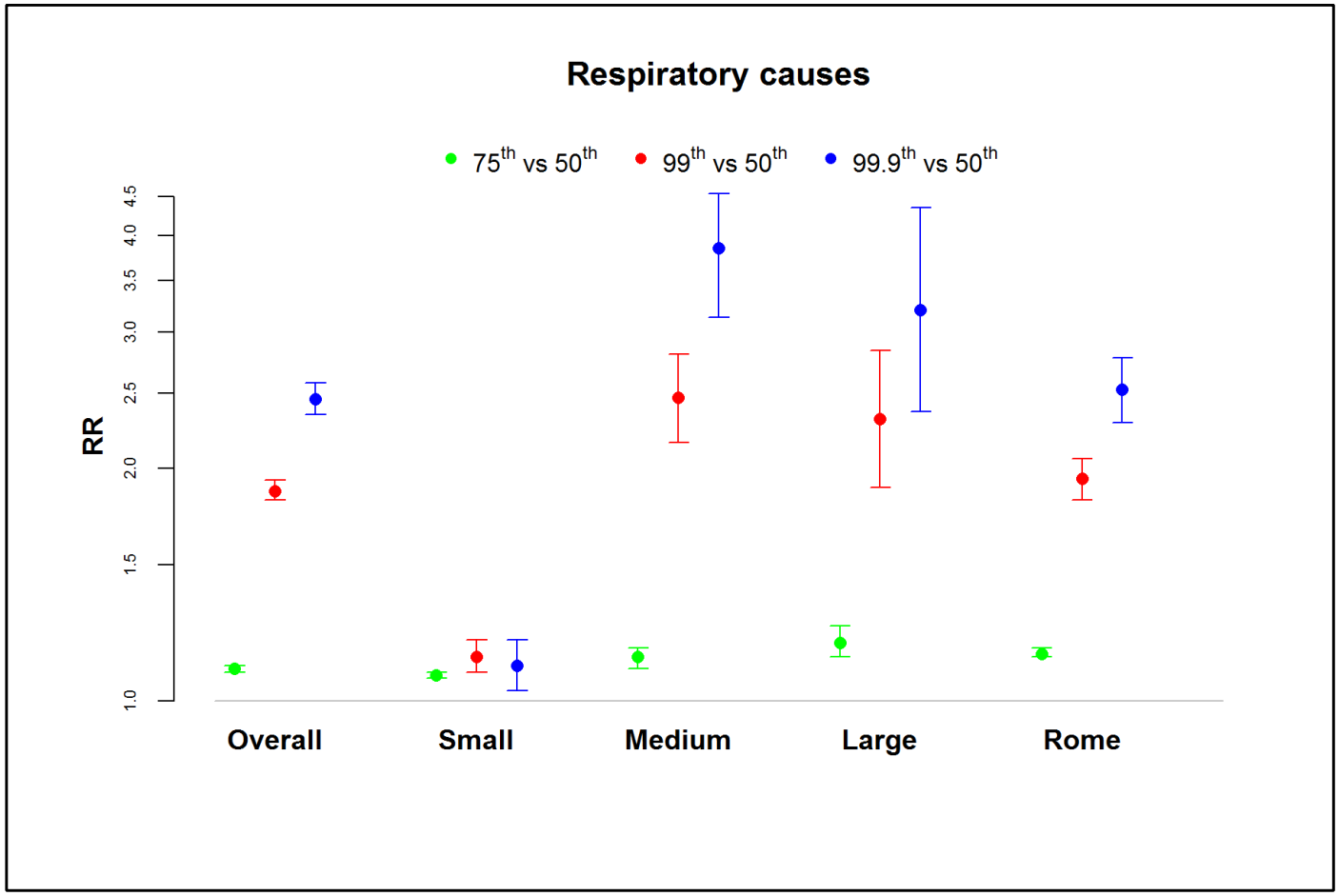

Table 5.7 Relative risk in natural, cardiovascular and respiratory mortality for increases in mean temperature above the 50th percentile of the Lazio regional distribution (fixed temperatures intervals for all municipalities).

				75th percentile		99th percentile		99.9th percentile	
		50th	75th	RR	95%CI	RR	95%CI	RR	95%CI
	Total Mortality								
Municipalities	small <15000	*21.0*	*23.9*	***1.10***	1.09 - 1.11	**1.71**	1.62 - 1.80	**2.11**	1.95 - 2.28
	medium>15000-40000	*21.0*	*23.9*	***1.12***	1.09 - 1.14	**1.85**	1.68 - 2.03	**2.34**	2.02 - 2.72
	large >40000-150000	*21.0*	*23.9*	***1.09***	1.07 - 1.11	**1.52**	1.38 - 1.68	**1.78**	1.52 - 2.07
	Rome	*21.0*	*23.9*	***1.04***	1.03 - 1.06	**1.44**	1.40 - 1.49	**1.72**	1.63 - 1.81
	Overall Lazio	*21.0*	*23.9*	***1.08***	*1.07 - 1.08*	***1.52***	*1.48 - 1.55*	***1.79***	*1.73 - 1.85*
	Cardiovascular Mortality								
Municipalities	small <15000	*21.0*	*23.9*	***1.11***	1.09 - 1.12	**1.73**	1.63 - 1.83	**2.14**	1.96 - 2.33
	medium>15000-40000	*21.0*	*23.9*	***1.08***	1.05 - 1.11	**1.59**	1.41 - 1.79	**1.91**	1.58 - 2.31
	large >40000-150000	*21.0*	*23.9*	***1.08***	1.05 - 1.11	**1.69**	1.47 - 1.94	**2.15**	1.73 - 2.67
	Rome	*21.0*	*23.9*	***1.05***	1.03 - 1.07	**1.62**	1.55 - 1.68	**2.06**	1.93 - 2.20
	Overall Lazio	*21.0*	*23.9*	***1.08***	*1.07 - 1.08*	***1.63***	*1.58 - 1.67*	***2.01***	*1.93 - 2.09*
	Respiratory Mortality								
Municipalities	small <15000	*21.0*	*23.9*	***1.08***	1.06 - 1.09	**1.09**	1.02 - 1.17	**1.06**	0.96 - 1.16
	medium>15000-40000	*21.0*	*23.9*	***1.11***	1.07 - 1.15	**2.72**	2.35 - 3.15	**4.56**	3.62 - 5.76
	large >40000-150000	*21.0*	*23.9*	***1.15***	1.09 - 1.20	**2.50**	2.01 - 3.10	**3.73**	2.65 - 5.24
	Rome	*21.0*	*23.9*	***1.08***	1.06 - 1.10	**1.78**	1.69 - 1.86	**2.30**	2.13 - 2.48
	Overall Lazio	*21.0*	*23.9*	***1.10***	*1.09 - 1.11*	***1.87***	*1.82 - 1.93*	***2.46***	*2.35 - 2.58*

Attributable Deaths

Table 5.8 shows the number of heat-attributable deaths by municipality classes in Lazio and in Rome by zones for temperature increases between the 50th and 75th percentile and for extreme temperatures (75th-99th percentile). Although estimates comprise 10 summers, the burden associated to heat was quite considerable. In Rome, the total number of heat attributable deaths for increases between 50-75th percentile accounted for 987 deaths (on average 98 per summer) in the period 2001-2010. While for the same temperature interval, 629 deaths were related to heat in the Lazio region. The highest burden was for more extreme temperatures in all municipality type groupings in Lazio and in Rome, with 4434 deaths in Rome and 3127 deaths in the Lazio region for temperatures between the 75th and 99th percentile. Interesting to note that in Rome and small municipalities, cardiovascular heat attributable deaths made up around 50% of the total heat-related deaths while for medium and large municipalities only around 35%. Overall, respiratory heat attributable deaths were a minor proportion, around 8% for Rome and Lazio (ranging between 5% and 15%). Cardiovascular heat-attributable deaths, for the two temperature intervals, were 500 and 2286 deaths respectively in Rome, and 234 and 1256 deaths in Lazio. Moreover, respiratory heat-attributable deaths for the two temperature intervals were respectively 81 and 377 in Rome, and 53 and 255 deaths in Lazio.

Years of life Lost (YLL)

From the simple calculations carried out for the whole Lazio region (Rome and Lazio municipalities combined) in the study period, the YLL were 16523 (on average 1652 YLL/year) associated to moderate summer temperatures (increases between 50th and 75th percentile). For extreme temperatures (75th to 99th percentile), the number of YLL was even greater; with 77271 over the study period (average of 7727 YLL).

Table 5.8 Heat Attributable Deaths. Attributable deaths for natural, cardiovascular and respiratory causes for mean temperature increases between the 50th – 75th and 75th- 99th percentile of area specific distributions. Summers (2000-2010).

			50-75th percentile			75-99th percentile		
		50th	AD	95%eCI		AD	95%eCI	
	Total Mortality							
Municipalities	small <15000	20.0	**84.5**	55.3	113.6	**831.2**	733.2	931.7
	medium>15000-40000	21.6	**315.7**	266.7	364.6	**1393.7**	1200.5	1567.8
	large >40000-150000	21.9	**229.0**	172.3	282.6	**902.5**	741.6	1064.7
	Rome	22.9	**987.8**	896.1	1080.1	**4434.4**	4013.7	4868.4
	Cardiovascular Mortality							
Municipalities	small <15000	20.0	**45.1**	31.4	59.5	**390.4**	344.5	438.2
	medium>15000-40000	21.6	**104.1**	76.5	132.0	**476.7**	367.6	571.8
	large >40000-150000	21.9	**84.8**	50.1	117.3	**388.8**	294.0	481.2
	Rome	22.9	**500.9**	461.1	544.8	**2285.5**	2106.5	2478.3
	Respiratory Mortality							
Municipalities	small <15000	20.0	**13.8**	12.0	15.6	**45.4**	39.6	51.1
	medium>15000-40000	21.6	**18.1**	13.9	22.1	**114.1**	99.7	128.4
	large >40000-150000	21.9	**21.3**	13.6	28.6	**95.1**	73.0	114.8
	Rome	22.9	**80.8**	74.0	87.9	**377.4**	345.3	410.7

5.3.4. Heat-related effects on hospital admissions

Conversely to what was observed for mortality, the increase in temperatures didn't seem to have an effect on hospital admissions, in particular for total natural and cardiovascular disease where curve were flat (Figures 5.16-5.18). An effect of heat was seen, to some extent, for respiratory hospital admissions with an increase in admissions with rising temperatures especially in small and medium sized municipalities.

The effect of heat on hospital admissions was limited, with non-significant estimates for all cause specific hospital admissions considered (Table 5.9 and Figures 5.19-5.21). Generally, there was no or a slight protective effect of moderate heat (50^{th} to 75^{th}) or extreme heat (50^{th}-99^{th}) on total natural admissions overall, except for small municipalities which had a statistically significant risk for increases in temperatures in the first temperature range ($RR50^{th}vs75^{th}$=1.010, 95%CI: 1.004-1.016). For cardiovascular hospital admissions no effect or a slight protective effect of heat was observed in Rome and small municipalities.

The association between respiratory admissions and heat was observed (figure 5.17 and figure 5.21), with a rising trend of risk in all municipalities. Statistically significant risks for temperature increases between the 50^{th} and 99^{th} percentile was observed only for the entire Lazio region and in small and medium municipalities (RR=1.065, 95%CI: 1.004-1.016; $RR50^{th}vs75^{th}$=1.173, 95%CI: 1.054-1.306, respectively). In the warm period considered, extremely low temperatures (Figure 5.18) between 5-12°C, seem to have a slight protective effect, noteworthy that the section of the curve only represents less than 1% of the values.

Heterogeneity in effect estimates by municipality population size was observed for natural admissions (for all temperature intervals) and for cardiovascular admissions only for temperature increases between the 50^{th} vs 75^{th} percentile (Table 5.12).

Figure 5.16 Mean temperature – hospital admissions association in the Lazio region and in Rome, summer (2001-2010).

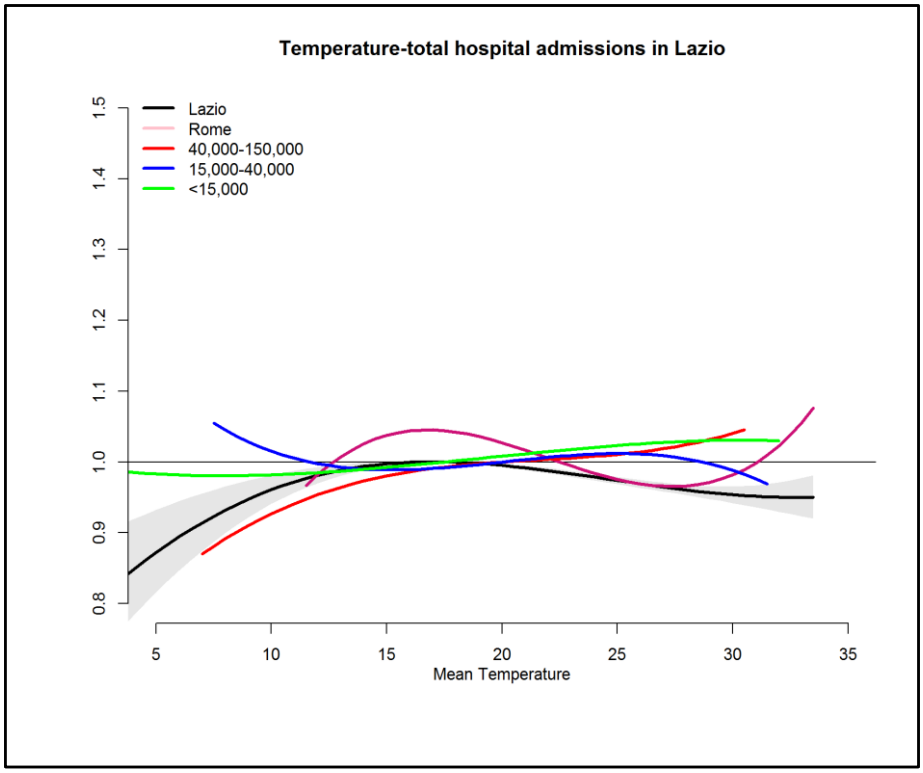

Figure 5.17 Mean temperature – cardiovascular admissions association in the Lazio region and in Rome, summer (2001-2010).

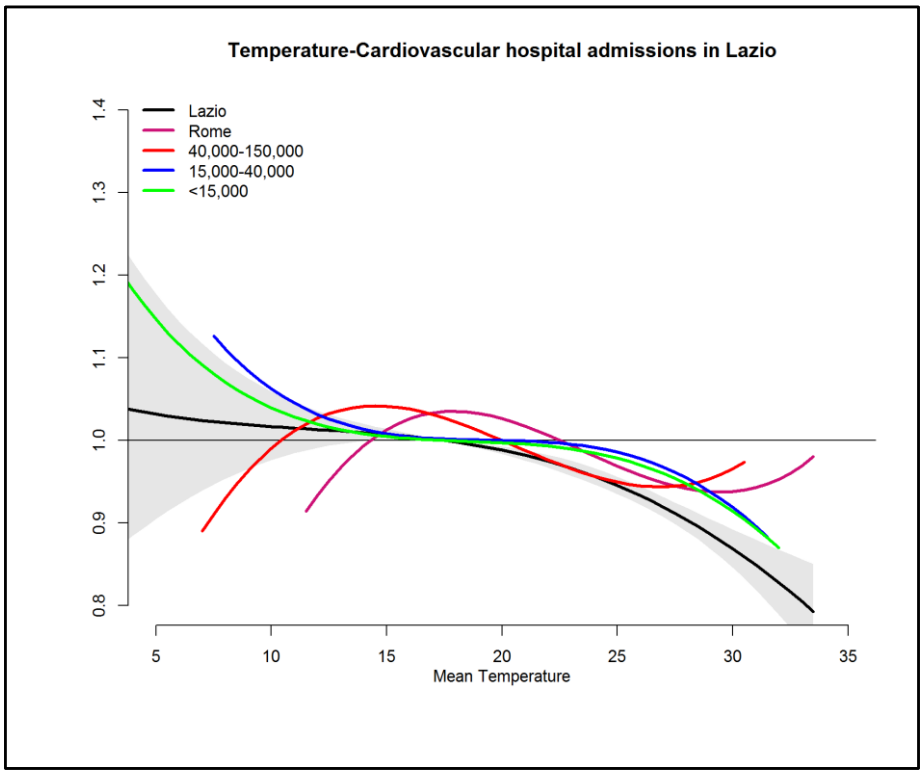

Figure 5.18 Mean temperature – respiratory admissions association in the Lazio region and in Rome, summer (2001-2010).

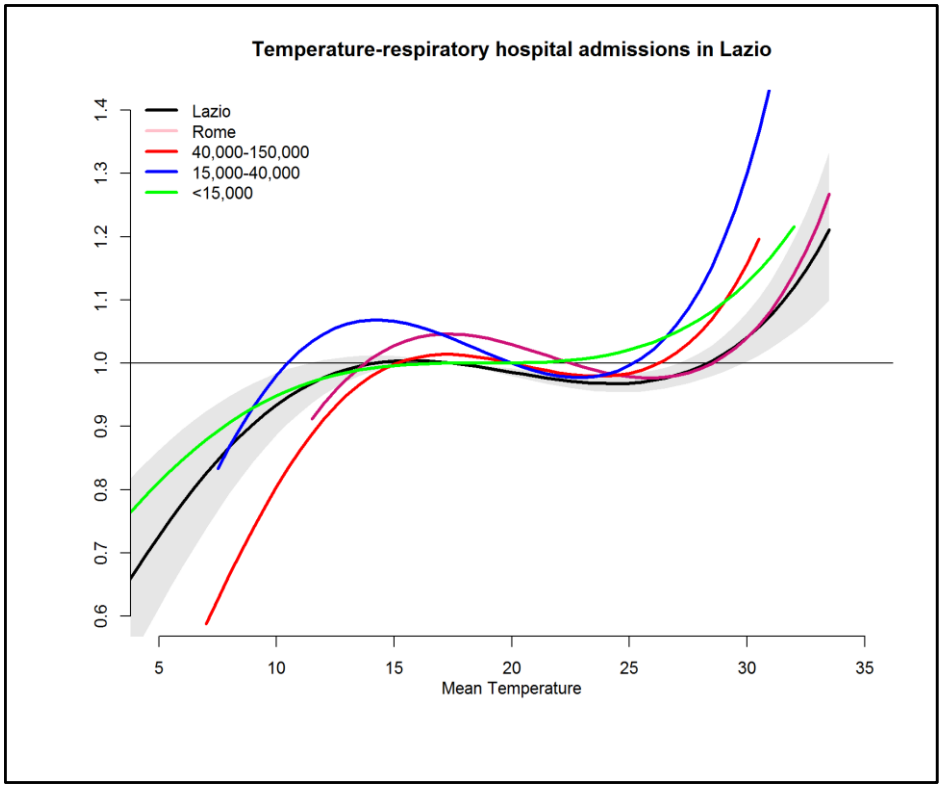

Table 5.9 Relative risk in natural, cardiovascular and respiratory hospital admissions for increases in mean temperature above the 50th percentile of area specific distributions.

	Hospital admissions	50th	75th	75th percentile RR	75th percentile 95%CI	99th percentile RR	99th percentile 95%CI	99.9th percentile RR	99.9th percentile 95%CI
	Natural								
Municipalities	small <15000	20.0	22.9	**1.010**	1.004 - 1.016	**1.031**	1.005 - 1.058	1.039	0.997 - 1.083
Municipalities	medium>15000-40000	21.6	24.3	1.007	0.999 - 1.015	1.016	0.981 - 1.053	1.018	0.963 - 1.077
Municipalities	large >40000-150000	21.9	24.6	1.006	0.998 - 1.015	1.035	0.997 - 1.074	1.051	0.994 - 1.111
Municipalities	Rome	22.9	25.1	**0.966**	0.963 - 0.970	**0.968**	0.951 - 0.985	0.992	0.964 - 1.021
Municipalities	*Overall Lazio*	*21.0*	*23.9*	***0.983***	*0.981 - 0.986*	***0.951***	*0.941 - 0.961*	***0.943***	*0.928 - 0.959*
	Cardiovascular								
Municipalities	small <15000	20.0	22.9	0.993	0.984 - 1.002	**0.953**	0.917 - 0.989	**0.928**	0.873 - 0.986
Municipalities	medium>15000-40000	21.6	24.3	0.992	0.975 - 1.008	0.948	0.880 - 1.022	0.924	0.823 - 1.039
Municipalities	large >40000-150000	21.9	24.6	**0.974**	0.957 - 0.991	0.972	0.899 - 1.050	0.985	0.877 - 1.106
Municipalities	Rome	22.9	25.1	**0.959**	0.951 - 0.966	**0.918**	0.886 - 0.953	**0.918**	0.866 - 0.974
Municipalities	*Overall Lazio*	*21.0*	*23.9*	***0.975***	*0.970 - 0.980*	***0.907***	*0.889 - 0.925*	***0.881***	*0.855 - 0.908*
	Respiratory								
Municipalities	small <15000	20.0	22.9	**1.006**	0.996 - 1.016	**1.065**	1.020 - 1.112	**1.216**	1.060 - 1.396
Municipalities	medium>15000-40000	21.6	24.3	1.002	0.980 - 1.025	**1.173**	1.054 - 1.306	**1.299**	1.101 - 1.533
Municipalities	large >40000-150000	21.9	24.6	0.996	0.968 - 1.024	1.090	0.960 - 1.237	1.160	0.959 - 1.403
Municipalities	Rome	22.9	25.1	**0.981**	0.970 - 0.993	1.029	0.973 - 1.087	1.078	0.987 - 1.178
Municipalities	*Overall Lazio*	*21.0*	*23.9*	*0.998*	*0.995 - 1.000*	***1.041***	*1.014 - 1.069*	***1.079***	*1.035 - 1.126*

Figure 5.19 Heat-related effects on total hospital admissions. Risks for increases in mean temperature between the 50th and 75th, 50th to 99th and 50th to extreme percentile of the area specific distributions. Estimates for small, medium, large municipalities in Lazio and Rome.

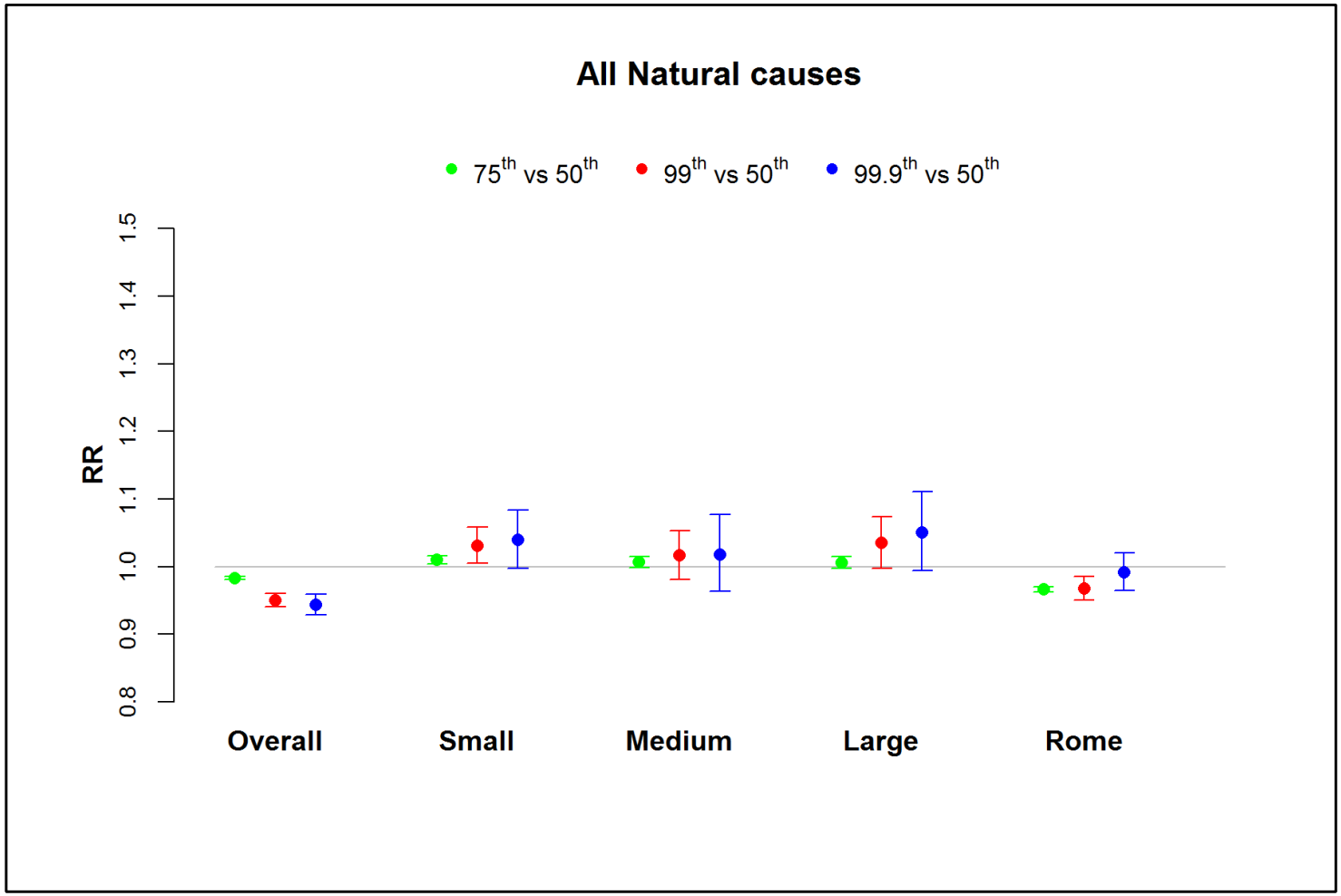

Figure 5.20 Heat-related effects on cardiovascular hospital admissions. Risks for increases in mean temperature between the 50th and 75th, 50th to 99th and 50th to extreme percentile of the area specific distributions. Estimates for small, medium, large municipalities in Lazio and Rome.

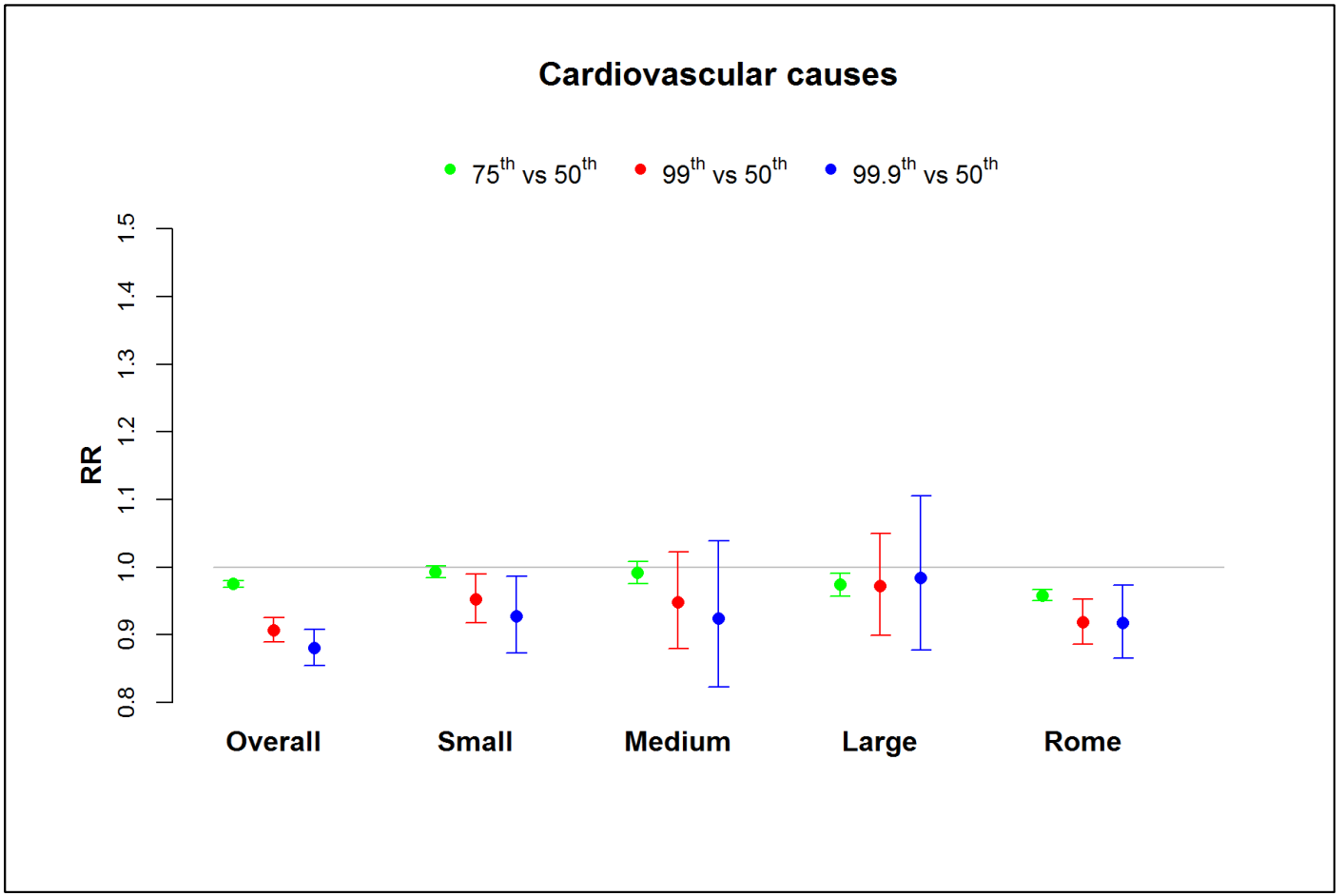

Figure 5.21 Heat-related effects on respiratory hospital admissions. Risk for increases in mean temperature between the 50th and 75th, 50th to 99th and 50th to extreme percentile of the area specific distributions. Estimates for small, medium, large municipalities in Lazio and Rome.

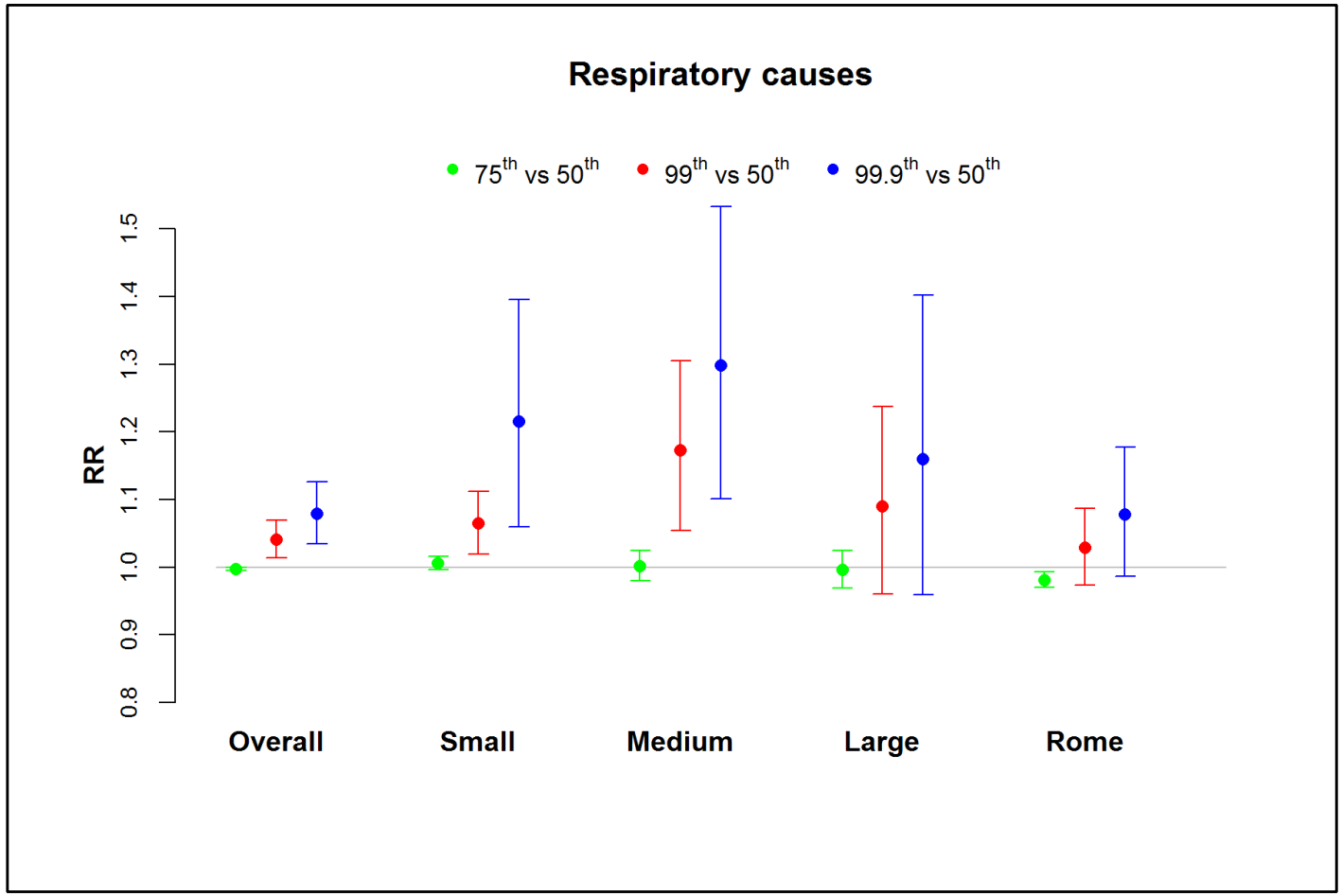

Sensitivity analysis without 2003

The summer of 2003 was an exceptional year across Europe, including Italy. To ensure the robustness of estimates and the role of such an extreme year the main analysis was re-run excluding 2003.

In table 5.10A the effect estimates were calculated on the overall temperature distribution (including 2003) as in the main analysis but excluding daily temperature and outcome data (mortality/admissions) for 2003 from the analysis. Results were pretty much comparable to main results for both mortality and hospital admissions.

Table 5.10B shows the effect estimates recalculated on the temperature distribution excluding 2003. Mortality effect estimates for mean temperature increases between the 50^{th} and 75^{th} percentile were comparable to the main analysis for the Lazio region, but not for Rome. Effect estimates were slightly lower when extreme temperature intervals were considered (50^{th} to 99^{th} percentile) compared to the main analysis. The risk in mortality for increases in mean temperature between the 50^{th} and 99^{th} percentile for the entire Lazio region went from an RR of 1.52 (CI95% 1.48-1.55) to a RR of 1.41 (CI95% 1.38-1.43). As expected, when extreme values were included (99.9^{th} percentile), risk estimates were more contained in magnitude when excluding 2003.

Hospital admission risk estimates excluding 2003 on the other hand remained unvaried even when considering extreme values, confirming the weak association between hospital admissions and heat. Only for Rome, a slight decline was observed when considering changes in temperature between the 50^{th} and 99.9^{th} percentile.

Table 5.10A Analysis excluding 2003. Relative risk in natural mortality and hospital admissions for increases in mean temperature between the 50th – 75th , 50th – 90th and 50th-99th percentile of the Lazio regional distribution (mean temperature distribution with 2003).

A					75th percentile			99th percentile			99.9th percentile		
	50th	75th	99th	99.9th	RR	95%CI		RR	95%CI		RR	95%CI	
Total Mortality													
small <15000	20.0	22.9	27.8	29.4	***1.07***	*1.06*	*1.08*	***1.54***	*1.47*	*1.61*	***1.92***	*1.79*	*2.07*
medium>15000-40000	21.6	24.3	28.5	29.8	***1.13***	*1.10*	*1.15*	***1.72***	*1.55*	*1.91*	***2.12***	*1.80*	*2.49*
large >40000-150000	21.9	24.6	28.6	29.8	***1.10***	*1.08*	*1.13*	***1.49***	*1.34*	*1.66*	***1.71***	*1.45*	*2.02*
Rome	22.9	25.5	29.5	30.8	***1.09***	*1.08*	*1.10*	***1.57***	*1.49*	*1.65*	***1.90***	*1.75*	*2.07*
Overall Lazio	21.0	23.9	28.8	30.2	***1.07***	*1.07*	*1.08*	***1.52***	*1.49*	*1.56*	***1.81***	*1.74*	*1.88*
Natural admissions													
small <15000	20.0	22.9	27.8	29.4	***1.01***	*1.00*	*1.02*	***1.03***	*1.00*	*1.06*	***1.04***	*0.99*	*1.09*
medium>15000-40000	21.6	24.3	28.5	29.8	***1.01***	*1.00*	*1.02*	***1.03***	*0.99*	*1.08*	***1.04***	*0.97*	*1.11*
large >40000-150000	21.9	24.6	28.6	29.8	***1.01***	*1.00*	*1.01*	***1.04***	*1.00*	*1.09*	***1.06***	*0.99*	*1.14*
Rome	22.9	25.5	29.5	30.8	***0.97***	*0.97*	*0.97*	***0.99***	*0.97*	*1.02*	***1.03***	*1.00*	*1.07*
Overall Lazio	21.0	23.9	28.8	30.2	***0.98***	*0.98*	*0.98*	***0.96***	*0.95*	*0.97*	***0.96***	*0.94*	*0.98*

Table 5.10A Analysis excluding 2003. Relative risk in natural mortality and hospital admissions for increases in mean temperature between the 50th – 75th , 50th – 90th and 50th-99th percentile of the Lazio regional distribution (mean temperature distribution without 2003).

B					75th percentile			99th percentile			99.9th percentile		
	50th	75th	99th	99.9th	RR	95%CI		RR	95%CI		RR	95%CI	
Total Mortality													
small <15000	19.8	22.6	27.1	28.5	***1.06***	*1.05*	*1.07*	***1.43***	*1.38*	*1.48*	***1.69***	*1.60*	*1.79*
medium>15000-40000	21.5	24.0	27.6	28.9	***1.11***	*1.09*	*1.13*	***1.53***	*1.42*	*1.65*	***1.83***	*1.63*	*2.07*
large >40000-150000	21.8	24.3	27.7	28.8	***1.09***	*1.07*	*1.11*	***1.37***	*1.27*	*1.48*	***1.53***	*1.36*	*1.72*
Rome	22.7	25.2	28.7	30.1	***1.05***	*1.04*	*1.06*	***1.30***	*1.26*	*1.33*	***1.46***	*1.40*	*1.51*
Overall Lazio	20.8	23.6	28.0	29.5	***1.06***	*1.06*	*1.07*	***1.41***	*1.38*	*1.43*	***1.66***	*1.61*	*1.71*
Natural admissions													
small <15000	19.8	22.6	27.1	28.5	***1.009***	*1.00*	*1.02*	***1.03***	*1.01*	*1.05*	***1.04***	*1.00*	*1.08*
medium>15000-40000	21.5	24.0	27.6	28.9	***1.007***	*1.00*	*1.02*	***1.03***	*0.99*	*1.06*	***1.03***	*0.98*	*1.09*
large >40000-150000	21.8	24.3	27.7	28.8	***1.004***	*1.00*	*1.01*	***1.03***	*1.00*	*1.06*	***1.05***	*1.00*	*1.10*
Rome	22.7	25.2	28.7	30.1	***0.965***	*0.96*	*0.97*	***0.95***	*0.94*	*0.96*	***0.96***	*0.95*	*0.98*
Overall Lazio	20.8	23.6	28.0	29.5	***0.982***	*0.98*	*0.98*	***0.96***	*0.95*	*0.97*	***0.96***	*0.94*	*0.97*

5.3.5 Effect of heat on mortality by urban development (%pct urban) and impervious surface (ISA)

The analysis of heat on mortality stratifying municipalities in the Lazio region and the urbanistic zones in Rome by indexes of urban development and impervious surfaces showed a trend in the heat-related effects (Figure 5.22-5.25). In Rome, the increase in temperature between the 50th percentile to extreme values (99th) was comprised between 48% and 60% for classes of urban development (Table 5.11). In the Lazio region, the risk increased from RR=1.05 (95%CI: 1.04-1.07) in the municipalities with percent urban below the 50th percentile to RR=1.10 (95%CI: 1.08-1.11) in those with percent urban above the 75th percentile. While for a rise in mean temperature between the 50th and 99th percentile, the greatest effect on mortality was observed for municipalities with a low urban development in the Lazio region (RR=1.87;95%CI: 1.79-1.95). The statistical test for heterogeneity showed that effects estimates (for all temperature intervals) were different by urban development strata only in the Lazio region (Table 5.12).

Overall, for ISA groupings heat effects were similar in Rome and Lazio, with slightly greater effects for medium level ISA. When considering results for ISA distribution in Lazio similar results were observed for temperature increases in the moderate range (50th to 75th percentile) compared to urban development; while when including more extreme temperatures (50th vs 99th percentile) greater effect estimates were estimated for medium and high ISA compared to urban development, while for low ISA a smaller risk was found compared to low urban development (Table 5.11). Estimates among ISA strata were different only for temperature increases between the 50th and 75th percentile (Table 5.12).

In Rome, classification by ISA gave slightly lower effect estimates (Figure 5.24 and 5.25). In zones which had a level of impervious surface encompassed between the 50th and 75th percentile (ISA= 49.5-76.6) a +12% increase in the risk of mortality was observed (Table 5.11).

Estimates for extreme temperatures had lower values compared to those found for urban development (Table 5.11). Overall, an increasing trend in effects by levels of exposure was observed but estimates by both ISA and percent urban strata were not statistically different in Rome (Table 5.12).

Figure 5.22 Mean temperature – mortality association in the Lazio region by urban development, summer (2001-2010).

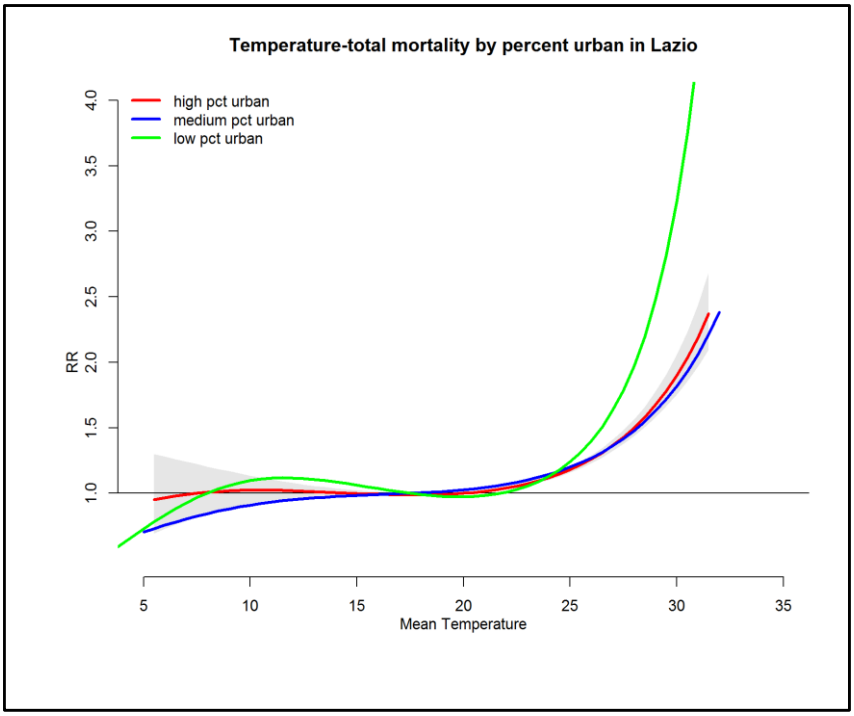

Figure 5.23 Mean temperature – mortality association in the Lazio region by ISA, summer (2001-2010).

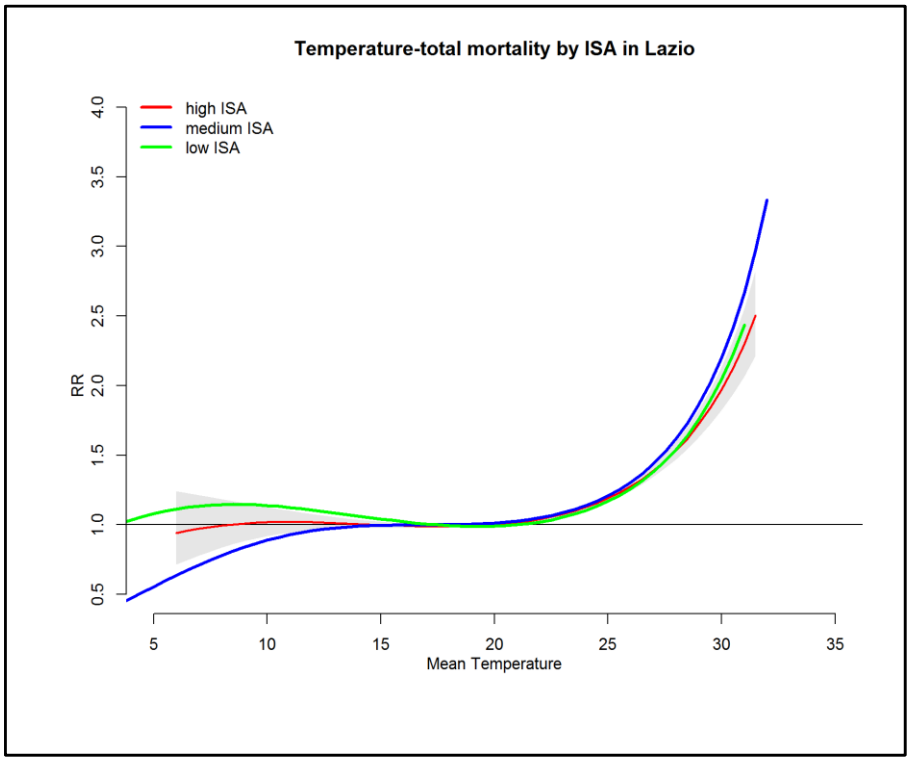

Figure 5.24 Mean temperature – mortality association in Rome region by urban development, summer (2001-2010).

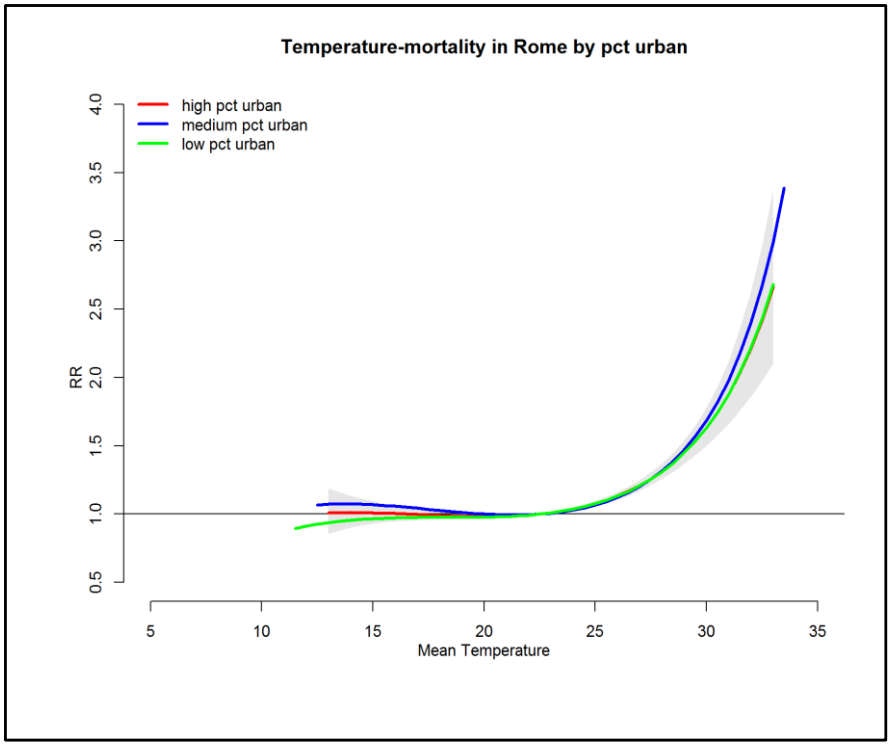

Figure 5.25 Mean temperature – mortality association in Rome by ISA, summer (2001-2010).

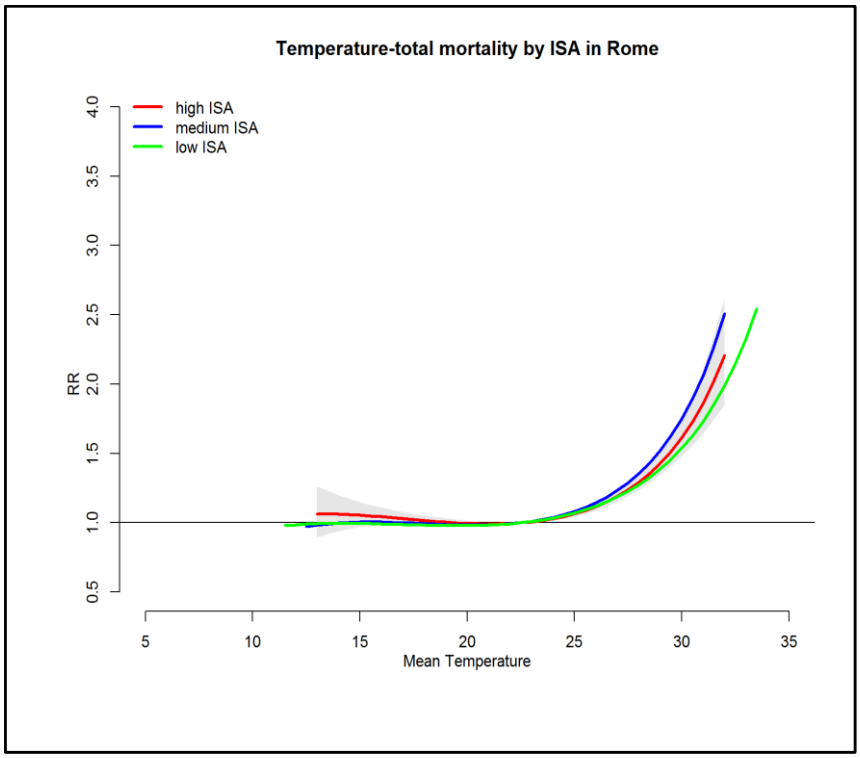

Table 5.11. Relative risk of natural, cardiovascular and respiratory mortality for increases in mean temperature considering distribution of percent urban and impervious surfaces in Rome and municipalities of the Lazio region.

			75th percentile		99th percentile		99.9th percentile	
			RR	95%CI	**RR**	95%CI	**RR**	95%CI
% urban	**Lazio**							
		low	**1.05**	1.04 - 1.07	**1.87**	1.79 - 1.95	**2.67**	2.48 - 2.87
		medium	**1.08**	1.06 - 1.09	**1.43**	1.35 - 1.51	**1.66**	1.52 - 1.82
		high	**1.10**	1.08 - 1.11	**1.53**	1.46 - 1.61	**1.79**	1.66 - 1.92
	Rome							
		low	**1.08**	1.07 - 1.10	**1.48**	1.38 - 1.59	**1.74**	1.56 - 1.95
		medium	**1.09**	1.07 - 1.12	**1.60**	1.47 - 1.75	**1.93**	1.69 - 2.21
		high	**1.11**	1.09 - 1.13	**1.57**	1.45 - 1.70	**1.91**	1.67 - 2.18
ISA	**Lazio**							
		low	**1.04**	1.03 - 1.05	**1.49**	1.42 - 1.56	**1.83**	1.69 - 1.98
		medium	**1.08**	1.07 - 1.10	**1.59**	1.50 - 1.68	**2.01**	1.83 - 2.21
		high	**1.10**	1.09 - 1.12	**1.56**	1.49 - 1.64	**1.84**	1.71 - 1.98
	Rome							
		low	**1.08**	1.06 - 1.10	**1.40**	1.31 - 1.50	**1.61**	1.43 - 1.80
		medium	**1.12**	1.09 - 1.14	**1.65**	1.53 - 1.79	**1.84**	1.66 - 2.05
		high	**1.10**	1.08 - 1.12	**1.55**	1.43 - 1.68	**1.90**	1.66 - 2.17

Table 5.12. Statistical testing of heterogeneity among strata specific mortality and hospital admission estimates for municipality size, ISA and percent urban levels.

	75th percentile		99th percentile		99.9th percentile	
	Q_res	P-value	Q_res	P-value	Q_res	P-value
Municipality size						
Total Mortality	28.45	0.000	9.09	0.028	7.23	0.065
Cardiovascular Mortality	22.03	0.000	18.00	0.000	12.89	0.005
Respiratory Mortality	53.75	0.000	286.72	0.000	279.71	0.000
Natural admissions	172.11	0.000	31.29	0.000	24.33	0.000
Cardiovascular admissions	28.81	0.000	0.09	0.384	1.13	0.770
Respiratory admissions	4.95	0.017	0.14	0.356	4.77	0.190
Lazio						
ISA levels	45.25	0.000	3.29	0.193	2.73	0.256
% urban levels	23.23	0.000	63.77	0.000	86.50	0.000
Roma						
ISA levels	6.31	0.043	9.52	0.009	4.20	0.123
% urban levels	3.06	0.216	2.29	0.318	1.66	0.436

Q_res: statistics of residual heterogeneity (among strata-specific estimates), based on Cochran-Q.

p-value: corresponding p-value. Null hypothesis: perfect homogeneity among strata-specific estimates. Alternative hypothesis: presence of heterogeneity

5.4 DISCUSSION

Results from the tome series study show that heat has a non-linear effect on mortality in rural, suburban and urban municipalities of the Lazio region as well as in Rome. Effects were observed for total, cardiovascular and respiratory causes of death. Risks for total mortality were similar for Rome and small municipalities, with the greatest effects in medium and large sized municipalities of the Lazio region. This pattern was true for both medium range temperatures (50^{th}-75^{th} percentile) and when including extreme temperature values. Medium and large municipalities were less in numerical terms, and possibly more diverse within the categories both in terms of population size, urbanistic characteristics, climatic and geographical conditions. Confidence intervals were wider in rural municipalities, notwithstanding estimates were still significant and did not overlap. A similar pattern was observed for cardiovascular mortality, with slightly higher effects when extreme temperatures were considered. Conversely for respiratory deaths, a different pattern was observed; with a very steep increase in the risk for extreme temperatures in all municipalities, except for the small ones in which effect estimates did not change much for the three temperature intervals. Overall for the entire region, a risk of 1.10 (95%CI: 1.09-1.11) for respiratory deaths was observed for temperature increases between the 50^{th} and 75^{th} percentile, which increased to (RR= 1.87 95%CI: 1.82-1.93) when extreme temperatures were included. In Rome, the mortality risk in the first temperature interval was 1.15 (95%CI: 1.14-1.17) and when extreme values were included estimates rose to 1.94 (95%CI: 1.82-2.06).

Conversely to mortality, hospital admissions effects were small or non-significant. For total admissions a suggestive effect of heat (lower CI limit was on the margin of statistical significance) was found only for small and large municipalities across the entire temperature range. No effect of heat was observed for cardiovascular admissions , or even protective in some municipality groupings of the Lazio region. These results are consistent with findings

from a project conducted in 15 European cities which found no effect in Mediterranean cities for cardiovascular admissions in summer.[12] Effects of heat, across the entire temperature range were observed for respiratory admissions in small and medium municipalities and overall in the Lazio Region. A suggestive rising trend in the effects of extreme heat on respiratory admissions was observed in all municipalities of the Lazio region including Rome. Respiratory admissions have been associated with heat in several studies conducted in Europe and findings here confirm results found in the literature[11,12,163,164]. Similarly Kovats and co-authors also found contrasting patterns of mortality and emergency hospital admissions in London, with an effect of heat only for respiratory admissions[164]. A study conducted in California on the other hand found a 2% excess risk in respiratory admissions for 10°F increases in apparent temperatures, while no effect was observed for cardiovascular disease, but only for ischemic stroke among the elderly was significant[163]. Williams et al. found an increase in emergency room visits for a 10°C increase in temperature but a decline hospital admissions in Perth, Australia.[13] In a similar study conducted in Adelaide heat effects on ambulance calls and ER visits were observed, while for hospital admissions only a weak association between temperature and respiratory admissions was observed, while no effects on cardiovascular admissions were shown[328] More detailed studies on specific sub-causes of admissions and ER visits rather than entire groupings could help disentangle this aspect.

One of the added values of the study it that it permitted to estimate the effects of heat for areas which had never been studied before, specifically rural and sub urban areas, finding a significant heat-related effect in the Lazio region. Moreover, rural (small municipalities) had comparable effect estimates to Rome for total and cardiovascular mortality. This finding was in accordance with the few previous studies conducted in rural small communities that found similar or a higher heat-related mortality for heat compared to urban areas [221,257,329,330]. A study carried out in Ohio, U.S., considered a synoptic approach to classify weather conditions on

each day and estimated excess deaths on days with oppressive conditions and other days in summer at county level[329]. A comparable effect of heat on mortality in urban and rural counties was found. Furthermore, Lee et al. found a slightly higher risk of death associated with temperature increases above 28°C for people living in rural areas compared to those living in urban areas of three States in SE USA[221]. Similar results were shown in a study on emergency room visits conducted in North Carolina, where higher rates of visits were observed in rural locations[331].

The novelty of the study is the use of 1x1km satellite-derived daily temperature data, which gave more accurate exposure measurements compared to traditional studies using ground monitoring networks. Guo et al. and Lee et al. found that spatio-temporal models gave slightly better model fits, possibly due to a reduced exposure error[21,221]. High-resolution temperatures enabled a better characterization of the spatial variation in the exposure compared to traditional monitoring stations which were limited in number and at considerable distances apart from one another. Furthermore, Lee and colleagues showed how the temperature distribution using high resolution data enabled to better estimate the effects of extremely hot temperatures in the US[221]. By using a more accurate measure of exposure the potential bias in effect estimates should be considerably reduced[21,22]. Important to note that spatial aggregations are still rather coarse, as death counts were at municipality level. It is recognized that the categorization of one municipality as entirely 'urban', 'suburban', or 'rural' might be an overgeneralization. If data by census tract or geo-located, attribution of exposure could have been more refined taking advantage of the fine scale exposure and land use attributes. Bennet et al. used a Bayesian spatial model to better capture the spatial differences in vulnerability to heat across the UK at district level[219].This approach could be a further step of the analysis carried out here, to better represent neighbouring municipalities and the spatial pattern of heat-related effects. It is however worth mentioning that in my thesis the dlnm approach was used, and the association

was considered non-linear to better capture the short-term effects of heat rather than the spatial pattern and this methodology is not integrated in the Bayesian framework as also reported by Bennet[219].

The different temperature distribution and the temperature-mortality curves depicted geographical differences in heat effects. Geographical differences in the effects of heat on mortality as have been widely documented around the world [7,8,191] and are dependent on local climates and population characteristics. In this study thresholds above which heat increases varied by municipality size as shown in the main analysis. This is suggestive of local population adaptation to local climates and having a different physiological response to heat to some extent. This was also confirmed in the sensitivity analysis using fixed temperature intervals on all municipalities. In fact results from this section showed that effects with the fixed intervals were larger for small municipalities and more contained in Rome suggesting that urban populations are exposed to higher temperatures, as shown by the temperature distribution, and might be more acclimatized [219,266,329,330,332]. Moreover, Lee et al. suggested that the warmer temperatures found in larger urban areas may lead to higher thresholds [221].

To try and account for the differences within each municipality with respect to the level of urbanization or built up environment, ISA and % urban development from CLC were considered in relation to heat-effects. Results showed a slight effect modification in the effects, with greater risks in heat-related mortality in municipalities with a higher level of ISA or % urban development. The differences were greater for the Lazio regional compared to Rome. Urban et al. found similar results among districts of the Czech Republic, areas with a higher population density and impervious surfaces had higher heat-related excess deaths [220]. Land use influences the thermal characteristics of an area and has been associated with vulnerability to heat-related mortality [183,297,300]. Greater heat vulnerability has been observed in areas with a

higher proportion of impervious surfaces, built-up environments and higher population density. On the contrary, the presence of green space and water bodies seems to reduce temperatures and areas with a greater presence of these factors are associated with lower risk estimates[183,292]. However, it should be noted that most of these latter studies only assess differential effects within urban areas and do not account for differences between urban and rural settings.

Socio-economic factors might also modify the temperature mortality association among populations in urban and rural areas[6,182,183,212,220]. Unfortunately, socio-economic factors were not available at the same spatial scale in this study but will be considered in the Rome study described in the next chapter. It is presumable that there are socio-economic differences between Rome and the rural and suburban areas in Lazio. A study conducted in Massachusetts showed that socio-economic factors had a dominant role in defining differential effects of heat rather than the level of urbanization characterized by population density and proportion of the impervious surface.[333] Noteworthy that socio-economic factors have been identified as risk factors mostly in the US[169,334], while in Europe the association is less clear.

The burden of heat-related deaths was also estimated and a considerable number of deaths was found for all municipalities in the Lazio Region and in Rome. Attributable deaths were found for both mild summer temperatures and for extreme values, with a greater total number of deaths in Rome, as expected due to the greater population exposed numerically.

Important to note that summer 2003 was included in the study period, when an exceptional heat wave occurred across Europe and Italy with a considerable number of excess deaths, potentially inflating the total number of deaths observed here for extreme heat. However, the sensitivity analysis excluding summer 2003 showed very similar patterns and results, with slightly lower estimates for the more extreme events, especially in Rome. A study conducted on the 2003 heat wave in Europe showed the difference in estimates excluding 2003, and in Rome the difference

was marginal compared to other cities such as Paris, London or Barcelona[320]. A further study on heat waves could help identify the effects and impacts of extreme events especially prolonged heatwaves and potential "added effect". However, this was not the primary interest here as the differences by size of population and municipality type was the main concern. A recent multi-country study found that Italian cites had one of the highest attributed risk fractions, and showed similar estimates for Rome.[157]

Berko et al., estimated the burden of extreme weather events in the US during 2006–2010 and found that nearly one-third of the deaths were attributed to extreme heat[257]. Heat-related impact estimates are important when considering future impacts of climate change and the potential role of adaptation measures. Two studies including Italian cities suggest that the introduction of heat plans and adaptation measures can reduce the burden of heat-related deaths.[229,335]

The burden considering YLL for the entire region provided additional information on the impacts of heat on the population in terms of premature death due to heat. An average of 9.300 YLL were estimated for each summer in the Lazio region for temperature increase between the 50th and 99th percentile. A recent study suggested that the impact of heat in terms of YLL is correlated to the presence of frail subjects in a population that might have a reduced life expectancy compared to the general population due to pre-existing medical conditions that make them more susceptible to heat.[326] YLL would be more contained if mortality displacement had been taken into account here. Notwithstanding, both impact estimates denote a significant burden in terms of exposure to heat, which will potentially rise in the future considering climate change and ageing of the Italian population.

Findings are suggestive of a key public health issue that needs to addressed with adequate resources now and in the future to improve response and reduce the impact. The estimates for sub-urban and rural areas can also be integrated into the regional heat warning systems and

heat plans to improve awareness and resilience among the local population and emergency response health services. In conclusion, findings from this study will be helpful for regional warning systems and public health heat prevention policies.

CHAPTER 6 – URBAN HEAT EFFECTS IN ROME

6.1 INTRODUCTION

People living in cities worldwide face a variety of health risks, among these, environmental factors like air pollution, noise, water contamination, proximity to industrial sites, waste and higher temperatures due to the UHI phenomenon play a key role. The acute effects of heat and extreme temperatures on health outcomes (mortality and hospital admissions) are well known in Italian cities.[12,157,161,179,208,320,336,337] However, most research in urban areas has been carried out with very coarse temperature exposure, typically using data from a single airport monitoring site thus not taking into account the spatial variation in temperatures within the urban context due to land use characteristics, urban micro meteorology and the UHI effect. This approximation is associated with a misclassification of the individual exposure, as all the subjects residing in an urban area are is given the same average exposure, thus potentially leading to an underestimation in the true heat-related effects.

Urban heat islands have been identified in Rome and other Italian cities.[91,127,128] Fabrizi et al. found a magnitude of +3-4°C in core urban areas of Rome at night compared to sub-rural zones, considering AATSR land surface data temperature and observed data[128]. A study comparing rural and urban monitoring stations, in three Italian cities found a UHI gradient of +1.9°C for Rome[278]. Morabito et al. compared LST temperatures in the different cities with building density and found the highest absolute LST difference (+3.8 °C) in Rome at night.[91]

Few studies have addressed variations in the effect of heat within cities. An important potential modifier of the heat effects is the presence of the urban heat island (UHI) effect due to the thermal capacity of buildings and impervious surfaces to retain heat. Within cities, zones with

densely packed buildings, narrow streets and limited green space are warmer that rural and suburban areas which have a higher proportion of green areas and less compact urban structures. Hence when considering the differential thermal properties and the micrometeorology within urban areas, land use and land cover are important. Stewart and Oke developed a standardized set of local climate zones, to classify urban and rural field sites based on surface properties[90]. This was accounted for in my thesis as satellite LST data captures temperatures at surface level and the relationship with land use and land cover were used to derive air temperature as described in chapter 4. Hence when characterizing the UHI intensity and thermal gradient for Rome, land use and the association with the micro climate is considered to some extent. Furthermore, vulnerability to heat among urban residents also depend on socio-economic factors, demographic characteristics and health status and these can vary greatly within urban areas thus also affecting response to heat [256,279,301].

This chapter presents the study conducted using the Rome Population Cohort to estimate the effect of heat on mortality by total, cardiovascular and respiratory causes using the case cross-over approach. The analysis considers potential individual and urban context factors that may modify vulnerability to heat. The novelty of the study is that it attributes the high resolution 1x1 km gridded air temperature, to each individual in the cohort at residential address who died between 2002-2010.

6.2 DATASET

6.2.1 The Rome Longitudinal Cohort

The Rome Longitudinal Study (RoLS)[338] is a population cohort where subjects were enrolled using the Rome Population Register at the 2001 Census (October 21st, 2001). The cohort has been used in numerous studies , especially regarding the long-term effects of air pollution on health outcomes[339–343]. Using record-linkage procedures Cesaroni and colleagues, attributed a series of socio-demographic characteristics to subjects included in the cohort using data from the Rome Population Register and national Census data.[338,344]

In particular, the following personal data were available from the population register:

- sex
- birth date
- place of birth
- residential history

and the following from the census:

- marital status (married, single, separated or divorced and widow/widowed)
- educational level (none, primary school, secondary school, high school and university)
- employment status (manual worker, non-manual workers, unemployed, housewife, retired, and other).

An area-based index of socioeconomic position, where the unit of observation was the census block was also taken into account. This is a composite indicator, obtained from a factor analysis performed on various socioeconomic census parameters (occupation, education, housing tenure, family composition, and foreign status (yes or no)). The four factors explained 84% of the variance: the first represented education, occupation and crowding in dwellings (49.5% of variance), the second immigration (14% of variance), the third family composition (11.3% of

variance), and the fourth home ownership (9.1% of variance).[345] The indicator was divided into 5 classes (very high, high, medium, low, very low), according to the quintiles of its distribution.

At census 2001, there were about 2.5 million inhabitants residing in Rome.[346] RoLS comprises 2,118,670 (84%) individuals, for which complete information was available. Researchers who built this cohort verified that differences for age and gender between subjects included and excluded from the analysis and these were not statistically significant.[338]

Pre-existing chronic conditions of diabetes (ICD-9-CM: 250), chronic obstructive pulmonary disease (ICD-9-CM: 490-492, 494, 496) (COPD) and cardiovascular diseases (ICD-9- CM: 390-459) were also accounted for by considering hospitalizations in the 5-year period before enrolment in the cohort[338]. Hospital admissions data were retrieved from the Lazio Regional Health Information System that collects individual discharge records from all hospitals in the region including Rome. Al subjects in the cohort were geocoded based on residential address in 2001 defined at census.

RoLS characteristics

RoLS population is made up of 1,119,878 (52.9%) females and 998,792 (47.1%) males, distributed as shown in the following population pyramid of age (Figure). The 35-39 age group represent the largest age class in the population, as a consequence of the period of strong birth growth that occurred in Italy in the 1960s, the so-called “baby boom”. After this period the number of birth severely decreased. Table 6.1 describes the principal socio-demographic characteristics of total population. Over 1.3 million (62%) subjects were born in Rome, while 806,517 (38%) were born elsewhere. Around 39% of the population was single and 48% were married, 34% of the subjects had a high school education and 44% were employed.

Figure 6.1. Age-sex population pyramid of Rome Longitudinal Study 2001

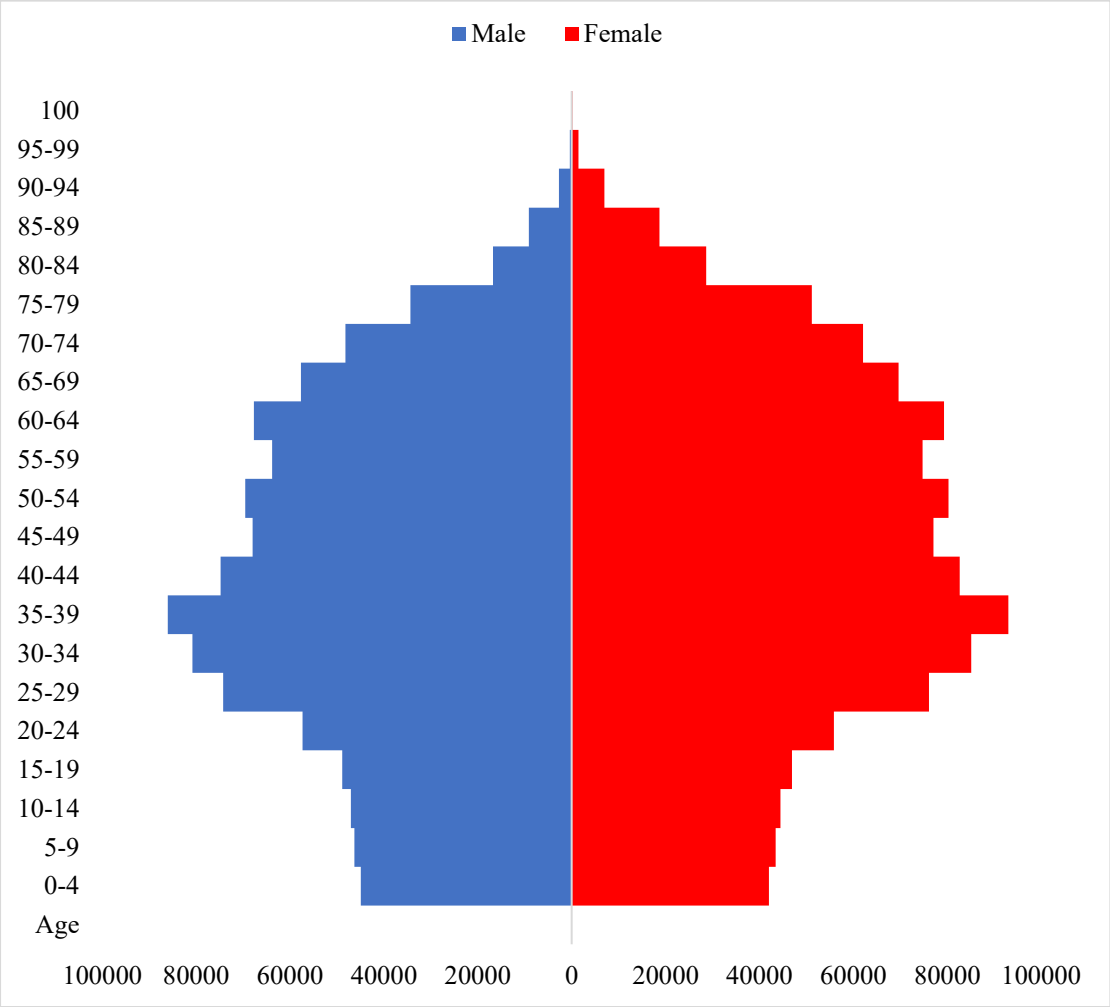

Table 6.1. Characteristics of the study population. Rome census 2001.

Characteristics	Population	
	N	%
Total	2,118,670	
Gender		
Men	998,792	47.1
Women	1,119,878	52.9
Mean age (SD)	*49.4 (22.2)*	
Place of Birth		
Rome	1,312,153	61.9
Other	806,517	38.1
Marital Status		
Married	1,012,816	47.8
Single	831,998	39.3
Separated	108,890	5.1
Widowed	164,966	7.8
Education		
None	146,305	7.3
Primary School	363,806	18.0
Secondary School	530,881	26.3
High School	685,104	34.0
University	290,543	14.4
Employment status		
Employed	820,873	44.4
Looking for first employment	58,698	3.2
Unemployed	86,140	4.7
Student	158,879	8.6
Housewife	314,770	17.0
Retired	336,530	18.2
Military or civil service	2,941	0.2
Unable to work	19,877	1.1
other	46,771	2.8
Area-based Socioeconomic Position		
Very High	397,835	18.8
High	420,005	19.8
Medium	422,943	20.0
Low	439,947	20.8
Very Low	437,930	20.7

6.2.2 Individual Temperature Exposure

Starting from the geo-coded individual addresses of subjects included in the cohort using GIS spatial joining techniques, the daily 1x1km gridded air temperature was attributed to each individual. Thus creating a time series of mean daily temperature data for each individual for the study period 2002-2010. Mean temperature (lag0-3) was considered as exposure.

6.2.3 Urban Heat Island Definition

The UHI intensity, measures the thermal difference between temperature at a given reference suburban point (T_{ref}) and temperatures in the single grid points (i) within the urban area (T_u).

$$\textbf{UHI intensity } \boldsymbol{id = Tuid - Trefd}$$

The suburban reference point was identified as the grid cell in which mean temperatures were lowest in the overall average mean summer temperature map for Rome for the entire study period. Once the point was identified, the difference between daily temperatures in each grid cell and the daily reference point was computed and the UHI intensity defined. The average UHI intensity for each grid cell was computed. This was then mapped for visual inspection. In the analysis UHI intensity was considered as a potential effect modifier of the temperature-mortality association. The variable was categorized into 2 classes, above and below the 50th percentile of the UHI intensity distribution only for the grid cells in which case events occurred. The grid cells in which residents live and die are the predominantly the areas with higher built environment, population density and impervious surfaces, the subset was made up of warmer grid cells. Considering the distribution for the entire UHI intensity would have given lower thresholds and most events would be allocated to the higher category. Two classes might be restrictive, but as UHI was evaluated with SEP it seemed reasonable not to have too many

categories. Ideally as UHI intensities are highest at night, minimum temperature values would have been the optimum to identify thermal gradients between urban and rural areas, but as mean temperature derived in chapter 4 was the temperature parameter available with a 1x1km resolution, the methodology employed here was the only feasible option. To a certain extent we can speculate the UHI intensity magnitude might be underestimated, but there should be no differences in the spatial pattern which is of greater interest here.

6.3 METHODS

Statistical modelling: Case-crossover design for the analysis of the short-term effect of heat on cause-specific mortality in the Rome Longitudinal Study.

All deaths occurring in the summer periods between 2002 and 2010 among subjects of the Rome Longitudinal Study were selected. Only fatal events occurring in the warm period (April to September) among subjects aged 35+ years at the time of death were considered. All residential addresses were geo-located, and the daily (lag0-3) exposure was attributed as the estimated mean temperature of the 1x1-km grid cell where the individual address was located.

In order to estimate the short-term association between daily mean (summer) temperature and mortality the case-crossover (CC) design[347] was used. This approach is a matched case-control design where each subject is a risk-set and the exposure on the event day (death) is compared to the average exposure on control days. It follows that each subject is the control of himself, therefore perfect adjustment for all time-invariant (e.g. sex, genetic factors, etc.) and slow-changing (age, smoking, BMI, socio-economic factors) confounders is achieved by design. Other time-varying factors (e.g. seasonality) can be adjusted for by modelling in the multivariate conditional logistic regression model. CC is the only possible approach when environmental exposures are estimated at the individual level and short-term effects are of interest. In contrast, conventional time-series studies are not applicable because they assume a homogeneous distribution of the exposure across the entire study area, and only focus on day-

to-day variability. Furthermore, CC allows evaluation of individual-level or address-level characteristics as potential effect modifiers of the relationship between Ta and the health outcome(s) of interest, under the hypothesis that some subgroups are more vulnerable to summer high temperatures, either because of individual characteristics (elderly, those living alone, people with chronic conditions, etc.), or because of contextual ones (socio-economic deprivation, degree of urbanization of the residential area, green space, presence of urban heat islands, etc.).

In the present study, control periods for each "case" were chosen as the same days of the week within the same time window (month and year)[324]. This strategy of controls selection, referred to as the "time-stratified" approach, has been shown to introduce negligible bias from long-term and seasonal time trends in either exposure or outcome, while at the same time minimizing the serial autocorrelation of the case and control time windows, as they are separated by seven days[348].

As in the time-series approach described in Chapter 5, the lagged non-linear association between high temperatures and mortality was accounted for by fitting a distributed-lag non-linear model (package *dlnm* in R)[322]. This model defines a two-dimensional function, the *cross-basis*, which incorporates both non-linear curves for the exposure-outcome relationship and lagged effects of the exposure on the outcome[323]. On the basis of the literature, a maximum lag of three days was set a priori and then allowed for non-linearity by fitting b-splines of the (lagged) temperature-mortality relationship with 3 degrees of freedom. Results are reported as odds ratios (and 95% CI) of mortality for temperature increases between the 50^{th} to the 75^{th} , 50^{th} to 95^{th} and 50^{th} to 99^{th} percentiles of the temperature distribution. For ease of description risks are denoted as relative risks.

As previously described, several individual-level and area-level characteristics were evaluated as potential effect modifiers. Each effect modifier was analysed singularly by conducting separate analyses for each level of the modifier. The individual-level variables included age (35-64, 65-74, 75-84 and 85+ years), gender, marital status (married, single, divorced, widowed), education level (primary, middle school, high school, university), occupational status (non-manual workers, manual/other workers, housewives, unemployed, retired and others), and a series of previous co-morbidities - past hospital admissions for cardiovascular diseases, diabetes or chronic-obstructive pulmonary diseases (COPD).

The area-level effect modifiers evaluated were: socio-economic position (at the census-block level), percent of urban development, impervious surfaces and UHI (defined at the 1x1-km grid level).

A sensitivity analysis was carried out to compare temperature effect estimates using traditional measured data from Ciampino airport monitoring station, temperature by urbanistic zone, used in the previous section and time series analysis and the individual temperature exposure considered here. The CC analysis was carried for each of the three exposures and effect estimates calculated. Attributable deaths using the three exposures were calculated using the same methodology described in the previous chapter[325] for increases in mean temperature between the 50^{th} and 75^{th} percentile and from the 50^{th} to the 99^{th} percentile. Results were compared to account for the misclassification in exposure might influence estimates.

The analyses were conducted using R (version 3.1.3; Institute for Statistics and Mathematics, WU Wien, Vienna, Austria) and STATA (version 13; StataCorp. 2013. Stata Statistical Software: Release 13. College Station, TX: StataCorp LP).

6.4 RESULTS

6.4.1. Mortality in the RoLS Cohort

Table 6.2 shows the descriptive statistics of deaths in the cohort by age, gender, comorbidity and individual factors. Over 57,000 deaths occurred during the summers in the period 2002-2010, of these around 40% were for CVD while only 3200 (5.6%) were for respiratory deaths. Deaths were mostly in the old (75-84=36.2%) and very old (85+=32.4%). Although the gender distribution was roughly even, around 40% of deaths among females were in the 85+ group, while among males the majority of deaths occurred in the 75-84 age group. It seems reasonable to have a higher proportion of widows/widowers and fewer single or divorced individuals when considering mortality as outcome in the cohort. Married individuals made up over 50% of the cohort. Regarding education, 48.7% of the cohort had a primary school education and only 11% had a university degree, this again reflects age distribution of the population in study. In the cohort, 53% were retired and 24% were housewives, only a limited proportion were still in the active workforce. Table 6.3 illustrates mortality distribution by SEP, urban development and impervious surface categories. Deaths by socio-economic position were evenly distributed with a slight skewness towards the richer subgroups. Regarding ISA and urban development around 50% of the deaths occurred in grid cells with a high ISA or urban development as expected considering the spatial domain in study.

Table 6.2. Number of deaths in the cohort during summer (May- September) by age, gender, cause , marital status, education , employment and co-morbidities in the study period (2002-2010).

		N	%			N	%
Total		**57,509**	**100.0**				
Cause				Education			
	Cardiovascular	23,302	40.5		University	6,424	11.2
	Respiratory	3,201	5.6		High school	10,389	18.1
Age group					Middle school	12,668	22.0
	35-64	6,972	12.1		Primary school	28,028	48.7
	65-74	11,087	19.3	Occupation			
	75-84	20,821	36.2		Non manual workers	3,461	6.0
	85+	18,629	32.4		Manual and other	2,240	3.9
Gender					Housewives	13,907	24.2
	Males	28,216	49.1		Unemployed	828	1.4
	Females	29,293	50.9		Retired	31,016	53.9
Marital status					Other	6,057	10.5
	Married	31,290	54.4	Co-morbidities			
	Single	5,027	8.7		CVD	19,545	34.0
	Divorced	2,269	3.9		COPD	4,995	8.7
	Widowed	18,923	32.9		Diabetes	4,885	8.5

Table 6.3. Number of deaths in the cohort during summer (May- September) by socio-economic position, impervious surface, percent urban development and urban heat island intensity in the study period (2002-2010).

		N	%
Total		**57,509**	**100.0**
Socio Economic position			
	High	11,734	20.4
	Mid-high	12,240	21.3
	Medium	11,489	20.0
	Mid-low	11,277	19.6
	Low	10,769	18.7
ISA			
	Low	15,374	26.7
	Medium	13,378	23.3
	High	28,757	50.0
Urban development			
	Low	14,376	25.0
	Medium	14,391	25.0
	High	28,742	50.0
UHI			
	Low	25,110	43.7
	High	32,399	56.3

6.4.2 Temperature Exposure

Figure 6.2 shows the average summer mean temperature distribution over the study period for Rome and the spatial distribution of deaths that occurred in the study period.

Tables 6.4a-b shows the temperature distribution in the warm season(May to September) with a fine spatial resolution, considering all the 1x1km grid cells for Rome (table 6.4a) and only in the grid cells where deaths occurred (cohort grid cells) (table 6.4b) over the entire study period. The mean temperature was of 22.2°C, with an interquartile range of 19.6°C to 25.1°C and the 99th percentile was 28.5°C considering the entire spatial domain. While considering cohort grid cells only (which is the exposure in the study domain) the mean was 23.1°C and IQR was comprised between 20.4°C and 26.1°C. It can be noted that tails of the temperature distribution in the cohort domain are truncated, with less extreme values for both high and low temperatures. We can also see an annual variability, with 2003 registering the highest temperatures for all percentiles considered, with +3°C on average throughout the distribution. In summer 2003, the 99th and maximum values reached 31.0°C and 34.1°C respectively. A seasonal trend in temperatures can also be observed with highest values in July and August and lower values at the beginning and end of the season. Mean temperatures in July and August were around 26°C in the cohort, while in May and September they were around 6°C lower (table 6.4a- b). The cohort dataset had slightly higher values. The 75th percentile in the cohort temperature distribution was 26°C for all summer and ranged between 20.9 and 27.4 in July, while the 99th percentile was of 20°C for all summer and ranged between 25.7°C in May and 30°C in August.

Figure 6.3 shows the UHI intensity in Rome and its spatial distribution. Central areas and the north eastern section of the city had the highest UHI intensities. Average values over the study

period ranged between 0.3°C and 2.9°C, with a mean value of 1.7°C during summer. The range in daily values had a greater variability between -0.2°C and 3.4°C (data not shown).

Figure 6.2. Map of average mean summer temperature over the study period and spatial location of death events that occurred in the study period (2002-2010).

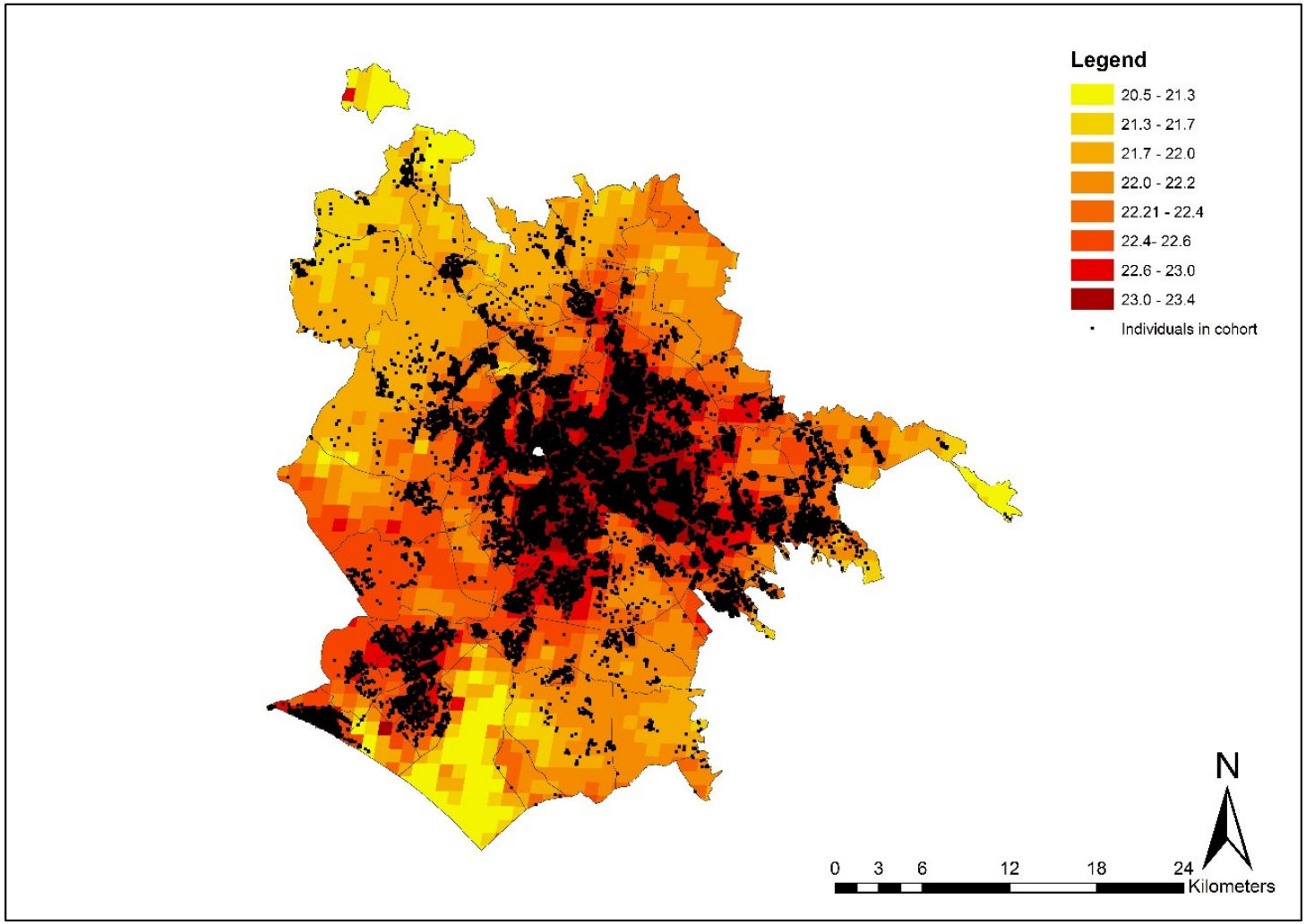

Figure 6.3. Map of average UHI intensity over the study period and spatial location of death events that occurred in the study period (2002-2010).

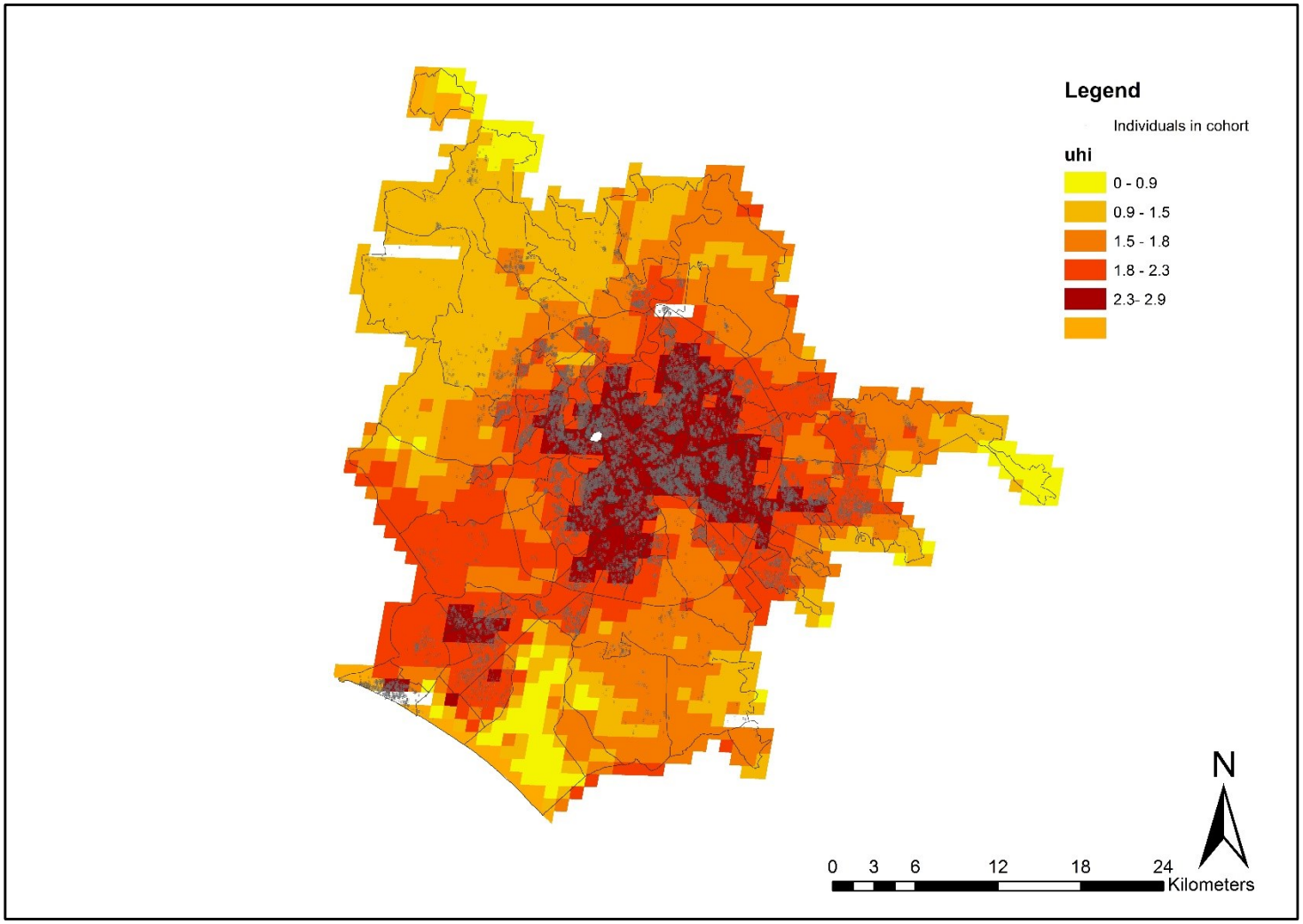

Table 6.4a. Mean Temperature distribution for Rome during summer (May- September), by month and by year in the study period (2002-2010).

	Min	p1	p5	p10	p25	p50	Mean	p75	p90	p95	p99	Max
2002	10.1	14.5	15.8	17.1	19.1	21.6	21.6	24.1	26.1	26.9	28.4	30.3
2003	14.3	17.7	18.9	19.6	21.0	25.2	24.6	27.9	29.0	29.5	30.3	36.2
2004	7.0	12.6	15.0	16.1	18.5	22.3	21.5	24.4	25.8	26.4	27.8	29.9
2005	13.1	15.2	16.4	17.3	19.3	21.9	21.7	24.0	25.7	26.7	27.8	29.4
2006	10.6	13.5	15.2	16.5	19.4	22.0	21.9	25.2	26.6	27.2	28.2	30.5
2007	12.6	14.7	16.0	16.9	19.3	22.1	21.9	24.5	26.6	27.6	29.2	31.8
2008	11.0	14.5	15.5	16.2	18.4	23.4	22.1	25.4	26.5	26.9	27.6	28.8
2009	12.7	14.8	17.3	18.8	20.7	22.8	22.9	25.5	26.6	27.3	28.2	30.4
2010	10.0	13.1	15.1	16.4	18.8	22.2	21.7	24.7	26.4	27.2	28.5	30.6
Month												
May	7.0	12.7	14.2	15.1	16.4	18.0	18.3	20.0	21.9	22.8	24.6	27.7
June	10.6	15.0	17.0	18.0	20.2	22.5	22.5	25.3	27.0	27.6	28.5	30.6
July	16.0	20.5	21.7	22.4	23.6	25.2	25.1	26.6	27.7	28.4	29.4	31.4
August	15.7	19.1	20.8	21.7	22.9	24.6	24.6	26.2	27.8	28.8	30.1	36.2
September	10.1	14.5	15.8	16.7	18.9	20.6	20.5	22.0	23.8	24.8	26.1	28.8
average	**11.3**	**14.5**	**16.1**	**17.2**	**19.4**	**22.6**	**22.2**	**25.1**	**26.6**	**27.3**	**28.5**	**30.9**

Table 6.4b. Mean Temperature distribution for cohort grid cells during summer (May- September), by month and by year in the study period (2002-2010).

variable	Min	p1	p5	p10	p25	p50	Mean	p75	p90	p95	p99	Max
2002	12.8	15.4	16.7	18.1	20.1	22.5	22.6	25.1	27.2	27.9	29.4	30.3
2003	17.0	18.8	19.9	20.7	22.1	26.6	25.6	28.7	29.7	30.2	31.0	34.1
2004	11.4	13.5	15.9	17.0	19.2	23.2	22.3	25.2	26.6	27.3	28.7	29.9
2005	14.8	16.6	17.4	18.2	20.0	22.7	22.6	24.9	26.7	27.6	28.6	29.3
2006	12.5	14.3	15.9	17.3	20.3	22.9	22.7	26.1	27.4	27.9	28.7	30.2
2007	14.3	15.5	16.6	17.5	20.0	23.0	22.7	25.4	27.4	28.3	29.9	31.7
2008	13.6	15.2	16.2	16.9	19.1	24.2	22.7	26.0	27.2	27.5	27.9	28.3
2009	14.3	15.8	18.0	19.6	21.4	23.8	23.7	26.4	27.5	28.2	29.0	30.4
2010	12.3	13.8	16.1	17.2	19.8	23.3	22.7	25.6	27.4	28.2	29.5	30.6
Month												
May	11.4	13.6	15.1	16.0	17.3	18.9	19.1	20.9	22.9	23.7	25.7	27.7
June	12.5	15.6	17.9	18.8	20.9	23.3	23.3	26.2	27.8	28.4	29.4	30.6
July	18.9	21.3	22.7	23.2	24.5	26.2	26.0	27.4	28.6	29.2	30.1	31.4
August	17.3	19.9	21.8	22.7	23.8	25.5	25.5	27.0	28.6	29.6	30.8	34.1
September	13.3	15.2	16.4	17.2	19.7	21.3	21.1	22.8	24.5	25.5	26.7	28.0
average	**13.7**	**15.4**	**17.0**	**18.1**	**20.2**	**23.6**	**23.1**	**26.0**	**27.4**	**28.1**	**29.2**	**30.5**

6.4.3 Short-term effects of heat on mortality in the Rome Population Cohort.

Figure 6.4 shows the dose-response curve for air temperature and cause specific mortality in Rome, the curve shows that during summer as temperatures progressively rise, around, 20-23°C, the risk of mortality increases, with statistically significant effects from around 25-26°C.

Figure 6.4 Mean temperature – mortality association in Rome, summer (2001-2010).

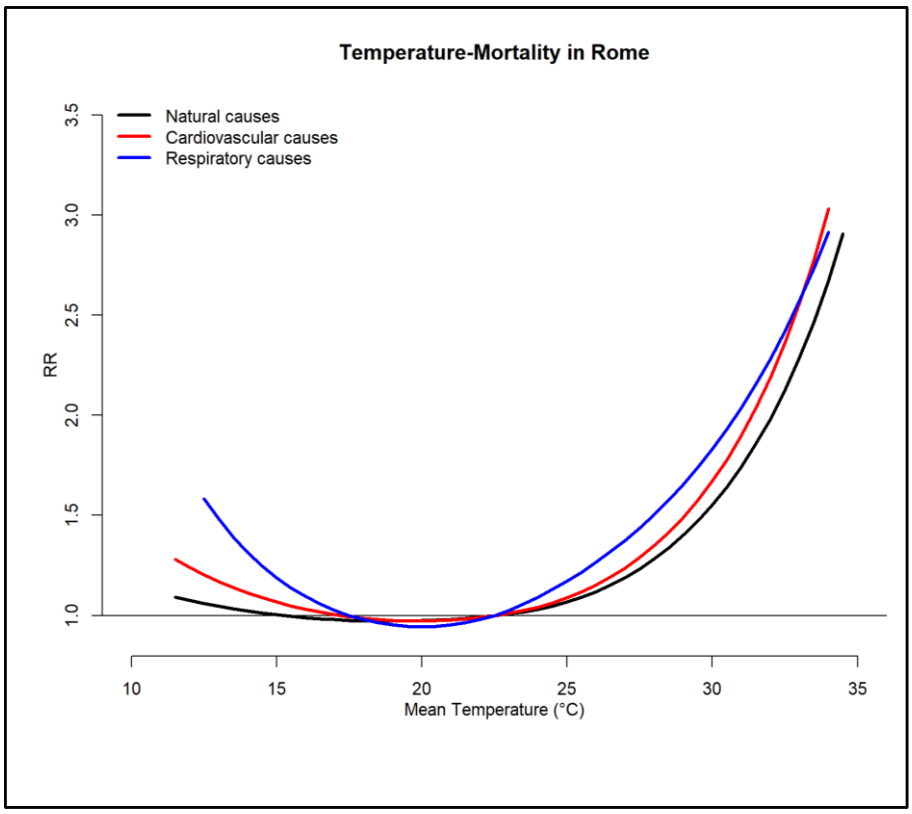

Figure 6.5 shows the relative risk in total mortality for increases in temperature from the 50th to 75th percentile and from the 50th to 99th percentile, results are reported by age groups, gender, and finally gender and age combined. The overall effect of heat on mortality, for an increase in temperature comprised between the 50th and 75th percentile (23.5 vs 26.2°C), in the Rome cohort was of 11%. While, when considering more extreme temperatures (50th to 95th) the risk rose to 34% for overall mortality (OR=1.34: CI95%: 1.28-1.40) (Table 6.5). Stratification by age showed a rising trend in effects; among younger adults the effect was non-significant and increased progressively with age from 1.06 (95%CI: 1.02-1.11) in the 65-74 age group to 1.18 (95%CI: 1.15-1.22) in the 85+ age group for temperature increases between the 50th and 75th percentile. For extreme temperatures, the pattern was similar and relative risks were higher, with significant increases in the risk of death due to temperature increases from the 50th to the 95th percentile of +10% in the 65-74 age group to 55% in the 85+ age group. Increases considering extreme values were no longer significant in the 65-74 age group, but remained significant even considering extreme estimates (50th to 99th percentile) (Table 6.5 and Figure 6.5). Statistical testing for heterogeneity confirmed differences by age groups for all temperature intervals (Table 6.11). When stratifying by gender an overall higher effect was observed for females with an OR of 1.14 (95%CI: 1.11-1.17) compared to OR=1.09 (95%CI: 1.06-1.11) in males for mean temperature increases between the 50th and 75th percentile. The gender difference for the first temperature interval (50thvs75th) was also confirmed by p-values and the Q statistical test as shown in table 6.11. When considering age and gender together, a greater risk was found for women considering moderate temperatures. The risk of death among elderly females increased from +7% in the 65-74 age group to +22% in the 85+ age group; while among males the increase in risk rose from +6% to +17%, respectively in the same age groups. A greater effect of extreme temperatures was observed among males with

risks comprised between 46% in the 65-74 age group to 86% in the 85+ age group (Table 6.5 and Figure 6.5).

Figure 6.6 shows the risk in total mortality for increases in temperature from the 50th to 75th percentile and from the 50th to 99th percentile, results are reported by marital status, occupation and level of education. The highest risk, when analysing marital status was for widows and widowers (OR=1.17: CI95% 1.13-1.20). For estimates stratified by education no clear trend was found, a slightly higher risk was observed for subjects with a primary school education (OR=1.13: CI95% 1.11-1.16), the second highest risk estimates were for individuals with a university degree. Occupation seemed to be linked to age as the categories with a greater risk were housewives (OR=1.13: CI95% 1.09-1.17), retired (OR=1.10: CI95% 1.07-1.13) which was also the largest category, and other types of workers (OR=1.20: CI95% 1.14-1.27) which is a miscellaneous category. The unemployed were very few and younger. Table 6.11 confirms statistically significant differences in estimates by marital status and occupation for temperature increases in the first two intervals only.

Analyses by cause (Table 6.6-6.7) showed similar age and gender patterns with a trend of increasing risk by age and greater effects among females for both cardiovascular and respiratory mortality. In general, respiratory risks were higher with an overall OR of 1.26 (CI95%: 1.13-1.31), while cardiovascular deaths had a risk of 1.14 (CI95%: 1.11-1.37) for temperature increases from the 50th to 75th percentile. For extreme temperatures, the risk of respiratory deaths was higher than other causes, especially for women aged 85+. Table 6.12 and confirm statistically significant differences in estimates by age, gender and marital status for temperature increases in the first two intervals only for cardiovascular disease. While respiratory disease show significant heterogeneity in estimates by age, females and ages groups and marital status across the entire temperature range (Table 6.13) .

Slightly different trends were observed for subjects with pre-existing chronic disease; although none were statistically significant (Tables 6.11-6.13). Having diabetes or a pre-existing cardiovascular condition were suggestive risk factors for cardiovascular mortality, while when considering respiratory disease, subjects with COPD, diabetes or pre-existing cardiovascular condition seemed to be slightly less at risk compared to those who didn't have the chronic condition (Tables 6.5-6.7).

Table 6.5 Heat-related effects on <u>total mortality</u>. Risk in mortality for increases in mean temperature between the 50th and 75th, 50th and 95th, 50 to 99th of the summer distribution in Rome by age groups, gender, age and gender combined and co-morbidities.

		75th percentile		95th percentile		99th percentile	
Total Mortality		**OR**	95%CI	**OR**	95%CI	**OR**	95%CI
All ages		**1.11**	1.09 - 1.13	**1.34**	1.29 - 1.40	**1.53**	1.43 - 1.63
	35-64	1.02	0.97 - 1.07	1.13	0.99 - 1.28	1.22	0.99 - 1.52
	65-74	**1.06**	1.02 - 1.11	**1.10**	1.00 - 1.22	1.12	0.94 - 1.32
	75-84	**1.11**	1.08 - 1.15	**1.38**	1.29 - 1.49	**1.62**	1.44 - 1.82
	85+	**1.18**	1.15 - 1.22	**1.55**	1.45 - 1.67	**1.87**	1.67 - 2.10
Gender							
	Males	**1.09**	1.06 - 1.11	**1.29**	1.21 - 1.37	**1.46**	1.32 - 1.61
	65-74	**1.06**	1.01 - 1.12	**1.16**	1.01 - 1.32	1.22	0.98 - 1.52
	75-84	**1.09**	1.05 - 1.14	**1.37**	1.24 - 1.51	**1.63**	1.38 - 1.92
	85+	**1.17**	1.01 - 1.37	**1.54**	1.11 - 2.14	**1.86**	1.09 - 3.17
	Females	**1.14**	1.11 - 1.17	**1.39**	1.31 1.47	**1.59**	1.44 - 1.74
	65-74	**1.07**	1.00 - 1.14	1.03	0.88 1.22	0.98	0.75 - 1.28
	75-84	**1.14**	1.09 - 1.19	**1.40**	1.26 1.55	**1.61**	1.36 - 1.91
	85+	**1.22**	1.11 - 1.33	**1.45**	1.17 1.79	**1.59**	1.12 - 2.25
Co-morbidity							
	CVD						
	yes	***1.13***	*1.10 - 1.17*	***1.40***	*1.31 - 1.50*	***1.62***	*1.45 - 1.82*
	no	**1.10**	1.08 - 1.12	**1.31**	1.24 - 1.38	**1.47**	1.35 - 1.60
	COPD						
	yes	***1.11***	*1.05 - 1.18*	***1.33***	*1.16 - 1.53*	***1.51***	*1.21 - 1.89*
	no	**1.11**	1.09 - 1.13	**1.34**	1.28 - 1.40	**1.53**	1.42 - 1.64
	DIABETES						
	yes	***1.14***	*1.08 - 1.21*	***1.31***	*1.14 - 1.51*	***1.42***	*1.13 - 1.79*
	no	**1.11**	1.09 - 1.13	**1.34**	1.28 - 1.40	**1.54**	1.43 - 1.65

Figure 6.5. Heat-related risks of mortality for increases in mean temperature between the 50th and 75th, 50 to 99th of the summer distribution in Rome by age groups, gender, age and gender combined.

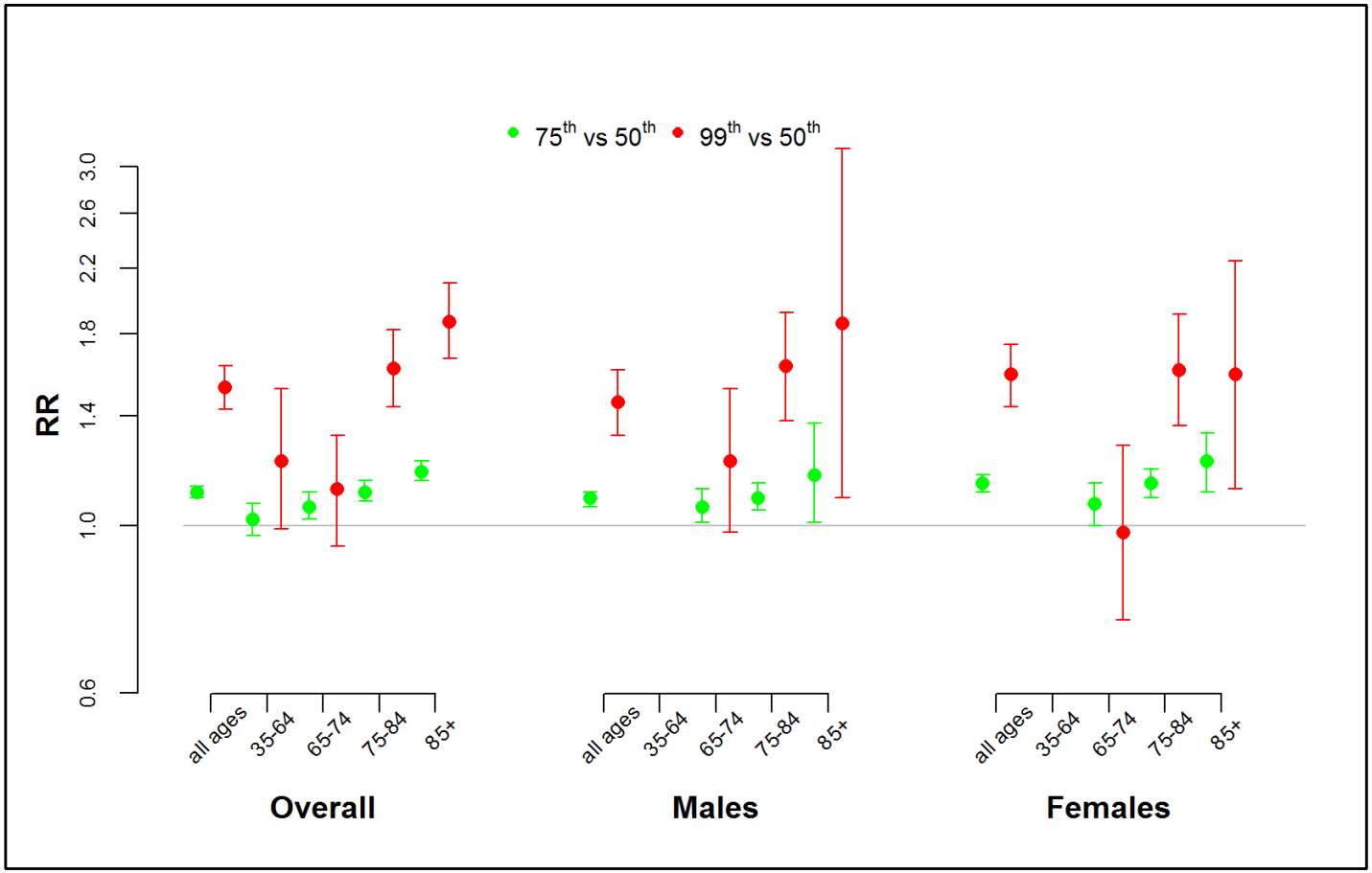

Figure 6.6. Heat-related risks of mortality for increases in mean temperature between the 50th and 75th, 50 to 99th of the summer distribution in Rome by marital status, education and occupation.

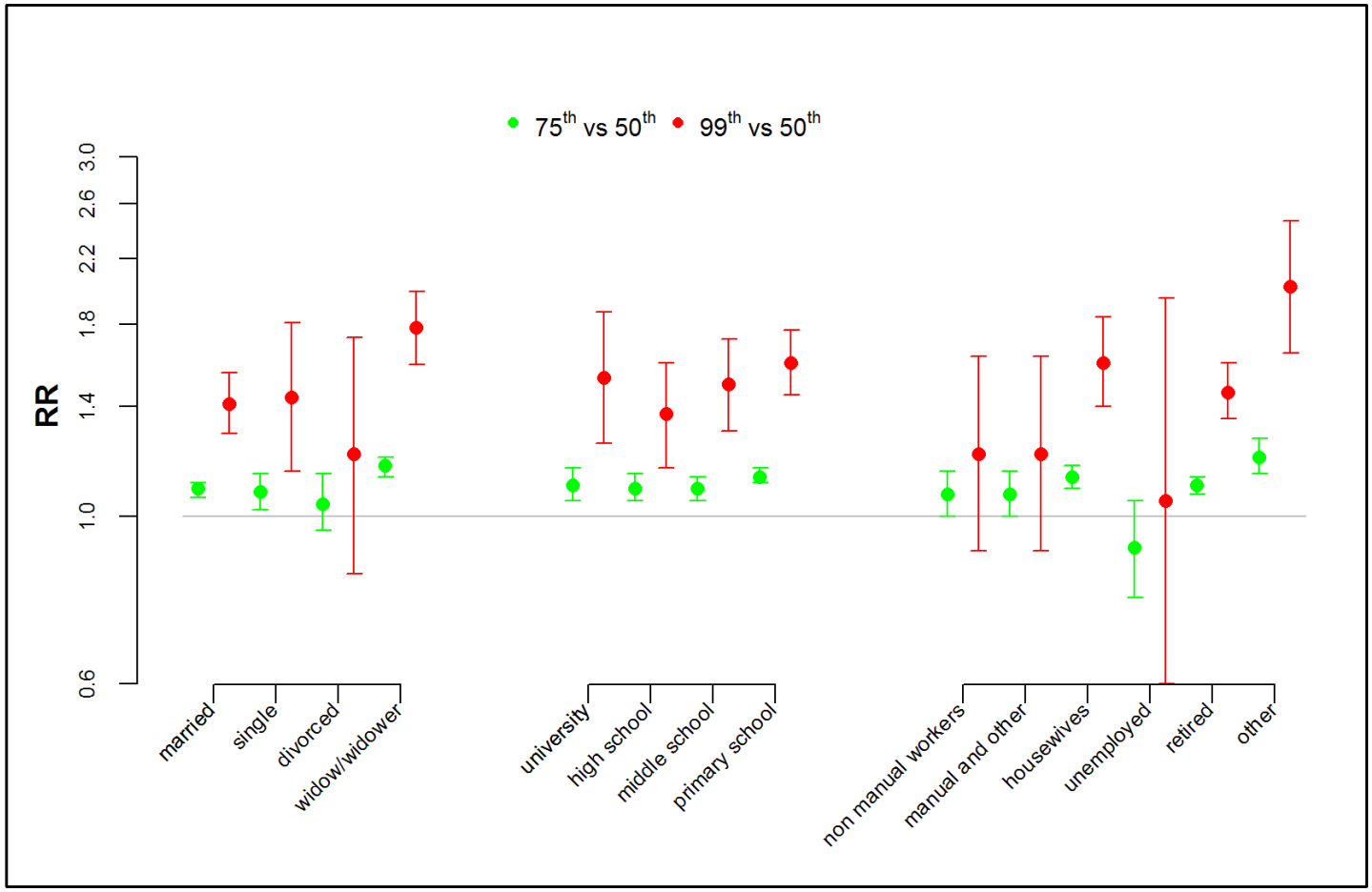

Table 6.6 Heat-related effects on cardiovascular mortality. Risk for increases in mean temperature between the 50th and 75th, 50th and 95th , 50th to 99th of the summer distribution in Rome by age groups, gender, age and gender combined and co-morbidities.

		75th percentile		95th percentile		99th percentile	
Cardiovascular Mortality		**OR**	95%CI	**OR**	95%CI	**OR**	95%CI
All ages		**1.14**	1.11 - 1.17	**1.41**	1.32 - 1.50	**1.63**	1.47 - 1.81
	65-74	**1.02**	0.95 - 1.11	**1.05**	0.86 - 1.28	**1.07**	0.77 - 1.48
	75-84	**1.13**	1.07 - 1.18	**1.39**	1.24 - 1.56	**1.61**	1.33 - 1.94
	85+	**1.21**	1.16 - 1.26	**1.59**	1.45 - 1.75	**1.91**	1.64 - 2.24
Gender							
	Males	**1.09**	1.05 - 1.13	**1.30**	1.18 - 1.43	**1.48**	1.26 - 1.73
	65-74	**0.99**	0.90 - 1.10	**1.07**	0.83 - 1.38	**1.15**	0.76 - 1.74
	75-84	**1.06**	0.99 - 1.13	**1.34**	1.13 - 1.58	**1.62**	1.24 - 2.12
	85+	**1.21**	1.13 - 1.30	**1.51**	1.28 - 1.78	**1.72**	1.31 - 2.26
	Females	**1.18**	1.14 - 1.23	**1.51**	1.38 1.64	**1.76**	1.53 - 2.03
	65-74	**1.08**	0.95 - 1.24	**1.03**	0.74 1.43	**0.95**	0.55 - 1.63
	75-84	**1.21**	1.13 - 1.29	**1.45**	1.23 1.70	**1.60**	1.23 - 2.08
	85+	**1.21**	1.15 - 1.27	**1.64**	1.46 1.84	**2.01**	1.66 - 2.44
Co-morbidity							
	CVD						
	Yes	**1.16**	1.12 - 1.21	**1.45**	1.31 - 1.60	**1.67**	1.42 - 1.97
	No	**1.12**	1.09 - 1.16	**1.38**	1.27 - 1.50	**1.60**	1.39 - 1.84
	COPD						
	Yes	**1.11**	1.01 - 1.21	1.20	0.97 - 1.48	1.25	0.88 - 1.76
	No	**1.14**	1.11 - 1.18	**1.43**	1.34 - 1.53	**1.68**	1.50 - 1.87
	DIABETES						
	Yes	**1.16**	1.06 - 1.27	1.20	0.97 - 1.48	1.17	0.82 - 1.66
	No	**1.14**	1.11 - 1.17	**1.43**	1.34 - 1.53	**1.69**	1.51 - 1.88

Table 6.7 Heat-related effects on respiratory mortality. Risk for increases in mean temperature between the 50th and 75th, 50th and 95th, 50th to 99th of the summer distribution in Rome by age groups, gender, age and gender combined and co-morbidities.

		75th percentile		95th percentile		99th percentile	
Respiratory mortality		**OR**	95%CI	**OR**	95%CI	**OR**	95%CI
all ages		**1.22**	1.13 - 1.31	**1.52**	1.29 - 1.80	**1.73**	1.32 - 2.28
	65-74	**0.87**	0.70 - 1.07	**0.75**	0.43 - 1.30	**0.69**	0.29 - 1.68
	75-84	**1.23**	1.09 - 1.40	**1.50**	1.13 - 2.00	**1.67**	1.04 - 2.66
	85+	**1.39**	1.24 - 1.57	**1.98**	1.54 - 2.54	**2.42**	1.60 - 3.65
Gender							
	Males	**1.17**	1.06 - 1.29	**1.54**	1.22 - 1.95	**1.88**	1.27 - 2.76
	65-74	**0.98**	0.76 - 1.27	**1.20**	0.60 - 2.41	**1.45**	0.48 - 4.41
	75-84	**1.25**	1.06 - 1.48	**1.70**	1.16 - 2.47	**2.05**	1.11 - 3.81
	85+	**1.24**	1.04 - 1.49	**1.68**	1.14 - 2.46	**2.03**	1.07 - 3.84
	Females	**1.28**	1.15 - 1.42	**1.51**	1.19 - 1.91	**1.61**	1.09 - 2.38
	65-74	**0.70**	0.49 - 1.01	**0.35**	0.14 - 0.88	**0.21**	0.05 - 0.93
	75-84	**1.20**	0.99 - 1.46	**1.28**	0.82 - 1.99	**1.27**	0.62 - 2.62
	85+	**1.52**	1.29 - 1.78	**2.23**	1.60 - 3.10	**2.72**	1.58 - 4.69
Co-morbidity							
	CVD						
	yes	**1.16**	1.03 - 1.30	**1.38**	1.05 - 1.82	1.54	0.98 - 2.41
	no	**1.26**	1.14 - 1.38	**1.62**	1.31 - 2.00	**1.87**	1.32 - 2.65
	COPD						
	yes	**1.16**	1.00 - 1.35	**1.48**	1.06 - 2.07	**1.75**	1.01 - 3.03
	no	**1.24**	1.14 - 1.35	**1.54**	1.27 - 1.87	**1.74**	1.26 - 2.39
	DIABETES						
	yes	1.12	0.88 - 1.42	1.52	0.78 - 2.95	1.92	0.65 - 5.64
	no	**1.23**	1.14 - 1.33	**1.53**	1.29 - 1.82	**1.74**	1.31 - 2.31

Table 6.8 Heat-related effects on total mortality. Risk for increases in mean temperature between the 50th and 75th, 50th to 95th , 50 to 99th of the summer distribution in Rome by SEP, UHI and SEP and UHI combined.

	75th percentile		95th percentile		99th percentile	
	OR	95%CI	**OR**	95%CI	**OR**	95%CI
Total Mortality						
SEP						
1. High	**1.12**	1.08 - 1.16	**1.37**	1.25 - 1.50	**1.58**	1.36 - 1.83
2. Mid-high	**1.10**	1.06 - 1.14	**1.31**	1.20 - 1.43	**1.49**	1.29 - 1.72
3. Medium	**1.15**	1.11 - 1.20	**1.38**	1.26 - 1.51	**1.54**	1.33 - 1.79
4. Mid-low	**1.11**	1.07 - 1.16	**1.35**	1.23 - 1.49	**1.55**	1.33 - 1.81
5. Low	**1.08**	1.04 - 1.12	**1.28**	1.15 - 1.41	**1.45**	1.23 - 1.71
UHI						
Low	**1.11**	1.08 - 1.13	**1.29**	1.20 - 1.38	**1.42**	1.26 - 1.60
High	**1.11**	1.09 - 1.14	**1.36**	1.30 - 1.44	**1.58**	1.45 - 1.71
SEP-UHI						
SEP=1-2 / UHI=Low	**1.10**	1.05 - 1.14	**1.22**	1.09 - 1.38	**1.31**	1.08 - 1.59
SEP=1-2 / UHI=High	**1.11**	1.07 - 1.15	**1.39**	1.29 - 1.49	**1.63**	1.45 - 1.84
SEP=3 / UHI=Low	**1.19**	1.12 - 1.27	**1.44**	1.21 - 1.71	**1.60**	1.21 - 2.13
SEP=3 / UHI=High	**1.12**	1.06 - 1.18	**1.34**	1.21 - 1.49	**1.52**	1.27 - 1.81
SEP=4-5 / UHI=Low	**1.08**	1.05 - 1.12	**1.28**	1.15 - 1.42	**1.44**	1.22 - 1.71
SEP=4-5 / UHI=High	**1.11**	1.07 - 1.16	**1.35**	1.23 - 1.47	**1.54**	1.33 - 1.78

Table 6.9 Heat-related effects on cardiovascular mortality. Risk for increases in mean temperature between the 50th and 75th, 50th to 95th, 50th to 99th of the summer distribution in Rome by SEP, UHI and SEP and UHI combined.

	75th percentile		95th percentile		99th percentile	
	OR	95%CI	**OR**	95%CI	**OR**	95%CI
Cardiovascular Mortality						
SEP						
1. High	**1.13**	1.07 - 1.20	**1.42**	1.24 - 1.63	**1.67**	1.33 - 2.08
2. Mid-high	**1.16**	1.10 - 1.23	**1.39**	1.21 - 1.59	**1.54**	1.23 - 1.93
3. Medium	**1.18**	1.11 - 1.26	**1.43**	1.24 - 1.64	**1.60**	1.28 - 2.01
4. Mid-low	**1.15**	1.08 - 1.22	**1.49**	1.28 - 1.73	**1.80**	1.41 - 2.30
5. Low	**1.08**	1.01 - 1.15	**1.32**	1.12 - 1.55	**1.54**	1.18 - 2.01
UHI						
Low	**1.14**	1.09 - 1.18	**1.35**	1.20 - 1.51	**1.50**	1.25 - 1.81
High	**1.14**	1.10 - 1.18	**1.44**	1.33 - 1.55	**1.69**	1.49 - 1.92
SEP-UHI						
SEP=1-2 / UHI=Low	**1.14**	1.06 - 1.21	**1.27**	1.05 - 1.53	**1.34**	0.99 - 1.82
SEP=1-2 / UHI=High	**1.15**	1.09 - 1.21	**1.45**	1.30 - 1.63	**1.71**	1.42 - 2.05
SEP=3 / UHI=Low	**1.25**	1.14 - 1.38	**1.68**	1.28 - 2.21	**2.02**	1.29 - 3.15
SEP=3 / UHI=High	**1.14**	1.05 - 1.24	**1.35**	1.15 - 1.58	**1.49**	1.15 - 1.94
SEP=4-5 / UHI=Low	**1.10**	1.03 - 1.16	**1.30**	1.09 - 1.54	**1.46**	1.10 - 1.94
SEP=4-5 / UHI=High	**1.13**	1.05 - 1.20	**1.49**	1.29 - 1.71	**1.84**	1.45 - 2.32

Table 6.10 Heat-related effects on respiratory mortality. Risk for increases in mean temperature between the 50th and 75th, 50th to 95th, 50th to 99th of the summer distribution in Rome by SEP, UHI and SEP and UHI combined.

	75th percentile		95th percentile		99th percentile	
	OR	95%CI	**OR**	95%CI	**OR**	95%CI
Respiratory Mortality						
SEP						
1. High	**1.06**	0.89 - 1.26	**1.02**	0.72 - 1.44	**0.96**	0.54 - 1.72
2. Mid-high	**1.29**	1.09 - 1.53	**1.89**	1.34 - 2.67	**2.43**	1.37 - 4.31
3. Medium	**1.37**	1.16 - 1.61	**1.60**	1.11 - 2.32	**1.65**	0.90 - 3.03
4. Mid-low	**1.26**	1.07 - 1.49	**1.93**	1.31 - 2.86	**2.61**	1.38 - 4.95
5. Low	**1.16**	0.99 - 1.37	**1.46**	0.93 - 2.29	**1.71**	0.83 - 3.54
UHI						
Low	**1.23**	1.11 - 1.38	**1.59**	1.19 - 2.14	**1.86**	1.14 - 3.03
High	**1.21**	1.09 - 1.33	**1.48**	1.21 - 1.81	**1.67**	1.20 - 2.32
SEP-UHI						
SEP=1-2 / UHI=Low	**1.07**	0.88 - 1.30	**1.47**	0.93 - 2.35	**1.92**	0.87 - 4.27
SEP=1-2 / UHI=High	**1.22**	1.04 - 1.42	**1.34**	1.00 - 1.79	**1.36**	0.85 - 2.18
SEP=3 / UHI=Low	**1.65**	1.26 - 2.16	**2.25**	1.06 - 4.80	**2.49**	0.74 - 8.41
SEP=3 / UHI=High	**1.20**	0.97 - 1.49	**1.35**	0.88 - 2.08	**1.40**	0.69 - 2.83
SEP=4-5 / UHI=Low	**1.21**	1.04 - 1.41	**1.45**	0.93 - 2.27	**1.60**	0.77 - 3.31
SEP=4-5 / UHI=High	**1.21**	1.01 - 1.44	**1.92**	1.30 - 2.83	**2.72**	1.45 - 5.12

Table 6.11 Statistical testing of heterogeneity among strata specific total mortality estimates by age groups, gender, age and gender combined, marital status, education, occupation, co-morbidities, SEP, UHI, ISA and level of urbanization.

	75th percentile		95th percentile		99th percentile	
	Q_res	P-value	Q_res	P-value	Q_res	P-value
Natural mortality						
Age	32.04	0.000	37.59	0.000	29.88	0.000
Sex	7.46	0.006	3.16	0.076	1.44	0.229
Among males: by age	6.24	0.044	6.43	0.040	5.45	0.065
Among females: by age	9.52	0.009	22.99	0.000	21.08	0.000
Marital status	15.98	0.001	16.02	0.001	11.29	0.010
Education	4.38	0.223	3.85	0.278	2.87	0.412
Occupation	20.98	0.001	19.91	0.001	14.69	0.012
Pre-CVD	2.31	0.129	2.45	0.118	1.78	0.183
Pre-COPD	0.00	0.959	0.00	0.944	0.01	0.922
Pre-Diabetes	0.98	0.322	0.04	0.786	0.38	0.535
SEP	6.27	0.180	1.66	0.799	0.71	0.950
UHI	0.17	0.680	1.76	0.185	2.01	0.157
ISA	4.38	0.112	0.92	0.630	0.52	0.771
% urban	1.61	0.447	0.02	0.992	0.07	0.964
Among SEP12: by UHI	0.21	0.644	3.09	0.079	3.59	0.058
Among SEP3: by UHI	2.37	0.124	0.45	0.502	0.11	0.745
Among SEP45: by UHI	0.90	0.344	0.51	0.476	0.29	0.588

Q_res: statistics of residual heterogeneity (among strata-specific estimates), based on Cochran-Q. p-value: corresponding p-value.

Null hypothesis: perfect homogeneity among strata-specific estimates. Alternative hypothesis: presence of heterogeneity

Table 6.12 Statistical testing of heterogeneity among strata specific cardiovascular mortality estimates by levels of age groups, gender, age and gender combined, marital status, education, occupation, co-morbidities, SEP, UHI, ISA and level of urbanization.

	75th percentile		95th percentile		99th percentile	
	Q_res	P-value	Q_res	P-value	Q_res	P-value
Cardiovascular mortality						
Age	21.44	0.000	15.70	0.001	10.61	0.014
Sex	9.40	0.002	5.03	0.025	2.66	0.103
Among males: age	12.29	0.002	4.85	0.089	2.60	0.272
Among females: age	2.21	0.332	7.30	0.026	7.40	0.025
Marital status	14.53	0.002	8.34	0.039	4.94	0.180
Education	5.66	0.129	1.40	0.706	1.06	0.787
Occupation	20.15	0.001	10.25	0.068	5.93	0.313
Pre-CVD	1.62	0.203	0.50	0.479	0.17	0.678
Pre-COPD	0.42	0.516	2.48	0.116	2.60	0.107
Pre-Diabetes	0.18	0.667	2.51	0.113	3.84	0.050
SEP	4.94	0.293	1.28	0.865	1.10	0.894
UHI	0.02	0.890	0.82	0.364	1.03	0.310
ISA	1.54	0.463	1.31	0.518	0.87	0.646
% urban	0.25	0.884	0.92	0.633	1.29	0.525
Among SEP12: UHI	0.08	0.773	1.50	0.220	1.79	0.181
Among SEP3: UHI	2.19	0.139	1.84	0.175	1.28	0.258
Among SEP45: UHI	0.36	0.546	1.46	0.228	1.49	0.222

Q_res: statistics of residual heterogeneity (among strata-specific estimates), based on Cochran-Q.

p-value: corresponding p-value. Null hypothesis: perfect homogeneity among strata-specific estimates. Alternative hypothesis: presence of heterogeneity

Table 6.13 Statistical testing of heterogeneity among strata specific respiratory mortality estimates by levels of age groups, gender, age and gender combined, marital status, education, occupation, co-morbidities, SEP, UHI, ISA and level of urbanization.

	75th percentile		95th percentile		99th percentile	
	Q_res	P-value	Q_res	P-value	Q_res	P-value
Respiratory mortality						
Age	18.92	0.000	12.12	0.007	7.59	0.055
Sex	1.35	0.245	0.02	0.893	0.30	0.584
Among males: age	2.82	0.244	0.80	0.671	0.31	0.856
Among females: age	15.07	0.000	15.25	0.000	11.02	0.004
Marital status	13.11	0.004	10.63	0.014	8.74	0.033
Education	4.26	0.235	4.00	0.261	5.41	0.144
Occupation	2.76	0.737	1.75	0.883	2.43	0.786
Pre-CVD	1.14	0.285	0.77	0.379	0.44	0.506
Pre-COPD	0.52	0.469	0.04	0.850	0.00	0.977
Pre-Diabetes	0.53	0.467	0.00	0.977	0.03	0.862
SEP	5.41	0.247	8.20	0.085	6.91	0.141
UHI	0.09	0.766	0.16	0.690	0.14	0.713
ISA	1.97	0.374	0.56	0.754	0.39	0.824
% urban	0.02	0.992	0.97	0.617	1.22	0.545
Among SEP12: UHI	1.02	0.312	0.12	0.729	0.54	0.462
Among SEP3: UHI	3.31	0.069	1.33	0.249	0.65	0.421
Among SEP45: UHI	0.00	0.998	0.85	0.356	1.16	0.281

Q_res: statistics of residual heterogeneity (among strata-specific estimates), based on Cochran-Q.

p-value: corresponding p-value. Null hypothesis: perfect homogeneity among strata-specific estimates. Alternative hypothesis: presence of heterogeneiy

Urban Heat Island Effect and Socioeconomic position.

Tables 6.8-6.10 show the risk of mortality for increases in temperatures between the 50^{th} - 75^{th}, 50^{th} - 95^{th} and 50^{th} - 99^{th} percentile stratified by urban context factors (SEP and UHI). Although the heat-related risk of mortality was significant in every SEP class, and effect estimates increased as the temperature range included more extreme values, there didn't seem to be a trend relating socio-economic inequality to heat-related deaths. The analyses by cause of death gave similar results (Tables 6.9-6.10). Statistical testing confirmed no significant difference in estimates by SEP (Tables 6.11-6.13).

Similarly, the analysis by UHI showed some differential effect only when extreme and very extreme temperatures occurred, with a greater risk in warmer areas (high UHI intensity) for cardiovascular and total deaths. While for respiratory deaths living in an area of low UHI seemed to be associated with a slightly greater mortality risk. However, it is noteworthy that confidence intervals of estimates by UHI category overlap and statistical testing showed no significant difference (Tables 6.11-6.13)

When considering the potential synergy between socio-economic conditions and UHI, no clear pattern was observed, only some slight no-significant differences in estimates. Among the high SEP group, when exposed to extreme temperatures, those living in hotter zones of the city (high UHI) had a higher risk of total mortality (SEP12UHIhigh OR=1.63 CI95% 1.45-1.84) compared to SEP12UHIlow OR=1.31 CI95% 1.08-1.59). A similar pattern was observed for cardiovascular deaths. Moreover, for respiratory and cardiovascular deaths, among individuals with a low SEP effect estimates were higher for those living in hotter areas (high UHI (table 6.9-6.10). Again, confidence intervals overlap and no significant differences were depicted (Table 6.11-6.13).

Impervious surfaces and urban development

When considering impervious surfaces and percent urban development by area, slightly different patterns emerged between the two variables and heat-effects (Table 6.14). Firstly, as for other spatial context attributes, an increasing trend in risk was observed when extreme temperatures were considered in the estimate range. For ISA, the risk of mortality was similar among subjects living in the different ISA class areas. When considering urban development, only among the high urban development (>75%) class, the effect differed between temperature intervals (confidence intervals did not overlap). For other temperature intervals, there was no difference in effect estimates by level of % urban and no statistical difference was shown (Table 6.11-6.13). It is plausible that individuals all reside in areas classified as continuous urban fabric and capture residential areas tout court explaining limited variability.

Looking at the correlations between UHI, ISA and percent urban it was interesting to note that ISA and UHI had a high correlation (0.76), while UHI and urban development had a lower correlation (0.57). Areas with low ISA and low UHI had potentially higher vegetative coverage and green space which contributes to mitigating the UHI intensity by producing more latent heat flux and less sensible heat flux.

Table 6.14 Heat-related effects on respiratory mortality. Risk estimates for increases in mean temperature between the 50th and 75th, 50th to 95th, 50th to 99th of the summer distribution in Rome by impervious surface and % urban development.

	75th percentile			95th percentile			99th percentile		
	OR	95%CI		**OR**	95%CI		**OR**	95%CI	
ISA									
low	**1.09**	1.06	1.13	**1.29**	1.17	1.42	**1.45**	1.24	1.69
med	**1.15**	1.11	1.19	**1.37**	1.26	1.49	**1.53**	1.33	1.76
high	**1.10**	1.08	1.13	**1.34**	1.27	1.42	**1.55**	1.41	1.69
urban development									
Low	**1.10**	1.06	1.14	**1.33**	1.22	1.46	**1.54**	1.32	1.79
med	**1.10**	1.07	1.14	**1.34**	1.24	1.45	**1.54**	1.35	1.76
high	**1.13**	1.10	1.15	**1.34**	1.27	1.42	**1.51**	1.38	1.66

Table 6.15 Heat-related effects on total mortality considering 3 temperature exposures. Risk estimates for increases in mean temperature between the 50th and 75th, 50th to 95th, 50th to 99th in Rome considering single monitoring site temperature, urbanistic zone average temperature and high resolution gridded temperature.

	75th percentile		95th percentile		99th percentile	
	OR	95%CI	**OR**	95%CI	**OR**	95%CI
Total Mortality						
T. at 1-km^2 grid	**1.11**	1.09 - 1.13	**1.34**	1.29 - 1.40	**1.53**	1.43 - 1.63
T. by urbanistic zone	**1.11**	1.09 - 1.13	**1.34**	1.28 - 1.40	**1.52**	1.42 - 1.63
T. from airport station	**1.11**	1.10 - 1.13	**1.32**	1.26 - 1.38	**1.48**	1.38 - 1.59
Cardiovascular Mortality						
T. at 1-km^2 grid	**1.14**	1.11 - 1.17	**1.41**	1.32 - 1.50	**1.63**	1.47 - 1.81
T. by urbanistic zone	**1.14**	1.11 - 1.17	**1.41**	1.32 - 1.51	**1.63**	1.46 - 1.81
T. from airport station	**1.14**	1.11 - 1.16	**1.40**	1.31 - 1.50	**1.61**	1.45 - 1.80
Respiratory Mortality						
T. at 1-km^2 grid	**1.22**	1.13 - 1.31	**1.52**	1.29 - 1.80	**1.73**	1.32 - 2.28
T. by urbanistic zone	**1.21**	1.12 - 1.30	**1.50**	1.27 - 1.78	**1.71**	1.29 - 2.27
T. from airport station	**1.20**	1.12 - 1.29	**1.47**	1.23 - 1.74	**1.64**	1.23 - 2.19

6.4.4 Sensitivity analysis – effect estimates with temperature exposure at different resolutions.

In order to evaluate the potential misclassification of exposure and effect estimates a sensitivity analysis was carried out. The same case-cross over model on total, cardiovascular and respiratory mortality, was carried out with fixed percentiles as for the main analysis, but considering three different exposures:

1. Single point measured mean temperature data (Ciampino airport),
2. Satellite derived temperature averaged by urbanistic zone (Lazio region time series analysis)
3. individual 1x1km gridded air temperature exposure.

The temperature distribution was less variable considering a single point of observed data while the high resolution gridded data had a wider distribution of daily temperatures. Results showed that for moderate increases in temperature (50^{th} to 75^{th} percentile) the effect estimates were equivalent, while when including more extreme values higher resolution exposure managed to capture the exponential increase in the effect slightly better. Dose-response curves in Figures 6.7-6.9 show how the monitoring station exposure distribution ended at lower temperatures, not even capturing the association with higher temperatures. Effect estimates considering each exposure are reported in table 6.15. The OR using weather station data was of 1.48 (CI95% 1.38-1.59) compared to 1.53 (CI95% 1.43-1.69) of the 1x1km gridded individual exposure for increases between the 50^{th} and 99^{th} percentile. Noteworthy that the increase is small and CI of estimates overlap. Similar patterns were observed for cardiovascular and respiratory causes. Moreover, for respiratory causes the slope of the curves for high resolution gridded data had a slightly steeper curve associated to higher effect estimates throughout the distribution above the turning point (Table 6.12).

Attributable deaths for increases in temperature between the 50th and 75th and 50th to the 99th percentile considering the three different exposures are summarized in Table 6.16. No great differences are observed when considering moderate heat attributable deaths, while differences are more relevant when extreme values are considered. The point source temperature exposure underestimates the impact of heat by around 100 deaths in the study period.

Table 6.16 Heat Attributable deaths for mean temperature increases between the 50th – 75th and 50th- 99th percentile considering three temperature exposures. Summers 2002-2010.

	75th percentile		99th percentile	
	AD	95%eCI	AD	95%eCI
Total Mortality				
T. at 1-km^2 grid	**620**	489 - 736	**2595**	2281 - 2889
T. by urbanistic zone	**636**	510 - 763	**2526**	2198 - 2813
T. from airport station	**639**	530 - 763	**2431**	2106 - 2728

Figure 6.7 Mean temperature – total mortality association in Rome by exposures, summer (2001-2010).

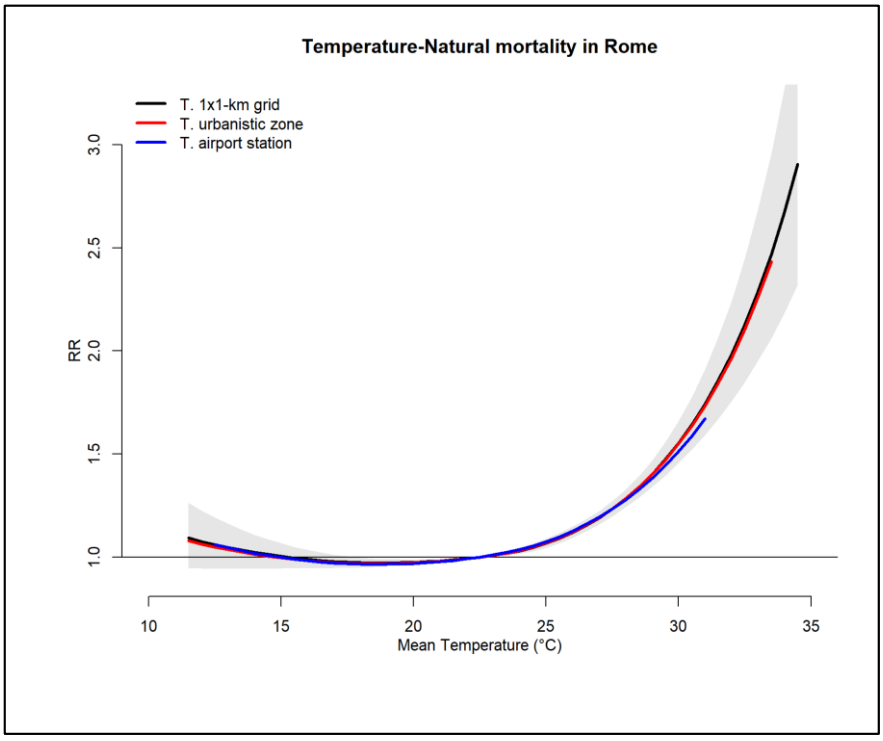

Figure 6.8 Mean temperature – cardiovascular mortality association in Rome by exposures, summer (2001-2010).

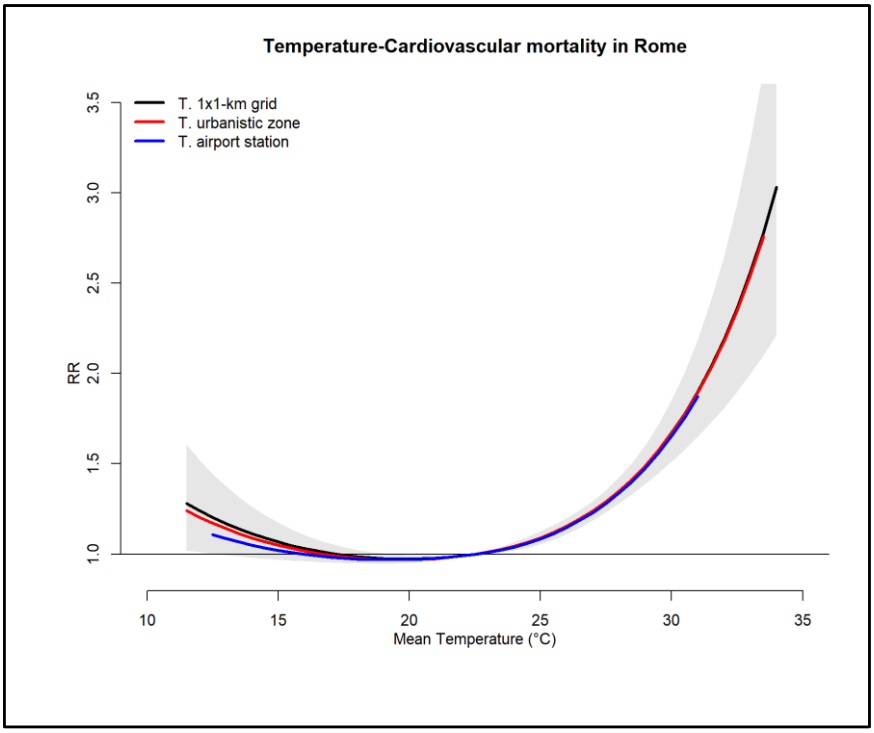

Figure 6.9 Mean temperature – respiratory mortality association in Rome by exposures, summer (2001-2010).

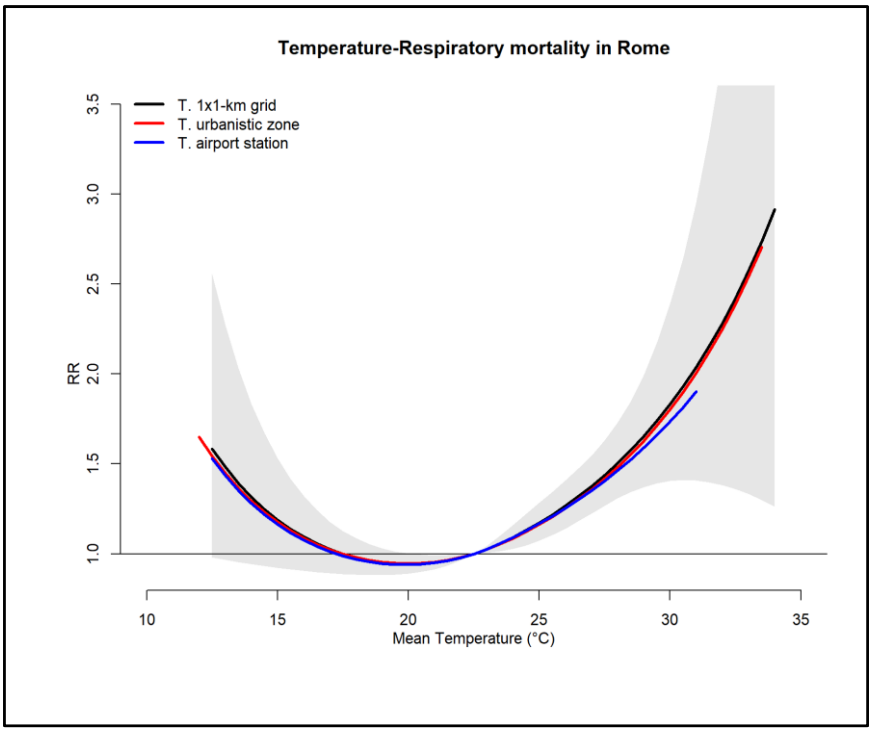

6.5 DISCUSSION

The case cross-over analysis conducted on the Rome cohort, confirms the significant non-linear effect of heat on mortality. The risk in total mortality associated to an increase in temperature in the moderate range (50^{th} vs 75^{th}) was of 1.11 (95%CI: 1.09-1.13) and when extreme values were included risk estimates rose to 1.53 (95%CI: 1.43-1.63). Overall risks for cause-specific mortality were higher; with an OR of 1.14 (95%CI: 1.11-1.17) for cardiovascular deaths and 1.22 (95%CI: 1.13-1.31) for respiratory deaths with a rising trend when more extreme temperature intervals were considered. A previous case cross-over study conducted in four Italian cities showed similar results for Rome.[179]

The study design and high spatio-temporal resolution exposure data permitted the estimation of hat related effects at individual level, and it is the first time such a study is carried out in a large city. Lee et al. found that spatiotemporal models gave slightly better model fits, possibly due to a reduced exposure error[221]. Spiegelman suggested that by using a more accurate measure of exposure the spatial dynamics of the environmental phenomenon are taken into account, thus potentially reducing the bias in effect estimates[22]. Moreover, the sensitivity analysis using different exposures showed how a more refined high-resolution exposure attributed to individual subjects provided more accurate effect estimates, especially for extreme exposures. This was true for both effect estimates and for impacts (attributable deaths). Dose-response curves and estimates show how the monitoring station exposure distribution ends at lower temperatures, not even capturing the effects of extreme heat, suggesting an underestimation in the effect of heat in Rome in previous studies using single point weather stations. Attributable deaths for temperature increases between the 50^{th} and 99^{th} percentile considering high resolution gridded data gave 100 extra heat-attributable deaths compared with single point source exposures.

The study also considered individual and spatial vulnerability factors, thus identifying potential effect modifiers. A modification in the heat-related risks was observed for several demographic factors across the temperature intervals. The risk of heat on mortality was modified by age and gender. An increasing trend in the risk of mortality was observed with age. The risk was non-significant in the 35-64 age group and increased from 1.06 (95%CI: 1.02-1.11) in the 65-74 age group to 1.18 (95%CI: 1.15-1.22) in the very old (85+ years). Females were at greater risk than males. Confidence intervals were somewhat wider among elderly males, as these were fewer numerically. Estimates for females were more stable, with greatest effects in old (75-84 years) and very old (85+). Age has been recognised as a susceptibility factor throughout the literature[5,8,169,179]. While for gender the findings are less clear, several studies have documented a greater vulnerability to heat among women both in terms of mortality and morbidity[218,248,249,349], while results are contrasting regarding susceptibility of males[5,221]. The need for further studies is confirmed also by the meta-analysis recently carried out by Benmarhnia[6].

Socio-economic variables such as marital status, education and occupation have been previously considered as risk factors to heat-related mortality.[169,181–183,256,293,299,350] A significant effect modification was observed by marital status and occupation. In this study greater heat-related effects were found for widows/widowers, potentially reflecting older age and living alone[290]. These findings confirm results in the literature.[179,252,287] Considering occupation, no effect was seen for non-manual and manual workers, the only significant effects were for housewives and retired again suggesting interaction with age. Non-manual workers may be somewhat protected, working in climate controlled indoor environments with air conditioning facilities that mitigate the effect of heat during working hours. Xu et al. found a greater risk among manual workers in Barcelona suggestive that outdoor and heavy load occupations impacted on heat stress.[183] Results from the Rome study show no effect

modification by education, which corresponds to findings from studies carried out in China[197,250,351], Latin America and in the USA [5,210,287]. However, it is worth mentioning that other studies also found a higher heat-related mortality risk among individuals with a lower level of education[169,319]. Zhang et al. found a greater effect among those with a higher education in central China[198], while Huang found a greater effect among those of low education level and SEP[218] When considering more comprehensive socio-economic indicators, there was no clear trend or effect modification in the association between heat and mortality by SEP in Rome. Studies conducted in the US have shown a clear trend by socio-economic status[180,256,352] with greater effects in deprived areas. A recent study conducted in Hong Kong gave similar results[299] while a study from Brazil showed no effect modification.[261] Milojevic et al. found that adjusting by neighbourhood level socio-economic deprivation in London had little effect on the association between temperature and mortality across high resolution temperature categories.[332]

Considering the UHI effect, results for Rome reported a suggestive (non-significantly different) modification when extreme temperatures values were estimated. Important to recall that high resolution temperatures were attributed at individual level, hence already taking into account the differential heat effects within the urban area. Smargassi et al[181] found that subjects living in postcode areas of Montreal with higher surface temperatures had a higher risk of dying during hot days, while Xu et al, Goggins et al. and Burkart et al. found that census blocks or areas with less vegetation or green space were associated with higher heat related effects.[182,183,290,292] The interaction between UHI and socioeconomic level gave a better characterization of these two phenomena in the urban area. Estimates were slightly different by UHI levels for high level SEP when extreme temperatures were considered, although not significantly different. This can be linked to the fact that in Rome most central areas are also the ones with high SEP, and are characterised by tight knit building structures, narrow streets

and reduced ventilation, making these areas potentially more exposed to nocturnal high UHI intensity. Furthermore, compared to cities in the US, air-conditioning in housing has become more common in the latest 10-15 years and this might also influence response to climate change and hotter summers.

A limit worth mentioning is that SEP was defined at census tract level and might not be very accurate, furthermore it was calculated using data from the 2001 census, hence somewhat dated. Further analysis will be conducted using the new socio-economic indicator derived for Rome from the 2010 census data and a more refined census block classification for peripheral new residential areas. Another limitation regarding vulnerability is the interaction with or confounding effect of air pollution during summer. The potential confounding effect is presumably very small considering heat estimates are greater in magnitude compared to air pollution estimates, while the synergistic effect of pollutants during heat waves and hot days might be relevant and requires investigation. However, attention should be posed on this aspect taking into account the causal pathways between the two exposures, namely air pollution and temperature, and health outcomes. As recently denoted by Buckley and colleagues[353] while the rationale for adjusting for temperature when estimating the effects of air pollution, is justifiable, as temperatures and meteorology alters air pollution concentrations (eg. Ozone) the inverse is not necessarily valid. Several studies have been carried out on the synergistic effect of temperature and air pollutants in particular for PM10 and ozone.[270,272,274,354] These aspects are important when considering public policy and prevention measures related to environmental exposures, as exposures especially in urban areas are concurrent as are subgroups most at risk, hence policy measures, or warning systems and surveillance could have an dual beneficial effect.

The study showed that urban populations are exposed to higher temperatures and might be more acclimatized[220,329,332] as also where Rome had slightly lower risk estimates for extreme heat intervals. However, the heat-related effects and impacts on mortality were still significant and need to be dealt with by improving population adaptation and public health response. These findings will be of great importance for the development of high resolution warning systems and public health response plans which in Rome entails the identification of frail elderly subjects who are then included in the GP active surveillance program during summer.[337] Identifying areas most at risk during heat waves, where susceptible subjects reside will ensure a more efficient management of the limited public health resources available.

CHAPTER 7 – OVERALL SUMMARY AND DISCUSSION

7.1 SUMMARY AND DISCUSSION

The research carried out had the scope of improving knowledge on the short-term effects of heat on mortality and hospital admissions. In reference to this, the aims of the thesis can be summarized as follows:

1. to define fine scale spatio-temporal air temperature data derived from LST using MODIS data, meteorological data and land use data for Italy with a 1x1km resolution over the period 2000-2010.
2. to estimate the effects and impacts of heat on mortality and morbidity in the Lazio region at municipal level using 1x1km satellite-derived mean air temperature during summer.
3. estimate the effects of heat on mortality within a large urban area taking into account the differential effect of heat due to individual factors (socio-demographics, pre-existing chronic disease), and area level factors (UHI intensity, socio-economic indicator, land use) using the Rome Longitudinal Population Cohort (ROLS). Exposure was attributed at individual level using the 1x1km predicted mean air temperature.

The thesis presents mixed-regression models to predict air temperature data using 1x1km satellite derived LST, land use and land cover variables and meteorological data from ground monitoring networks. The performance of these complex models, using random out-of-sample cross validation, was extremely good in the stage 1 model (only on grid cells with both LST and observed data) with a mean R^2 value of 0.96 and RMSPE of 1.1°C and R^2 of 0.89 and 0.97

for the spatial and temporal domains respectively. The model was also validated with regional weather forecasting model data and gave excellent results (R^2=0.95 RMSPE=1.8°C). The models for each year were able to capture spatial temperature gradients across Italy as well as temporal differences at the annual, seasonal and daily interval. The advantages of the data are that they cover the entire Italian domain, thus providing fine scale resolution daily time series, for areas in which meteorological data are usually unavailable, enabling the evaluation of temperature variations and health risks across space in a more detailed manner. The monitoring of temperature fluctuations over time at national, regional or city level can be carried out. This is important when considering climate change; to identify areas at risk where greatest temperature increases have occurred, or where the change in temperatures may have secondary effects on the environment, ecosystems or on biodiversity. Climate change models or re-analysis modelled data of current and past weather and climate can also be compared with this data to look at temporal trends across Italy. Furthermore, the exposure data was used to define the UHI in Rome, in terms of air temperature rather than simply surface temperature data as done in most studies[181,182]. The intensity of the UHI was calculated for each day comparing urban 1x1 km grid squares with a fixed sub-urban point. The mean daily intensity of the UHI was of +1.7°C, reaching maximum values of +3.4°C. The study carried out shows the spatio-temporal distribution of the UHI intensity and its variation in terms of association to land use and land cover changes, urban sprawl and other factors[106,355–357]. Wang et al. used LST data to evaluate changes in the UHI in Phoenix, Arizona over a 14 year period and found that the areas that had changed the most were the outskirts of the city, as urban, residential and impervious surfaces expanded reducing the natural vegetation in the peripheral areas[358]. A study conducted in the US on UHI spatial distribution and intensity among US cities and their change over time, also found that surface UHI depended on the size of the urban area, the level of urbanization and land use characteristics[359]. An increase in UHI intensity and total area of UHI, during

summer and winter, was observed in a study conducted in 35 Chinese cities between 2000-2015[360]. The derived data can be used to evaluate changes in the UHI intensity in Italian cities over time.

The high resolution air temperature dataset provides a very attractive alternative source of data to be used in environmental epidemiological studies in Italy. It provides a temperature index, namely mean temperature, which has been widely used in time series studies[4,6,18,361] and with a daily temporal resolution which is the time interval traditionally considered in these studies.

Mean temperature data developed in the first part of research was then was used in two studies aimed at estimating the health effects of heat, the first in the Lazio region to account for geographical differences in effects and impacts of heat on mortality and hospital admissions between urban, sub-urban and rural settings. While the second study specifically addressed effect modification in the heat-related risk due to individual level and area level factors in the city of Rome. Findings not only confirmed the well-known effects and impacts of heat on health outcomes, but gave some additional insights into the heterogeneous effect at geographical level and considering individual and urban landscape characteristics.

The time series study conducted in the Lazio region, found a significant effect of heat on mortality in all municipalities, with an overall relative risk of 1.08 (95% CI :1 .07-1.08) for an increase in temperature between the 50th and 75th percentile of the summer distribution with differences amongst rural, suburban and urban areas. The highest effects on total mortality were observed for medium and large sized municipalities. Conversely, when comparing the effect on total mortality for increases between the 50th and the 99th percentile, Rome and small municipalities had a similar risk (RR=1.53 95% CI: 1.47-1.60 and RR=1.54 95% CI: 1.47-1.59 respectively). For all areas considered, an increasing trend in the effects of mortality was observed when extreme temperatures were included. Studies carried out in Europe, the US and

worldwide confirm findings of an increased risk when more extreme temperatures are considered.[7,8,18,193,214,362,363]

For cardiovascular deaths, effect estimates were similar to those found for total mortality, with a rising trend as more extreme temperatures were considered. Furthermore, a spatial pattern also emerged for cardiovascular deaths in which the effects increased steadily with population size of municipalities. Compared with all total mortality, the risk for increases in mean temperature between the 50th and the 99th percentile was slightly higher, ranging between RR=1.55 95% CI: 1.48-1.62 in small municipalities to RR=1.78 95% CI: 1.69-1.87 in Rome. Greater risks for cardiovascular deaths have been documented around the world[7,10,234,251,275,330,351,362,364,365], as well as in the Mediterranean[8,172]. A limited selection of studies found a non-significant effect of heat on cardiovascular deaths.[169,244,366] The association between cardiovascular disease and heat was also studied in greater detail, specifically considering ischaemic heart disease, myocardial infarction (MI) and other heart disease. Guo et al.[367] found an increase in IHD mortality during days with high temperatures in China, while a study conducted in Germany found a significant increase in IHD, other heart disease and cerebrovascular disease.[234] A recent review confirmed the risk of myocardial infarction during hot days, with risks comprised between +7% and +40% increase in MI rates.[233]

Finally, respiratory deaths had greater effect estimates overall in the Lazio region (RR=1.87 95%CI: 1.82-1.93) considering extreme temperatures (50th to the 99th percentile). Conversely to what was observed for natural and cardiovascular deaths, the effect on respiratory deaths in rural areas (small municipalities) was limited and did not increase across the temperature range. The greatest effects were found in medium and large municipalities. For all municipalities, except small ones, a steep rise in respiratory death effect estimates occurred when extreme

values were considered. The literature confirms higher effects on respiratory deaths compared to cardiovascular deaths associated to heat exposure.[8,179,275,368]

On the contrary, the analyses conducted on hospital admissions, elucidated small or no effects of heat. An increase in admissions was observed only for respiratory causes, with a statistically significant effect in small and medium sized municipalities and overall estimates when considering temperatures between the 50th and 99th percentile. Similar results were found for Rome in a European multi-city study[12] with a +3.9 (CI95%: 0.5-7.4) percent change in hospitalizations for temperature increases above the 90th percentile of maximum apparent temperature. The study also showed that the increase was mainly among the very old.[12]

Several hypotheses have been put forward as to why hospitalizations are less associated to extreme heat events compared to mortality; firstly the timeliness between exposure and health event. Deaths occur rapidly, within three days (lag 0-3) and subjects do not receive or seek treatment or care in time, as their health status degenerates very rapidly, in fact most deaths have been reported to be out-of-hospital.[169,179,287] This is mostly true for cardiovascular causes. Secondly the underlying mechanisms that may lead to death or hospitalization may play a crucial role for both cardiovascular and respiratory events. For cardiovascular events several explanations have been put forward. Heat stress causes greater surface blood circulation and sweating and leads to an increase in heart rate. It has been suggested that heat stress causes an increase in red blood cell counts, platelet counts and blood viscosity, and may lead to heart failure, MI or stroke.[192,233–235] Conversely, mechanisms associated with heat are less clear for respiratory events, on hot days the respiratory system is under greater stress and causes exacerbation of chronic respiratory disease among those with pre-existing respiratory conditions.[5,10,12,242] Several studies have shown an increase in respiratory admissions[20,164] and more specifically among subjects with COPD.[20,179,253,255,287,369]

A sensitivity analysis was carried out considering fixed temperature values as temperature intervals for all municipality groupings rather than their own distributions. Estimates were higher for small municipalities and more contained in Rome suggesting that rural populations are less acclimatized to high temperature absolute values as suggested by the few studies comparing rural and urban areas.[221,257,329,330]

Heat attributable deaths were also calculated for each temperature interval for municipalities in the Lazio region and in Rome. Impact estimates are important for public health and policy makers as they quantify the risks, giving an idea of the entity of the burden in more comprehensive terms. Heat attributable deaths for temperatures between the 75th and 99th percentile were respectively 4434 deaths in Rome and 3127 deaths in other municipalities of the Lazio region over the 10 summer periods considered. In terms of YLL the burden comprised of around 7727 YLL each summer in the Lazio region for temperature increase between the 50th and 99th percentile. These numbers can help raise awareness on the impacts of heat and the knowledge base on the heat burden among public health bodies and encourage the uptake of policy and prevention measures. Attributable deaths and attributable risk fractions are also important when we consider future impacts on health under climate change scenarios. The IPCC Vth Assessment Report stated *"…warming of the climate system is unequivocal, and since the 1950s, many of the observed changes are unprecedented over decades to millennia*" and that "*It is extremely likely that human influence has been the dominant cause of the observed warming since the mid-20th century*"[370]. The rapid increase of greenhouse gases in the atmosphere is expected to increase both mean temperatures and temperature variability around the world.[370] Europe and the Mediterranean are among the areas most at risk in terms of temperature increases[2]. The WHO carried out a risk assessment to quantify the effects of climate change on global mortality by 2030s and 2050s, showing a relevant impact of heat across Europe[1]. Another recent publication by the WHO, estimated heat-related deaths in

European countries for the mid and late 21st century considering RCP scenarios and found that heat impacts will dramatically increase, in particular for countries of the Mediterranean[3]. Both studies however stress the need for higher spatial resolution estimates both in terms of health estimates and climate change prediction data, as well as the importance of including adaptation scenarios into the models. These aspects are very important in Italy as every year heat waves have a significant impact on mortality [229,314]. Future climate change predictions have shown that the Mediterranean will be one of the areas most affected, with an increase in the frequency and intensity of extreme events, especially heat waves[2]. Results from this research can be used to make more accurate predictions of the future heat-related burdens under different climate change scenarios at national level. This will provide policy makers with a map of current and future risks in order to further promote adequate adaptation and mitigation strategies according to local population characteristics and geo-climatic conditions and resources available.

The case cross-over study conducted in Rome provided more precise estimates of heat on cause-specific mortality as temperature exposure was assigned at individual level, with each person in the cohort having their specific spatio-temporal daily air temperature time series. Comparing temperature exposures with different resolutions, suggest that effect estimates and attributable deaths with high resolution gridded data are more accurate, reducing misclassification especially for extreme temperature intervals. Furthermore, the study helped identify effect modifiers of the temperature-mortality association considering individual and area level factors.

Results for total and cardiovascular mortality were similar to the time series study, with slightly higher estimates potentially due to the more accurate exposure attribution at individual level compared to zonal estimates of the times series study. The overall risk in mortality for increases in mean temperature between the 50th and 99th percentile was 1.53 (95%CI: 1.43-1.63) for total

mortality, 1.63 (95%CI: 1.47-1.81) for cardiovascular deaths and 1.73 (95%CI: 1.32-2.28) for respiratory deaths.

Individual vulnerability factors were identified, with age being the primary risk factor and a positive trend depicted, with the very old (85+) being at greater risk. Females seemed to be more vulnerable to heat when stratifying by gender, however, when considering the interaction between gender and age the effects of extreme temperatures were higher among elderly males. This suggesting that initial female vulnerability was related to a higher proportion of elderly females. Age has been recognised as a susceptibility factor throughout the literature as a result of the reduced thermoregulatory capacity in the elderly,[5,6] while evidence regarding gender susceptibility is still inconsistent.

Although having a pre-existing disease did not seem to modify estimates in a significant way, some suggestive patterns were observed and need to be investigated further. In particular having a pre-existing cardiovascular condition seemed to be a risk factor for total and cardiovascular mortality, while subjects with diabetes or COPD didn't seem to be at greater risk during extreme heat. Previous studies conducted in the US[20,255] and in Hong Kong.[253] 2016) have shown a greater risk of death during extreme heat among persons with diabetes and COPD, which contrast with our findings. Stafoggia et al. also found a greater risk for subjects with previous hospitalizations for COPD and cardiovascular disease, specifically heart failure and stroke.[371] A possible explanation for contrasting findings here is that these subjects are under medical control and constant surveillance, and are more aware of the risks during heat waves. Specifically, since 2006 subjects aged over 65 years with pre-existing chronic disease were all identified as susceptible to heat and included in the regional GP active surveillance program during summer.[228,337] Another possible explanation is that chronic conditions were defined considering hospitalizations in the 5 years prior to enrolment in the cohort at baseline

2001, so health status might have modified over time among the group as well as in those classified as not having the chronic condition, thus giving a potential distorted case mix. In light of these findings, pre-existing conditions should have been re-defined for every individual considering different temporal intervals within the cohort to account for new insurgence of cases as well as more severe subjects with repeated hospitalizations over time.

Individual level socio-economic variables such as marital status and occupation were also found to be effect modifiers of heat-related deaths. The greatest effect modification was found for widows/widowers, housewives and retired individuals, potentially reflecting older age or living alone as also suggested in other studies.[169,179,180,252,256] Education level did not show a clear trend either, with the highest effects of heat among subjects with primary education only and those with a university degree. Stratification of these variables by age might have helped disentangle this difference, and possibly identify two risk groups but limited power due to smaller counts by category might be a caveat.

When considering neighbourhood socioeconomic factors, while the literature suggests a greater risk for those living in lower SEP areas possibly due to their limited resources and means of response and health status[5,6,218,256,299,300] in the present study no risk gradient was found by SEP in Rome. Important to note that the index used was an area-based indicator which included a series of socio-economic variables and might not be entirely representative of the individual characteristics of all subjects in the cohort throughout the time period in study. However, it is worth mentioning that when the index was defined validation with individual socio-economic variables and an income index had a good correlation.[345] Moreover, socio-economic differentials in terms of the effects on heat might have a diverse role by age group, the proportion of very old might be greater in the high and medium high socio-economic groups compared to the more disadvantaged groups.

Location within the city, in terms of urban development, impervious surface and UHI were suggestive effect modifiers of the heat-mortality association among subjects included in the Rome cohort. The assumption here was that the urban climate and thermal characteristics within a city vary spatially and these differences might modify the response of individuals to heat. Typically, hotter zones will have an added heat load while subjects in cooler zones (presence of green areas, low building density and impervious surfaces) will have a reduced heat load during heat waves or hot days. This is the typical UHI phenomenon whereby urban areas have a positive thermal differential compared to rural areas.[78] Factors affecting the UHI and its intensity are the size of the city, its urban geometry and characteristics, population density and surrounding land use and local climate.[30,90,106,372–374].Several studies have defined spatial vulnerability maps of heat within urban areas considering the UHI and socio-demographic data.[279,301,375–377] In the present study, slightly greater risks of total and cardiovascular mortality in warmer areas (high UHI intensity) were found for temperature increases between the 50th and 95th and 50th and 99th percentile, although differences were not statistically different. When combining UHI and SEP levels, a greater risk was observed among those with a high SEP (SEP1UHIhigh RR=1.63 CI95% 1.45-1.84; SEP1UHIlow RR=1.31 CI95% 1.08-1.59). Furthermore, among those of low SEP in Rome, a greater risk of cardiovascular and respiratory mortality was found among those living in hotter areas (high UHI) when considering an increase in temperature between the 50th and 99th percentile. Noteworthy that differences in temperature effects between UHI and non-UHI areas were non-significant. These findings confirm results from the literature conducted on total mortality only. A study carried out in Montreal, considered UHI using land surface LST and housing value as proxy of SEP, found a greater UHI differential for post code areas with a high housing value[181]. Conversely, a study conducted in Hong Kong only found a differential risk by UHI and SEP among those of low SEP[182]. Moreover, Milojevic et al. found that adjusting for neighbourhood

level socioeconomic deprivation did not modify the association between temperature and mortality when high resolution temperature was considered.[332] The latter study is the only one similar to the one conducted in Rome, in terms of high resolution air temperature exposure, although purely modelled un-validated data, potentially including spatial differences in effects by design.

Other studies indirectly accounted for the differential effect of heat within urban areas by looking at green areas and the potential role of cooling.[20,183,235,292,378–381] Some studies found that vegetation/green space modified the effect of heat within urban areas[292,381] but it is worth noting that temperature was considered from a single point source and the spatial thermal conditions were not taken into account directly. Xu et al. did not find a modification in the effect of heat for green areas per se in Barcelona but for perception of little greenness in the surrounding areas by local residents.[183]

The study carried out for my thesis also considered impervious surfaces (ISA) and urban development land cover classes as indicators of the built environment as a proxy of sealed surfaces and building materials. These indicators were considered both in the time series study and in the Rome case cross-over to identify areas with higher urban development and impervious surfaces which can contribute to modifying thermal conditions. Results from the study suggest that residing in areas with a high percent of impervious surfaces was a risk factor for heat-related mortality. A study conducted in Germany comparing urban and rural areas, found a positive correlation between district mortality rates and the proportion of each district covered by sealed surfaces during time periods of high heat stress[281], which is similar to what was found in Rome and the Lazio region. Madrigano et al. found a higher risk of MI during heat wave days among those living in high density housing.[235] Two studies from the US considered population density at post code level as potential effect modifier and found a greater

risk in areas with higher population density, poverty and lower level education.[20,287] Overall, area level socio-economic indicators, the built environment and urban microclimate conditions influenced the heat-related risk of mortality in Rome.

7.2 STRENGTHS AND LIMITATIONS

7.2.1 Strengths

This is the first dataset with such a high spatio-temporal resolution in Italy and will be of great importance for both environmental and epidemiological studies on the health effects of climate change. The model permits estimation of daily temperature data in grid cells even when satellite data is not available taking into account the association with surrounding grid cells. The methodology developed is replicable in other contexts and can be updated to include more recent years. The high spatial and temporal resolution of exposure data provides a valuable dataset which can be used for nationwide studies on temperature and other environmental exposures for which temperature might be a confounder or effect modifier, for example air pollution studies. Furthermore, the richness of the dataset, also in terms of land use and land cover variables from different sources, having not only a good spatial scale but also spatio-temporal variables (NDVI), is also an added value, offering the possibility of integrating additional spatial and spatio-temporal parameters with a standardized geographical framework. The estimated UHI intensity was not a measure of the surface temperature, as provided in many other studies, but of air temperature which is a direct measure to be used in epidemiological studies.

The analyses carried out, evaluated and compared the effects of heat for different temperature intervals in different settings taking into account geographical and population characteristics. Considering the Bradford Hill framework[382–384] and the issue of causality in the context of an environmental exposure, air temperature, to whom the entire population is exposed to some considerations can be made. Significant effect estimates were observed for cause-specific mortality in urban, rural and suburban contexts for different temperature ranges and a gradient was observed for more extreme temperature values. Higher effects and impacts were observed when considering extreme temperatures and these were coherent using both the time-series and

case-cross over approach. The findings were consistent with previous research conducted around the world, and potential biological mechanisms have been discussed in the literature. However, better evidence on the causal processes is still needed to specifically address this issue. Causal modelling frameworks have recently been proposed such as the propensity score[385] or instrumental variable approach[386] to assess the causal effects of environmental exposures[387]. These approaches can be used to have better insights into the issue of causality when studying health effects of temperatures. The temporal criteria, which is one of the most important in epidemiological terms for causality, was fully satisfied as exposure proceeds the onset of the health outcome (death) or onset of the disease. Being an environmental exposure to which we are all exposure to, limits the specificity of health effects and it is not plausible to exclude it completely. Adaptation measures to contrast heat effects can be adopted. The difference-in-difference approach or regression discontinuity approach[388], have been recently proposed as a quasi-experimental technique for evaluating the impact on health of heat prevention plans[389] or air pollution warning systems[390,391] or other public health interventions.[392] Benmarhnia and collegues evaluated the effectiveness of heat action plan in Montreal by applying the difference-in-differences approach. Mortality on days when warnings were issued (temperatures above a set threshold) were compared to days below the threshold and years before and after the introduction of the heat plan were compared[389]. This quasi-experimental approach gives a more appropriate evaluation of public health measures, however it is worth noting that as the exposure is not actually reduced or taken out, as in other applications of this approach, some limitations in this context remain. The choice of pre and post years may modify results and the introduction of heat plan may not necessarily mean his is the most appropriate cut-point in the time series.

Estimates for urban, sub-urban and rural areas were calculated and showed a significant effect of heat on cause-specific mortality in all settings in the Lazio region. Effect estimates and

impacts for rural and sub-urban settings were provided for the first time. The case cross-over study conducted in a large urban area, provided important findings on the differential effect of heat by areal and individual characteristics. The case cross-over approach is also very strong at it rules out all confounding by factors that do not vary over time or are slow varying, while short-term varying confounders that might influence the short-term variation were included in the model (season, day of the week, summer reduction in mortality) making findings more reliable.

7.2.2 Limitations

Some limitations of the several studies carried out are worth mentioning:

- The complex exposure method requires a copious amount of data to implement the models and procedures are time consuming to set up the dataset. Meteorological data from weather stations had a heterogeneous coverage across Italy and is still partial in some areas, mainly due to the difficulty in retrieving regional data from some of regional environment agencies.
- External validation of the model was conducted only for central Italy on one year. This was mainly due to limited data availability and retrieval in the time available to me. The choice of a high resolution regional scale forecast model meant that potential models from which to choose was limited and often weather forecast data from past periods are not stored. This could be overcome by having access to data for all Italy, or in alternative using re-analysis data but losing out on spatial resolution, which is already higher than our 1x1km grid.
- Mean temperature was used as exposure only, maximum or minimum temperatures could not be estimated due to the limited or heterogeneous measurement of the observed data for these indices from different sources. The data set for the quantification of maximum

or minimum temperature would have been a subset and model performance would have been less accurate at national level. The definition of these parameters could be looked into considering specific areas where data is available.

- One limitation of the spatiotemporal exposure estimates provided in my work is the potential discrepancy between personal temperature exposures and ambient estimates at 1km^2 resolution. The epidemiological literature has well documented the lack of accurate measurements of personal exposures to environmental exposures, such as temperature or air pollutants, and that this can lead to health effect estimates that are potentially bias or have a reduced statistical power[393]. Even finely resolved predictions from spatiotemporal models such as the ones estimated here, are prone to measurement error: classical/classical-like error due to model parameter estimation and Berkson/Berkson-like error due to spatial smoothing[394]. While with classical error health effect estimates tend towards null value, both error types might reduce the statistical power[395]. Unfortunately, it is impossible to quantify the amount of bias on health effect estimates induced by the exposure modelling strategy, because individual temperature measurements in the study subjects (or a random sample of them) are not available. However, as my study was focused on day-to-day variability it is plausible to assume that measurement error should not be a major concern, as I expect that spatial differentials in daily temperatures are not extreme, and should have been adequately captured by the exposure model.
- When considering urban areas and the UHI intensity, higher spatial resolution satellite data would have improved UHI characterization. Noteworthy that gaining in spatial resolution would not have given daily temporal data. UHI intensity is highest at night, so defining UHI considering nocturnal data only might have given a different magnitude in terms of UHI intensity and slightly diverse pattern. Unfortunately, in the time available it was not possible to pursue this aspect.

- Green space was not directly considered as an effect modifier into the analysis but might have been worth including to highlight the role of vegetation in terms of cooling as well as general landscape added value and how these might influence heat-related mortality. However, the fine resolution temperature exposure and UHI indirectly includes thermal cooling by vegetation as satellite LST data was used and models included land use and NDVI.
- Considering the two health effect studies, the area in study was restricted with respect to initial idea of carrying out a national study on mortality and hospital admissions. Unfortunately, I had to succumb to the curse of Italian bureaucracy and its interminably long and time-consuming procedures.
- The case cross-over models adjust for confounders that do not vary in time or are slow changing factors by design, while short-term varying confounders included in the model were season, day of the week, summer reduction in mortality. Other factors that vary in the short-term and are associated with the outcome were not considered. Air pollution is one factor that might have been worth considering and might have caused some residual confounding. However, pollution effect estimates in the short-term are extremely small, hence can be considered negligible in the context of temperature effects which are much greater. Lee et al. did not find a confounding effect of particles in summer in a study on temperature effects conducted in the US.[221] Moreover, air pollution data with the same resolution was not readily available within my time frame. The synergistic effects of temperatures and different pollutants (ozone, particles) in summer would have been interesting to explore as evidence in the literature is still unclear.

7.3 FUTURE WORK

The following additional work would have been of interest if time and data would have permitted.

First of all, in order to give more robust results and evaluate the geographical differences in effect estimates and impacts of heat in rural, suburban and rural areas a national wide study should be carried out. This will be pursued as a collaboration has been set up with the Italian institute of Statistics (ISTAT) to have access to daily total deaths for all municipalities in Italy. Hopefully national hospital admissions data will also be obtained from the Ministry of Health to fulfil this research gap and provide estimates on the risk of respiratory admissions associated to high temperatures. Furthermore, to better represent the spatial differences of heat-related effects at the national scale, the use of appropriate spatial models such as the Bayesian approach implemented by Bennett and colleagues in the UK[219] is required. This will allow to estimate both the magnitude of the risk and the confidence, in terms of posterior probability, that local risk estimates are different from regional or national risks providing appropriate representation of the spatial pattern.

Once national estimates are produced, future heat-related death burdens under climate change scenarios should be explored, considering high resolution climate change projections from regional scale models which would permit to consider high spatial scale differences in impacts and climate variations.

Another important aspect which was not considered in my thesis is the temporal variation in heat related effects, or changes over time. This would help improve evidence on the role of contributing factors to changes in effect estimates and impacts over time, such as temperature changes (increasing temperatures, change in seasonality) or variations in population

vulnerability due to population ageing, health status, etc. Furthermore, a study on the temporal variations with a specific focus on heat wave events, could improve the evidence on the role of adaptation measures put in place since 2004 in Italy, with more detailed quantifications at national level, also allowing for comparisons between areas which have heat plans and prevention measures and areas which do not.

Furthermore, recent studies have looked at the longer time frames (annual) in relation to extreme temperatures and the short-term effects on health outcomes trying to address whether the peaks in mortality during extreme events are just a short-term displacement of deaths or if they are life shortnening.[396,397] Armstrong et al. found that annual mortality was associated with deviations of temperatures from normal, in particular rising in years that experienced extreme heat or cold spells in a multi country study.[396] Similarly, Goggins et al. found that mortality increases associated with extreme temperature were not solely due to short-term forward displacement of deaths in Hong Kong.[397] Recent studies have studied the short and long-term effects simultaneously thus looking at the daily acute effects of environmental exposures and the long term variability[315,398]. This has been typically done for air pollution but could be also applied to temperature effects.

With regards to urban areas, a greater focus on the differential effects by UHI seems necessary considering the results reported in the Rome study. The use of higher spatial resolution satellite data from LANDSAT, Quickbird, Rapid Eye or data from the forthcoming Sentinel satellites would also help define the UHI more accurately. Data fusion techniques have recently been developed and could be used in order to combine the high spatial and temporal resolution of different satellite data sources[316,399] Moreover, a standardized definition of UHI in other Italian cities is desirable.

Always with reference to other urban areas, the conduction of case cross-over studies to see how both individual and area level vulnerability factors modify heat related deaths is needed. The main requirement would be to retrieve mortality data at individual level from cohort studies or local registries in order to geocode individuals and maintain the high resolution individual exposure. The use of data aggregated by census tract would somewhat loose out the added value of the high resolution of the research. Another aspect which was marginally studied were the pre-existing health conditions of individuals which might be vulnerability factors among the population during heat. By extending the set of pre-existing disease and taking into account the number of hospitalizations over longer time periods can help identify subgroups at risk to whom prevention should be targeted.

Finally, data from different sources and effect estimates could be integrated to define vulnerability maps to heat combining heat exposure, land use characteristics, socio-demographics and health effects by area in Italy thus providing public health with a very useful tool.

CHAPTER 8 – CONCLUSIONS

In conclusion, the use of high resolution satellite derived air temperature data was of great use to evaluate the differential effects of heat at regional level and within urban areas. The time series study was able to show that heat has significant effects and impacts on cause-specific mortality in suburban and rural areas, with risk estimates comparable to those found in urban areas. The heat-related risk in urban areas were also confirmed. High temperatures also had an effect on respiratory hospital admissions.

The study conducted in Rome, using a population cohort and high-resolution temperature data attributed at individual level showed the significant effect of heat on mortality. Important suggestions of the differential effect of heat within urban settings in terms of individual characteristics and factors that influence urban thermal properties (UHI and land use features) where elucidated. These aspects need to be taken into consideration when planning prevention measures to improve adaptation and response. Heat warning systems for large urban areas should also take into account the spatial differences of heat-related effects and the factors that influence urban climate. Finally, results from the thesis can be used to predict future heat-related mortality under different climate change scenarios and provide valuable insights into the future burden of heat.

REFERENCES

1. Simon Hales, Sari Kovats, Simon Lloyd DC-L. Quantitative risk assessment of the effects of climate change on selected causes of death , 2030s and 2050s. *Risk Assessment IWorld Heal Organ*. 2014:128. doi:ISBN 978 92 4 150769 1.
2. Kovats, R.S., R. Valentini, L.M. Bouwer, E. Georgopoulou, D. Jacob, E. Martin, M. Rounsevell and J-FS. IPCC VTH REPORT Europe. In: Climate Change 2014: Impacts, Adaptation, and Vulnerability. 2014:1267-1326.
3. Kendrovski V, Baccini M, Martinez GS, Wolf T, Paunovic E, Menne B. Quantifying projected heat mortality impacts under 21st-Centurywarming conditions for selected European countries. *Int J Environ Res Public Health*. 2017;14(7). doi:10.3390/ijerph14070729.
4. Basu R. Relation between Elevated Ambient Temperature and Mortality: A Review of the Epidemiologic Evidence. *Epidemiol Rev*. 2002;24(2):190-202. doi:10.1093/epirev/mxf007.
5. Basu R, Brabyn L, Zawar-Reza P, et al. High ambient temperature and mortality: a review of epidemiologic studies from 2001 to 2008. *Environ Health*. 2009;8(1):40. doi:10.1186/1476-069X-8-40.
6. Benmarhnia T, Deguen S, Kaufman JS, Smargiassi A. Vulnerability to heat-related mortality: A systematic review, meta-analysis, and meta-regression analysis. *Epidemiology*. 2015;26(6):781-793. doi:10.1097/EDE.0000000000000375.
7. Curriero FC, Heiner KS, Samet JM, Zeger SL, Strug L, Patz J a. Temperature and mortality in 11cities of the eastern United States. *Am J Epidemiol*. 2002;155(1):80-87.
8. Baccini M, Biggeri A, Accetta G, et al. Heat Effects on Mortality in 15 European Cities. *Epidemiology*. 2008;19(5):711-719. doi:10.1097/EDE.0b013e318176bfcd.
9. Bunker A, Wildenhain J, Vandenbergh A, et al. Effects of Air Temperature on Climate-Sensitive Mortality and Morbidity Outcomes in the Elderly; a Systematic Review and Meta-analysis of Epidemiological Evidence. *EBioMedicine*. 2016;6:258-268. doi:10.1016/j.ebiom.2016.02.034.
10. Braga ALF, Zanobetti A, Schwartz J. The effect of weather on respiratory and cardiovascular deaths in 12 U.S. cities. *Environ Health Perspect*. 2002;110(9):859-863. doi:10.1289/ehp.02110859.
11. Schwartz J, Samet JM, Patz JA. Hospital admissions for heart disease: The effects of temperature and humidity. *Epidemiology*. 2004;15(6):755-761. doi:10.1097/01.ede.0000134875.15919.0f.
12. Michelozzi P, Accetta G, De Sario M, et al. High temperature and hospitalizations for cardiovascular and respiratory causes in 12 european cities. *Am J Respir Crit Care Med*. 2009;179(5):383-389. doi:10.1164/rccm.200802-217OC.
13. Williams S, Nitschke M, Weinstein P, Pisaniello DL, Parton KA, Bi P. The impact of summer temperatures and heatwaves on mortality and morbidity in Perth, Australia 1994-2008. *Environ Int*. 2012;40(1):33-38. doi:10.1016/j.envint.2011.11.011.
14. Phung D, Guo Y, Thai P, et al. The effects of high temperature on cardiovascular admissions in the most populous tropical city in Vietnam. *Env Pollut*. 2016;208(Pt A):33-39. doi:10.1016/j.envpol.2015.06.004.
15. Ye X, Wolff R, Yu W, Vaneckova P, Pan X, Tong S. Ambient Temperature and Morbidity: A Review of Epidemiological Evidence. *Environ Health Perspect*. 2011;120(1):19-28. doi:10.1289/ehp.1003198.
16. WHO. Methods of assessing human health vulnerability and public health adaptation to climate change. *World Heal Organ*. 2003;(1):112.
17. Keiko Natsume, Tokuo Ogawa, Jumichi Sugenoya, Norikazu Ohmishi and KI. Prefered ambient temperature for old and young men in summer and winter. *Int J Biometeorol*. 1992;36:1-4.
18. Anderson BG, Bell ML. Weather-related mortality: how heat, cold, and heat waves affect mortality in the United States. *Epidemiology*. 2009;20(2):205-213. doi:10.1097/EDE.0b013e318190ee08.
19. Armstrong B. Models for the relationship between ambient temperature and daily mortality. *Epidemiology*. 2006;17(6):624-631. doi:10.1097/01.ede.0000239732.50999.8f.
20. Zanobetti A, O'Neill MS, Gronlund CJ, Schwartz JD. Susceptibility to mortality in weather extremes: Effect modification by personal and small-area characteristics. *Epidemiology*. 2013;24(6):809-819.

doi:10.1097/01.ede.0000434432.06765.91.

21. Guo Y, Barnett AG, Tong S. Spatiotemporal model or time series model for assessing city-wide temperature effects on mortality? *Environ Res*. 2013;120:55-62. doi:10.1016/j.envres.2012.09.001.

22. Spiegelman D. Approaches to uncertainty in exposure assessment in environmental epidemiology. *Annu Rev Public Health*. 2010;31:149-163. doi:10.1146/annurev.publhealth.012809.103720.

23. Stewart ID. A systematic review and scientific critique of methodology in modern urban heat island literature. *Int J Climatol*. 2011;31(2):200-217. doi:10.1002/joc.2141.

24. Wong KV, Paddon A, Jimenez A. Review of World Urban Heat Islands: Many Linked to Increased Mortality. *J Energy Resour Technol*. 2013;135. doi:10.1115/1.4023176.

25. Voelkel J, Shandas V, Haggerty B. Developing high-resolution descriptions of urban heat islands: A public health imperative. *Prev Chronic Dis*. 2016;13(9). doi:10.5888/pcd13.160099.

26. Benali A, Carvalho AC, Nunes JP, Carvalhais N, Santos A. Estimating air surface temperature in Portugal using MODIS LST data. *Remote Sens Environ*. 2012;124(May):108-121. doi:10.1016/j.rse.2012.04.024.

27. Kloog I, Chudnovsky A, Koutrakis P, Schwartz J. Temporal and spatial assessments of minimum air temperature using satellite surface temperature measurements in Massachusetts, USA. *Sci Total Environ*. 2012;432:85-92. doi:10.1016/j.scitotenv.2012.05.095.

28. Shi L, Liu P, Kloog I, Lee M, Kosheleva A, Schwartz J. Estimating daily air temperature across the Southeastern United States using high-resolution satellite data: A statistical modeling study. *Env Res*. 2016;146:51-58. doi:10.1016/j.envres.2015.12.006.

29. Kloog I, Nordio F, Coull BA, Schwartz J. Predicting spatiotemporal mean air temperature using MODIS satellite surface temperature measurements across the Northeastern USA. *Remote Sens Environ*. 2014;150:132-139. doi:10.1016/j.rse.2014.04.024.

30. Ngie A, Abutaleb K, Ahmed F, Darwish A, Ahmed M. Assessment of urban heat island using satellite remotely sensed imagery: A review. *South African Geogr J*. 2014;96(2):198-214. doi:10.1080/03736245.2014.924864.

31. Midekisa A, Senay GB, Wimberly MC. Multisensor earth observations to characterize wetlands and malaria epidemiology in Ethiopia. *Water Resour Res*. 2014. doi:10.1002/2014WR015634.

32. Xu Z, Liu Y, Ma Z, Toloo G, Hu W, Tong S. Assessment of the temperature effect on childhood diarrhea using satellite imagery. *Sci Rep*. 2014;4. doi:10.1038/srep05389.

33. Nordio F, Kloog I, Coull BA, et al. Estimating Spatio-Temporal Resolved Pm10 Aerosol Mass Concentrations Using Modis Satellite Data and Land Use Regression Over Lombardy, Italy. *Atmos Environ*. 2013;74:227-236. wos:000320969500026.

34. Lee M, Kloog I, Chudnovsky A, et al. Spatiotemporal prediction of fine particulate matter using high-resolution satellite images in the Southeastern US 2003–2011. *J Expo Sci Environ Epidemiol*. 2015;(April):1-8. doi:10.1038/jes.2015.41.

35. Stafoggia M, Schwartz J, Badaloni C, et al. Estimation of daily PM 10 concentrations in Italy (2006-2012) using finely resolved satellite data, land use variables and meteorology. *Environ Int*. 2016:1-49. doi:10.1016/j.envint.2016.11.024.

36. Kloog I, Sorek-Hamer M, Lyapustin A, et al. Estimating daily PM2.5and PM10across the complex geo-climate region of Israel using MAIAC satellite-based AOD data. *Atmos Environ*. 2015;122:409-416. doi:10.1016/j.atmosenv.2015.10.004.

37. Kloog I, Nordio F, Coull BA, Schwartz J. Incorporating Local Land Use Regression And Satellite Aerosol Optical Depth In A Hybrid Model Of Spatio- Temporal PM2 . 5 Exposures In The Mid-Atlantic States Incorporating Local Land Use Regression And Satellite Aerosol Optical Depth In A Hybrid Model Of. 2012.

38. Cresswell MP, Morse a. P, Thomson MC, Connor SJ. Estimating surface air temperatures, from Meteosat land surface temperatures, using an empirical solar zenith angle model. *Int J Remote Sens*. 1999;20(6):1125-1132. doi:10.1080/014311699212885.

39. Czajkowski K, Goward S, Stadler S, Walz A. Thermal Remote Sensing of Near Surface Environmental Variables: Application Over the Oklahoma Mesonet. *Prof Geogr*. 2000;52(2):345-357.

doi:10.1111/0033-0124.00230.

40. Wan ZWZ, Dozier J. A generalized split-window algorithm for retrieving land-surfacetemperature from space. *IEEE Trans Geosci Remote Sens*. 1996;34(4). doi:10.1109/36.508406.

41. Wan Z, Zhang Y, Zhang Q, Li Z-LL. Quality assessment and validation of the MODIS global land surface temperature. *Int J Remote Sens*. 2004;25(1):261-274. doi:10.1080/0143116031000116417.

42. Jin ML, Dickinson RE. Land Surface Skin Temperature Climatology: Benefitting From the Strengths of Satellite Observations. *Environ Res Lett*. 2010;5(4 LB-3630). doi:10.1088/1748-9326/5/4/044004.

43. Vogt J V., Viau A a., Paquet F. Mapping regional air temperature fields using satellite-derived surface skin temperatures. *Int J Climatol*. 1997;17:1559-1579. doi:10.1002/(SICI)1097-0088(19971130)17:14<1559::AID-JOC211>3.0.CO;2-5.

44. Qin Z, A K. Review article Progress in the remote sensing of land surface temperature and ground emissivity using NOAA ± AVHRR data. *Remote Sens*. 1999;20(12).

45. Vancutsem C, Ceccato P, Dinku T, Connor SJ. Evaluation of MODIS land surface temperature data to estimate air temperature in different ecosystems over Africa. *Remote Sens Environ*. 2010;114:449-465. doi:10.1016/j.rse.2009.10.002.

46. Benmecheta A, Abdellaoui A, Hamou A. A Comparative Study of Land Surface Temperature Retrieval Methods From Remote Sensing Data. *Can J Remote Sens*. 2013;39(1 LB-1350):59-73. wos:000328371900006.

47. Snyder WC, Wan Z, Zhang Y, Feng YZ. Classification-based emissivity for land surface temperature measurement from space. *Int J Remote Sens*. 1998;19(14):2753-2774. doi:10.1080/014311698214497.

48. Price JC. Land surface temperature measurements from the split window channels of the NOAA 7 Advanced Very High Resolution Radiometer. *J Geophys Res*. 1984;89(D5):7231. doi:10.1029/JD089iD05p07231.

49. Pinheiro ACT, Descloitres J, Privette JL, Susskind J, Iredell L, Schmaltz J. Near-real time retrievals of land surface temperature within the MODIS Rapid Response System. *Remote Sens Environ*. 2007;106:326-336. doi:10.1016/j.rse.2006.09.006.

50. Wan Z, Zhang Y, Zhang Q, Li Z. Validation of the land-surface temperature products retrieved from Terra Moderate Resolution Imaging Spectroradiometer data. *Remote Sens Environ*. 2002;83(1-2):163-180. doi:10.1016/S0034-4257(02)00093-7.

51. Wan Z. New refinements and validation of the collection-6 MODIS land-surface temperature/emissivity product. *Remote Sens Environ*. 2014;140(1):36-45. doi:10.1016/j.rse.2013.08.027.

52. Wan Z. New refinements and validation of the MODIS Land-Surface Temperature/Emissivity products. *Remote Sens Environ*. 2008;112(1):59-74. doi:10.1016/j.rse.2006.06.026.

53. Tatem AJ, Goetz SJ, Hay SI. Europe PMC Funders Group Terra and Aqua : new data for epidemiology and public health. 2004;6(1):33-46.

54. U.S. Geological Survey. Landsat—Earth observation satellites. *Fact Sheet*. 2015;2020(August):1-4. doi:10.3133/fs20153081.

55. Cristóbal J, Ninyerola M, Pons X. Modeling air temperature through a combination of remote sensing and GIS data. *J Geophys Res*. 2008;113(D13):D13106. doi:10.1029/2007JD009318.

56. Kim J, Hogue TS. Evaluation and sensitivity testing of a coupled Landsat-MODIS downscaling method for land surface temperature and vegetation indices in semi-arid regions. *J Appl Remote Sens*. 2012;6(1):063569-1. doi:10.1117/1.JRS.6.063569.

57. Yang JS, Wang YQ, August P V. Estimation of Land Surface Temperature Using Spatial Interpolation and Satellite-Derived Surface Emissivity. *J Environ Informatics*. 2004;4(1):37-44. doi:10.3808/jei.200400035.

58. Hou P, Chen Y, Qiao W, Cao G, Jiang W, Li J. Near-surface air temperature retrieval from satellite images and influence by wetlands in urban region. *Theor Appl Climatol*. 2013;111(1-2):109-118. doi:10.1007/s00704-012-0629-7.

59. Al H et. The Advanced Very High Resolution Radiometer (AVHRR): a brief reference guide. 1992:1183-1188.

http://webapp1.dlib.indiana.edu/virtual_disk_library/index.cgi/4646607/FID2394/avhrr2.htm.

60. EUMETSAT. THE EUMETSAT POLAR SYSTEM KEEPING A CLOSER EYE ON WEATHER AND CLIMATE. https://www.eumetsat.int/website/wcm/idc/idcplg?IdcService=GET_FILE&dDocName=PDF_BR_PRG02&RevisionSelectionMethod=LatestReleased&Rendition=Web.

61. EUMETSAT. Meteosat: Europe's Geostationary Meteorological Satellites. 2015:1-16. https://www.eumetsat.int/website/wcm/idc/idcplg?IdcService=GET_FILE&dDocName=PDF_BR_PRG01_EN&RevisionSelectionMethod=LatestReleased&Rendition=Web.

62. Zakšek K, Schroedter-Homscheidt M. Parameterization of air temperature in high temporal and spatial resolution from a combination of the SEVIRI and MODIS instruments. *ISPRS J Photogramm Remote Sens*. 2009;64(4):414-421. doi:10.1016/j.isprsjprs.2009.02.006.

63. Fu G, Shen Z, Zhang X, Shi P, Zhang Y, Wu J. Estimating air temperature of an alpine meadow on the Northern Tibetan Plateau using MODIS land surface temperature. *Acta Ecol Sin*. 2011;31(1):8-13. doi:10.1016/j.chnaes.2010.11.002.

64. Rosenfeld A, Dorman M, Schwartz J, Novack V, Just AC, Kloog I. Estimating daily minimum, maximum, and mean near surface air temperature using hybrid satellite models across Israel. *Environ Res*. 2017;159(March):297-312. doi:10.1016/j.envres.2017.08.017.

65. Pelta R, Chudnovsky AA. Spatiotemporal estimation of air temperature patterns at the street level using high resolution satellite imagery. *Sci Total Environ*. 2017;579:675-684. doi:10.1016/j.scitotenv.2016.11.042.

66. Yao Y, Zhang B. MODIS-based air temperature estimation in the southeastern Tibetan Plateau and neighboring areas. *J Geogr Sci*. 2012;22(1):152-166. doi:10.1007/s11442-012-0918-1.

67. Zhang W, Huang Y, Yu Y, Sun W. Empirical models for estimating daily maximum, minimum and mean air temperatures with MODIS land surface temperatures. *Int J Remote Sens*. 2011;32(24):9415-9440. doi:10.1080/01431161.2011.560622.

68. Xu YM, Qin ZH, Shen Y. Study on the estimation of near-surface air temperature from MODIS data by statistical methods. *Int J Remote Sens*. 2012;33(24):7629-7643. doi:10.1080/01431161.2012.701351.

69. Lai YJ, Li CF, Lin PH, Wey TH, Chang CS. Comparison of Modis Land Surface Temperature and Ground-Based Observed Air Temperature in Complex Topography. *Int J Remote Sens*. 2012;33(24 LB-2330):7685-7702. wos:000306836700005.

70. Recondo C, Peón JJ, Zapico E, Pendás E. Empirical models for estimating daily surface water vapour pressure, air temperature, and humidity using MODIS and spatiotemporal variables. Applications to Peninsular Spain. *Int J Remote Sens*. 2013;34(22):8051-8080. doi:10.1080/01431161.2013.828185.

71. Nieto H, Sandholt I, Aguado I, Chuvieco E, Stisen S. Air temperature estimation with MSG-SEVIRI data: Calibration and validation of the TVX algorithm for the Iberian Peninsula. *Remote Sens Environ*. 2011;115:107-116. doi:10.1016/j.rse.2010.08.010.

72. Stisen S, Sandholt I, Nørgaard A, Fensholt R, Eklundh L. Estimation of diurnal air temperature using MSG SEVIRI data in West Africa. *Remote Sens Environ*. 2007;110(2):262-274. doi:10.1016/j.rse.2007.02.025.

73. Prihodko L. Estimation of air temperature from remotely sensed surface observations. *Remote Sens Environ*. 1997;60:335-346. doi:10.1016/S0034-4257(96)00216-7.

74. Cai M, Yang S, Zhao C, Zeng H, Zhou Q. Estimation of daily average temperature using multisource spatial data in data sparse regions of Central Asia. *J Appl Remote Sens*. 2013;7(1):073478. doi:10.1117/1.JRS.7.073478.

75. Zhu W, Lű A, Jia S. Estimation of daily maximum and minimum air temperature using MODIS land surface temperature products. *Remote Sens Environ*. 2013;130:62-73. doi:10.1016/j.rse.2012.10.034.

76. Wloczyk C, Borg E, Richter R, Miegel K. Estimation of instantaneous air temperature above vegetation and soil surfaces from Landsat 7 ETM+ data in northern Germany. *Int J Remote Sens*. 2011;32(24):9119-9136. doi:10.1080/01431161.2010.550332.

77. Sandholt I, Rasmussen K, Andersen J. A simple interpretation of the surface temperature/vegetation index space for assessment of surface moisture status. *Remote Sens Environ*. 2002;79(2-3):213-224.

doi:10.1016/S0034-4257(01)00274-7.

78. Voogt J. A, Oke T. R. Thermal remote sensing of urban climates. *Remote Sens Environ*. 2003;86(3):370-384. doi:10.1016/S0034-4257(03)00079-8.

79. Sun YJ, Wang JF, Zhang RH, Gillies RR, Xue Y, Bo YC. Air temperature retrieval from remote sensing data based on thermodynamics. *Theor Appl Climatol*. 2005;80(1):37-48. doi:10.1007/s00704-004-0079-y.

80. Prince SD, Goetz SJ, Dubayah RO, Czajkowski KP, Thawley M. Inference of surface and air temperature, atmospheric precipitable water and vapor pressure deficit using advanced very high-resolution radiometer satellite observations: Comparison with field observations. *J Hydrol*. 1998;212-213(1-4):230-249. doi:10.1016/S0022-1694(98)00210-8.

81. Şahin M, Sahin M, Şahin M. Modelling of air temperature using remote sensing and artificial neural network in Turkey. *Adv Sp Res*. 2012;50(7):973-985. doi:10.1016/j.asr.2012.06.021.

82. Mao KB, Tang HJ, Wang XF, Zhou QB, Wang DL. Near-surface air temperature estimation from ASTER data based on neural network algorithm. *Int J Remote Sens*. 2008;29(20):6021-6028. doi:10.1080/01431160802192160.

83. Nichol JE, Fung WY, Lam K s., Wong MS. Urban heat island diagnosis using ASTER satellite images and 'in situ' air temperature. *Atmos Res*. 2009;94:276-284. doi:10.1016/j.atmosres.2009.06.011.

84. Nichol J, Wong MS. Mapping Urban Environmental Quality Using Satellite Data and Multiple Parameters. *Environ Plan B-Planning Des*. 2009;36(1 LB-4760):170-185. wos:000263711600011.

85. Oke TR. City size and the urban heat island. *Atmos Environ*. 1973;7:769-779. doi:10.1016/0004-6981(73)90140-6.

86. Arnfield a. J. Micro- and mesoclimatology. *Prog Phys Geogr*. 2003;27(3):435-447. doi:10.1191/030913303767888518.

87. Souch C, Grimmond S. Applied climatology: urban climate. *Prog Phys Geogr*. 2006;30(2):270-279. doi:10.1191/0309133306pp484pr.

88. Basara JB, Basara HG, Illston BG, Crawford KC. The Impact of the Urban Heat Island during an Intense Heat Wave in Oklahoma City. *Adv Meteorol*. 2010;2010:1-10. doi:10.1155/2010/230365.

89. Wong K V., Chaudhry S. Use of Satellite Images for Observational and Quantitative Analysis of Urban Heat Islands Around the World. *J Energy Resour Technol*. 2012;134(4):042101. doi:10.1115/1.4007486.

90. Stewart ID, Oke TR. Local climate zones for urban temperature studies. *Bull Am Meteorol Soc*. 2012;93(12):1879-1900. doi:10.1175/BAMS-D-11-00019.1.

91. Morabito M, Crisci A, Messeri A, et al. The impact of built-up surfaces on land surface temperatures in Italian urban areas. *Sci Total Environ*. 2016;551-552:317-326. doi:10.1016/j.scitotenv.2016.02.029.

92. Zhou B, Rybski D, Kropp JP. On the statistics of urban heat island intensity. *Geophys Res Lett*. 2013;40(20):5486-5491. doi:10.1002/2013GL057320.

93. Zhou J, Chen YH, Zhang X, Zhan WF. Modelling the Diurnal Variations of Urban Heat Islands With Multi-Source Satellite Data. *Int J Remote Sens*. 2013;34(21):7568-7588. doi:10.1080/01431161.2013.821576.

94. Grimmond CSB, Blackett M, Best MJ, et al. The International Urban Energy Balance Models Comparison Project: First Results from Phase 1. *J Appl Meteorol Climatol*. 2010;49(6):1268-1292. doi:10.1175/2010JAMC2354.1.

95. Weng Q, Rajasekar U, Hu X. Modeling Urban Heat Islands and Their Relationship With Impervious Surface and Vegetation Abundance by Using ASTER Images. *IEEE Trans Geosci Remote Sens*. 2011;49(10):4080-4089.

96. Schwarz N, Lautenbach S, Seppelt R. Exploring indicators for quantifying surface urban heat islands of European cities with MODIS land surface temperatures. *Remote Sens Environ*. 2011;115(12):3175-3186. doi:10.1016/j.rse.2011.07.003.

97. Peng S, Piao S, Ciais P, et al. Surface urban heat island across 419 global big cities. *Environ Sci Technol*. 2012;46:696-703. doi:10.1021/es2030438.

98. Zhang P, Imhoff ML, Wolfe RE, Bounoua L. Characterizing Urban Heat Islands of Global Settlements Using Modis and Nighttime Lights Products. *Can J Remote Sens*. 2010;36(3 LB-3880):185-196. wos:000284352700004.

99. Cheval S, Dumitrescu A. The July Urban Heat Island of Bucharest as Derived From Modis Images. *Theor Appl Climatol*. 2009;96(1-2 LB-4630):145-153. wos:000264965500013.

100. Cheval S, Dumitrescu A. The summer surface urban heat island of Bucharest (Romania) retrieved from MODIS images. *Theor Appl Climatol*. 2015;121(3-4):631-640. doi:10.1007/s00704-014-1250-8.

101. Retalis A, Paronis D, Lagouvardos K, Kotroni V. The Heat Wave of June 2007 in Athens, Greece-Part 1: Study of Satellite Derived Land Surface Temperature. *Atmos Res*. 2010;98(2-4 LB-3580):458-467. wos:000284983400028.

102. Tomlinson CJ, Chapman L, Thornes JE, Baker CJ. Derivation of Birmingham's Summer Surface Urban Heat Island From Modis Satellite Images. *Int J Climatol*. 2012;32(2 LB-2240):214-224. wos:000299103000005.

103. Tran H, Uchihama D, Ochi S, Yasuoka Y. Assessment with satellite data of the urban heat island effects in Asian mega cities. *Int J Appl Earth Obs Geoinf*. 2006;8:34-48. doi:10.1016/j.jag.2005.05.003.

104. Qiao Z, Tian GJ, Xiao L. Diurnal and Seasonal Impacts of Urbanization on the Urban Thermal Environment: a Case Study of Beijing Using Modis Data. *Isprs J Photogramm Remote Sens*. 2013;85:93-101. wos:000326558200010.

105. Wu C-DD, Lung S-CCC, Jan J-FF. Development of a 3-D urbanization index using digital terrain models for surface urban heat island effects. *ISPRS J Photogramm Remote Sens*. 2013;81:1-11. doi:10.1016/j.isprsjprs.2013.03.009.

106. Zhou D, Zhao S, Liu S, Zhang L, Zhu C. Surface urban heat island in China's 32 major cities: Spatial patterns and drivers. *Remote Sens Environ*. 2014;152:51-61. doi:10.1016/j.rse.2014.05.017.

107. Effat HA, Hassan OAK. Change detection of urban heat islands and some related parameters using multi-temporal Landsat images; a case study for Cairo city, Egypt. *Urban Clim*. 2014;10(P1):171-188. doi:10.1016/j.uclim.2014.10.011.

108. Bokaie M, Zarkesh MK, Arasteh PD, Hosseini A. Assessment of Urban Heat Island based on the relationship between land surface temperature and Land Use/ Land Cover in Tehran. *Sustain Cities Soc*. 2016;23:94-104. doi:10.1016/j.scs.2016.03.009.

109. Liu K, Su H, Zhang L, Yang H, Zhang R, Li X. Analysis of the urban heat Island effect in shijiazhuang, China using satellite and airborne data. *Remote Sens*. 2015;7(4):4804-4833. doi:10.3390/rs70404804.

110. Imhoff ML, Zhang P, Wolfe RE, Bounoua L. Remote Sensing of the Urban Heat Island Effect Across Biomes in the Continental Usa. *Remote Sens Environ*. 2010;114(3 LB-4020):504-513. wos:000274820700005.

111. Jin MS. Developing an Index to Measure Urban Heat Island Effect Using Satellite Land Skin Temperature and Land Cover Observations. *J Clim*. 2012;25(18 LB-1740):6193-6201. wos:000309038000009.

112. Rajasekar U, Weng QH. Urban heat island monitoring and analysis using a non-parametric model: A case study of Indianapolis. *ISPRS J Photogramm Remote Sens*. 2009;64(1):86-96. doi:10.1016/j.isprsjprs.2008.05.002.

113. Xie HJ, Chang NB, Daranpob A, Prado D. Assessing the Long-Term Urban Heat Island in San Antonio, Texas Based on Moderate Resolution Imaging Spectroradiometer/Aqua Data. *J Appl Remote Sens*. 2010;4. wos:000278050800001.

114. Zhang Y, Yiyun C, Qing D, Jiang P. Study on Urban Heat Island Effect Based on Normalized Difference Vegetated Index:A Case Study of Wuhan City. *Procedia Environ Sci*. 2012;13:574-581. doi:10.1016/j.proenv.2012.01.048.

115. Ho HC, Knudby A, Xu Y, Hodul M, Aminipouri M. A comparison of urban heat islands mapped using skin temperature, air temperature, and apparent temperature (Humidex), for the greater Vancouver area. *Sci Total Environ*. 2016;544:929-938. doi:10.1016/j.scitotenv.2015.12.021.

116. Chen X-LL, Zhao H-MM, Li P-XX, Yin Z-YY. Remote sensing image-based analysis of the relationship between urban heat island and land use/cover changes. *Remote Sens Environ*.

2006;104(2):133-146. doi:10.1016/j.rse.2005.11.016.

117. Zhang LJ, Wen XP, Wang J, Zhou Y. Research on the relationship of surface temperature and urban heat island using the thermal infrared remote sensing image. 2014;889-890:1634-1637. doi:10.4028/www.scientific.net/AMR.889-890.1634.

118. Aslan N, Koc-San D. Analysis of relationship between urban heat island effect and Land use/cover type using Landsat 7 ETM+ and Landsat 8 OLI images. In: Zdimal V, Ramasamy SM, Skidmore A, et al., eds. Vol 41. Akdeniz University, Faculty of Science, Department of Space Sciences and Technologies, Antalya, Turkey Akdeniz University, Remote Sensing Research and Application Centre, Antalya, Turkey: International Society for Photogrammetry and Remote Sensing; 2016:821-828. doi:10.5194/isprsarchives-XLI-B8-821-2016.

119. Stathopoulou M, Cartalis C, Petrakis M. Integrating Corine Land Cover data and Landsat TM for surface emissivity definition: application to the urban area of Athens, Greece. *Int J Remote Sens*. 2007;28(15):3291-3304. doi:10.1080/01431160600993421.

120. Klok L, Zwart S, Verhagen H, Mauri E. The Surface Heat Island of Rotterdam and Its Relationship With Urban Surface Characteristics. *Resour Conserv Recycl*. 2012;64:23-29. doi:10.1016/j.resconrec.2012.01.009.

121. Li YY, Zhang H, Kainz W. Monitoring Patterns of Urban Heat Islands of the Fast-Growing Shanghai Metropolis, China: Using Time-Series of Landsat Tm/Etm+ Data. *Int J Appl Earth Obs Geoinf*. 2012;19:127-138. wos:000309028500011.

122. Mallick J, Rahman A, Singh CK. Modeling Urban Heat Islands in Heterogeneous Land Surface and Its Correlation With Impervious Surface Area by Using Night-Time Aster Satellite Data in Highly Urbanizing City, Delhi-India. *Adv Sp Res*. 2013;52(4 LB-740):639-655. wos:000322093900009.

123. Meng F, Liu M. Remote-Sensing Image-Based Analysis of the Patterns of Urban Heat Islands in Rapidly Urbanizing Jinan, China. *Int J Remote Sens*. 2013;34(24 LB-300):8838-8853. wos:000327237000012.

124. Xie QJ, Zhou ZX, Teng MJ, Wang PC. A Multi-Temporal Landsat Tm Data Analysis of the Impact of Land Use and Land Cover Changes on the Urban Heat Island Effect. *J Food Agric Environ*. 2012;10(2 LB-15760):803-809. wos:000305165300067.

125. Xiong YZ, Huang SP, Chen F, Ye H, Wang CP, Zhu CB. The Impacts of Rapid Urbanization on the Thermal Environment: a Remote Sensing Study of Guangzhou, South China. *Remote Sens*. 2012;4(7 LB-1950):2033-2056. wos:000306759700009.

126. Xu YM, Qin ZH, Wan HX. Spatial and Temporal Dynamics of Urban Heat Island and Their Relationship With Land Cover Changes in Urbanization Process: a Case Study in Suzhou, China. *J Indian Soc Remote Sens*. 2010;38(4 LB-15850):654-663. wos:000288560900009.

127. Anniballe R, Bonafoni S, Pichierri M. Spatial and temporal trends of the surface and air heat island over Milan using MODIS data. *Remote Sens Environ*. 2014;150:163-171. doi:10.1016/j.rse.2014.05.005.

128. Fabrizi R, Bonafoni S, Biondi R. Satellite and Ground-Based Sensors for the Urban Heat Island Analysis in the City of Rome. *Remote Sens*. 2010;2(5):1400-1415. doi:10.3390/rs2051400.

129. Pichierri M, Bonafoni S, Biondi R. Satellite air temperature estimation for monitoring the canopy layer heat island of Milan. *Remote Sens Environ*. 2012;127:130-138. doi:10.1016/j.rse.2012.08.025.

130. Qiao Z, Tian G. Dynamic monitoring of the footprint and capacity for urban heat island in Beijing between 2001 and 2012 based on MODIS. *Yaogan Xuebao/Journal Remote Sens*. 2015;19(3):476-484. doi:10.11834/jrs.20154165.

131. Stathopoulou M, Cartalis C. Downscaling Avhrr Land Surface Temperatures for Improved Surface Urban Heat Island Intensity Estimation. *Remote Sens Environ*. 2009;113(12 LB-4390):2592-2605. wos:000271771300005.

132. Kourtidis K, Georgoulias AK, Rapsomanikis S, et al. A study of the hourly variability of the urban heat island effect in the Greater Athens Area during summer. *Sci Total Env*. 2015;517:162-177. doi:10.1016/j.scitotenv.2015.02.062.

133. Zaksek K, Ostir K. Downscaling Land Surface Temperature for Urban Heat Island Diurnal Cycle Analysis. *Remote Sens Environ*. 2012;117:114-124. wos:000300459300010.

134. Constantinescu D, Cheval S, Caracaş G, Dumitrescu A. Effective monitoring and warning of Urban Heat Island effect on the indoor thermal risk in Bucharest (Romania). *Energy Build*. 2016;127:452-468. doi:10.1016/j.enbuild.2016.05.068.

135. Meng F, Shan BY, Liu M. Remote-Sensing Evaluation of the Relationship Between Urban Heat Islands and Urban Biophysical Descriptors in Jinan, China. *J Appl Remote Sens*. 2014;8. wos:000330565900001.

136. Mathew A, Khandelwal S, Kaul N. Spatial and temporal variations of urban heat island effect and the effect of percentage impervious surface area and elevation on land surface temperature: Study of Chandigarh city, India. *Sustain Cities Soc*. 2016;26:264-277. doi:10.1016/j.scs.2016.06.018.

137. Shen H, Huang L, Zhang L, Wu P, Zeng C. Long-term and fine-scale satellite monitoring of the urban heat island effect by the fusion of multi-temporal and multi-sensor remote sensed data: A 26-year case study of the city of Wuhan in China. *Remote Sens Environ*. 2016;172:109-125. doi:10.1016/j.rse.2015.11.005.

138. Aniello C, Morgan K, Busbey A, Newland L. Mapping micro-urban heat islands using LANDSAT TM and a GIS. *Comput Geosci*. 1995;21(8):965-969. doi:10.1016/0098-3004(95)00033-5.

139. Zhu X, Chen G, Sha W, Iwasaki T, Li W, Wen Z. The role of rapid urbanization in surface warming over eastern China. *Int J Remote Sens*. 2014;35(24):8295-8308. doi:10.1080/01431161.2014.985397.

140. Jalan S, Sharma K. Spatio-temporal assessment of land use/ land cover dynamics and urban heat island of Jaipur city using satellite data. In: Dadhwal VK, Seshasai MVR, Hakeem A, Diwakar PG, Raju PLN, eds. Vol XL-8. 1st ed. Department of Geography, Mohanlal Sukhadia University, Udaipur, India Department of Geography, University of Rajasthan, Jaipur, India: International Society for Photogrammetry and Remote Sensing; 2014:767-772. doi:10.5194/isprsarchives-XL-8-767-2014.

141. Aminipouri M, Knudby A. Spatio-temporal analysis of surface urban heat island (SUHI) using MODIS land surface temperature (LST) for summer 2003-2012, A case study of the Netherlands. In: Department of Geography, Simon Fraser UniversityBC, Canada: Institute of Electrical and Electronics Engineers Inc.; 2014:3192-3193. doi:10.1109/IGARSS.2014.6947156.

142. Qiu WX, Xu HX, He ZW. Dynamic Monitoring and Evaluation on Urban Heat Island Effects Using Remote Sensing Technology. *Sensors and Transducers*. 2013;23(SPEC.ISSUE):122-126. https://www.scopus.com/inward/record.uri?eid=2-s2.0-84889007732&partnerID=40&md5=7ec227a272d8fbe7125e92b19154df51.

143. Zhang C, Xu H. Study on the evolution tendency of the urban heat island effect in Xichang City using Remote Sensing. 2013. doi:10.1109/Geoinformatics.2013.6626172.

144. Li X, Li W, Middel A, Harlan SL, Brazel AJ, Turner BL. Remote sensing of the surface urban heat island and land architecture in Phoenix, Arizona: Combined effects of land composition and configuration and cadastral-demographic-economic factors. *Remote Sens Environ*. 2016;174:233-243. doi:10.1016/j.rse.2015.12.022.

145. Feizizadeh B, Blaschke T. Examining Urban Heat Island Relations to Land Use and Air Pollution: Multiple Endmember Spectral Mixture Analysis for Thermal Remote Sensing. *Ieee J Sel Top Appl Earth Obs Remote Sens*. 2013;6(3 LB-970):1749-1756. wos:000320871800072.

146. Li G, Zhang F, Jing Y, Liu Y, Sun G. Response of evapotranspiration to changes in land use and land cover and climate in China during 2001-2013. *Sci Total Env*. 2017;596-597:256-265. doi:10.1016/j.scitotenv.2017.04.080.

147. Rinner C, Hussain M. Toronto's Urban Heat Island—Exploring the Relationship between Land Use and Surface Temperature. *Remote Sens*. 2011;3(12):1251-1265. doi:10.3390/rs3061251.

148. Mohan M, Kikegawa Y, Gurjar BR, Bhati S, Kolli NR. Assessment of Urban Heat Island Effect for Different Land Use-Land Cover From Micrometeorological Measurements and Remote Sensing Data for Megacity Delhi. *Theor Appl Climatol*. 2013;112(3-4 LB-1110):647-658. wos:000318246300024.

149. Rajasekar U, Weng Q. Spatio-temporal modelling and analysis of urban heat islands by using Landsat TM and ETM+ imagery. *Int J Remote Sens*. 2009;30(13):3531-3548. doi:10.1080/01431160802562289.

150. Wen XP, Yang XF, Hu GD. Relationship Between Land Cover Ratio and Urban Heat Island From Remote Sensing and Automatic Weather Stations Data. *J Indian Soc Remote Sens*. 2011;39(2 LB-2900):193-201. wos:000293960200007.

151. Zhou J, Zhang X. Modeling the monthly variations of urban heat island in Beijing City with MODIS surface products. In: Jiangsu Key Laboratory of Resources and Environmental Information Engineering, China University of Mining and Technology, Xuzhou, China School of Resources and Environment, University of Electronic Science and Technology of China, Chengdu, China: Atlantis Press; 2013:338-341. https://www.scopus.com/inward/record.uri?eid=2-s2.0-84907387748&partnerID=40&md5=1d8906b14563523a6dfa478f16660f87.

152. Sharifi E, Lehmann S. Correlation analysis of surface temperature of rooftops, streetscapes and urban heat island effect: Case study of central Sydney. *J Urban Environ Eng*. 2015;9(1):3-11. doi:10.4090/juee.2015.v9n1.003011.

153. Gallo KP, McNab AL, Karl TR, Brown JF, Hood JJ, Tarpley JD. The Use of NOAA AVHRR Data for Assessment of the Urban Heat Island Effect. *J Appl Meteorol*. 1993;32(5):899-908. doi:10.1175/1520-0450(1993)032<0899:TUONAD>2.0.CO;2.

154. Tomlinson CJ, Chapman L, Thornes JE, Baker CJ. Including the urban heat island in spatial heat health risk assessment strategies: a case study for Birmingham, UK. *Int J Health Geogr*. 2011;10:42. doi:10.1186/1476-072X-10-42.

155. Rooney C, McMichael AJ, Kovats RS, Coleman MP. Excess mortality in England and Wales, and in Greater London, during the 1995 heatwave. *J Epidemiol Community Heal*. 1998;52(8):482-486. doi:10.1136/jech.52.8.482.

156. Semenza JC, McCullough JE, Flanders WD, McGeehin MA, Lumpkin JR. Excess hospital admissions during the July 1995 heat wave in Chicago. *Am J Prev Med*. 1999;16(4):269-277. doi:10.1016/S0749-3797(99)00025-2.

157. Gasparrini A, Guo Y, Hashizume M, et al. Mortality risk attributable to high and low ambient temperature: a multicountry observational study. *Lancet*. 2015;386(9991):369-375. doi:10.1016/S0140-6736(14)62114-0.

158. Donoghue ER, Graham MA, Jentzen JM, Lifschultz BD, Luke JL, Mirchandani HG. Criteria for the diagnosis of heat-related deaths: National Association of Medical Examiners. Position paper. National Association of Medical Examiners Ad Hoc Committee on the Definition of Heat-Related Fatalities. *Am J Forensic Med Pathol*. 1997;18(0195-7910 LA-eng PT-Guideline PT-Journal Article PT-Practice Guideline):11-14.

159. Huynen MMTE, Martens P, Schram D, Weijenberg MP, Kunst AE. The impact of heat waves and cold spells on mortality rates in the Dutch population. *Environ Health Perspect*. 2001;109(5):463-470. doi:10.1289/ehp.01109463.

160. Kyselý J. Mortality and displaced mortality during heat waves in the Czech Republic. *Int J Biometeorol*. 2004;49(2):91-97. doi:10.1007/s00484-004-0218-2.

161. Michelozzi P, de'Donato F, Bisanti L, et al. Heat Waves in Italy: Cause Specific Mortality and the Role of Educational Level and Socio-Economic Conditions. In: Kirch W, Menne B, Bertollini R, eds. *Extreme Weather Events and Public Health Responses*. Springer; 2005:121-127.

162. Koken PJM, Piver WT, Ye F, Elixhauser A, Olsen LM, Portier CJ. Temperature, air pollution, and hospitalization for cardiovascular diseases among elderly people in Denver. *Environ Health Perspect*. 2003;111(10):1312-1317. doi:10.1289/ehp.5957.

163. Green RS, Basu R, Malig B, Broadwin R, Kim JJ, Ostro B. The effect of temperature on hospital admissions in nine California counties. *Int J Public Health*. 2010;55(2):113-121. doi:10.1007/s00038-009-0076-0.

164. Kovats RS, Hajat S, Wilkinson P. Contrasting patterns of mortality and hospital admissions during hot weather and heat waves in Greater London, UK. *Occup Environ Med*. 2004;61(11):893-898. doi:10.1136/oem.2003.012047.

165. Morabito M, Modesti PA, Cecchi L, et al. Relationships between weather and myocardial infarction: A biometeorological approach. *Int J Cardiol*. 2005;105(3):288-293. doi:10.1016/j.ijcard.2004.12.047.

166. Wexler RK. Evaluation and treatment of heat-related illnesses. *Am Fam Physician*. 2002;65(11):2307-2314.

167. K Bhaskaran, S Hajat AH. Effects of ambient temperature on the incidence of myocardial infarction.

168. Lin S, Luo M, Walker RJ, Liu X, Hwang S-A, Chinery R. Extreme High Temperatures and Hospital

Admissions for Respiratory and Cardiovascular Diseases. *Epidemiology*. 2009;20(5):738-746. doi:10.1097/EDE.0b013e3181ad5522.

169. O'Neill MS, Zanobetti A, Schwartz J. Modifiers of the temperature and mortality association in seven US cities. *Am J Epidemiol*. 2003;157(12):1074-1082. doi:10.1093/aje/kwg096.

170. O'Neill MS, Hajat S, Zanobetti A, Ramirez-Aguilar M, Schwartz J. Impact of control for air pollution and respiratory epidemics on the estimated associations of temperature and daily mortality. *Int J Biometeorol*. 2005;50(2):121-129. doi:10.1007/s00484-005-0269-z.

171. Hajat S, Haines a. Associations of cold temperatures with GP consultations for respiratory and cardiovascular disease amongst the elderly in London. *Int J Epidemiol*. 2002;31:825-830. doi:10.1093/ije/31.4.825.

172. Ballester F, Corella D, Pérez-Hoyos S, Sáez M, Hervás A. Mortality as a function of temperature. A study in Valencia, Spain, 1991-1993. *Int J Epidemiol*. 1997;26(3):551-561. doi:10.1093/ije/26.3.551.

173. Díaz J, García R, López C, Linares C, Tobías A, Prieto L. Mortality impact of extreme winter temperatures. *Int J Biometeorol*. 2005;49(3):179-183. doi:10.1007/s00484-004-0224-4.

174. Pattenden S, Nikiforov B, Armstrong BG. Mortality and temperature in Sofia and London. *J Epidemiol Community Health*. 2003;57(8):628-633. doi:10.1136/jech.57.8.628.

175. Hajat S, Armstrong BG, Gouveia N, Wilkinson P. Mortality displacement of heat-related deaths: A comparison of Delhi, S??o Paulo, and London. *Epidemiology*. 2005;16(5):613-620. doi:10.1097/01.ede.0000164559.41092.2a.

176. Gouveia N, Fletcher T. Time series analysis of air pollution and mortality: Effects by cause, age and socioeconomic status. *J Epidemiol Community Health*. 2000;54(10):750-755. doi:10.1136/jech.54.10.750.

177. Gasparrini A, Armstrong B. The impact of heat waves on mortality. *Epidemiology*. 2011;22(1):68-73. doi:10.1097/EDE.0b013e3181fdcd99.

178. Barnett AG, Hajat S, Gasparrini A, Rocklöv J. Cold and heat waves in the United States. *Environ Res*. 2012;112:218-224.

179. Stafoggia M, Forastiere F, Agostini D, et al. Vulnerability to heat-related mortality: A multicity, population-based, case-crossover analysis. *Epidemiology*. 2006;17(3):315-323. doi:10.1097/01.ede.0000208477.36665.34.

180. Medina-Ramón M, Schwartz J. Temperature, temperature extremes, and mortality: A study of acclimatisation and effect modification in 50 US cities. *Occup Environ Med*. 2007;64(12):827-833. doi:10.1136/oem.2007.033175.

181. Smargiassi a, Goldberg MS, Plante C, Fournier M, Baudouin Y, Kosatsky T. Variation of daily warm season mortality as a function of micro-urban heat islands. *J Epidemiol Community Health*. 2009;63(8):659-664. doi:10.1136/jech.2008.078147.

182. Goggins WB, Chan EYY, Ng E, Ren C, Chen L. Effect modification of the association between short-term meteorological factors and mortality by urban heat islands in Hong Kong. *PLoS One*. 2012;7(6):e38551. doi:10.1371/journal.pone.0038551.

183. Xu Y, Dadvand P, Barrera-Gomez J, et al. Differences on the effect of heat waves on mortality by sociodemographic and urban landscape characteristics. *J Epidemiol Community Heal*. 2013;67(6):519-525. doi:10.1136/jech-2012-201899.

184. Weerasinghe DP, MacIntyre CR, Rubin GL. Seasonality of coronary artery deaths in New South Wales, Australia. *Heart*. 2002;88(1):30-34. doi:10.1136/heart.88.1.30.

185. Braga AL, Zanobetti A, Schwartz J. The time course of weather related deaths. *Epidemiology*. 2001;12:662-667.

186. Rainham DGC, Smoyer-Tomic KE. The role of air pollution in the relationship between a heat stress index and human mortality in Toronto. *Environ Res*. 2003;93(1):9-19. doi:10.1016/S0013-9351(03)00060-4.

187. Steadman RG. A Universal Scale of Apparent Temperature. *J Clim Appl Meteorol*. 1984;23(12):1674-1687. doi:10.1175/1520-0450(1984)023<1674:AUSOAT>2.0.CO;2.

188. Höppe P. The physiological equivalent temperature - a universal index for the biometeorological assessment of the thermal environment. *Int J Biometeorol*. 1999;43(2):71-75. doi:10.1007/s004840050118.

189. Barnett AG, Tong S, Clements ACA. What measure of temperature is the best predictor of mortality? *Environ Res*. 2010;110(6):604-611. doi:10.1016/j.envres.2010.05.006.

190. Brooke Anderson G, Bell ML, Peng RD. Methods to calculate the heat index as an exposure metric in environmental health research. *Environ Health Perspect*. 2013;121(10):1111-1119. doi:10.1289/ehp.1206273.

191. Guo YLLY-LL, Gasparrini A, Armstrong B, et al. Global variation in the effects of ambient temperature on mortality: A systematic evaluation. *Epidemiology*. 2014;25(6):781-789. doi:10.1097/EDE.0000000000000165.

192. Keatinge WR, Donaldson GC, Cordioli E, et al. Heat related mortality in warm and cold regions of Europe: observational study. *BMJ*. 2000;321(7262):670-673. doi:10.1136/bmj.321.7262.670.

193. Gasparrini A, Guo Y, Hashizume M, et al. Temporal Variation in Heat-Mortality Associations: A Multicountry Study. *Environ Health Perspect*. 2015;123(11):1200-1207. doi:10.1289/ehp.1409070.

194. Guo Y, Gasparrini A, Armstrong BG, et al. Heat wave and mortality: A multicountry, multicommunity study. *Environ Health Perspect*. 2016;125(8). doi:10.1289/EHP1026.

195. Chen R, Li T, Cai J, Yan M, Zhao Z, Kan H. Extreme temperatures and out-of-hospital coronary deaths in six large Chinese cities. *J Epidemiol Community Health*. 2014;68(12):1119-1124. doi:10.1136/jech-2014-204012.

196. Wang C, Chen R, Kuang X, Duan X, Kan H. Temperature and daily mortality in Suzhou, China: a time series analysis. *Sci Total Env*. 2014;466-467:985-990. doi:10.1016/j.scitotenv.2013.08.011.

197. Yang C, Meng X, Chen R, et al. Long-term variations in the association between ambient temperature and daily cardiovascular mortality in Shanghai, China. *Sci Total Environ*. 2015;538:524-530. doi:10.1016/j.scitotenv.2015.08.097.

198. Zhang Y, Yu C, Bao J, Li X. Impact of temperature on mortality in Hubei, China: a multi-county time series analysis. *Sci Rep*. 2017;7:45093. doi:10.1038/srep45093.

199. Ha J, Shin YS, Kim H. Distributed lag effects in the relationship between temperature and mortality in three major cities in South Korea. *Sci Total Environ*. 2011;409(18):3274-3280. doi:10.1016/j.scitotenv.2011.05.034.

200. Kwon BY, Lee E, Lee S, Heo S, Jo K, Kim J. Vulnerabilities to temperature effects on acute myocardial infarction hospital admissions in South Korea. *Int J Environ Res Public Health*. 2015;12(11):14571-14588. doi:10.3390/ijerph121114571.

201. Lin YK, Chang CK, Wang YC, Ho TJ. Acute and prolonged adverse effects of temperature on mortality from cardiovascular diseases. *PLoS One*. 2013;8(12):e82678. doi:10.1371/journal.pone.0082678.

202. Nitschke M, Tucker GR, Bi P. Morbidity and mortality during heatwaves in metropolitan Adelaide. *Med J Aust*. 2007;187(11-12):662-665. doi:10.1017/CBO9781107415324.004.

203. Schaffer A, Muscatello D, Broome R, Corbett S, Smith W. Emergency department visits, ambulance calls, and mortality associated with an exceptional heat wave in Sydney, Australia, 2011: A time-series analysis. *Environ Heal A Glob Access Sci Source*. 2012;11(1). doi:10.1186/1476-069X-11-3.

204. Pearce JL, Hyer M, Hyndman RJ, Loughnan M, Dennekamp M, Nicholls N. Exploring the influence of short-term temperature patterns on temperature-related mortality: a case-study of Melbourne, Australia. *Environ Heal A Glob Access Sci Source*. 2016;15(1):1-10. doi:10.1186/s12940-016-0193-1.

205. Vaneckova P, Bambrick H. Cause-Specific Hospital Admissions on Hot Days in Sydney, Australia. *PLoS One*. 2013;8(2). doi:10.1371/journal.pone.0055459.

206. McMichael AJ, Wilkinson P, Kovats RS, et al. International study of temperature, heat and urban mortality: The 'ISOTHURM' project. *Int J Epidemiol*. 2008;37:1121-1131. doi:10.1093/ije/dyn086.

207. Seposo XT, Dang TN, Honda Y. Evaluating the Effects of Temperature on Mortality in Manila City (Philippines) from 2006-2010 Using a Distributed Lag Nonlinear Model. *Int J Env Res Public Heal*. 2015;12(6):6842-6857. doi:10.3390/ijerph120606842.

208. Leone M, D'Ippoliti D, De Sario M, et al. A time series study on the effects of heat on mortality and evaluation of heterogeneity into European and Eastern-Southern Mediterranean cities: Results of EU CIRCE project. *Environ Heal A Glob Access Sci Source*. 2013;12(1). doi:10.1186/1476-069X-12-55.

209. Hashizume M, Wagatsuma Y, Hayashi T, Saha SK, Streatfield K, Yunus M. The effect of temperature on mortality in rural Bangladesh-a population-based time-series study. *Int J Epidemiol*. 2009;38(6):1689-1697. doi:10.1093/ije/dyn376.

210. Bell ML, O'Neill MS, Ranjit N, Borja-Aburto VH, Cifuentes L a, Gouveia NC. Vulnerability to heat-related mortality in Latin America: a case-crossover study in Sao Paulo, Brazil, Santiago, Chile and Mexico City, Mexico. *Int J Epidemiol*. 2008;37(4):796-804. doi:10.1093/ije/dyn094.

211. Phung D, Guo Y, Nguyen HTL, Rutherford S, Baum S, Chu C. High temperature and risk of hospitalizations, and effect modifying potential of socio-economic conditions: A multi-province study in the tropical Mekong Delta Region. *Environ Int*. 2016;92-93:77-86. doi:10.1016/j.envint.2016.03.034.

212. O'Neill MS, Zanobetti A, Schwartz J. Disparities by race in heat-related mortality in four US cities: The role of air conditioning prevalence. *J Urban Heal*. 2005;82(2):191-197. doi:10.1093/jurban/jti043.

213. Bobb JF, Peng RD, Bell ML, Dominici F. Heat-related mortality and adaptation to heat in the United States. *Environ Health Perspect*. 2014;122(8):811-816. doi:10.1289/ehp.1307392.

214. Tobias A, Armstrong B, Gasparrini A, Diaz J. Effects of high summer temperatures on mortality in 50 Spanish cities. *Env Heal*. 2014;13(1):48. doi:10.1186/1476-069x-13-48.

215. Gasparrini A, Guo Y, Hashizume M, et al. Changes in Susceptibility to Heat during the Summer: A Multicountry Analysis. *Am J Epidemiol*. 2016;183(11):1027-1036. doi:10.1093/aje/kwv260.

216. Wang C, Zhang Z, Zhou M, et al. Nonlinear relationship between extreme temperature and mortality in different temperature zones: A systematic study of 122 communities across the mainland of China. *Sci Total Env*. 2017;586:96-106. doi:10.1016/j.scitotenv.2017.01.218.

217. Ma W, Wang L, Lin H, et al. The temperature-mortality relationship in China: An analysis from 66 Chinese communities. *Env Res*. 2015;137:72-77. doi:10.1016/j.envres.2014.11.016.

218. Huang Z, Lin H, Liu Y, et al. Individual-level and community-level effect modifiers of the temperature-mortality relationship in 66 Chinese communities. *BMJ Open*. 2015;5(9). doi:10.1136/bmjopen-2015-009172.

219. Bennett JE, Blangiardo M, Fecht D, Elliott P, Ezzati M. Vulnerability to the mortality effects of warm temperature in the districts of England and Wales. *Nat Clim Chang*. 2014;4(4):269-273. doi:10.1038/nclimate2123.

220. Urban A, Burkart K, Kysely J, et al. Spatial Patterns of Heat-Related Cardiovascular Mortality in the Czech Republic. *Int J Env Res Public Heal*. 2016;13(3). doi:10.3390/ijerph13030284.

221. Lee M, Shi L, Zanobetti A, Schwartz JD. Study on the association between ambient temperature and mortality using spatially resolved exposure data. *Environ Res*. 2016;151:610-617. doi:10.1016/j.envres.2016.08.029.

222. Kloog I, Melly SJ, Coull BA, Nordio F, Schwartz JD. Using Satellite-Based Spatiotemporal Resolved Air Temperature Exposure to Study the Association between Ambient Air Temperature and Birth Outcomes in Massachusetts. *Env Heal Perspect*. 2015;123(10):1053-1058. doi:10.1289/ehp.1308075.

223. Davis RE, Knappenberger PC, Michaels PJ, Novicoff WM. Changing heat-related mortality in the United States. *Environ Health Perspect*. 2003;111(14):1712-1718. doi:10.1289/ehp.6336.

224. Ostro B, Rauch S, Green R, Malig B, Basu R. The effects of temperature and use of air conditioning on hospitalizations. *Am J Epidemiol*. 2010;172(9):1053-1061. doi:10.1093/aje/kwq231.

225. O'Neill M. Air Conditioning and Heat-Related Health Effects.Pdf. *Appl Env Sci Public Heal*. 2003;1:9-12. http://www.hsph.harvard.edu/clarc/pubs/endnote53-o'neill.pdf.

226. Smoyer-Tomic KE, Rainham DGC. Beating the heat: Development and evaluation of a Canadian hot weather health-response plan. *Environ Health Perspect*. 2001;109(12):1241-1248. doi:10.1289/ehp.011091241.

227. Weisskopf MG, Anderson HA, Foldy S, et al. Heat wave morbidity and mortality, Milwaukee, Wis, 1999 vs 1995: An improved response? *Am J Public Health*. 2002;92(5):830-833. doi:10.2105/AJPH.92.5.830.

228. Schifano P, Cappai G, Sario M, Bargagli AM, Michelozzi P. Who should heat prevention plans target? A heat susceptibility indicator in the elderly developed based on administrative data from a cohort study. *Heal Aging Res*. 2013;2(2):1-10. doi:10.12715/har.2013.2.2.

229. de' Donato FK, Leone M, Scortichini M, et al. Changes in the effect of heat on mortality in the last 20 years in nine European cities. Results from the PHASE project. *Int J Environ Res Public Health*. 2015;12(12):15567-15583. doi:10.3390/ijerph121215006.

230. Khosla R, Guntupalli KK. HEAT-RELATED ILLNESSES. *Crit Care Clin*. 1999;15(2):251-263. doi:10.1016/S0749-0704(05)70053-1.

231. Kilbourne EM. The spectrum of illness during heat waves. *Am J Prev Med*. 1999;16(4):359-360. doi:10.1016/S0749-3797(99)00016-1.

232. Bouchama A, Dehbi M, Mohamed G, Matthies F, Shoukri M, Menne B. Prognostic factors in heat wave related deaths: a meta-analysis. *Arch Intern Med*. 2007;167(20):2170-2176. doi:10.1001/archinte.167.20.ira70009.

233. Bhaskaran K, Hajat S, Haines A, Herrett E, Wilkinson P, Smeeth L. Effects of ambient temperature on the incidence of myocardial infarction. *Heart*. 2009;95(21):1760-1769. doi:10.1136/hrt.2009.175000.

234. Breitner S, Wolf K, Peters A, Schneider A. Short-term effects of air temperature on cause-specific cardiovascular mortality in Bavaria, Germany. *Heart*. 2014;100(16):1272-1280. doi:10.1136/heartjnl-2014-305578.

235. Madrigano J, Mittleman MA, Baccarelli A, et al. Temperature, myocardial infarction, and mortality: Effect modification by individual-and area-level characteristics. *Epidemiology*. 2013;24(3):439-446. doi:10.1097/EDE.0b013e3182878397.

236. Keatinge WR, Coleshaw SRK, Easton JC, Cotter F, Mattock MB, Chelliah R. Increased platelet and red cell counts, blood viscosity, and plasma cholesterol levels during heat stress, and mortality from coronary and cerebral thrombosis. *Am J Med*. 1986. doi:10.1016/0002-9343(86)90348-7.

237. Hoffmann P, Heinke SchlüNzen K. Weather pattern classification to represent the urban heat island in present and future climate. *J Appl Meteorol Climatol*. 2013;52(12):2699-2714. doi:10.1175/JAMC-D-12-065.1.

238. Halonen JI, Zanobetti A, Sparrow D, Vokonas PS, Schwartz J. Relationship between outdoor temperature and blood pressure. *Occup Environ Med*. 2011. doi:10.1136/oem.2010.056507.

239. Barnett AG, Sans S, Salomaa V, Kuulasmaa K, Dobson AJ. The effect of temperature on systolic blood pressure. *Blood Press Monit*. 2007;12(3):195-203. doi:10.1097/MBP.0b013e3280b083f4.

240. Wilker EH, Yeh G, Wellenius GA, Davis RB, Phillips RS, Mittleman MA. Ambient temperature and biomarkers of heart failure: A repeated measures analysis. *Environ Health Perspect*. 2012;120(8):1083-1087. doi:10.1289/ehp.1104380.

241. Bind M-A, Zanobetti A, Gasparrini A, et al. Effects of temperature and relative humidity on DNA methylation. *Epidemiology*. 2014;25(4):561-569. doi:10.1097/EDE.0000000000000120.

242. Green D, Bambrick H, Tait P, et al. Differential Effects of Temperature Extremes on Hospital Admission Rates for Respiratory Disease between Indigenous and Non-Indigenous Australians in the Northern Territory. *Int J Env Res Public Heal*. 2015;12(12):15352-15365. doi:10.3390/ijerph121214988.

243. Arbuthnott KG, Hajat S. The health effects of hotter summers and heat waves in the population of the United Kingdom: A review of the evidence. *Environ Heal A Glob Access Sci Source*. 2017;16. doi:10.1186/s12940-017-0322-5.

244. Yi W, Chan AP. Effects of temperature on mortality in Hong Kong: a time series analysis. *Int J Biometeorol*. 2015;59(7):927-936. doi:10.1007/s00484-014-0895-4.

245. Iniguez C, Schifano P, Asta F, Michelozzi P, Vicedo-Cabrera A, Ballester F. Temperature in summer and children's hospitalizations in two Mediterranean cities. *Env Res*. 2016;150:236-244. doi:10.1016/j.envres.2016.06.007.

246. Xu Z, Hu W, Su H, et al. Extreme temperatures and paediatric emergency department admissions. *J Epidemiol Community Health*. 2014;68(4):304-311. doi:10.1136/jech-2013-202725.

247. Díaz J, Linares C, Tobías A. Impact of extreme temperatures on daily mortality in Madrid (Spain)

among the 45-64 age-group. *Int J Biometeorol*. 2006;50(6):342-348. doi:10.1007/s00484-006-0033-z.

248. Ebi KL. weather changes associated with hospitalizations for cardiovascular disease and stroke in California, 1983-1998. 2004.

249. Wichmann J, Andersen ZJ, Ketzel M, Ellermann T. Apparent Temperature and Cause-Specific Mortality in Copenhagen , Denmark : A Case-Crossover Analysis. 2011:3712-3727. doi:10.3390/ijerph8093712.

250. Zhang J, Li TT, Tan JG, Huang CR, Kan HD. Impact of temperature on mortality in three major Chinese cities. *Biomed Env Sci*. 2014;27(7):485-494. doi:10.3967/bes2014.080.

251. Yang X, Li L, Wang J, Huang J, Lu S. Cardiovascular mortality associated with low and high temperatures: Determinants of inter-region vulnerability in China. *Int J Environ Res Public Health*. 2015;12(6):5918-5933. doi:10.3390/ijerph120605918.

252. Basagana X. Heat Waves and Cause-specific Mortality at all Ages. 2011;22(6). doi:10.1097/EDE.0b013e31823031c5.

253. Sun S, Tian L, Qiu H, et al. The influence of pre-existing health conditions on short-term mortality risks of temperature: Evidence from a prospective Chinese elderly cohort in Hong Kong. *Environ Res*. 2016;148:7-14. doi:10.1016/j.envres.2016.03.012.

254. Zanobetti A, O'Neill MS, Gronlund CJ, Schwartz JD. Summer temperature variability and long-term survival among elderly people with chronic disease. *Proc Natl Acad Sci*. 2012;109(17):6608-6613. doi:10.1073/pnas.1113070109.

255. Schwartz J. Who is sensitive to extremes of temperature? A case-only analysis. *Epidemiology*. 2005;16(1):67-72. doi:10.1097/01.ede.0000147114.25957.71.

256. Gronlund CJ. Racial and socioeconomic disparities in heat-related health effects and their mechanisms: a review. *Curr Epidemiol Rep*. 2014;1(3):165-173. doi:10.1007/s40471-014-0014-4.

257. Berko J, Ingram DD, Saha S, Parker JD. Deaths attributed to heat, cold, and other weather events in the United States, 2006-2010. *Natl Health Stat Report*. 2014;(76):1-15. http://www.scopus.com/inward/record.url?eid=2-s2.0-84908133087&partnerID=40&md5=a55980275ef8a783119fb8cc27e58f2b.

258. Chung Y, Lim YH, Honda Y, et al. Mortality related to extreme temperature for 15 Cities in Northeast Asia. *Epidemiology*. 2015;26(2):255-262. doi:10.1097/EDE.0000000000000229.

259. Vargo J, Stone B, Habeeb D, Liu P, Russell A. The social and spatial distribution of temperature-related health impacts from urban heat island reduction policies. *Environ Sci Policy*. 2016;66:366-374. doi:10.1016/j.envsci.2016.08.012.

260. Benmarhnia T, Oulhote Y, Petit C, et al. Chronic air pollution and social deprivation as modifiers of the association between high temperature and daily mortality. *Env Heal*. 2014;13(1):53. doi:10.1186/1476-069x-13-53.

261. Gouveia N, Hajat S, Armstrong B. Socioeconomic differentials in the temperature-mortality relationship in São Paulo, Brazil. *Int J Epidemiol*. 2003;32(3):390-397. doi:10.1093/ije/dyg077.

262. Willers SM, Jonker MF, Klok L, et al. High resolution exposure modelling of heat and air pollution and the impact on mortality. *Env Int*. 2016;89-90:102-109. doi:10.1016/j.envint.2016.01.013.

263. Taylor J, Wilkinson P, Picetti R, et al. Comparison of built environment adaptations to heat exposure and mortality during hot weather, West Midlands region, UK. *Env Int*. 2017. doi:10.1016/j.envint.2017.11.005.

264. Taylor J, Davies M, Mavrogianni A, et al. Mapping indoor overheating and air pollution risk modification across Great Britain: A modelling study. *Build Environ*. 2016;99:1-12. doi:10.1016/j.buildenv.2016.01.010.

265. Krüger EL. Urban heat island and indoor comfort effects in social housing dwellings. *Landsc Urban Plan*. 2015;134:147-156. doi:10.1016/j.landurbplan.2014.10.017.

266. Smoyer KE, Rainham DG, Hewko JN. Heat-stress-related mortality in five cities in Southern Ontario: 1980-1996. *Int J Biometeorol*. 2000;44:190-197. doi:10.1007/s004840000070.

267. Henits L, Mucsi L, Liska CM. Monitoring the changes in impervious surface ratio and urban heat island

intensity between 1987 and 2011 in Szeged, Hungary. *Env Monit Assess*. 2017;189(2):86. doi:10.1007/s10661-017-5779-8.

268. Ren C, Williams GM, Morawska L, Mengersen K, Tong S. Ozone modifies associations between temperature and cardiovascular mortality: analysis of the NMMAPS data. *Occup Env Med*. 2008;65(4):255-260. doi:10.1136/oem.2007.033878.

269. Ren C, Williams GM, Tong S. Does particulate matter modify the association between temperature and cardiorespiratory diseases? *Environ Health Perspect*. 2006;114(11):1690-1696. doi:10.1289/ehp.9266.

270. Breitner S, Wolf K, Devlin RB, Diaz-Sanchez D, Peters A, Schneider A. Short-term effects of air temperature on mortality and effect modification by air pollution in three cities of Bavaria, Germany: a time-series analysis. *Sci Total Env*. 2014;485-486:49-61. doi:10.1016/j.scitotenv.2014.03.048.

271. Jhun I, Fann N, Zanobetti A, Hubbell B. Effect modification of ozone-related mortality risks by temperature in 97 US cities. *Environ Int*. 2014;73:128-134. doi:10.1016/j.envint.2014.07.009.

272. Analitis A, de' Donato F, Scortichini M, et al. Synergistic Effects of Ambient Temperature and Air Pollution on Health in Europe: Results from the PHASE Project. *Int J Environ Res Public Health*. 2018;15(9):1856. doi:10.3390/ijerph15091856.

273. Li J, Woodward A, Hou X-YY, et al. Modification of the effects of air pollutants on mortality by temperature: A systematic review and meta-analysis. *Sci Total Env*. 2017;575:1556-1570. doi:10.1016/j.scitotenv.2016.10.070.

274. Scortichini M, De Sario M, de'Donato F, et al. Short-Term Effects of Heat on Mortality and Effect Modification by Air Pollution in 25 Italian Cities. *Int J Environ Res Public Health*. 2018;15(8):1771. doi:10.3390/ijerph15081771.

275. Hajat S, Kovats RS, Lachowycz K. Heat-related and cold-related deaths in England and Wales: who is at risk? *Occup Environ Med*. 2007;64(August):93-100. doi:10.1136/oem.2006.029017.

276. Gasparrini A, Armstrong B, Kenward MG. Distributed lag non-linear models. *Stat Med*. 2010;29(21):2224-2234. doi:10.1002/sim.3940.

277. Rocklöv J, Ebi K, Forsberg B. Mortality related to temperature and persistent extreme temperatures: a study of cause-specific and age-stratified mortality. *Occup Environ Med*. 2011;68:531-536. doi:10.1136/oem.2010.058818.

278. De'donato FK, Stafoggia M, Rognoni M, et al. Airport and city-centre temperatures in the evaluation of the association between heat and mortality. *Int J Biometeorol*. 2008;52(4):301-310. doi:10.1007/s00484-007-0124-5.

279. Reid CE, O'Neill MS, Gronlund CJ, et al. Mapping community determinants of heat vulnerability. *Environ Health Perspect*. 2009;117(11):1730-1736. doi:10.1289/ehp.0900683.

280. Tan J, Zheng Y, Tang X, et al. The urban heat island and its impact on heat waves and human health in Shanghai. *Int J Biometeorol*. 2010;54:75-84. doi:10.1007/s00484-009-0256-x.

281. Gabriel KMA a, Endlicher WR. Urban and rural mortality rates during heat waves in Berlin and Brandenburg, Germany. *Environ Pollut*. 2011;159(8-9):2044-2050. doi:10.1016/j.envpol.2011.01.016.

282. Kershaw SE, Millward AA. A spatio-temporal index for heat vulnerability assessment. *Environ Monit Assess*. 2012;184(12):7329-7342. doi:10.1007/s10661-011-2502-z.

283. Henderson SB, Wan V, Kosatsky T. Differences in heat-related mortality across four ecological regions with diverse urban, rural, and remote populations in British Columbia, Canada. *Heal Place*. 2013;23:48-53. doi:10.1016/j.healthplace.2013.04.005.

284. Hondula DM, Davis RE, Rocklöv J, Saha M V. A time series approach for evaluating intra-city heat-related mortality. *J Epidemiol Community Health*. 2013;67:707-712. doi:10.1136/jech-2012-202157.

285. White-Newsome JL, Brines SJ, Brown DG, et al. Validating satellite-derived land surface temperature with in situ measurements: A public health perspective. *Environ Health Perspect*. 2013;121(8):925-931. doi:10.1289/ehp.1206176.

286. Li P, Xin J, Bai X, et al. Observational studies and a statistical early warning of surface ozone pollution in Tangshan, the largest heavy industry city of North China. *Int J Env Res Public Heal*. 2013;10(3):1048-1061. doi:10.3390/ijerph10031048.

287. Medina-Ramón M, Zanobetti A, Cavanagh DP, Schwartz J. Extreme temperatures and mortality: Assessing effect modification by personal characteristics and specific cause of death in a multi-city case-only analysis. *Environ Health Perspect*. 2006;114(9):1331-1336. doi:10.1289/ehp.9074.

288. Basu R, Malig B. High ambient temperature and mortality in California: exploring the roles of age, disease, and mortality displacement. *Environ Res*. 2011;111(8):1286-1292. doi:10.1016/j.envres.2011.09.006.

289. Laaidi K, Zeghnoun A, Dousset B, et al. The impact of heat islands on mortality in Paris during the August 2003 heat wave. *Environ Health Perspect*. 2012;120(2):254-259. doi:10.1289/ehp.1103532.

290. Goggins WB, Ren C, Ng E, Yang C, Chan EYY. Effect modification of the association between meteorological variables and mortality by urban climatic conditions in the tropical city of Kaohsiung, Taiwan. *Geospat Health*. 2013;8(1):37-44. https://www.scopus.com/inward/record.uri?eid=2-s2.0-84896515931&partnerID=40&md5=d7266771a628b306a1501e1410fcea6c.

291. Ho HC, Knudby A, Walker BB, Henderson SB. Delineation of spatial variability in the temperature-mortality relationship on extremely hot days in greater Vancouver, Canada. *Environ Health Perspect*. 2017;125(1):66-75. doi:10.1289/EHP224.

292. Burkart K, Meier F, Schneider A, Breitner S, Canário P, Alcoforado MJ. Modification of Heat-Related Mortality in an Elderly Urban Population by Vegetation (Urban Green) and Proximity to Water (Urban Blue): Evidence from Lisbon, Portugal. *Environ Health Perspect*. 2016;124(7):927-934.

293. Huang G, Zhou W, Cadenasso ML. Is everyone hot in the city? Spatial pattern of land surface temperatures, land cover and neighborhood socioeconomic characteristics in Baltimore, MD. *J Environ Manage*. 2011;92(7):1753-1759. doi:10.1016/j.jenvman.2011.02.006.

294. Johnson DP, Wilson JS, Luber GC. Socioeconomic indicators of heat-related health risk supplemented with remotely sensed data. *Int J Health Geogr*. 2009;8:57. doi:10.1186/1476-072X-8-57.

295. Johnson DP, Stanforth A, Lulla V, Luber G. Developing an applied extreme heat vulnerability index utilizing socioeconomic and environmental data. *Appl Geogr*. 2012;35(1-2):23-31. doi:10.1016/j.apgeog.2012.04.006.

296. Milojevic A, Wilkinson P, Armstrong B, et al. Impact of London's Urban Heat Island on Heat-related Mortality. *Epidemiology*. 2011;22(1):S182-S183. doi:10.1097/01.ede.0000392239.91165.65.

297. Kestens Y, Brand A, Fournier M, et al. Modelling the variation of land surface temperature as determinant of risk of heat-related health events. *Int J Health Geogr*. 2011;10(1):7. doi:10.1186/1476-072X-10-7.

298. Steeneveld GJ, Koopmans S, Heusinkveld BG, van Hove LWA, Holtslag AAM. Quantifying urban heat island effects and human comfort for cities of variable size and urban morphology in the Netherlands. *J Geophys Res*. 2011;116(D20):D20129. doi:10.1029/2011JD015988.

299. Wong MS, Peng F, Zou B, Shi WZ, Wilson GJ. Spatially Analyzing the Inequity of the Hong Kong Urban Heat Island by Socio-Demographic Characteristics. *Int J Env Res Public Heal*. 2016;13(3). doi:10.3390/ijerph13030317.

300. Buscail C, Upegui E, Viel J-F. Mapping heatwave health risk at the community level for public health action. *Int J Health Geogr*. 2012;11:38. doi:10.1186/1476-072X-11-38.

301. Taylor J, Wilkinson P, Davies M, et al. Mapping the effects of urban heat island, housing, and age on excess heat-related mortality in London. *Urban Clim*. 2015;14:517-528. doi:10.1016/j.uclim.2015.08.001.

302. Heaviside C, Vardoulakis S, Cai XM. Attribution of mortality to the urban heat island during heatwaves in the West Midlands, UKHeaviside, C., Vardoulakis, S., Cai, X.M., 2016. Attribution of mortality to the urban heat island during heatwaves in the West Midlands, UK. Env. Heal. 15 Suppl 1,. *Env Heal*. 2016;15 Suppl 1:27. doi:10.1186/s12940-016-0102-7.

303. Morabito M, Crisci A, Gioli B, et al. Urban-hazard risk analysis: Mapping of heat-related risks in the elderly in major Italian cities. *PLoS One*. 2015;10(5):1-18. doi:10.1371/journal.pone.0127277.

304. Xu S. An approach to analyzing the intensity of the daytime surface urban heat island effect at a local scale. *Environ Monit Assess*. 2009;151(1-4):289-300. doi:10.1007/s10661-008-0270-1.

305. Cai G, Du M, Xue Y. Monitoring of urban heat island effect in Beijing combining ASTER and TM data.

Int J Remote Sens. 2011;32:1213-1232. doi:10.1080/01431160903469079.

306. Mehta AJ, Kloog I, Zanobetti A, et al. Associations between changes in City and address specific temperature and QT interval - The VA normative aging study. *PLoS One*. 2014;9(9). doi:10.1371/journal.pone.0106258.

307. Prata F. Land Surface Temperature Measurement from Space : AATSR Algorithm Theoretical Basis Document. 2002. https://www.eumetsat.int/website/home/Data/Training/TrainingLibrary/DAT_2043202.html.

308. Heymann Y, Steenmans C, Croissille G, Bossard M. CORINE Land Cover. Technical Guide. *Off Publ Eur Communities*. 1994;(November):1-94. http://www.eea.europa.eu/publications/COR0-landcover.

309. Homer C, Huang C, Yang L, Wylie B, Coan M. Development of a 2001 national land-cover database for the United States. *Photogramm Eng Remote Sens*. 2004;70(7):829-840. doi:10.14358/PERS.70.7.829.

310. arnfield 2017. Köppen climate classification. In: Encyclopædia Britannica, inc. https://www.britannica.com/science/Koppen-climate-classification.

311. Cotton WR, Pielke Sr. RA, Walko RL, et al. RAMS 2001: Current status and future directions. *Meteorol Atmos Phys*. 2003;82(1-4):5-29. doi:10.1007/s00703-001-0584-9.

312. Li Y, Zhao M, Motesharrei S, Mu Q, Kalnay E, Li S. Local cooling and warming effects of forests based on satellite observations. *Nat Commun*. 2015;6:1-8. doi:10.1038/ncomms7603.

313. Zhang M, Lee X, Yu G, et al. Response of surface air temperature to small-scale land clearing across latitudes. *Environ Res Lett*. 2014;9(3). doi:10.1088/1748-9326/9/3/034002.

314. Michelozzi P, De' Donato F, Scortichini M, et al. [On the increase in mortality in Italy in 2015: analysis of seasonal mortality in the 32 municipalities included in the Surveillance system of daily mortality]. *Epidemiol Prev*. 2016;40(1):22-28. doi:10.19191/EP16.1.P022.010.

315. Shi L, Zanobetti A, Kloog I, et al. Low-Concentration PM and Mortality: Estimating Acute and Chronic Effects in a Population-Based Study. *Environ Health Perspect*. 2016;(JANUARY):46-52. doi:10.1289/ehp.1409111.

316. Weng Q, Fu P, Gao F. Generating daily land surface temperature at Landsat resolution by fusing Landsat and MODIS data. *Remote Sens Environ*. 2014;145:55-67. doi:10.1016/j.rse.2014.02.003.

317. Hazaymeh K, Hassan QK. Fusion of MODIS and landsat-8 surface temperature images: a new approach. *PLoS One*. 2015;10(3):e0117755. doi:10.1371/journal.pone.0117755.

318. Sidiqui P, Huete A, Devadas R. Spatio-temporal mapping and monitoring of Urban Heat Island patterns over Sydney, Australia using MODIS and Landsat-8. In: Gamba P, Xian G, Liang S, Weng Q, Chen JM, Liang S, eds. University of Technology Sydney (UTS), Sydney, Australia: Institute of Electrical and Electronics Engineers Inc.; 2016:217-221. doi:10.1109/EORSA.2016.7552800.

319. Michelozzi P, De Sario M, Accetta G, et al. Temperature and summer mortality: geographical and temporal variations in four Italian cities. *J Epidemiol Community Health*. 2006;60(5):417-423.

320. D'Ippoliti D, Michelozzi P, Marino C, et al. The impact of heat waves on mortality in 9 European cities: results from the EuroHEAT project. *Environ Health*. 2010;9:37. doi:10.1186/1476-069X-9-37.

321. Armstrong BG, Gasparrini A, Tobias A. Conditional Poisson models: A flexible alternative to conditional logistic case cross-over analysis. *BMC Med Res Methodol*. 2014;14(1):1-6. doi:10.1186/1471-2288-14-122.

322. Gasparrini A. Distributed Lag Linear and Non-Linear Models in R: The Package dlnm. *J Stat Softw*. 2011;43(8):1-20. doi:http://dx.doi.org/10.18637/jss.v043.i08.

323. Gasparrini A. Modelling lagged associations in environmental time series data: A simulation study. *Epidemiology*. 2016;27(6):835-842. doi:10.1097/EDE.0000000000000533.

324. Levy D, Lumley T, Sheppard L, Kaufman J, Checkoway H. Referent selection in case-crossover analyses of health effects of air pollution. *Epidemiology*. 2001;12:186-192.

325. Gasparrini A, Leone M. Attributable risk from distributed lag models. *BMC Med Res Methodol*. 2014;14(1):1-8. doi:10.1186/1471-2288-14-55.

326. Baccini M, Kosatsky T, Biggeri A. Impact of Summer Heat on Urban Population Mortality in Europe

during the 1990s: An Evaluation of Years of Life Lost Adjusted for Harvesting. *PLoS One*. 2013;8. doi:10.1371/journal.pone.0069638.

327. WHO. WHO methods and data sources for country - level causes of death. 2017. http://www.who.int/healthinfo/global_burden_disease/GlobalCOD_method_2000_2015.pdf.

328. Williams S, Nitschke M, Sullivan T, et al. Heat and health in Adelaide, South Australia: Assessment of heat thresholds and temperature relationships. *Sci Total Environ*. 2012;414:126-133. doi:10.1016/j.scitotenv.2011.11.038.

329. Sheridan SC, Dolney TJ. Heat, mortality, and level of urbanization: Measuring vulnerability across Ohio, USA. *Clim Res*. 2003;24(3):255-265. doi:10.3354/cr024255.

330. Urban A, Davidkovova H, Kysely J, Dale AG, Frank SD. Heat- and cold-stress effects on cardiovascular mortality and morbidity among urban and rural populations in the Czech Republic The effects of urban warming on herbivore abundance and street tree condition. *Int J Biometeorol*. 2014;58:1057-1068. doi:10.1289/ehp.1307496 10.1007/s00484-013-0693-4.

331. Kovach MM, Konrad CE, Fuhrmann CM. Area-level risk factors for heat-related illness in rural and urban locations across North Carolina, USA. *Appl Geogr*. 2015;60:175-183. doi:10.1016/j.apgeog.2015.03.012.

332. Milojevic A, Armstrong BG, Gasparrini A, Bohnenstengel SI, Barratt B, Wilkinson P. Methods to Estimate Acclimatization to Urban Heat Island Effects on Heat- and Cold-Related Mortality. *Environ Health Perspect*. 2016;124(7):1016-1022. doi:10.1289/ehp.1510109.

333. Hattis D, Ogneva-Himmelberger Y, Ratick S. The spatial variability of heat-related mortality in Massachusetts. *Appl Geogr*. 2012;33(1):45-52. doi:10.1016/j.apgeog.2011.07.008.

334. Barichivich J, Briffa KR, Myneni RB, et al. A Weekly Indicator of Surface Moisture Status from Satellite Data for Operational Monitoring of Crop Conditions. *Sci Total Env*. 2017;10(1):483-489. doi:10.1038/srep40326.

335. Schifano P, Leone M, De Sario M, et al. Changes in the effects of heat on mortality among the elderly from 1998-2010: results from a multicenter time series study in Italy. *Environ Heal*. 2012;11(1):58. doi:10.1186/1476-069X-11-58.

336. Baccini M, Kosatsky T, Analitis A, et al. *Impact of Heat on Mortality in 15 European Cities: Attributable Deaths under Different Weather Scenarios*. Vol 65.; 2011:64-70. doi:10.1136/jech.2008.085639.

337. Michelozzi P, de' Donato FK, Bargagli AM, et al. Surveillance of Summer Mortality and Preparedness to Reduce the Health Impact of Heat Waves in Italy. *Int J Environ Res Public Health*. 2010;7(5):2256-2273. doi:10.3390/ijerph7052256.

338. Cesaroni G, Badaloni C, Romano V, Donato E, Perucci CA, Forastiere F. Socioeconomic position and health status of people who live near busy roads: The Rome Longitudinal Study (RoLS). *Environ Heal A Glob Access Sci Source*. 2010;9(1):1-12. doi:10.1186/1476-069X-9-41.

339. Stafoggia M, Cesaroni G, Peters A, et al. Long-term exposure to ambient air pollution and incidence of cerebrovascular events: Results from 11 European cohorts within the ESCAPE project. *Environ Health Perspect*. 2014;122(9):919-925. doi:10.1289/ehp.1307301.

340. Beelen R. et al. Natural Cause Mortality and Long-Term Exposure to Particle Components: An Analysis of 19 European Cohorts within the Multi-Center ESCAPE project. *Environ Health Perspect*. 2015;123(November 2012):525-533. doi:http://dx.doi.org/10.1289/ehp.1408095.

341. Guxens M, Ghassabian A, Gong T, et al. Air pollution exposure during pregnancy and childhood autistic traits in four European population-based cohort studies: The ESCAPE project. *Environ Health Perspect*. 2016;124(1):133-140. doi:10.1289/ehp.1408483.

342. Beelen R, Raaschou-Nielsen O, Stafoggia M, et al. Effects of long-term exposure to air pollution on natural-cause mortality: An analysis of 22 European cohorts within the multicentre ESCAPE project. *Lancet*. 2014;383(9919):785-795. doi:10.1016/S0140-6736(13)62158-3.

343. Cesaroni G, Forastiere F, Stafoggia M, et al. Long term exposure to ambient air pollution and incidence of acute coronary events: prospective cohort study and meta-analysis in 11 European cohorts from the ESCAPE Project. *BMJ*. 2014;348(2):f7412. doi:10.1136/bmj.f7412.

344. Cesaroni G, Badaloni C, Gariazzo C, et al. Long-term exposure to urban air pollution and mortality in a cohort of more than a million adults in Rome. *Environ Health Perspect*. 2013;121(3):324-331. doi:10.1289/ehp.1205862.

345. Cesaroni G, Agabiti N, Rosati R, Forastiere F, Perucci CA. An index of socioeconomic position based on 2001 Census, Rome. *Epidemiol Prev*. 2006;30(6):352-357.

346. ISTAT. Popolazione residente e abitazioni nelle grandi province italiane. 2001.

347. Maclure M. The Case-Crossover Design : A Method for Studying Transient Effects on the Risk of Acute Events. 1991;133(2):144-153.

348. Janes H, Sheppard L, Lumley T. Case – Crossover Analyses of Air Pollution Exposure Data Referent Selection Strategies and Their Implications for Bias. 2005;16(6):717-726. doi:10.1097/01.ede.0000181315.18836.9d.

349. Li Y, Cheng Y, Cui G, et al. Association between high temperature and mortality in metropolitan areas of four cities in various climatic zones in China: a time-series study. *Env Heal*. 2014;13:65. doi:10.1186/1476-069x-13-65.

350. Chan EYY, Goggins WB, Kim JJ, Griffiths SM. A study of intracity variation of temperature-related mortality and socioeconomic status among the Chinese population in Hong Kong. *J Epidemiol Community Heal*. 2012;66(4):322-327. doi:10.1136/jech.2008.085167.

351. Wang X, Li G, Liu L, Westerdahl D, Jin X, Pan X. Effects of extreme temperatures on cause-specific cardiovascular mortality in China. *Int J Environ Res Public Health*. 2015;12(12):16136-16156. doi:10.3390/ijerph121215042.

352. Harlan SL, Chowell G, Yang S, et al. Heat-related deaths in hot cities: estimates of human tolerance to high temperature thresholds. *Int J Env Res Public Heal*. 2014;11(3):3304-3326. doi:10.3390/ijerph110303304.

353. Buckley JP, Samet JM, Richardson DB. Does air pollution confound studies of temperature? *Epidemiology*. 2014. doi:10.1097/EDE.0000000000000051.

354. Chen K, Wolf K, Breitner S, et al. Two-way effect modifications of air pollution and air temperature on total natural and cardiovascular mortality in eight European urban areas. *Environ Int*. 2018;116(December 2017):186-196. doi:10.1016/j.envint.2018.04.021.

355. Heusinkveld BG, Steeneveld GJ, Van Hove LWA, et al. Spatial variability of the rotterdam urban heat island as influenced by urban land use. *J Geophys Res*. 2014;119(2):677-692. doi:10.1002/2012JD019399.

356. Zhou W, Huang G, Cadenasso ML. Does spatial configuration matter? Understanding the effects of land cover pattern on land surface temperature in urban landscapes. *Landsc Urban Plan*. 2011;102(1):54-63. doi:10.1016/j.landurbplan.2011.03.009.

357. Hwang RL, Lin CY, Huang KT. Spatial and temporal analysis of urban heat island and global warming on residential thermal comfort and cooling energy in Taiwan. *Energy Build*. 2017;152:804-812. doi:10.1016/j.enbuild.2016.11.016.

358. Wang C, Myint SW, Wang Z, Song J. Spatio-temporal modeling of the urban heat island in the Phoenix metropolitan area: Land use change implications. *Remote Sens*. 2016;8(3). doi:10.3390/rs8030185.

359. Li XX, Zhou Y, Asrar GR, Imhoff M, Li XX. The surface urban heat island response to urban expansion: A panel analysis for the conterminous United States. *Sci Total Environ*. 2017;605-606:426-435. doi:10.1016/j.scitotenv.2017.06.229.

360. Zhou W, Peng B, Shi J, et al. Estimating high resolution daily air temperature based on remote sensing products and climate reanalysis datasets over glacierized basins: A case study in the Langtang Valley, Nepal. *Remote Sens*. 2017;9(9). doi:10.3390/rs9090959.

361. Gasparrini A, Guo Y, Hashizume M, et al. Temporal variation in heat–mortality associations: A multicountry study. *Environ Health Perspect*. 2015;123(11):1200-1207. doi:10.1289/ehp.1409070.

362. Gasparrini A, B. A, S. K. The effect of high temperatures on cause-specific mortality in England and Wales. *Occup Environ Med*. 2012;69(1):56-61. http://oem.bmj.com/content/69/1/56.full.pdf%5Cnhttp://ovidsp.ovid.com/ovidweb.cgi?T=JS&PAGE=reference&D=emed10&NEWS=N&AN=2011705783.

363. Zhao Q, Zhang Y, Zhang W, et al. Ambient temperature and emergency department visits: Time-series analysis in 12 Chinese cities. *Env Pollut*. 2017;224:310-316. doi:10.1016/j.envpol.2017.02.010.

364. Yu, Weiwei K, Wang, et al. Daily average temperature and mortality among the elderly: a meta-analysis and systematic review of epidemiological evidence. *Int J Biometeorol*. 2012;56(4):569-581. doi:10.1007/s00484-011-0497-3.

365. Huang J, Wang J, Yu W. The lag effects and vulnerabilities of temperature effects on cardiovascular disease mortality in a subtropical climate zone in China. *Int J Environ Res Public Health*. 2014;11(4):3982-3994. doi:10.3390/ijerph110403982.

366. Goodman PG, Dockery DW, Clancy L. Cause-specific mortality and the extended effects of particulate pollution and temperature exposure. *Environ Health Perspect*. 2004;112(2):179-185. doi:10.1289/ehp.6451.

367. Huang W, Li J, Guo Q, Mansaray LR, Li X, Huang J. A satellite-derived climatological analysis of urban heat Island over Shanghai during 2000-2013. *Remote Sens*. 2017;9(7):1-27. doi:10.3390/rs9070641.

368. Li Y, Ma Z, Zheng C, Shang Y. Ambient temperature enhanced acute cardiovascular-respiratory mortality effects of PM2.5 in Beijing, China. *Int J Biometeorol*. 2015;59(12):1761-1770. doi:10.1007/s00484-015-0984-z.

369. Rocklöv J, Forsberg B, Ebi K, Bellander T. Susceptibility to mortality related to temperature and heat and cold wave duration in the population of Stockholm County, Sweden. *Glob Health Action*. 2014;7(1). doi:10.3402/gha.v7.22737.

370. Stocker, T.F., D. Qin, G.-K. Plattner, M. Tignor, S.K. Allen, J. Boschung, A. Nauels, Y. Xia VB and PMM (eds. . IPCC, 2013: Summary for Policymakers. Climate Change 2013: The Physical Science Basis. Contribution of Working Group I to the Fifth Assessment Report of the Intergovernmental Panel on Climate Change. In: Cambridge University Press, Cambridge, United Kingdom and New York, NY, USA; 2013. www.ipcc.ch/report/ar5/wg1/.

371. Stafoggia M, Forastiere F, Agostini D, et al. Factors affecting in-hospital heat-related mortality: a multi-city case-crossover analysis. *J Epidemiol Community Health*. 2008;62(3):209-215. doi:10.1136/jech.2007.060715.

372. Yang C, Lei B, Wang Y, Zhang S. Remote sensing of the spatial pattern of urban heat island effects and its influencing factors using TM data: a case study in core areas of Chongqing City. *Yingyong Jichu yu Gongcheng Kexue Xuebao/Journal Basic Sci Eng*. 2014;22(2):227-238. doi:10.3969/j.issn.1005-0930.2014.02.004.

373. Tang J, Di L, Xiao J, Lu D, Zhou Y. Impacts of land use and socioeconomic patterns on urban heat island. *Int J Remote Sens*. 2017;38(11):3445-3465. doi:10.1080/01431161.2017.1295485.

374. Lin RP, Qi XH, Ye SL. Spatial-Temporal characteristics of urban heat islands and driving mechanisms in a coastal Valley-Basin city: A case study of Fuzhou City. *Shengtai Xuebao/ Acta Ecol Sin*. 2017;37(1):294-304. doi:10.5846/stxb201607251516.

375. Ho HC, Knudby A, Sirovyak P, Xu Y, Hodul M, Henderson SB. Mapping maximum urban air temperature on hot summer days. *Remote Sens Environ*. 2014;154:38-45. doi:10.1016/j.rse.2014.08.012.

376. Hondula DM, Davis RE, Leisten MJ, Saha M V., Veazey LM, Wegner CR. Fine-scale spatial variability of heat-related mortality in Philadelphia County, USA, from 1983-2008: A case-series analysis. *Environ Heal A Glob Access Sci Source*. 2012;11(1):1-11. doi:10.1186/1476-069X-11-16.

377. Harlan SL, Brazel AJ, Prashad L, Stefanov WL, Larsen L. Neighborhood microclimates and vulnerability to heat stress. *Soc Sci Med*. 2006;63(11):2847-2863. doi:10.1016/j.socscimed.2006.07.030.

378. Dang TN, Seposo XT, Duc NH, et al. Characterizing the relationship between temperature and mortality in tropical and subtropical cities: a distributed lag non-linear model analysis in Hue, Viet Nam, 2009-2013. *Glob Heal Action*. 2016;9:28738. doi:10.3402/gha.v9.28738.

379. Chen D, Wang X, Thatcher M, et al. Urban vegetation for reducing heat related mortality [Trends of urban haze in Jiangsu Province China over the past 33 years] Developing resilient green roofs in a dry climate Challenges associated with projecting urbanization-induced heat-related mortalit. *Env Pollut*. 2014;192:275-284. doi:10.1007/s40471-014-0014-4 10.1016/j.envpol.2014.05.002 10.1016/j.scitotenv.2014.05.040 10.1016/j.scitotenv.2014.04.130.

380. Du H, Cai W, Xu Y, Wang Z, Wang Y, Cai Y. Quantifying the cool island effects of urban green spaces using remote sensing Data. *Urban For Urban Green*. 2017;27:24-31. doi:10.1016/j.ufug.2017.06.008.

381. Son J-YY, Lane KJ, Lee J-TT, Bell ML. Urban vegetation and heat-related mortality in Seoul, Korea. *Environ Res*. 2016;151:728-733. doi:10.1016/j.envres.2016.09.001.

382. Bradford-Hill A. The Enviroment and Disease: Association or Causation? *Proc R Soc Med*. 1965;58:295-300. doi:DOI: 10.1016/j.tourman.2009.12.005.

383. Rooney AA, Boyles AL, Wolfe MS, Bucher JR, Thayer KA. Systematic review and evidence integration for literature-based environmental health science assessments. *Environ Health Perspect*. 2014;122(7):711-718. doi:10.1289/ehp.1307972.

384. Fedak KM, Bernal A, Capshaw ZA, Gross S. Applying the Bradford Hill criteria in the 21st century: How data integration has changed causal inference in molecular epidemiology. *Emerg Themes Epidemiol*. 2015;12(1):1-9. doi:10.1186/s12982-015-0037-4.

385. Baccini M, Mattei A, Mealli F, Bertazzi PA, Carugno M. Assessing the short term impact of air pollution on mortality: A matching approach. *Environ Heal A Glob Access Sci Source*. 2017;16(1):1-12. doi:10.1186/s12940-017-0215-7.

386. Schwartz J, Bind MA, Koutrakis P. Estimating Causal Effects of Local Air Pollution on Daily Deaths: Effect of Low Levels. *Environ Health Perspect*. 2017;125(1):23-29. doi:10.1289/EHP232.

387. Bae S, Kim H-C, Ye B, Choi W-J, Hong Y-S, Ha M. Causal Inference in Environmental Epidemiology. *Envirionmental Heal Toxicol*. 2017;32:e2017015. doi:10.5620/eht.e2017015.

388. Bor J, Moscoe E, Mutevedzi P, Newell ML, Bärnighausen T. Regression discontinuity designs in epidemiology: Causal inference without randomized trials. *Epidemiology*. 2014. doi:10.1097/EDE.0000000000000138.

389. Benmarhnia T, Bailey Z, Kaiser D, Auger N, King N, Kaufman JS. A difference-in-differences approach to assess the effect of a heat action plan on heat-related mortality, and differences in effectiveness according to sex, age, and socioeconomic status (Montreal, Quebec). *Environ Health Perspect*. 2016;124(11):1694-1699. doi:10.1289/EHP203.

390. Chen H, Li Q, Kaufman JS, et al. Effect of air quality alerts on human health: a regression discontinuity analysis in Toronto, Canada. *Lancet Planet Heal*. 2018;2(1):e2-e3. doi:10.1016/S2542-5196(17)30185-7.

391. Neidell M. Air quality warnings and outdoor activities: Evidence from Southern California using a regression discontinuity design. *J Epidemiol Community Health*. 2010;64(10):921-926. doi:10.1136/jech.2008.081489.

392. Bakolis I, Kelly R, Fecht D, et al. Protective Effects of Smoke-free Legislation on Birth Outcomes in England: A Regression Discontinuity Design. *Epidemiology*. 2016;27(6):810-818. doi:10.1097/EDE.0000000000000534.

393. Armstrong BG. Effect of measurement error on epidemiological studies of environmental and occupational exposures. *Occup Environ Med*. 1998. doi:10.1136/oem.55.10.651.

394. Szpiro AA, Paciorek CJ, Sheppard L. Does more accurate exposure prediction necessarily improve health effect estimates? *Epidemiology*. 2011. doi:10.1097/EDE.0b013e3182254cc6.

395. Sheppard L, Burnett RT, Szpiro AA, et al. Confounding and exposure measurement error in air pollution epidemiology. *Air Qual Atmos Heal*. 2012. doi:10.1007/s11869-011-0140-9.

396. Armstrong B, Bell ML, Coelho MSZS, et al. Longer-term impact of high and low temperature on mortality: An international study to clarify length of mortality displacement. *Environ Health Perspect*. 2017;125(10). doi:10.1289/EHP1756.

397. Goggins WB, Yang C, Hokama T, Law LSK, Chan EYY. Using Annual Data to Estimate the Public Health Impact of Extreme Temperatures. *Am J Epidemiol*. 2015;182(1):80-87. doi:10.1093/aje/kwv013.

398. Kloog I, Coull B a, Zanobetti A, Koutrakis P, Schwartz JD. Acute and chronic effects of particles on hospital admissions in New-England. *PLoS One*. 2012;7(4):e34664. doi:10.1371/journal.pone.0034664.

399. Wu M, Li H, Huang W, et al. Generating daily high spatial land surface temperatures by combining ASTER and MODIS land surface temperature products for environmental process monitoring Exploring the Effects of Atmospheric Forcings on Evaporation: Experimental Integration of the Atmos. *Env Sci*

Process Impacts. 2015;17(8):1396-1404. doi:10.3390/s150717666 10.1039/c5em00254k.

APPENDIX

TABLE 1. LITERATURE REVIEW SEARCH

Search	Query
#1	Environmental Monitoring/methods* [mesh]
#2	LST [title/abstract]
#3	“Land surface temperature”
#4	“satellite data” [title/abstract] OR satellite sensors” [title/abstract] OR “satellite surface temperature”
#5	MODIS [title/abstract]
#6	“remote sensing”[title/abstract]
#7	Remote Sensing Technology [mesh]
#8	#1 or #2 or #3 or #4 or #5 or #6 or #7
#9	"air temperature" [title/abstract]
#10	#8 AND #9 Limit "2013/01/01"[PDat] : "2018/01/04"[PDat]
#11	“urban heat island” [title/abstract]
#12	UHI [title/abstract]
#13	#2 OR satellite[title/abstract]
#14	#12 OR #13 OR #9
#15	#13 AND #14 Limit "2013/01/01"[PDat] : "2018/01/04"[PDat]
#16	“heat stress” [title/abstract]
#17	Heat stress disorders [mesh]
#18	"Hot Temperature/adverse effects"[Mesh]
#19	Hospitalization[MESH]
#21	Mortality[title/abstract]
#22	Death*[title/abstract]
#23	#16 OR #17 OR #18 OR #19 OR #20 OR #21 OR #22 Limit "2013/01/01"[PDat] : "2017/12/31"[PDat]
#24	#23 AND #14
#25	#23 AND #9

Table 2. Summary of studies included in the literature review on methods to derive air temperature from LST.

Authors	Title	Year	Study area	Satellite\sensor	Description\method	Results\notes
Benali et al.	Estimating air surface temperature in Portugal using MODIS LST data	2012	Portugal	TERRA\MODIS	Estimate T max, T min and T avg for a 10 year period based on LST and auxiliary data using a statistical approach. An optimization procedure with a mixed bootstrap and jackknife resampling was employed.	MEF (Model Efficiency Index) >0.90 and RMSE <2°C.
Benmecheta et al.	A Comparative Study of Land Surface Temperature Retrieval Methods From Remote Sensing Data	2013	overview different algorithms	overview different algorithms	Overview of the different algorithms used for the estimation of land surface temperature as well as a comparative list of methods . Mostly single split window tecniques.	Compare, and analyze the various extraction methods for LST in terms of their computational algorithms, their different input parameters, and their relative accuracy to make them more readily usable by a broader cross-section of nontechnical practitioners
Cai et al.	Estimation of Daily Average Temperature Using Multisource Spatial Data in Data Sparse Regions of Central Asia	2013	Ili river basin, central Asia	MODIS	TVX Klemen method.	Correlation coefficient varies from 0.90 to 0.94 and the RMSE is 3°C
Cresswell	Estimating Surface Air Temperatures, From Meteosat Land Surface Temperatures, Using an Empirical Solar Zenith Angle Model	1999	Africa	METEOSAT	Empirical hour-specificmodels to estimate the air temperature fromthe Land Surface Temperature and the sun zenith angle.	The algorithms achieve an accuracy of within 3 degrees C for over 70% of the Meteosat temperatures processed.
Cristobal et al.	Modeling Air Temperature Through a Combination of Remote Sensing and Gis Data	2008	Spain	LANDSAT, MODIS AND AVHRR	Multiple regression analysis combining geographical variables (altitude, latitude, continentality and solar radiation) with LST, NDVI and albedo	best models are obtained when remote sensing variables are combined with geographical variables (R2=0.6; RMSE=1.76°C for daily temp). LST and NDVI are the most powerful predictors.

Authors	Title	Year	Study area	Satellite\sensor	Description\method	Results\notes
Czajkowski et al.	Thermal Remote Sensing of Near Surface Environmental Variables: Application Over the Oklahoma Mesonet	2000	Oklahoma, USA	AVHRR	Surface tempertaure, air tempertaure and humidity were derived from TIR AVHRR data and NDV using TVX method. estimates were validated using Mesonet weather forecasts.	Good performance, but also highlighted differences at the state level and by variable in study.
Fu et al.	Estimating air temperature of an alpine meadow on the Northern Tibetan Plateau using MODIS land surface temperature	2011	Tibettan plateau	TERRA AQUA\MODIS	A linear estimation of air temperature of an alpine meadow on Northern Tibetan Plateau at heights of 1.5m–2.1m by using MODIS land surface temperature (LST) data was conducted	MODIS LST data were accurate enough to linearly estimate daily minimum and nighttime mean air temperatures, but not for daytime maximum tempertuares.
Hou et al.	Near-Surface Air Temperature Retrieval From Satellite Images and Influence by Wetlands in Urban Region	2013	Beijing , China	LANDSAT TM	Near-surface air temperature (NSAT) retreival method that employs Landsat Thematic Mapper images using an Energy Balance Bowen Ratio model is developed. This model is established based on the energy balance over land and the Bowen ratio	Meanprediction error 2.2°C. proximity ot wetlands influences temperature .
Kilibarda et al.	Spatio-temporal interpolation of daily temperatures for global land areas at 1 km resolution	2014	Globally resolution 1x1km, for 2011	MODIS	Predictions in space and time were made for the mean, maximum and minimum temperature using spatio-temporal regression-kriging with a time series of MODIS 8 day images, topographic layers (DEM and TWI) and a geometric temperature trend as covariates.	shows use of MODIS data : creates 1km global daily temperatures using interpolation (krigging) of MODIS data.
Kim et al.	Evaluation and Sensitivity Testing of a Coupled Landsat-Modis Downscaling Method for Land Surface Temperature and Vegetation Indices in Semi-Arid Regions	2012	Korea	MODIS and LANDSAT , LST AND NDVI	Estimating T-a near the land surface based on moisture conditions of the atmosphere and surface using multiple regression algorithms.	The fused Landsat + MODIS NDVI product also shows good correlation to ground-based data and is relatively consistent except during the acute (monsoon) growing season. downscaling over arid areas landsat modis
Kloog et al.	Temporal and spatial assessments of minimum air temperature using satellite surface temperature measurements in Massachusetts, USA.	2012	Massachussettes USA	MODIS	Land use regression, meteorological variables and spatial smoothing to calibrate between Ts and Ta on a daily basis and then predict Ta for days when satellite Ts data were not available. Mixed regression models with daily random slopes to calibrate MODIS Ts data with monitored Ta measurements. GAMS with spatial smoothing to estimate Ta in days with missing Ts.	The spatial patterns of Ta within the study domain identified distinguishing between urban and rurral settings. Good performance of model also when Ta and LST missing.

Authors	Title	Year	Study area	Satellite\sensor	Description\method	Results\notes
Kloog et al.	Predicting spatiotemporal mean air temperature using MODIS satellite surface temperature measurements across the Northeastern USA	2014	NE USA	MODIS	mixed model regressions to calibrate Ts and Ta measurements, regressing Ta measurements against day-specific random intercepts, and fixed and random Ts slopes. Then fill in the cells with missing Ts values,regress the Ta predicted from the first mixed effects model against the mean of the Ta measurements on that day, separately for each grid cell.	mean out-of-sample R2=0.95. Method shows that Ts can be used t estimate Ta.
Lai et al.	Comparison of Modis Land Surface Temperature and Ground-Based Observed Air Temperature in Complex Topography	2012	Taiwan	TERAA AQUA\MODIS	Regression analysis to define monthyl mean Ta using LST and observed Ta.	Correlation coef >0.90, STDEV<2. Possible sources of bias between T-s and T-a: (1) the significant influences caused by soil moisture between wet and dry seasons; (2) the difference between ground-based weather station elevation and 1 km grid-averaged elevation; and (3) interaction among the satellite view, solar zenith angle and terrain gradient
Mao et al.	Near-Surface Air Temperature Estimation From Aster Data Based on Neural Network Algorithm	2008		ASTER	MODTRAN4 is used to simulate radiance transfer from the ground with different combinations of land surface temperature, near surface air temperature, emissivity and water vapour content. The dynamic learning neural network is used to estimate near surface air temperature	The mean and the standard deviation of estimation error are about 2.0K and 2.3K
Nichol et al.	Spatial Variability of Air Temperature and Appropriate Resolution for Satellite-Derived Air Temperature Estimation	2008	Hong Kong	ASTER	The spatially variable relationship between air and surface temperature was evaluated using spatial resampling and buffering around air temperature points	Differences in the spatial scales of air temperature in these regions are attributed mainly to structural factors of land cover such as city block size, building density and % green areas, and secondarily to the climatic conditions.
Nieto et al	Air temperature estimation with MSG-SEVIRI data: Calibration and validation of the TVX algorithm for the Iberian Peninsula	2011	Iberian peninsula	SEVERI LST and NDVI	Estimate NDVImax using observed air temperature to calibrate the NDVImax for each vegetation type.A spatio-temporal assessment of residuals has been performed to evaluate the accuracy of retrievals in terms of daily and seasonal variation, land cover, landscape heterogeneity and topography	The effect of vegetation types and climates and the potential variation in NDVI of the effective full cover has not been subject for investigation.

Authors	Title	Year	Study area	Satellite\sensor	Description\method	Results\notes
Pelta et al.	Spatiotemporal estimation of air temperature patterns at the street level using high resolution satellite imagery	2016	Tel Aviv	LANDSAT BT	Mixed regression models with daily random slopes to calibrate Landsat BT dat awith mon itored Air tempertaure measurements	Good model performance, authors assess temporal changes in spatial distribution of temperature derived from TM and compare to modis data
Prihodko	Estimation of air temperature from remotely sensed surface observations	1997	Kansas	NOAA\AVHRR	Ta estimated directly from remotely sensed observations using the (observed) correlation between a spectral vegetation index and surface temperature (temperature-vegetation index).	A strong correlation (r=0.93) was found between the satellite estimates and measured air temperatures with a mean error of 2.92°c. Positive bias satellite estimates.
Recondo et al	Empirical Models for Estimating Daily Surface Water Vapour Pressure, Air Temperature, and Humidity Using Modis and Spatiotemporal Variables	2013	Spain	TERRA MODIS	Regression models to estimate daily surface water vapour pressure, air temperature and relative humidity over cloud-free land areas of Spain using MODIS and spatiotemporal variables	Model results compared with previous algorithms developed in the same area and MODIS standard products.
Resenfeld et al.	Estimating daily minimum, maximum, and mean near surface air temperature using hybrid satellite models across Israel	2017	Israel	TERRA AQUA MODIS LST	Regression models and IPW to estimate min, max and mean Ta from LST, meteorology and land use data	Model performance was excellent for both days with and without available Ts observations for both Aqua and Terra. Using both AQUA and TERRA rpovides more Ta parameters to use in epi studies.
Sahin et al.	Modelling of air temperature using remote sensing and artificial neural network in Turkey	2012	Turkey	NOAA-AVHRR	Estimate mean monthly temperatures using RS and artifical neural networks (ANN)	Correlation coefficient (R), and root mean squared error (RMSE) were 0.991-1.254 K respectively.
Shi et al.	Estimating daily air temperature across the Southeastern United States using high-resolution satellite data: A statistical modeling study	2016	South eastern USA	MODIS TERRA	Mixed regression models to derive Ta from LST, land use and meteorology.	Model performance was very good also in a humid climate and complex terrin and LU like SE USA. Model was validated with re-forecast model temperatures and had good performance.
Singh et al.	A New Method to Determine Near Surface Air Temperature From Satellite Observations	2006	global scale all sea surfaces	AVHRR and SSM/I	Satellite observed parameters of total precipitable water (W), atmospheric boundary layer (similar to 500 m) water vapour (Wb), and sea surface temperature (SST) are used to derive Ta	Global mean root mean square (rms) error for instantaneous Ta estimates is 1.4 degrees C

Authors	Title	Year	Study area	Satellite\sensor	Description\method	Results\notes
Stisen et al.	Estimation of Diurnal Air Temperature Using Msg Seviri Data in West Africa	2007	West Africa	geostationary MSG SEVIRI	multiple daily air temperature estimates can be achieved using the contextual temperature-vegetation index method using thermal split window channels in combination with the red NIR channels.	the model gave good results and maps of air temperature with 15 min intervals and 3 km spatial resolution for application in a distributed hydrological model were developed.
Sun et al.	Air Temperature Retrieval From Remote Sensing Data Based on Thermodynamics.	2005	North China plain	MODIS	Crop water stress index and aerodynamic resistance, were used to build a quantitative relationship between the land surface temperature and the ambient air temperature	Derived values have an accuracy of 3°C for more than 80% of data processed compared to in situ data.
Vancutsem et al.	Evaluation of MODIS land surface temperature data to estimate air temperature in different ecosystems over Africa	2010	Africa	MODIS	The main objective of this study was to explore the possibility of retrieving high-resolution Ta data from the Moderate Resolution Imaging Spectroradiometer (MODIS) Ts products over different ecosystems in Africa.	Two factors to retrieve maximum Ta from Ts, (NDVI) (SZA), were analyzed. MODIS nighttime products provide a good estimation of minimum Ta over different ecosystem. Maximum Ta varies according to the seasonality, the ecosystems, the solar radiation, and cloud-
Vogt	Mapping regional air temperature fields using satellite-derived surface skin temperatures	1997	Andalusia, Spain	NOAA\AVHRR	Mapping and monitoring the spatial distribution of daily maximum air temperatures with NOAA-AVHRR images. Regression analysis between the daily maximum air temperature (T-max) and the mean surface skin temperature (T-s) retrieved for 11 km(2) image windows centred over each station,	T-max is strongly linked to LST in the given environment (mean R-2 = 0.823) , mean error of about 2 to 2.5 K.
White-Newsome et al.	Validating satellite-derived land surface temperature with in situ measurements: a public health perspective	2013	Detriot	LANDSAT TM	Compare LST and SI to air temperature measurements	Report high correlation between satellite and air tempertaures but do not use one to define the other
Wloczyk et al.	Estimation of Instantaneous Air Temperature Above Vegetation and Soil Surfaces From Landsat 7 Etm+ Data in Northern Germany	2011	Germany	LANDSAT ETM+	The temperature-vegetation index method using multispectral band data was used to retrieve Ta	The satellite-derived air temperatures (60 m spatial resolution) are compared with in situ measurements, showing an average error of about 3 K(RMS). Results are good for all seasons.

Authors	Title	Year	Study area	Satellite\sensor	Description\method	Results\notes
Xu et al.	Study on the Estimation of Near-Surface Air Temperature From Modis Data by Statistical Methods	2012	Yangtze River Delta	AQUA MODIS	regression models to estimate air temperature from satellite-derived land surface temperature and other environmental parameters over 4 land surface types.	The estimation error of air temperature tends to be lower as spatial window size increases, suggesting that the model performances are improved by spatially averaging land surface characteristics.
Yao et al.	Modis-Based Air Temperature Estimation in the Southeastern Tibetan Plateau and Neighboring Areas.	2012	Tibet	MODIS	Regression model to estimate monthly mean air temperatures in the southeastern Tibetan Plateau and its neighboring areas. Spatio-temporal analysis of monthly mean Ts vs. monthly mean Ta are carried out.	MODIS Ts data combining with observed data could be used to rather accurately estimate air temperature in mountain regions.
Zaksek et al.	Parameterization of Air Temperature in High Temporal and Spatial Resolution From a Combination of the Seviri and Modis Instruments	2009	Europe	MSG, SEVERI and MODIS NDVI and LST	Downsacaling of SEVERI data using LSt and NDVi MODIS. Thenempirical parameterization that requires albedo, down-welling surface short-wave flux, relief characteristics and NDVI data	Daytime RMSD = 2.0 K with a bias of -0.01 K and a correlation coefficient of 0.95. very promising, considering the high temporal (30 min) and spatial resolution (1000 m) of the results.
Zhang et al.	Empirical Models for Estimating Daily Maximum, Minimum and Mean Air Temperatures With Modis Land Surface Temperatures	2011	China	TERRA AQUA MODIS\LST	Regression models between day and night LST and Ta minimum and maximium from observed Meteo data in China. Coupled LST measurement models were also developed.	Night-time LST was best predictor for estimating daily T-min, T-mean and even T-max when considering both the performance of the models and the availability of the LST data. No significant difference between LSTs of TERRA and AQUA for estimating daily air temperatures.
Zheng et al.	Monthly Air Temperatures Over Northern China Estimated by Integrating Modis Data With Gis Techniques	2013	N. China	MODIS LST and NDVI	A hybrid method combining stepwise regression modeling and spatial interpolation techniques. Stepwise regression modeling was applied to construct the relationship between air temperatures (T-mean, T-min, and T-max-the dependent variables) , geographical, (MODIS). Spatial interpolation used to correct the residual values	average RMSE values at 0.86 degrees, 1.10 degrees, and 1.13 degrees C for T-mean, T-min, and T-max.
Zhu et al.	Estimation of daily maximum and minimum air temperature products temperature using MODIS land surface	2013	Xiangride River basin in the north Tibetan Plateau	MODIS (from both TERRA and AQUA) , LANDSAT	temperature-vegetation index (TVX) method to estimate air temperature. Subtraction method that merges the spatial detail of higher-resolution imagery (Landsat) with the temporal change observed in coarser or moderate-resolution imagery (MODIS).	Applying the temporal difference between MODIS images observed at two different dates to a higher-resolution Landsat image allows prediction of a combined or fused image (Landsat + MODIS) at a future date.

Table 3 Summary of studies included in the literature review on urban heat islands defined using satellite data.

Authors	Title	Year	area study	satellite\sensor\other data	Aim	METHOD description	Results\intensity UHI
Aniello et al.	Mapping Micro-Urban Heat Islands Using Landsat Tm and a Gis	1996	Dallas, Texas	LANDSAT	use satellite data to identify micro UHI and woodland areas in Texas	tree cover was merged with thermal data from LANDSAT images.	micro-urban heat islands are resulting from the lack of tree cover related to newly developed residential neighborhoods, parking lots, business districts, apartment complexes, and shopping centers
Anminipouri et al.	Spatio-temporal analysis of surface urban heat island (SUHI) using MODIS land surface temperature (LST) for summer 2003-2012, A case study of the Netherlands	2014	Netherlands	MODIS LST, NDVI	define UHI in cities the netherlands	mapping UHI and considering role of green space and land cover to mitigate UHI	NDVI reduces surface temperature
Aslan et al	Analysis of relationship between urban heat island effect and Land use/cover type using Landsat 7 ETM+ and Landsat 8 OLI images	2016	Antalya	LANDSAT MODIS NDVI	Assess factors influencing UHI, temporal changes	regression analysis to evaluate which factors correlated to LST and influence UHI	Maximum LST values were detected for dry agriculture, urban, and bareland classes, while minimum LST values were detected for vegetation and irrigated agriculture classes. Uhi increased from 5.6 °C to 6.8°C.
Bektas Balcik	Determining the impact of urban components on land surface temperature of Istanbul by using remote sensing indices	2014	Istanbul	LANDSAT TM 5	Identify factor influencing the UHI in terms of Land cover, land use indicies.	An Index Based Built-up Index (IBI) Soil-Adjusted Vegetation Index, Normalized Difference Built-up Index, and Modified Normalized Difference Water Index) was used to derive artificial surfaces in the study area. An ecological evaluation index of the region was calculated to explore the impact of both the vegetated land and the artificial surfaces on the UHI.	the quantitative relationship of urban components (artificial surfaces, vegetation, and water) and LST was examined using multivariate statistical analysis, and the correlation coefficient was 0.829. Areas with a high rate of urbanization will accelerate the rise of LST and UHI in Istanbul.
Bokaie et al.	Assessment of Urban Heat Island based on the relationship between land surface temperature and Land Use/ Land Cover in Tehran	2016	Tehran	LANDSAT - LU/LC, NDVI	mapping of UHI and defining factors which modify LST in urban area.	Definition of LST from LANDSAT, correlation between LST and LU/LC	NDVI, water features negative correlation with LST
Chen et al.	Remote Sensing Image-Based Analysis of the Relationship Between Urban Heat Island and Land Use/Cover Changes	2006	Pearl river delta, China	LANDSAT TM+, NDVI	Identify land use factors influencing UHI using satellite data and vegetation indexes	o retrieve the brightness temperatures from LANDSAT and compare to land use/cover types	correlations between NDVI, NDWI, NDBaI and temperature are negative when NDVI is limited in range, but positive correlation is shown between NDBI and temperature
Chen et al.	The Influence of Socioeconomic and Topographic Factors on Nocturnal Urban Heat Islands: a Case Study in Shenzhen, China,	2012	Shezen , china	ASTER, elevation, SES	factors affeting UHI	relationships between nocturnal UHIs and socioeconomic or topographic factors were analysed using traditional regression analysis	+5K night. elevation and land use pop density influence UHI
Cheval et al.	The July Urban Heat Island of Bucharest as Derived From Modis Images	2009	Bucarest, Romania	MODIS	Define the extension, geometry, and magnitude of UHI using the surface thermal data.	The magnitude of the heat island was calculated by comparing the average temperature inside its limits and the average temperature of the 5 km (a) and of the 10 km (b) buffers around it	UHI and the surrounding area of Bucharest is higher and more variable during the daytime, and is noticeably related to the land cover

Authors	Title	Year	area study	satellite\sensor\other data	Aim	METHOD description	Results\intensity UHI
Cheval et al.	The summer surface urban heat island of Bucharest (Romania) retrieved from MODIS images	2015	Bucarest, Romania	MODIS LST	the study proposes a methodology to delimit and quantify the average SUHI based on the statistical significance of the shift between the urban area and its surroundings	The thermal difference between the SUHI and several surrounding buffers defines the SUHI's intensity	land cover exerts a strong influence on Bucharest's LST
Connors et al	Landscape Configuration and Urban Heat Island Effects: Assessing the Relationship Between Landscape Characteristics and Land Surface Temperature in Phoenix, Arizona	2013	Pheonix	ASTER LSt and land cover data	explore the relationship between land surface temperature and spatial pattern for three different land uses: mesic residential, xeric residential, and industrial/commercial.	measure correlation between LSt and land covers, ANOVA on land cover types and regression model between LST and and cover types.	
Da Costa et al.	Identification of Urban Heat Islands in Ilha Solteira-Sp Municipality Using Geotecnologies	2010	Ilha Solteira-SP, Brazil	LANDSAT TM	aimed to identify the main thermal variations in the urban area	transformation of Landsat TM data into values of surface temperature and their comparison to distinct urban land use	land cover surfaces classified as guilding and paved buildings had highe LST
Deng et al.	Estimating Very High Resolution Urban Surface Temperature Using a Spectral Unmixing and Thermal Mixing Approach	2013		LANDSAT	physically based method, (VHR spectral unmixing and thermal mixing (VHR-SUTM) approach) wa used to estimate LST	considering both spectral and thermal properties, spectral unmixing was used to estimate fractional urban compositions for a comprehensive representation of heterogeneous urban surfaces. Further, VHR LST was modeled as a summation of the thermal	high estimation accuracy (RMSE of 2.02 K and MAE of 1.51 K)
Deng et al.	Examining the Impacts of Urban Biophysical Compositions on Surface Urban Heat Island: a Spectral Unmixing and Thermal Mixing Approach	2013	USA	LANDSAT LST NDVI	Study the thermal proprties of Land cover to determine how they influence urban thermal pattern	A two-step physically based method, the spectral unmixing and thermal mixing (SUTM) model, to examine the impacts of typical land cover compositions on urban thermal pattern. Compare SUTM model with NDVI, %ISA and %GV.	SUTM outperforms all regression models both rural and urban contexts. NDVI and %GV have poor performance in urban areas. Soil influenced modeling performance
Duan et al.	Spatiotemporal variation of urban heat island in Zhengzhou City based on RS	2011	Zhengzhou City	LANDSAT	Analyse the causes of Uhi in Zhengzhou over time.	brightness temperature and meteorological data were considerd to estimate UHI	UHI of Zhengzhou has increased especially in NE and SW of the city probably as a result of reduction of vegetation cover.
Effat et al	Change detection of urban heat islands and some related parameters using multi-temporal Landsat images; a case study for Cairo city, Egypt	2014	Cairo	LANDSAT LST , NDVI	map and detect changes in land-cover and heat islands over Cairo through three decades using multi-temporal Landsat TM satellite data	comparison of images	growth in urban area, NDVI seasonal fluctuations
Fabrizi et al.	Satellite and Ground-Based Sensors for the Urban Heat Island Analysis in the City of Rome	2010	Rome	ENVISAT - AATSR	Define the Uhi of Rome through LST and Ta data	algorithm employing satellite brightness temperatures for the estimation of the air temperature belonging to the layer of air closest to the surface	3-4K
Feizizadeh et al.	Examining Urban Heat Island Relations to Land Use and Air Pollution: Multiple Endmember Spectral Mixture Analysis for Thermal Remote Sensing	2013	Tabriz, Irad	ASTER + land use/land cover (LULC),	to identify UHI and to investigate their relationship to land use/land cover (LULC) and air pollution	integration of Spectral Mixture Analysis and Endmember Remote Sensing Indices to derive LST, to identify UHI and to investigate their relationships to land use/land cover (LULC) and air pollution	that LST is highly influenced by LULC and that UHIs are closely linked to LST and LULC. As expected, LST is sensitive to vegetation and moisture and low temperatures are found in water bodies and vegetated areas. High temperatures are related to construction zones and industrial sites which are not necessarily located in the city centre

Authors	Title	Year	area study	satellite\sensor\other data	Aim	METHOD description	Results\intensity UHI
Fung et al.	Derivation of Nighttime Urban Air Temperatures Using a Satellite Thermal Image	2009	Hong Kong	ASTER	idenitfy UHI in Hong Kong on winter nights using satellite derived surface temperature and in situ measurements. Derive Ta from LST and mobile transverse techniques.	Regression analysis was used to derive Ta from LST.	2-3.5 °C ntensity of UHI, maximum 12°C. Good correlation between the in situ surface and air temperature pair of readings. LST compared with in situ sruface measurements, bias 1.1°C.
Giannaros et al.	Numerical Study of the Urban Heat Island Over Athens (Greece) With the WRF Model	2013	Athens	AVHRR	Evaluate UHI using WRF model and satellite data.	WRF model coupled with NOAA satellite data was tested against observations to study the UHI in Athens.	UHI >4°c at night. The diurnal cycle Canopy-UHI, with high nighttime values, decrease following sunrise, and an increase after sunset. Inclusion of the LST data into WRF model resulted in a small reduction in the temperature bias.
Hamadi et al.	Estimating Urban Heat Island Effects on the Temperature Series of Uccle (Brussels, Belgium) Using Remote Sensing Data and a Land Surface Scheme	2010	Bruxelles, Belgium		estimate the UHI using different sources of data, validate finidings of satellite data.	estimate the UHI using ground monitors, satellite data and land use chnarcteristics includedin Town energy balance scheme.	UHI rising at a rate +2.5 C per decade for minimum temperature
Ho et al.	A comparison of urban heat islands mapped using skin temperature, air temperature, and apparent temperature (Humidex), for the greater Vancouver area	2016	Vancouver	Ta, AppT, LST	Map UHI in vancouver using LST data, apaprent tmepertuare and air temperature form monitors	Forest regression model	skin temperature was poorly correlated with both air temperature (R2=0.38) and apparent temperature (R2=0.39).
Hung et al.	Assessment with satellite data of the urban heat island effect in Asian mega cities.	2006	Asian cities	MODIS TERRA AND AQUA	UH1 patterns were analyzed in association with urban vegetation covers and surface energy fluxes derived from high-resolution Landsat ETM+ data	A Gaussian approximation was applied in order to quantify spatial extents and magnitude of individual UHIs for inter-city comparison	land-surface temperature (LST) and land use maps produced to describe UHI in Mega Asian cities
Imhoff et al.	Remote Sensing of the Urban Heat Island Effect Across Biomes in the Continental Usa	2010	USA	LANDSAT-ISA and MODIS - impervious srface	Use LST MODIS and ISA Landsat data to analyse the UHI and its relationship with size, intensity and ecological settings in 38 cities.	Development intensity zones based on %ISA are defined for each urban area emanating outward from the urban core to the non-urban rural areas nearby and used to stratify sampling for land surface temperatures and NDVI.	ecological context significantly influences the amplitude of summer daytime UHI (urban-rural temperature difference) the largest (8 degrees C average) observed for cities built in biomes dominated by temperate broadleaf and mixed forest. ISA is the primary driver for increase in temperature explaining 70% of the total variance in LST
Jalan et al	Spatio-temporal assessment of land use/ land cover dynamics and urban heat island of Jaipur city using satellite data	2014	Jaipur, India	LANDSAT - LULC	Spatio-temporal changes in UHI can be quantified through Land Surface Temperature (LST) derived from satellite imageries.	analyzes the spatial distribution and temporal variation of LST in context of changes in LULC	The study concludes that UHI of Jaipur city has intensified and extended over new areas.
Jin et al.	Developing an Index to Measure Urban Heat Island Effect Using Satellite Land Skin Temperature and Land Cover Observations	2012	Pheonix	MODIS	estimate UHI using skin LSt and observed Ta		This new index has advantages of high spatial resolution and aerial coverage to better record UHI intensity than T-2m
Jusuf et al.	The Influence of Land Use on the Urban Heat Island in Singapore	2007	Singapore	LANDSAT	identify land use types which have the most influence to the increase of ambient temperature in Singapore	remote sensing data and geographical information system (GIS) to obtain a macro view of Singapore	land usage will influence urban temperature

Authors	Title	Year	area study	satellite\sensor\other data	Aim	METHOD description	Results\intensity UHI
Klok et al.	The Surface Heat Island of Rotterdam and Its Relationship With Urban Surface Characteristics	2012	Rotterdam, the Netherlands	LANDSAT, NOAA-AVHHR	Define surface HI in Rotterdam using LST.	Compare urban and rural LST, explain differences by land surface characteristics	12°C during the day, 9°C during the night. the SHI is largest in areas with scarce vegetation, high fraction of impervious surface, low albedo
Kourtidis et al	A study of the hourly variability of the urban heat island effect in the Greater Athens Area during summer	2015	Athens Greece	AATSR, ASTER, AVHRR and MODIS observed data	mapping of the hourly spatiotemporal evolution of the urban heat island (UHI) effect	Comparison between observed station data, modelled data ClimUrb and LST for different satellites	LST can be up to 5K lower than the respective Tair during nighttime, while it can be up to 15K higher during the rest of the day.
Li et al.	Monitoring Patterns of Urban Heat Islands of the Fast-Growing Shanghai Metropolis, China: Using Time-Series of Landsat Tm/Etm+ Data	2012	Shanghai	LANDSAT TM/ETM+, LULC	quantifying the impact of land-use/land cover (LULC) change on patterns of surface urban heat island	Estimate the relationships between surface UHI pattern and pixel-based biophysical features, population density, road density.	Change in LULC , reduction vegetation cover for more urban cover types, influence spatiotemporal pattern UHI
Li et al.	Remote sensing of the surface urban heat island and land architecture in Phoenix, Arizona: Combined effects of land composition and configuration and cadastral-demographic-economic	2016	Phoenix arizona	LANDSAT , LU, census data, NDVI	Define factors that influence UHI	Multiple ordinary least squares regressions (OLS) were used to determine the effects of land architecture and demographic-economic variables (independent variables) on the LST (dependent variable)	land configuration has a stronger influence on LST than land compositio
Liu et al	Urban Surface Heat Fluxes Infrared Remote Sensing Inversion and Their Relationship With Land Use Types	2012	Kumagaya, Japan	ASTER	Analyze the influence of different land use types on the surface heat fluxes and energy balance	PCACA model and theoretical position algorithm	Increase of urban impervious surfaces area can increase sensible heat flux and the Bowen ratio, increasing of urban Ts and Ta
Liu et al	Quantifying spatial-temporal pattern of urban heat Island in Beijing: An improved assessment using land surface temperture time series observations from landsat, modis and Chinese new satellite	2015	Beijung	LANDSAT MODIS	quantify the spatial-temporal patterns of surface urban heat island (SUHI) by investigating the relationship between Land surface temperature (LST) and the land-cover types	Spatial and Temporal Adaptive Fusion Model (STARFM) developed by Gao et al. was employed to create the high spatial resolution LST time series	No obvious linear relationships were observed between mean subplot LST and impervious surfaces LSMs. Green space reduced UHI
Lo and Quattrocchi	Land-Use and Land-Cover Change, Urban Heat Island Phenomenon, and Health Implications: a Remote Sensing Approach	2006	Atlanta	LANDSAT, MSS and TM images	Describe change in land cover and UHI Atlanta between 1973-97	Compare LANDSAT images LST and NDVI	Land surface change(loss forested land) has increased in surface temperature and a decline in NDVI .
Lo et al.	Application of High-Resolution Thermal Infrared Remote Sensing and Gis to Assess the Urban Heat Island Effect	1997	Atlanta	NDVI+ atlas data	study changes in the thermal signatures of urban land cover types between day and night	A spatial model of warming and cooling characteristics of commercial, residential, agricultural, vegetation, and water features was developed using a GIS approach	There is a strong negative correlation between NDVI and irradiance of residential, agricultural and vacant/transitional land cover types, indicating that the irradiance of a land cover type is greatly influenced by the amount of vegetation present
Mallick et al.	Land Surface Emissivity Retrieval Based on Moisture Index From Landsat Tm Satellite Data Over Heterogeneous Surfaces of Delhi City,	2012	Delhi, India	LANDSAT7, emissivity, LULC	derive emissivity using ND mositure index in urban areas,	estimated emissivity values over few land use/land cover (LULC) classes of LANDSAT TM have been compared with the literature values and field measurement emissivity data using infrared thermometer	strong correlation is observed between surface temperatures with NDMI over different LULC classes. Regression model results show that surface temperatures can be predicted if NDMI values are known

Authors	Title	Year	area study	satellite\sensor\other data	Aim	METHOD description	Results\intensity UHI
Mallick et al.	Modeling Urban Heat Islands in Heterogeneous Land Surface and Its Correlation With Impervious Surface Area by Using Night-Time Aster Satellite Data in Highly Urbanizing City, Delhi-India,	2013	Delhi, India	LANDSAT + ASTER, LULC, ISA	Identification and assessment of UHI in Delhi	methodology takes into account spatially-relative surface temperatures and impervious surface fraction (ISA) value to measure surface UHI intensity between the urban land cover and rural surroundings, validation through ground measurements	CBD and industrial areas +4°C, chnages in surface temperature are due to human activity, cange LULC pattern and vegetation density
Mathew et l.	Spatial and temporal variations of urban heat island effect and the	2016	Chandigarh city,India	MODIS , LULC	compare UHI variation conisdering imeprvious surfaces, elevation	Correlation , linear regression	Positive relationship has been found between LST and %ISA with a consistent rising trend. Negative
Meng et al	Remote-Sensing Image-Based Analysis of the Patterns of Urban Heat Islands in Rapidly Urbanizing Jinan, China	2013	Jinan china	LANDSAT, LST LULC	The results show that significant changes in land use and land cover occurred over the study period	geographical information system (GIS) and remote sensing (RS) approach, the changes in this urban area's LULC were explored, see how influence UHI	Spatially, there were significant LST gradients from the city centre to surrounding rural areas
Meng et al	Remote-Sensing Evaluation of the Relationship Between Urban Heat Islands and Urban Biophysical Descriptors in Jinan, China,	2014	Jinan china	LANDSAT	evaluate correlaton between LST and impervious surface, water, and vegetation to see how the influence UHI	impervious surfaces have a positive exponential relationship with LST, while the water and vegetation are both negatively correlated with temperature	increased from 0.42 in 1992 to o.55 in 2011
Mohan et al.	Assessment of Urban Heat Island Effect for Different Land Use-Land Cover From Micrometeorological Measurements and Remote Sensing Data for Megacity Delhi	2013	Delhi, India	MODIS	definition of UHI using satellite data and LULC	compare skin observed data to LST satellite data	Dense urban areas and highly commercial areas were observed to have highest UHI with maximum hourly magnitude peaking up to 10.7 A degrees C and average daily maximum UHI reaching 8.3 A degrees C. modis overestimated compared to in situ skin measurements
Morabito et al.	The impact of built-up surfaces on land surface temperatures in Italian urban areas	2016	Italy	MODIS	map heat vulnerability using LSt and urban density (built up environment)	Linear regression analysis	Statistically significant linear relationships (p b 0.001) between built-up surfaces and spatial LST variations
Ngie et al.	Assessment of urban heat island using satellite remotely sensed imagery: A review	2014	Review		review of studies use LST to derive UHI	overview of the UHI background concepts and provides details of satellite remote sensing data and processing techniques to retrieve LST	LSt mostly valid in large urbna reas
Nichol et al.	Remote Sensing of Urban Heat Islands by Day and Night	2005	Hong Kong	LANDSAT TM+, ASTER	Identify UHI daily and nighttime pattern	Compare night-time ASTER image, with daytime LANDSAT image	Lower temperature gradients between different LC types at night time (dominant meso-scale climatic patterns), suggestive of processes operating in the Urban Boundary Layer (UBL), as opposed to the Urban Canopy Layer (UCL) which is dominant in the daytime
Nichol et al.	Urban Heat Island Diagnosis Using Aster Satellite Images and 'in Situ' Air Temperature	2009	Hong Kong	ASTER	Use Thermal Satellite data and in situ air tempertaures to identify the causes of UHI	Use of a cloud free ASTER image and in situ data, to define the differences in UHI between surface and Ta. Land cover, urban structure are considered.	two datasets showing a similar amplitude and general trend, but with the surface exhibiting much higher local variability than air temperature. Advection model seems more probable cause of UHI over large urban areas while in smaller ones the physical structure model is more plausible.

Authors	Title	Year	area study	satellite\sensor\other data	Aim	METHOD description	Results\intensity UHI
Nichol et al.	Temporal Characteristics of Thermal Satellite Images for Urban Heat Stress and Heat Island Mapping	2012	Hong Kong	ASTER	Map UHI and identify temporal patterns of heat stress in Hong Kong using LSt and Ta.	Compare LSt and in situ mesurements to identify UHI	nightime thermal images more representative of Ta due to stable BL wiht lower wind and tempertuare inversion. LSt and Ta are highly correlaed at night. Images useful for identifiying hot spots.
Qiao e al.	Diurnal and Seasonal Impacts of Urbanization on the Urban Thermal Environment: a Case Study of Beijing Using Modis Data	2013	Biejing, china	MODIS high resolution, LST NDVI	explore the effect of urbanization on UHI	Vegetation had a notable cooling effect as the normalized vegetation difference index (NDVI) increased during summer. However, when the NDVI reached a certain value, the nighttime LST shifted markedly in other seasons	Urban land was the most important contributor to increases in regional LSTs
Rajasekar et al.	Urban Heat Island Monitoring and Analysis Using a Non-Parametric Model: a Case Study of Indianapolis	2009	Nine counties in central Indiana	MODIS - ASTER LULC	analyze the diurnal varaition of UHI at regional level in 9 counties in Indiana.	Three dimensional (3-D) models of the day and night images were generated and visually explored for patterns through animation. The diurnal temperature profiles and UHI intensity attributes (minimum, maximum and	Skin temperature magnitude of UHI LST 1-3°C night. The areas with maximum heat signatures were found to have a strong correlation with impervious surfaces.
Retalis	The Heat Wave of June 2007 in Athens, Greece-Part 1: Study of Satellite Derived Land Surface Temperature	2010	Athens	AQUA MODIS LST and land SAF	Estimate the heat wave in Athens 2007 considering the UHI effect	estimate the temperature anomaly and the temporal evolution of the heatwave comparing LST and Ta.	Significant correlation beween satellite data at common overpass times, daytime differences vary between 2 5 to 5 8 degrees ma di UHI o tra satellite measurements
Rinner et al.	Toronto's Urban Heat Island-Exploring the Relationship Between Land Use and Surface Temperature	2011	Torornto, Canada		Explore the relationship between LSt and land use in Toronto	analyze whether characteristic land uses within an urban area are associated with higher or lower surface temperatures suing LST.	statistically significant differences between high average temperatures for commercial and resource/industrial land use (29.1 degrees C), and low average temperatures for parks, recreational land, water bodies (23.1 degrees C).
Schwarz	Exploring indicators for quantifying surface urban heat islands of European cities with MODIS land surface temperatures	2011	263 European cities	MODIS monthly mean Temperature	we compared the eleven different indicators for quantifying surface urban heat islands	Research should take into account the differences and instabilities of the indicators chosen for quantifying surface urban heat islands and should use several indicators in parallel for describing the surface urban heat island of a city	different indicators show only weak correlations
Schwarz et al.	Relationship of Land Surface and Air Temperatures and Its Implications for Quantifying Urban Heat Island Indicators-an Application for the City of Leipzig (Germany)	2012	Leipzig (Germany)		Estimate UHI combining Ta and LST	define relationship between LST and Ta to define UHI	Intensity of UHI depends on the indicator selected
Sharifi et al.	Correlation analysis of surface temperature of rooftops, streetscapes and urban heat island effect: Case study of central Sydney	2015	Sydney	LST	explore the most heat resilient urban features at precinct scale	Compare the surface temperature of streetscapes and buildings' rooftops (dominant urban horizontal surfaces) to LST	higher open space ratio and street network intensity correlate significantly to higher sUHI effect at precinct scale.
Sidiqui et al.	Spatio-temporal mapping and monitoring of Urban Heat Island patterns over Sydney, Australia using MODIS and Landsat-8	2016	Syndey	MODIS LST LULC - LANDSAT	monitoring, mapping and characterizing UHI patterns over time and space	The UHI intensities were extracted and a Gaussian approximation was then applied in order to quantify spatial extent, centre and magnitude of UHI intensities	The daytime UHI intensity in Sydney could be as large as 7 - 8 °C in summer day. Increasing trend in daytime UHI magnitudes for Sydney.

Authors	Title	Year	area study	satellite\sensor\other data	Aim	METHOD description	Results\intensity UHI
Sobrino	Evaluation of the Surface Urban Heat Island Effect in the City of Madrid by Thermal Remote Sensing	2013	Madrid, Spain	DESIREX	Define the UHI in Madrid	The DESIREX imagery was used to retrieve the SUHI effect by applying the temperature and emissivity separation (TES) algorithm	+5K night, validation with observed Ta are within 1K
Steutker et al.	Satellite measured growth of the urban heat island ììof Houston, Texas.	2003	Houston	NOAA - AVHRR	growth and variation of UHI in Houston	Comparison of 82 nighttime scenes taken between 1985 and 1987 and 125 nighttime scenes taken between 1999 and 2001	mean growth in magnitude of 0.8K 35%, the surface UHI intensity ranged from 1.06 to 4.25 °C depending on season and weather conditions
Stewart	A systematic review and scientific critique of methodology in modern urban heat island literature	2011	190 studies on UHI		ti review quality of methods and recommend improvements	not on satellite data but ground measurements of UHI	limits include half of the studies fail to control the confounding effects of weather, relief or time on reported 'urban' heat island magnitudes
Strathopoulou et al.	Daytime Urban Heat Islands From Landsat Etm+ and Corine Land Cover Data: an Application to Major Cities in Greece	2007	Athens, Thessaloniki, Patra, Volos and Heraklion	LANDSAT ETM+	assessing the thermal urban environment as well as for defining heat islands in urban areas in Greek cities	define the link between surface emissivities, land surface temperatures and urban surface characteristics	Identify hot spots in cities
Strathopoulou et al.	Downscaling AVHRR Land Surface Temperatures for Improved Surface Urban Heat Island Intensity Estimation	2009	Athens	AVHRR - LCL Corine	Downscale AVHRR data to obtain better spatial prediction of UHI using different methods. LST data and Corinne land cover data then used to quantify UHI.	Four downscaling techniques using different scaling factors were considered to downscale 1-km LST image data provided by AVHRR to obtain data at 120m resolution. Data was validated with LANDSAT TM images.	downscaling techniques improved estimation of LST.
Strathpolou et al.	Integrating Corine Land Cover data and Landsat TM for surface emissivity definition: application to the urban area of Athens, Greece	2007	Athens	LANDSAT ETM+, CLC corine, NDVI	define emissivity from satellite data in urban areas with different land covers	combine use of the land cover/land use information provided by CLC database with Landsat data for the definition and correlation of emissivity with various land covers and land uses	statistically significant differences in emissivity associated with different land cover types
Strathpolou et al.	A surface heat island study of Athens using high-resolution satellite imagery and measurements of the optical and thermal properties of commonly used building and paving materials	2009	Athens		Analyze the spatial structure of the thermal urban environment	Identify hot surfaces within the urban areas using ETM+ are identified and related to the urban surface characteristics and land use from Corinne and Greek land use.	Identify hot spots in cities
Sun et al.	An Erdas Image Processing Method for Retrieving Lst and Describing Urban Heat Evolution: a Case Study in the Pearl River Delta Region in South China	2010	Pearl river delta, china	LST and NDVI	estimate UHI using LST	Erdas image method to define uhi. The LST is classified based on normalized statistical method, and the normalized heat images are computed between different times.	LST increased areas mainly locate along the major roads in the eastern bank of the Pearl River
Tomlinson et al.	Derivation of Birmingham's Summer Surface Urban Heat Island From Modis Satellite Images,	2012	Birmingham	MODIS + observed data	map the average variation in heat island intensity		5K CBD during stable conditions, cold spots laso identified

Authors	Title	Year	area study	satellite\sensor\other data	Aim	METHOD description	Results\intensity UHI
Tomlinson et al.	Comparing Night-Time Satellite Land Surface Temperature From Modis and Ground Measured Air Temperature Across a Conurbation	2012	Birmingham	MODIS + observed data		compares nighttime LST data to air temp data from dataloggers	night-time air temperature is consistently higher than the satellite-measured LST
Unger et al.	Modeling of the Urban Heat Island Pattern Based on the Relationship Between Surface and Air Temperatures	2010			develop an easy to use method for early night-time near-surface air temperature pattern estimation based on surface temperature data	define the relationship between air and sruface temperature using measurements collected.	Ta depends on LST surrounding area.
Voogt	Effects of urban surface geometry on remotely-sensed surface temperature.	1998	Vancouver	Airborne thermal scanner ¯ ights	investigate the magnitude of e□ective anisotropic variations in urban surface thermal emissions for select land-use areas		strong directional variations in the observed surface temperature
Wen et al.	Relationship Between Land Cover Ratio and Urban Heat Island From Remote Sensing and Automatic Weather Stations Data	2011	Guangzhou	CBERS	investigates the relationship between land cover ratio and UHI	the correlation coefficient between hourly mean temperature and land cover ratio, ED and MFRACT was calculated	UHI higher a t night, stations with higher impervious ratio and lower ED had more serious heat island effect
Weng et al.	Modeling Urban Heat Islands and Their Relationship With Impervious Surface and Vegetation Abundance by Using Aster Images	2011	Indiannapolis	ASTER	characterize UHI using LSt , impervious surfaces and land cover	kernel convolution modeling method for 2-D LST imagery to characterize and model the UHI as a Gaussian process.	UHI intensity possessed a stronger correlation with both greenness and imperviousness indexes than with GV and IS abundance
White-Newsome et al.	Validating satellite-derived land surface temperature with in situ measurements: a public health perspective	2013	Detroit	LANDSAT TM5	Assess the correlations between LST and SI (% surface imperviousness) with actual ground temperatures.	Associations between these ground-based temperatures and the average LSTs and SI were evaluated. Spearman correlation coefficients and p-values were calculated	Satellite-derived LST and SI values were significantly correlated with 24-hr average and August monthly average ground temperatures at all but two of the radii examined (100 m for LST and 0 m for SI). SI and LST useful to lok at spatial variation but less useful for
Wu et al.	Development of a 3-D Urbanization Index Using Digital Terrain Models for Surface Urban Heat Island Effects	2013	Taipei and Yilan, Taiwan	MODIS	Identify the UHI in Taiwan cities. The correlation between 3DUI and surface temperatures were also assessed.	To assess SUHI at finer spatial scale, three-dimensional Urbanization Index (3DUI) with a 5-m spatial resolution was developed to quantify urbanization from a 3-D perspective using Digital Terrain Models (DTMs).	UHI intensity greater during heat wave days, up to +10.2 °C in Taiwan and +7.5°C in Yilan. Correlation etween 3Dui and LST was >0.6.
Xie et al.	Assessing the Long-Term Urban Heat Island in San Antonio, Texas Based on Moderate Resolution	2010	San Antonio Texas	MODIS AQUA LST, NDVI	assess the uHI in San Antonio and long term change		6-7K higher than rural area. UHI in ccentral and also in areas to the north

Authors	Title	Year	area study	satellite\sensor\other data	Aim	METHOD description	Results\intensity UHI
Xie et al.	A Multi-Temporal Landsat Tm Data Analysis of the Impact of Land Use and Land Cover Changes on the Urban Heat Island Effect	2012	Wuhan	LANDSAT 5 TM	Define the relationship between UHI and LULC	RS techniques were applied to derive information on LULC and land surface temperature (LST) to describe UHI.	seasonal difference sin vegetation and land cover influence UHI intensity.
Xiong et al.	The Impacts of Rapid Urbanization on the Thermal Environment: a Remote Sensing Study of Guangzhou, South China	2012	Guangzhou	LANDSAT + LULC		thermal remote sensing and spatial statistics methods, here we analyze four Landsat TM/ETM+ images to investigate the spatiotemporal variations in the land surface temperature (LST) over five land use/land cover	high temperature anomalies were closely associated with built-up land and densely populated and heavily industrialized districts. LST is related positively with NDBI and negatively with NDVI
Xu et al.	Remote Sensing of the Urban Heat Island and Its Changes in Xiamen City of Se China	2004	Xiamen City, China	Landsat TM/ETM+	describe the UHI of Xiamen	Satellite thermal infrared images were used to determine surface radiant temperatures. Urban-Heat-Island Ratio Index(URI) defined.	Urban area has expanded and more recent images show the UHI has been reduced or disappeared as rural areas changed LC and have similar thermal properties
Xu et al.	Modelling of Urban Sensible Heat Flux at Multiple Spatial Scales: a Demonstration Using Airborne Hyperspectral Imagery of Shanghai and a Temperature Emissivity	2008	Shanghai	Operative Modular Imaging Spectrometer (OMIS	map spatial variations in turbulent sensible heat flux	the Operative Modular Imaging Spectrometer (OMIS), along with a survey map and meteorological data, to derive the land cover information and surface parameters. Compare LUMPS and Rama input data	At 30m resolution, LUMPS and ARM methods produce similar results, less than 15 W m(-2) difference in mean Q(H) averaged over the entire study area
Xu et al.	Spatial and Temporal Dynamics of Urban Heat Island and Their Relationship With Land Cover Changes in Urbanization Process: a Case Study in Suzhou, China,	2010	Suzhou, China	LANDSAT	to study the spatial and temporal variations of heat island and their relationships with land cover changes in Suzhou	Land cover classifications were derived to quantify urban expansions and brightness temperatures was used to express urban thermal environment	show good correspondence between heat island variations with urban area expansions
Xu et al.	Correlation analysis of the urban heat island effect and the spatial and temporal distribution of atmospheric particulates using TM images in Beijing	2013	Beijing	LANDSAT	analyze the correlation between the urban heat island effect and the spatial and temporal concentration distributions of atmospheric particulates in Beijing	uses NDVI, NDWI and DVI (difference veg index)	(1) a direct correlation between UHI and DVI; (2) indirect correlation among UHI, NDWI and DVI; and (3) an indirect correlation among UHI, NDVI, and DVI
Xu et al.	An approach to analyzing the intensity of the daytime surface urban heat island effect at a local scale	2009		LANDSAT 7	Evaluate the intensity of daytime UHI	A landscape index (LI) is proposed to evaluate the intensity of the daytime surface urban heat island (SUHI) effect.	LI can be used to compare SUHI daytime intensity in different areas.
Yang	Spatial and Temporal Characteristics of Beijing Urban Heat Island Intensity.	2013	Beijing, China	oberved Ta data, 56 monitoring stations	Define UHI in Beijing using observed data		seasonal patterns of UHI are identified and hot spot areas
Zaksek et al.	Downscaling Land Surface Temperature for Urban Heat Island Diurnal Cycle Analysis	2012	central Europe	geostationanry SEVIRI	Downscale SEVIRI data (good temporal scale but poor spatial) to monitor the diurnal cycle UHI. (1km spatial and 15min temporal).	For each SEVIRI pixel a multiple regression was run on the low resolution data. Regression equation was then used on the high resolution data in order to estimate LST of high spatial and temporal resolutions	downscaled pixel data was compared to MODIS, RMSE 2.5°K

Authors	Title	Year	area study	satellite\sensor\other data	Aim	METHOD description	Results\intensity UHI
Zhang et al	Spatial-Temporal Patterns of Urban Anthropogenic Heat Discharge in Fuzhou, China, Observed From Sensible Heat Flux Using Landsat Tm/Etm Plus Data	2013	Fuzhou, China	LANDSAT TM+\ETM+	Estimate the anthropogenic heat discharge in the form of sensible heat flux in complex urban environments.	Spatial and temporal distributions of anthropogenic heat flux were analysed as a function of land-cover type, percentage of impervious surface area, and FVC	that anthropogenic heat release probably plays a significant role in the UHI effect, RS important for mapping UHI and can differentiate anthropogenic heat from solar radiative fluxes.
Zhang et al.	Exploring the Influence of Impervious Surface Density and Shape on Urban Heat Islands in the Northeast United States Using Modis and Landsat	2012	USA cities	MODIS and LANDSAT, ISA-impervious surface area	assess the surface urban heat island (UHI) signature and its relationship to settlement size and shape, development intensity distribution, and land cover composition	Our study indicates that for cities of similar size, the ISA density distribution within the urban area and the shape of the urbanized area as measured by area to perimeter ratio are significant modulators of UHI magnitude.	Stratification based on ISA allows the definition of hierarchically ordered urban zones that are consistent across urban settlements and scales. settlement size, shape, and development intensity significantly influenced the amplitude of summer daytime UHI.
Zhang et al.	Characterizing Urban Heat Islands of Global Settlements Using Modis and Nighttime Lights Products	2010	global cities	MODIS LST and nighttime light products and ISA (impervious surface area)	Define UHI in urban areas using MODIS and night lights	spatial analysis to assess the urban heat island (UHI) signature on LST amplitude and its relationship with development intensity, size, and setting.	Ecological context and settlement size significantly influence the amplitude of summer daytime UHI. UHI 3.8°C in cities with biomes dominated by forests; +1.9°C UHI in cities embedded in grass-shrub biomes; weak UHI or sometimes an urban heat sink (UHS) in cities in arid
Zhang et al.	Analysis of Land Use/Land Cover Change, Population Shift, and Their Effects on Spatiotemporal Patterns of Urban Heat Islands in Metropolitan Shanghai, China	2013	Shanghai	Landsat ETM+	quantify spatiotemporal changes in UHI related to changes in LULC change/pop shifts from 1997 to 2008.	Integrated approach of remote sensing, geographical information systems (GIS), and statistical analysis.	changes in LULC and population shifts resulted in significant variation in the spatiotemporal patterns of the UHIs due to the loss of water bodies and vegetated surfaces
Zhang et al. 2005	The Diurnal and Seasonal Characteristics of Urban Heat Island Variation in Beijing City and Surrounding Areas and Impact	2005	Biejing, china	MODIS EOS	Study the urban heat island (UHI) spatial distribution of the diurnal and seasonal variabilities and its driving forces	analyze the relationships among UHI distribution and landcover categories, topographic factor, vegetation greenness, and surface evapotranspiration	+4-6°C LST between Beijing city and suburb areas; significant UHI mainly appears in the summer; negative correlation between NDVI and LST; high latent heat exchange is evident, high evapotraspiration in
Zhou et al.	Modelling the Diurnal Variations of Urban Heat Islands With Multi-Source Satellite Data	2013	Biejing, china	LST		a diurnal temperature cycle genetic algorithm (DTC-GA) approach was used to generate the hourly 1km land-surface temperature (LST) by integrating multi-source satellite data	all diurnal cycles, daytime UHIs varied significantly but night-time UHIs were stable. Seasonal cycles are also variable
Zhou et al.	On the statistics of urban heat island intensity	2013	EU cities	review	study UHI in European cities by means of remotely sensed land surface temperature data.	Defining cities as spatial clusters of urban land cover, we investigate the relationships of the UHI intensity, with the cluster size and the temperature of the surroundings	
Zhou et al.	Maximum Nighttime Urban Heat Island (Uhi) Intensity Simulation by Integrating Remotely Sensed Data and Meteorological Observations	2011	Beijing, China	MODIS, meteorological data	Describe the temporal variation in UHI Beijing.	SVM regression models were developed to predict the MNUHII from the following variables: the normalized difference vegetation index (NDVI), surface albedo, atmospheric aerosol optical depth (AOD), relative humidity (RH), sunshine hour (SH), and precipitation (PREP)	RH and AOD were the most important factors that influenced the MNUHII, precipitation attenuates UHI. Other meteorological factors should be considered with sruface characteristics in defining UHI.
Zhou etal.	Relationships Between Land Cover and the Surface Urban Heat Island: Seasonal Variability and Effects of Spatial and Thematic Resolution of Land Cover Data on Predicting Land Surface Temperatures	2014		LANDSAT 7 TM	Investigate the relationship between land surface temperature (LST) and land use/land cover (LULC) and its seasonality.	ten models were defined to evaluate effects of spatial and thematic resolution of LULC data on the observed relationships between LST and LULC variables for each season	Percent of iA88:H98mperviousness was the best predictor on LST with relatively consistent explanatory power across seasons. Vegetation related variables, particularly tree canopy, were good predictor of LST during summer.

Table 4. Summary of studies included in the literature review on heat effects on mortality and hospital admissions by total, cardiovascular and respiratory causes.

STUDY DESIGN: TIME SERIES

OUTCOME: MORTALITY

Study	Country, period	Population	Outcome measure	Exposure	Main results
Kunst et al. 1993	The Netherlands; *1979-1987*	all ages	Percentage change in daily mortality for 1°C increase in mean temperature above 16.5°C (lag 0)	mean temperature	All causes **all ages** =+1.76 CVD all ages =+1.75 RESP **all ages** =+3.31 External causes all ages=+2.46 Evidence of harvesting effect for cardiovascular mortality at lag 7-30 days
Saez et al. 1995	Barcelona (Spain); *1985-1989*	all ages, 65+	Absolute change in daily mortality for 1°C in maximum/minimum temperature Percentage change of mortality during unusual periods of hot temperature	1. daily minimum and maximum temperature. 2. Unusual periods during summer (>3 consecutive days with temperature/humidity exceeding its 85th percentile)	All causes all ages=0.564 deaths; **65+** =1.293 deaths CVD All ages=1.111 deaths RESP all ages=0.144 deaths Unusual periods: All causes: all ages =+1.7% **65+** =+2% CVD all ages=+4.2% RESP all ages=+13.2%

Study	Country, period	Population	Outcome measure	Exposure	Main results
Ballester et al. 1997	Valencia (Spain); *1991-1993*	all ages +70	Relative risk (RR) of death for 1°C increase above 24°C	mean temperature	<u>All causes</u> all ages RR=1.037 (lag 3-6) **70+** RR=1.050 (lag 1-2) <u>CVD</u> **all ages** RR =1.037 (lag 3-6) <u>RESP</u> **all ages** RR=1.101 (lag 7-14) <u>Malignant tumors</u> **all ages** RR=1.037 (lag 0)
Alberdi et al. 1998	Madrid (Spain); *1986-1992*	all ages 65+	Absolute change in daily mortality for 1°C increase in temperature during summer (lag 1)	maximum temperature	<u>All causes</u> **all ages** =0.97 <u>CVD</u> **65+** significant absolute change (data not shown)
Rossi et al. 1999	Milan (Italy), *1980-1989*	all age	Relative risk (RR) of death above a cause-specific threshold (lag 0)	mean temperature	<u>All causes</u> **all ages** RR=1.14 (above 29°C) <u>Myocardial infarction</u> **all ages** RR= 1.44 (above 27°C) <u>Heart failure</u> **all ages** RR= 1.47 (above 27°C) <u>RESP</u> Effect of temperature above 20°C (lag 1) (data not shown)
Hales et al. 2000	Christchurch (New Zealand), *1988-1993*	all ages 65+	Percentage change in mortality for 1°C increase in maximum temperature above 20.5°(lag 0)	maximum temperature	<u>All causes</u> **all ages** =+1% **65+** = +0.9% No interaction between high temperatures and particulate air pollution.

Study	Country, period	Population	Outcome measure	Exposure	Main results
Michelozzi et al. 2000	Rome (Italy), *1987-1996,* summer (15 May-30 September)	65+	Percentage change in mortality for 1°C increase in mean temperature	mean, minimum and maximum temperature	<u>All causes</u> **All ages**=+2.3% No association between relative humidity and mortality. Significant interaction between temperature and humidity with a greater effect when the dew point was over 15°C.
Braga et al. (2001, 2002)	12 cities (U.S.); *1986-1993*	all ages	Percentage change in mortality for 1°C increase in mean temperature above 30°C	mean temperature	<u>All causes</u> all ages =+4% **cold cities**: MI =+6% CVD =+1% COPD =+25% **Hot cities:** MI =+4% (lag 4-6) COPD =+6% (lag 3-4) CVD: no effect Harvesting effect for heat
Curriero et al. 2002	11 eastern (U.S.) cities; *1973-1994*	age groups: 0-64 65-75 75+ years	Percentage change in mortality for 1°C increase in mean temperature above city-specific thresholds.	Mean temperature	<u>All causes</u> Tampa (Florida)= +0.12% above 27.1°C Chicago (Illinois)= +0.54% above 18.4°C Baltimore (Maryland)= 0.54% above 21.4°C Atlanta (Georgia)= +1.22% above 24.6°C Greatest heat effects on cardiovascular and respiratory causes No effect on other causes (maily cancer).

Study	Country, period	Population	Outcome measure	Exposure	Main results
Diaz et al. 2002a	Seville (Spain); 1986-1997 summers (June-September)	age 65+ age 75+	Percentage change in mortality for 1°C increase in temperature above 41°C.	maximum temperature	<u>All causes</u> **65**+ =+38% **75**+ =+51% <u>CVD</u> **65**+ =+49% <u>RESP</u> **65+** =+29%
Diaz et al. 2002b	Madrid (Spain), *1986-1997* (June-September)	age groups: 65-74 >75	Percentage change in mortality for 1°C increase in temperature above 36.5°C	maximum and minimum temperature	<u>All causes</u> **65-74**:men=+14.7%; women=+16.2% 75+: men=+12.6%; women=+28.4% <u>CVD</u>: **65-74**: men=+9.4%; women=+11.7% **75+:** men:=+9.3%; women=+34.1% <u>RESP</u>: **65-74** :men =+17.2%; women=+23.0% **75**+ :men =+26.1%; women:=+17.6%
Hajat et al. 2002	London (UK), 1976-1996	all ages	Percentage change in mortality during days with smoothed (3-days moving average) mean temperature >97th percentile (21.5°C) (lag 0)	mean temperature, any day with the 3 day moving average above the 99th, 97th, 95th centiles	<u>All causes</u> **all ages** = +3.34% <u>CVD</u> **all ages**=+3.01% <u>RESP</u> **all ages**=+5.46%

Study	Country, period	Population	Outcome measure	Exposure	Main results
Gouveia et al. 2003	São Paulo (Brazil); *1991-1994*	age groups: 0-14, 15-64, 65+	Percentage change in mortality for 1°C increase in mean temperature above 20°C (lag 0-1).	Mean temperature	All causes: **<15** =+2.6% **15-64**=+1.5% **65**+=+2.5% CVD **65**+=+2.0% RESP **15-64** =+2.1% **65**+ =+2.3% Other natural causes **15-64**= +2.3% **65**+ =+2.9% Heat effect lower in the elderly in the highest socioeconomic group

Study	Country, period	Population	Outcome measure	Exposure	Main results
O'Neill et al. 2003	7 cities (U.S.); *1986-1993* *Pooled analysis*	age groups: 0-64 65+	Percentage change in mortality at 29°C apparent temperature relative to 15°C.	mean apparent temperature	<u>All causes</u> **≥65** = +5.6% **0-64**=+4.8% Black= +8.6% (lag 0) White= +4.1% high-school education or less= +5.2% post-high school education =+0.5% n.s. **0-64** =+ 4.8% **65**+ =+5.6% <u>CVD</u> All ages n.s. **0-64** =n.s. **65**+ n.s <u>RESP</u> **All ages** n.s **0-64** =n.s. **65**+ n.s
Pattenden et al. 2003	Sofia, 1996-1999 London, 1993-1996	All ages	Percentage change in mortality for 1 C° above 21°C for London and 21.6°C for Sofia (90th centile)	mean temperature	<u>All causes</u> All ages=+1.9% in London (lag 0-1) All ages=+3.5% in Sofia

Rainham et al. 2003	Toronto (Canada); *1980-1996*	age groups: 0-65 and 65+	Relative risk (RR) of death for an increase in humidex between the 50th and 95th percentile range.	Humidex	<u>All causes:</u> **all ages** RR =1.06 **<65** RR=1.05 **65+** RR=1.06 Air pollution appears to have a small but consistent confounding effect on humidex effect estimates.
El-Zein et al. 2004	Beirut (Lebanon) *1997-1999*	All ages, 65+	Percentage change in mortality for 1°C increase in mean temperature above 27.5°C (lag 1-2)	mean temperature	<u>All causes</u> All age =+19.6% **65+** =+25.7%
Goodman et al. 2004	Dublin (Ireland); 1980-1996	age groups: 0-64, 65-74 and 75+	Percentage change in mortality for 1°C increase in minimum temperature (lag 0).	Minimum temperature	<u>All causes</u> **all ages** = +0.4% **65-74**= +0.7% <u>CVD</u> N.S. <u>RESP</u> : **all ages**= +0.8%

Hajat et al. 2005	Delhi, São Paulo, London, *1991-1994*	All ages, age groups: 0-14, 15-64, 65+	Percentage change in mortality for 1°C increase in temperature above 20°C.	Mean temperature	<u>All causes</u> **all ages**: Delhi=+2.4% (lag 0-28) Sao Paulo=+1.6% (lag 0) London=+1.4% (lag 0) <u>CVD</u> **all ages** = +4.3% (lag 0-7) Sao Paulo=+1.2% (lag 0) London=+0.9% (lag 0) <u>RESP</u> **all ages**=+4.5% (lag 0-7) Sao Paulo=+4.0% (lag 0-28) London=+5.9% (lag 0-28) <u>All other causes</u>: **all ages**=+2.8% (lag 0-7) Sao Paulo=+1.8% (lag 0) London=+1.6% (lag 0)
Kim et al. 2006	6 cities (Korea); 1994 to 2003 Multicenter study	All ages	Percentage change in mortality for 1°C increase in mean temperature and Heat Index (Steadman 1979) above city specific threshold	mean threshold	<u>All causes</u> **All age** Seoul=+16.3% Daegu=+9.1% Incheon =+7.01% Gwangju =+6.7% Daejeon n.s. Busan n.s. **65+** Seoul=+17.1% Daegu=+5.9% Incheon=+4.7% Gwangju=+2.6% Daejeon n.s. Busan n.s.

Michelozzi et al. 2006	4 italian cities; June-September *2003-2004*	All ages	Percentage change in mortality for 1°C increases in maximum apparent temperature between 26°C to 36°C	maximum apparent temperature	<u>All causes</u> **All age** (2003) Torino=+7.8% (26-28°C) Milano=+10.7% (26-34°C) Roma=+32% (26-36°C) Bologna=+27.2% (26-36°C) **All age** (2004) Milano= +15.2% (26-36°C) Torino=+ 11.7% (26-30°C)
Hajat et al. 2007	England and Wales (UK)	All ages	Relative risk (RR)of death for 1°C increase in temperature above the 95th percentile.	Mean temperature	<u>All causes:</u> **All ages**: Strongest effects for respiratory disease and deaths from external causes **0-64**: greatest effect on external causes **85+:** greatest effect on respiratory disease

Baccini et al. 2008	15 cities Mediterranean and North-Continental; *1990-2000* *Pooled analysis*	All ages	Percentage change in mortality for 1°C increase above a city-specific threshold in **Mediterranean** (Athens, Rome, Barcelona, Valencia, Turin, Milan and Ljubljana) and **North-Continental** cities (Prague, Budapest, Zurich, Paris, Helsinki, Stockholm, London Dublin).	Apparent temperature (Threshold 29.4°C **Mediterranean** cities and 23.3°**C north-continental** cities)	<u>All causes:</u> Mediterranean cities: **all ages** =+3.12% North-Continental cities: All ages=+1.84% **15-64** n.s. **65-74** n.s. **75+(**Mediterranean cities=+4.22%; North-Continental cities=+2.07%) <u>CVD</u>: Mediterranean cities: **all ages**=+3.7% North-Continental cities: **all ages**=+2.4% **15-64** n.s. **65-74** n.s. **75+(**Mediterranean cities=+4.6%; North-Continental cities=+2.5%) <u>RESP:</u> Mediterranean cities: **all ages**=+6.7% North-Continental cities: **all ages**=+6.1% **15-64** n.s. **65-74** n.s. **75+(** Mediterranean cities=+8.1; North-Continental cities=+6.6)

Study	Country, period	Population	Outcome measure	Exposure	Main results
Ishigami et al.2008	Budapest;1993-2001 London; 1993-2003 Milan;1999-2004	All ages	Relative risk (RR) of death for 1°C of temperature above the 95th percentile (lag 0-1)	mean temperature threshold: Budapest>24°C London>20°C Milan >26°C	<u>All causes</u> **0-14**= significant only in females in London **15-64** and **65-74**=significant in both males and females in all cities Effect greater in 75-84 e 85+. **<75** (Budapest RR=1.03; London RR=1.03; Milan RR=1.12 **75+** (Budapest RR=1.06; London RR=1.06; Milan RR=1.17 <u>CVD</u> **<75** Budapest RR=1.04; London RR=1.03; Milan RR=1.15 **75+** Budapest RR=1.08; London RR=1.06; Milan RR=1.20 <u>RESP</u> **<75** Budapest RR=1.06; London RR=1.05; Milan RR=1.37 **75**+ Budapest RR=1.08; London RR=1.08; Milan RR=1.22 <u>External causes:</u> **<75** Budapest RR=1.04; London RR=1.06; Milan RR=1.21 **75+** Budapest RR=1.02; London RR=1.10; Milan RR=1.18
Anderson et al. 2009	107 communities (USA) 1987-2000 Pooled analysis	All ages	Percentage change in mortality comparing 99 percentile vs 90 percentile	Mean temperature	<u>All causes</u> <u>All ages= 3%</u>

Study	Country, period	Population	Outcome measure	Exposure	Main results
McMichael et al. 2008	12 cities from low and middle-income countries (Delhi, Monterrey, Mexico City, Chiang Mai, Bangkok, Salvador, São Paulo, Santiago, Cape Town, Ljubljana, Bucharest and Sofia)	All ages	Percentage change in mortality for 1°C above a city-specific threshold.	Mean temperature	<u>All causes</u> **all ages** +0.77% in Mexico City - +18.8 in Monterrey Ljubljana=3.12%; Bucharest=3.30%; Sofia=2.88%; Delhi=3.94%; Monterrey=18.8%; Mexico City=0.77%, Chiang Mai n.s.; Bangkok=5.78%; Salvador=2.48%; São Paulo=3.46%; Santiago=1.04%; Cape Town n.s. <u>CVD:</u> **all ages** +1.05% in Mexico City to +17.6% in Monterrey. Ljubljana=+3.35%; Bucharest=+3.92%; Sofia=+3.43%;Delhi=+3.94%; Monterrey=+17.6%; Mexico City=+1.05%, Chiang Mai not estimable; Bangkok= not estimable;Salvador=+14.7%; São Paulo=+3.26%; Santiago=+1.47%; <u>Non cardiovascular disease:</u> **all ages** +1.68% in São Paulo - +5.10% in Sofia. Ljubljana=+1.77%; Bucharest=+1.87%; Sofia=+5-10%; Delhi=+4.30%; Monterrey=+49.3%; Mexico City=+1.53% n.s., Chiang Mai not estimable; Bangkok=+7.52%; Salvador=+2.61%; São Paulo=+1.68%; Santiago=not estimable; Cape Town=not estimable

Study	Country, period	Population	Outcome measure	Exposure and threshold	Main results
Hashizume et al. 2009	(Bangladesh); *1994-2002*	All ages	Percentage change in mortality for 1°C increase above a threshold	mean temperature heat threshold 31°C	CVD **All ages** = +62.9% Elderly= +108.1%
Muggeo et al. 2009	Palermo (Italy): 1997-2001 Santiago (Chile): *1989-1991*	All ages	Percentage change in mortality for 1°C increase in temperature above identified threshold	mean temperature	All causes Santiago **≥65** =+5.48% Palermo **0-64** =+10.2% **≥65** =+17.6% CVD **All ages**=+17.7%
Stafoggia et al. 2009	Rome (Italy), *1997-2004*	Elderly 65+	Relative risk (RR) of death at 30°C (lag 0-1) relative to 20°C	apparent temperature	All causes All ages RR=1.39 CVD All ages RR=1.44 RESP All ages RR=1.70
Iniguez et al. 2010	13 cities (Spain) *1990-1996*	All ages	Percentage change in mortality for 1 ºC increase in temperature from MMT	mean temperature MMT	All causes 7**0+=** increase from 0.47% to 4.83%. Significant effect 9/13 cities Cardio-RESP All ages: increase from 0.87% to 7.72%. significant effect: 7/13 cities

Study	Country, period	Population	Outcome measure	Exposure and threshold	Main results
Rocklov et al. 2010	3 regions (Sweden), June-August, *1998-2005*	65+	Relative risk (RR) of death for 1°C increase in temperature above the threshold of the 90th percentile (lag 0-1)	mean temperature	<u>All cause:</u> **All ages** RR=1.051
Almeida et al. 2010	Lisbon and Oporto (Portugal); summer (April to September)	65+	Percentage change in mortality per 1°C increase in mean daily temperature	Mean apparent temperature	<u>All causes</u> **All ages** LISBON +2.1% OPORTO +1.5% **>65** LISBON +2.7% OPORTO +1.8% <u>CVD:</u> **All ages** LISBON +2.4% OPORTO +2.1% **>65** LISBON +2.8% OPORTO +2.2% <u>RESP</u> LISBON: n.s. for all ages **>65** OPORTO +3.0%

Study	Country, period	Population	Outcome measure	Exposure and threshold	Main results
Ha et al. 2011	Seoul, Daegu, and Incheon (South Korea) *1992-2007*	All ages 65+	Percentage change in mortality per 1°C increase in temperature above the thresholds (lag 0-1)	mean temperature	All causes: Seoul **All ages**=+7.97% **≥65** =+8.51% Daegu All ages=+6.12% **≥65**=+6.82% Incheon All ages=+3.85% **≥65**=+3.89% <u>CVD</u> all ages=+ 10.2%
Gomez-Acebo et al. 2011	Cantabra (Spain); June-September *2003-2006*	All ages	Percentage change in mortality per 1 degrees C increase in temperature	maximum temperature	All causes: **All ages**=+2.0% (1.1, 3.0) When stratifying by age, temperatures have no effect on mortality in people younger than 65; moreover, maximum temperature has no effect in people older than 90
Yu et a. 2011	Brisbane (Australia) 1996-2004	All ages 65+	Percentage change in mortality per 1°C increase in temperature above the threshold	Mean temperature	<u>CVD</u> **All ages**: 3.5% (0.4 to 6.7) (lag 0-1) 8.4% (1.1 to 16.2) (lag 0-21) **65+:** 3.7% (0.4 to 7.1) **65+:** 8.0% (0.3 to 13.2) (lag 0-21)
Gasparrini et al. 2011	108 communities (USA), 1987–2000	All ages	Relative risk (RR) between the median city-specific temperature during heat-wave days and the 75th p annual distribution	1)Tmean (main effect) 2) heatwave added effect: ≥4 days with Tmean ≥99th annual T distribution(alternative definitions are used	<u>All causes</u> Main effect RR=7.7 Added effect RR=2.8

Study	Country, period	Population	Outcome measure	Exposure and threshold	Main results
Rocklov et al. 2011	Stockholm (Sweden); June-August 1990-2002	All ages	Relative risk (RR) of death for 1°C of temperature in minimum apparent temperature or for day number of extreme days (lag 0-1)	1)apparent minimum Temperature (main effect) 2)Extreme heat: n° of days with Tappmax >98th pctile	<u>All causes</u> All ages Main effect RR=1.006 Extreme heat RR=1.024 <u>CVD</u> Main effect RR=1.004 n.s. Extreme heat RR=1.020 n.s. <u>RESP</u> Main effect RR=1.014 n.s. Extreme heat RR=1.039% n.s.
Goldberg et al. 2011	Montreal (Canada) 1984-2007	All ages	Percentage change in mortality comparing 99th to 75th percentile	maximum temperature	All causes **All ages**: +28.4% (lag 0-14) +11.9% (lag 0)
Gasparrini et al. 2012	10 regions England and Wales (UK); 1993-2006 summers (June-September) pooled analysis	All ages Ages groups: age groups: 0-64, 65-74; 75-84; 85+	Percentage change in mortality for 1°C increase above the threshold* (lag 0-1)	maximum temperature	<u>All causes</u> All ages=+2.1% <u>Cardiovascular disease</u> All ages=+1.8% <u>Pulmonary heart diseases</u> All ages=+8.3% <u>Asthma</u> All ages=+5.5% <u>Extra-pyramidal disorders</u> All ages=5.5% <u>Arrhythmias</u> All ages=5.0% Evidence of a heat-related increase in mortality for almost all of the cause-of-death and age groups

Study	Country, period	Population	Outcome measure	Exposure and threshold	Main results
Barnett et al. 2012	107 cities (U.S); 1987-2000	All ages	Percentage change in daily mortality for 10°F increase in temperature.	Temperature	<u>All causes</u> all ages=+4.7% (summer 1987) all ages=-0.4% n.s. (summer 2000)
Tobias et al. 2012	52 cities (Spain); *1995-2004* (June to September)	All ages	Relative risk (RR) of death above a specific thresholds	minimum and maximum temperatures	<u>All causes</u> **All ages** RR= 1.24 Zamora RR= 2.70 Madrid RR= 1.31 Seville RR= 1.32;
Williams et al. 2012	Adelaide (Australia); 1993-2009	All ages	Incidence rate ratio (IRR) in the mortality for 10 °C increases in daily maximum temperatures over thresholds	maximum and minimum temperature	No effect on mortality
Wu et al. 2013	4 cities (China);2006-2010	All ages 0-64; 65+	RR for 1. °C increase of temperature above the hot threshold	Mean temperature	<u>All causes</u> All ages: Changsha RR=1.020 Lag 0 higher RR in 65+ Kunming RR=1.017 Guangzhou RR=1.029 higher RR in 65+ Zhuhai RR=1.023 higher RR in 65+
Lin et a. 2013	4 cities (Taiwan); 1994-2007	All ages	RR at 31 degrees C Comparing to centered temperature at 27 degrees C	Mean temperature	Cerebrovascular diseases All ages: RR = 1.14 Lag 0-3 Heart diseases RR = 1.22 IHD RR = 1.09 n.s.

Study	Country, period	Population	Outcome measure	Exposure and threshold	Main results
Guo 2013	5 cities (China); 2004-2008	All ages	RR at the 99th percentile of temperature (extremely hot temperature) compared with the 90th percentile	Mean temperature	IHD All ages: RR=1.17 (lag 0-2)
Breitner 2014	3 cities (Germany); 1990-2006	All ages, 75+	RR for temperature from the 90th (20.0 degrees C) to the 99th centiles (24.8 degrees C)	Mean temperature	cardiovascular causes all ages RR=1.10 (lag 0-1) 75+: 1.12 IHD all ages RR=1.06 75+: 1.09 Other heart disease All ages: RR=1.14 75+ 1.15 Cerebrovascular disease All ages RR= 1.12 75+ 1.14
Tobias 2014	50 cities (Spain);1990-2004	All ages	% change between the 99th and 90th percentiles	Maximum temperature	All causes All ages: 14.6% Heterogeneity among cities
Guo 2014	23 countires 306 cities	All ages	% change between 99^{th} percentile and MMT	Mean temperature	Heterogeneity among cities , MT changes by region, heat effects short lag

Study	Country, period	Population	Outcome measure	Exposure and threshold	Main results
Wang 2014	Suzhou, China;2005-2008	All ages	RR at 99th percentile of temperature, 32.6 degrees C) compared with the minimum mortality temperature (26 degrees C)	Mean temperature	<u>All causes</u> All ages: RR= 1.43 lag 0-3

Li 2014	4 cities (China); 2004-2012	All ages, 0-14,15-29,30-54,55-64,65-74,75+	RR per 1°C increase	Maximum temperature	<u>All-cause</u> Harbin all ages: RR= 1.045,30-54: 1.061,55-64: 1.072,65-74: 1.030,75+: 1.061 0-14,15-29 n.s Nanjing all ages: RR=1.032, 55-64: 1.063, 65-74: 1.053, 75+: 1.056 0-14,15-29,30-54 n.s. Shenzhen all ages: RR=1.040, 0-5: 1.058, 30-54: 1.072; 75+ 1.074 15-29, 55-64, 65-74 n.s. Chongqing all ages: RR=1.055,30-54: 1.149,55-64: 1.112, 65-74:1.083,75+: 1.057 Greater effects in females <u>CVD causes</u> Harbin all ages: 1.046 Nanjing 1.050 Shenzhen 1.075 Chongqing 1.069 <u>Respiratory causes</u> Harbin all ages: 1.080 Nanjing, Shenzhen, Chongqing n.s. <u>Digestive causes</u> Harbin Shenzhen Nanjing n.s. Chongqing all ages: 1.236 <u>Endocrine and metabolic causes</u> Harbin all ages 1.232 Nanjing 1.125 Shenzhen 1.319 Chongqing 1.236

Study	Country, period	Population	Outcome measure	Exposure and threshold	Main results
Benmarhnia 2014	Paris, France;2004-2009	All ages,65+	Mortality rates attributable to summer temperatures (per 100,000)	Mean temperature	All causes All ages: 5.37 65+: 33.57 Effect modification by air pollution and social deprivation and by deprivation in the high polluted group
Yi 2015	Hong Kong;2002-2011	All ages,0-64, 65-74,75+	RR at 31.5 degrees C, 99th percentile of temperature) relative to 27.8 degrees C (75th percentile of temperature	Mean temperature	All causes All ages: RR= 1.09 lag 0-3 Higher effects in 65-74 than 75+ years or 0-64 Cardiopulmonary All ages: 1.14 Cardiovascular n.s. Respiratory All ages: 1.33
Yang 2015	26 regions in the south and west of China; 2008-2011	All ages	% change for 1°C increment above the high temperature threshold 90th percentile	Mean temperature	CVD causes All ages: % change from 0% to 18.25% Effect modifiers: number of hospital beds per 10,000 population, % residents engaged in industrial occupations, % women

Study	Country, period	Population	Outcome measure	Exposure and threshold	Main results
Huang 2015	66 Chinese communities; 2006-2011	All ages	% change for 1°C increment above the MMT	Mean temperature	<u>All causes</u> All ages: % change=3.44% Effect modifiers: age, sex, place of death, cause of death and education level
Gasparrini 2015	384 locations in Australia, Brazil, Canada, China, Italy, Japan, South Korea, Spain, Sweden, Taiwan, Thailand, UK, and USA; 1985 and 2012	All ages	attributable deaths for heat	Mean temperature	All causes: all ages: 0·42% (Lag 0-21)
Gasparrini 2015	272 locations in Australia, Canada, Japan, South Korea, Spain, UK, and USA; 1985-2001 and 1996-2012	All ages	RR at 99th percentile (or 90th percentile) compared with minimum mortality temperature	Mean temperature	<u>All causes</u> Australia All ages: RR=1.272 (lag 0-9) Canada All ages: RR=1.124 (lag 0-9) Japan All ages: RR=1.098 (lag 0-9) South Korea All ages: RR= 1.109 (lag 0-9) Spain All ages: RR=1.434 (lag 0-9) UK All ages: RR=1.167 (lag 0-9) USA All ages: RR=1.091 (lag 0-9) The analysis suggests a decrease in the mortality risk associated with heat in Japan, Spain and USA

Study	Country, period	Population	Outcome measure	Exposure and threshold	Main results
Pearce 2016	Melbourne, Australia, 1999-2006	65+ years	% change above the 90th percentile as compared to days in the referent 25–75 percentile	Mean temperature	All causes All ages: 6% (lag 0-11)
Sun 2016	Hong Kong, 1998-2001	65+ years	% change extreme hot temperature (99th percentile of temperature, 30.4 °C) compared to at 75th percentile (19.5 °C)	Mean temperature	All causes Patients with diabetes, CVD, COPD n.s. (lag 0-3)
Petitti 2016	Maricopa County, Arizona; 2000-2011	All ages	RR at the highest recorded temperatures	minimum, mean, and maximum temperature	CVD All ages: RR> 1.05
Yang 2016	16 large Chinese cities; 2007–2013	All ages	Attributable fraction to temperature above the 97.5th percentiles	Mean temperature	Stroke All ages: 1.4% (lag 0-14)
Seposo 2016	3 cities (Philippines)	All ages	RR at 99th temperature percentile compared to the 70th percentile	Mean temperature	All causes All ages RR 2.48 (lag 0-2)

Zhang 2017	12 counties (central China); 2009-2012	All ages	RR at 99th percentile compared to reference temperature was 27.7 °C	Mean temperature	All causes All ages: 1.097 (lag 0-2) Heterogeneity among counties Higher effects in 75+, females, those dying outside the hospital, those with higher education

STUDY DESIGN: CASE CROSSOVER
OUTCOME: MORTALITY

Study	Country, period	Population	Outcome	Exposure	Main results
Stafoggia et al. 2006	4 Italian cities 1997-2003	35+	OR of dying at 30° C relative to 20°C.	mean apparent temperature	<u>All causes</u> 35+ OR=1.34; 65+ OR=1.39; 75+ OR=1.43 CVD 35+ OR=1.46 ; 65+ OR=1.46 ; 75+ OR=1.50 Psychoses: 35+ OR=1.70; 65+ OR=1.75 ;75+ OR=1.67 Depression : 35+ OR=1.71 ; 65+ OR=1.82; 75+ OR=1.80 Conduction disorders 35+ OR=1.77 ; 65+ OR=1.86; 75+ OR=2.12 Marital status 35+ OR=1.50
Medina-Ramon et al. 2007	50 cities (U.S); *1989-2000*	all ages	Percentage change in mortality in days with minimum temperature ≥ 99th percentile	minimum temperature	<u>All causes</u> **all ages**=+5.74% (lag 0-2) <u>CVD</u> **all ages** =+4.68% (lag 1)
Kolb et al. 2007	Canada 1984-2003	65+	Percentage change in mortality for 5°C increase of maximum temperature (lag 0-2)	Mean and maximum temperature	<u>Congestive heart failure</u> **65+** 20-25°C: =+1.05 25-30°C: =+1.26 30-33.1°C:=+1.20 <u>No association after 3 days</u>

Study	Country, period	Population	Outcome	Exposure	Main results
Bell et al. 2008	3 Latin American cities (San Paolo, Santiago, Mexico city); *1998-2002*	all ages	Percentage change in mortality in days at the 95th percentile of mean apparent temperature compared with the 75th percentile.	Mean apparent temperature	<u>All causes</u>: **all ages** Santiago: n.s.; Sao Paulo: +4.43%; Mexico City: n.s. No effect for sex <u>CVD</u> **all ages** Santiago: n.s. Sao Paulo: n.s. Mexico City: n.s. <u>RESP</u> **all ages** Santiago: n.s. Sao Paulo: +12.22% Mexico City: n.s.
Basu et al. 2008	9 California counties (U.S); *1999-2003*	All ages	Percentage change in mortality for 10°F in mean apparent temperature	mean apparent temperature	<u>All causes</u> <u>all ages</u> ≤ 1 =+4.9% ≤ 5 =+4.2%, n.s. 5-17 n.s. 18-64 n.s. **≥ 65** =+2.2% **≥ 75** =+2.6% **≥ 85** =+1.7% <u>CVD</u> **all ages**=+2.6% <u>Ischemic disease:</u> **all ages**=+2.5% <u>Myocardial infarction</u> **all ages**=+2.7%, n.s. <u>Conduction disorders</u> **all ages** =+5.4%, n.s.

Study	Country, period	Population	Outcome	Exposure	Main results
Basagana et al. 2011	Catalonia region (Spain); 1983-2006	All ages age group: <1 year	Relative risk (RR) of death in hot days with maximum temperature above the 95th percentile compared with no hot days	Maximum temperature and humidity	<u>All causes (lag 0-2):</u> **All ages** RR=1.19 <**1 year** RR=1.53 <u>CVD</u> **All ages** RR=1.22 <u>RESP</u>. **All ages** RR=1.21 <u>Mental and nervous system disorders</u> **All ages** RR=1.30 <u>External causes:</u> **All ages** RR=1.23 <u>Infectious disease:</u> **All ages** RR=1.22 Effect for all main causes at lags 0–2
Wichmann et al. 2011	Copenhagen (Denmark); 1999-2006	All ages	Percentage change in mortality per IQR increase in maximum apparent temperature	Maximum apparent temperature	<u>CVD</u> **All ages** =-6.9% **>80** = - 8.3% <u>RESP</u> **All ages**= n.s.
Chen 2016	Ontario province (Canada); 1996-2010	All ages	% change for 5°C increase in temperature	Mean temperature	All causes 2.5% (lag 0) <u>Respiratory in-hospital deaths</u> 26.0%
Willers 2016	Rotterdam 1995-2009	All ages	% change between the 90 and 99% of the thermal index	Maximum temperature, maximum UTCI, maximum radiant temperature	All causes All ages: % change= from 4% to 10.6% for the three indicators (lag1) synergistic effects of high temperatures and air pollution

STUDY DESIGN: TIME SERIES
OUTCOME: MORBIDITY

Study	Country, period	Population	Outcome measure	Exposure	Main results
Koken et al. 2003	Denver Colorado (U.S.), 1993-1997 (July and August)	65+	Percentage change in hospital admissions for cardiovascular disease	maximum temperature	A 25th-75th centile increase (from 28.3°C to 34.2°C) in temperature was associated with a 18%, 13%, 28%, and 13% increase in hospitalization respectively for acute myocardial infarction, coronary atherosclerosis, pulmonary heart disease and congestive heart failure, but not with cardiac dysrhythmias. During increases in both temperature and ozone, males have an increased risk of hospitalization compared with females.
Kovats et al. 2004	Greater London (UK), April 1994-March 2000	all ages age groups 0-5, 5-14, 15-64, 65-74, 75+ years	Percentage change in hospital admissions for 1°C above a cause- and age-specific threshold.	Mean temperature	All causes: **0-4** =0.24% Respiratory diseases: all ages=5.5% **65-74**=7.7% **75+=** 10.8% Renal diseases **all ages** =1.30% Slightly increase in total admissions among children under 5 years (0.2% increase for each degree above 12°C).

Study	Country, period	Population	Outcome measure	Exposure	Main results
Schwartz et al. 2004	12 US cities, 1986-1994	65+	Relative risk (RR) of hospital admissions at 80°F (32.2°C) compared with 0°F (-17.8°C).	mean temperature	CVD **65+** RR=1.15 (lag 0) Effect of hot temperatures immediate (lag 0), with evidence of harvesting. The effects of hot temperature disappeared within 10 days. No clear pattern of humidity on cardiovascular admissions.

Ebi 2004	3 US California; 1983-1997 and January-June 1998	All ages	Percentage change in hospital admission for 3°C increase in minimum temperature	Minimum and maximum temperature	<u>Acute Myocardial infarction</u> **55-69** Los Angeles:men=6.7%; women=-11.2%; San Francisco men =0.8%; women=1.4%, n.s.; Sacramento:men =22.3%; women=24.1% <u>Angina pectoris</u> **55-69** Los Angelesmen=-1.2%, n.s.; women=-2.5%, n.s.; San Franciscomen=2.0%; women=10.7% Sacramentomen=8.85%, n.s.; women=18.7% **70+** Los Angeles:men=-6.5%; women=-5.8%; San Francisco:men: 9.9%; women=12.5%; Sacramento: men=10.5%; women=11.9%, n.s. <u>Heart failure</u> **55-69** Los Angeles:men =-11.9%; women= -8.1% San Franciscomen=5.7%; women=6.5%; Sacramentomen=19.8; women=17.2, n.s. 70+ Los Angeles:men =-6.4; women= -2.8, n.s. San Franciscomen =9.9; women=8.4. Sacramentomen=9.2, n.s.; women=14.9 <u>Ictus</u> **55-69** Los Angeles: men=-4.9%; women=-4.0%, n.s. San Francisco: men=4.1%; women=10.6%; Sacramento: men=16.0%; women=28.3%

Study	Country, period	Population	Outcome measure	Exposure	Main results
Morabito et al. 2005	Florence (Italy), 1998-2002	all population, age groups 0-64 and 65+ years	Percentage change in hospital admissions every 2 hours of severe discomfort (apparent temperature above the 90th percentile) per day.	Mean temperature. Severe hot discomfort days: with apparent temperature >90th centile;	Myocardial infarction **all ages** =+10% (lag 3) **<65** effect only in males=+3% (lag 0) **65+** =no effect (lag 0)
Linarez et al. 2007	Spain (Madrid); *1995-2000*	All ages	Absolute and percentage change in emergency hospital admissions above the daily mean for a 1°C increase in temperature above 36°C.	Maximum and minimum temperature	All causes **All ages**=4.6% n.s. **>75**=17.9% RESP **>75**=27.5% No association with admissions due to circulatory diseases,
Dawson et al. 2008	Scotland (UK) *1990-2005*	All ages	Percentage change in emergency hospital admissions for 1°C increase in mean temperature preceding 24h	Maximum, minimum and mean temperature	Ischemic stroke All ages =+2.1%
Lin et al. 2009	New York, (USA); *1991-2004*	All ages	Percentage change in hospital admissions for 1°C above the threshold of the temperature	Mean apparent temperature, mean temperature and 3-day moving average of apparent temperature	Respiratory diseases All ages=+2.7%-+3.1% cardiovascular diseases all ages=+1.4%-3.6% At high temperatures, admission rates increased for chronic airway obstruction, asthma, ischemic heart disease, and cardiac dysrhythmias, but decreased for hypertension and heart failure.

Study	Country, period	Population	Outcome measure	Exposure	Main results
Michelozzi et al.2009	15 europeans cities; *1990-2001*	**All ages**	Percentage change in emergency hospital admissions for 1°C increase in maximum apparent temperature above a city-specific threshold	maximum apparent temperature	CDV **All ages** all cities=-0.6; Mediterranean cities : n.s.; North-Continental: n.s.) **65-74** n.s. **75+** n.s. Cerebrovascular diseases: **65-74** n.s. **75+** all cities=-1.5%; Mediterranean cities n.s. North-Continental: n.s.
Wang et al. 2009	Brisbane (Australia); 1996-2005	**All ages**	Relative risk (RR) of hospital admissions for 1°C increase in minimum and maximum temperature	Maximum, minimum and mean temperature	primary intracerebral 294aemorrhage <65 RR=1.12 ≥65 RR=0.99 n.s There is not statistical significant relationship between maximum temperature and ischemic stroke emergency admissions for any age groups.
Bhaskaran et al. 2010	England and Wales	**Median age 70**	Percentage change of hospital admissions for 1°C increase in temperature	Mean temperature	No effect

Study	Country, period	Population	Outcome measure	Exposure	Main results
Green et al-2010	9 U.S. California counties; 1999-2005	All ages	Percentage change per 10°F increases in mean daily apparent temperature.	Mean apparent temperature	Respiratory diseases **All ages** lag 0 =+2.0 n.s. lag 1=+0.8 n.s. pneumonia=+3.7% **< 5** =+5.9% 1**9–64** =+4.1% Neither asthma nor chronic obstructive pulmonary disease (chronic bronchitis or emphysema) was associated with apparent temperature Ischemic diseases: **65+=**3.5% Acute renal failure All ages=+7.4% 65+=10.7% <u>Dehydration</u> All ages=10.8% **5–18** = +19.75
Bayentin et al. 2010	Quebec (Canada) 1989-2006	**All ages** age groups 45-66, 65+	Percentage change in hospital admissions for 1°C increase above a threshold	Mean temperature	<u>Ischemic heart diseases</u> Women aged 45-65 years were more affected by extreme heat in comparison to men of the same age (range 1.21-10.7)

Study	Country, period	Population	Outcome measure	Exposure	Main results
Pudpong et al. 2011	Chiang Mai (Thailand); 2002-2006	All ages Age groups: 0-14 ≥65	Percentage change in the hospital visits/ admissions for 1 °C increase in temperature above the identified threshold (if applicable).	Mean temperature	**Daily out-patient visits** All causes All ages=+9.4% 0-14= +6.6% ≥65 =+10.8% CVD All ages=+19.2% (lag 0-13) Diabetic All ages=+26.3% (lag 0-13) **Hospital admissions** **All causes** All ages=+5.4%, n.s. (lag 0-13) Intestinal diseases All ages=+5.8% (lag 0-13) 0-14= +13.1% (lag 0-13)
Williams et al. 2012	Adelaide (Australia) 1993-2009	All ages	Incidence rate ratio (IRR) in the ambulance call-outs, emergency department (ED) presentations and hospital admissions for 10 °C increases in daily maximum temperatures over thresholds	maximum and minimum temperature	Daily ambulance call-outs all-age IRR=1.049 65+ IRR= 1.065 ED All causes **All ages** **65+** IRR= 1.036 Mental health All ages IRR=1.079 **65+** IRR=1.143 Heat relates **All ages** IRR= 6.511 **Hospital admissions** **All ages** IRR=1.034 No effect on Eds and admissions for renal causes, on CVD RESP admissions

Study	Country, period	Population	Outcome measure	Exposure	Main results
Chan et al. 2013	Hong Kong; 1998-2009	All ages <15; 15-59; 60-74; 75+	% change for every increase of 1 degrees C above 29 degrees C	Mean temperature	All causes % change=1.9% lag0-10 Respiratory causes: <15 % change 19.5 15-59 % change 8.2 60-74 % change 7.1 75+ % change 4.9 Infectious diseases <15 % change 7 15-59 % change 0.9 n.s. 60-74 % change 2.6 n.s. 75+ % change 9.6
Zhang 2014	Shanghai; 2006-2011	All ages, 65+	% change in Hospital admissions for 1 degrees C above optimum temperature 25°C	Mean temperature	respiratory diseases all ages: 2.15% greater in females and 65+ years
Kwon 2015	South Korea;2004-2012	All ages	RR of risk in hospital admissions per 1°C increase above threshold temperature (28.5 °C)	Mean temperature	AMI All ages: n.s. 75 years: RR=1.16 20-74 n.s. Urban: 1.10 rural n.s.
Phung 2016a	Mekong Delta Region (Vietnam)	All ages	% change of risk in hospital admissions for 1 °C increase above 21 °C, which is the minimum temperature	Mean temperature	All causes All ages: 1.3% (lag 0) infectious diseases all ages: 2.2% respiratory diseases all ages: 1.1% cardiovascular diseases n.s.
Phung 2016b	Ho Chi Minh City (Vietnam)	All ages	RR in hospital admissions for 99th percentile (31.3 °C) in comparison with the threshold 29.6 °C.	Mean temperature	CVD All ages Temperature effect lasted from to 0 to 5 days

Study	Country, period	Population	Outcome measure	Exposure	Main results
Lam 2016	Hong Kong; 2004–2011	All ages, 0-4,5-14, 15-59, 60+ years	RR in hospital admissions for 30°C vs 27°C	Mean temperature	Asthma RR=1.19 (lag 0-3) 0-4years n.s 5-14 1.32 15-59 1.52 (lag 0-12) 60+ 1.17

STUDY DESIGN: CASE CROSSOVER STUDIES
OUTCOME: MORBIDITY

Study	Country, period	Population	Outcome	Exposure	Main results
Fletcher et al. 2012	New York (USA); 1991-2004 (July-August)	All ages	Odds ratio (OR) for hospitalization per 5°F increase (lag 0-1)	Mean temperature	Renal diseases All ages OR=1.09
Wichmann et al. 2011	Copenhagen 1999-2006	19+	Percentage change in hospital admissions per IQR increase in maximum apparent temperature (lag 0-4)	Maximum apparent temperature	Respiratory diseases **19+=**6.5% **66-80**=9.8% Strongest effect for women, lowest and second highest SES groups No effect for cerebrovascular diseases
Wichmann et al. 2012	Copenhagen (Denmark) 1999-2006	19+	Percentage change in hospital admissions per IQR increase in temperature (lag 0-4)	Maximum apparent temperature	Myocardial infarction No effect
Chen 2017	Nanchang hospital (China); 2008-2015	All ages	Odds ratio (ORs) for admissions	Extreme high temperature (mean temperature> 34.8° C or maximum temperature> 39.9° C)	Ischemic Stroke OR = 1.18 (lag 0-3) haemorrhagic stroke OR = 1.34
Zanobetti 2013	135 US cities	65+	Odds ratio (ORs) for CVD Dadmissions	Minimum and maximum temperatures <1st Percentile, >99th	Atrial fibrillation:6%, Alzheimer:8% Dementia:6%

Table 3.4 Summary of studies included in the literature review on the differential effects of heat on mortality within urban areas considering the Urban heat island effect and socio-economic factors.

Authors	Year	Title	Study area	Exposure data source	Exposure indicator/satellite sensor	Aim	Method	Results
Johnson et al.	2009	Socioeconomic indicators of heat-related health risk supplemented with remotely sensed data.	Philadephia	LANDSAT TM	LST, National Land Cover data	to improve spatial delineation of risk from extreme heat events in urban environments by integrating sociodemographic risk factors with estimates of land surface temperature derived from thermal remote sensing data.	logistic regression models to identify models that better predict intra-urban variations in risk from extreme heat events.	Model with LST and socioeconomic variables performed the best in predicting heat- related mortality.
Smargassi et al.	2009	Variation of daily warm season mortality as a function of micro-urban heat islands.	Montreal, Canada	LANDSAT 7	ETM+	To evaluate whether people located in micro-urban heat islands are at higher risk of mortality during hot summer days	Case cross-over analysis on tempertaure and casue specific mortality, stratified by UHI and dwelling value by post code.	Subjects located in hotter area of the city were at greater risk of dying during hot days.
Tan et al.	2010	The urban heat island and its impact on heat waves and human health in Shanghai.	Shanghai	urban monitoring network	air temperature, UHIintensity	To investigate the health effects of the urban heat island in Shanghai	Examine summer mortality rates in Shanghai by UHI area	UHI worsens the adverse health effects from exposure to extreme thermal conditions.
Huang et al.	2011	Is everyone hot in the city? Spatial pattern of land surface temperatures, land cover and neighborhood socioeconomic characteristics in Baltimore, MD.	Baltimore, MD	LANDSAT 7	ETM+, LULC, socio-economic variables by census block	To define UHI and explore how this temperature variation relates to social factors by census-based block group	Correlate LST to socio-economic parameters. Map the spatial relationship of land surface temperatures to social factors	LST is higher in areas that are characterized by low income, high poverty, less education, more ethnic minorities, more elderly people and greater risk of crime
Kestens et al.	2011	Modelling the variation of land surface temperature as determinant of risk of heat-related health events.	Quebec Province, Canada	LANDSAT	LST, NDVI, land cover, water bodies	To estimate exposure to temperatures in urban areas based on satellite and meteorological data	GLM to estimate surface temperatures using meteorological, land use, NDVI and other parameters	Land cover and NDVI were strong predictors of LST
Steeneveld et al.	2011	Quantifying Urban Heat Island Effects and Human Comfort for Cities of Variable Size and Urban Morphology in the Netherlands	The Netherlands	observed data	Ta ad Humidity	Identify the UHI intensities in Dutch cities , linking UHI to green and blue space, population density and	Model relationship between UHI and parameters that influence thermal conditions in urban areas	Mean daily maximum UHI of 2.3 K in dutch cities
Thomlinson et al.	2011	Including the Urban Heat Island in Spatial Heat Health Risk Assessment Strategies: a Case Study for Birmingham, Uk,	Birmingham	MODIS	LST	To define a hazard index based on UHI and urban characteristics	Spatial risk assessment methodology in order to highlight potential heat health risk areas	"very high" risk areas within the city centre, and a number of pockets of "high risk" areas scattered throughout the conurbation

Authors	Year	Title	Study area	Exposure data source	Exposure indicator/satellite sensor	Aim	Method	Results
Buscail et al.	2012	Mapping heatwave health risk at the community level for public health action.	Rennes, France	LANDSAT 7	ETM+, LST, NDVI, water bodies	To identify high risk areas at the community level considering socioeconomic, land use and LST	A land-use regression model was performed to predict the LST considering land use and socioeconomic parameters.	highest risks observed in a north–south central
Goggins et al.	2012	Effect modification of the association between short-term meteorological factors and mortality by urban heat islands in Hong Kong.	Hong Kong	MODIS,	NDVI, SVF. Land use characteristics	evaluate whether people living in heat island areas of Hong Kong are at greater risk of mortality in summer	GAMs were used to estimate the association between meteorological variables and mortality during summer	A 1°C rise above 29°C was associated with a 4.1% (95% CI: 0.7-7.6%) increase in natural mortality in areas with high UHI compared to 0.7% (95% CI: 22.4-3.9%) in low UHI areas
Laaidi et al.	2012	The impact of heat islands on mortality in Paris during the August 2003 heat wave.	Paris	AVHHR	LST	To valuate the health impact of heat waves in urban areas, assess the daily and cumulative Tmin and Tmax exposure to heat, and implement indicators of heat exposure for elderly people in relation to residence.	Conditional logistic regression model, adjusted for age and other potential confounders by area of residence	Urban hot spots were associated with higher risk of death during the 2003 heat wave
Goggins et al.	2013	Effect modification of the association between meteorological variables and mortality by urban climatic conditions in the tropical city of Kaohsiung, Taiwan	Kaohsiung, Taiwan	Urban climatic mapping	UHI, Ta	To stratify districts into 3 urban heat risk categories based on thermalload and dynamic potential	Time series analysis on temperature and mortality stratified by 3 categories.	greater risk in level 1 - high thermal load and low dynamic potential. Ti reduce impact heat greater mitigation policies need to be introduced.
Xu et al.	2013	Differences on the effect of heat waves on mortality by sociodemographic and urban landscape characteristics	Barcelona, Spain	MODIS	VCF	To identify the most heat-vulnerable areas by mapping heat vulnerability	Time-stratified case-crossover analysis on daily mortality and tempertaure, by socioeconomic or built environment characteristics	The effect of heat on mortality was higher in the census tracts with a large percentage of old buildings , manual workers, limited greeen areas
Heaton et al.	2014	Characterizing urban vulnerability to heat stress using a spatially varying coefficient model	Houston, texas	HRLADS , UCM	UHI defined with HRLDAS, apparent Temperature, HUMIDEX, land cover UCM	To identify heat variable with greatest effects on mortality and socio-economic characteristics with higher risk	Poisson regression models with spatially varying coefficients within a Bayesian hierarchical framework	Census blocks most at risk are those with higher temperatures and greater proportion of elderly

Authors	Year	Title	Study area	Exposure data source	Exposure indicator/satellite sensor	Aim	Method	Results
Taylor et al.	2015	Mapping the effects of urban heat island, housing, and age on excess heat-related mortality in London	London, UK	obserbed and modelled Ta	Ta, number heat days	Vulnerability mapping of heat using predefined UHI, land use and population characteristics	Characteristics were mapped and during the LUCID project activity period results were incorporated and heat and weather conditions by wards were evaluated.	Dwelling type and UHI playing an important role in the spatial variation of relative risk of mortality and overall excess in mortality due to heat
Burkart et al.	2016	Modification of Heat-Related Mortality in an Elderly Urban Population by Vegetation (Urban Green) and Proximity to Water (Urban Blue): Evidence from Lisbon, Portugal	Lisbon, Portugal	MODIS	LST, NDVI	To estimate differential effect of tempertaure on mortality due to green and blue features within urban area	GAM models with stratification by quantiles of greeness, UHI and distance from ocean (water body)	cooler areas , closer to water body and with more green had lower risk in excess mortality
Heaviside et al.	2016	Attribution of mortality to the urban heat island during heatwaves in the West Midlands, UK	West Midlands UK	WRF weather forecast model	modelled Ta + observed Ta data	To estimate heat-related mortality during the 2003 heat wave considering UHI and estimate future impacts under CC	Considers a population weighted mean to evaluate impact of 2003 heat wave in West Midlands and HIA future CC impacts.	UHI contributes to around 50% excess deaths, under CC scenarios heatwaves could have 3 times the impact in the future.
Ho et al	2016	Delineation of spatial variability in the temperature-mortality relationship on extremely hot days in greater Vancouver, Canada	Vancouver, canada	LANDSAT 5 and 7	TM & ETM+, humidex, apparent temperature	To assess the spatial variability of heat-related mortality effects considering different mapping of UHI and social deprivation	Case cross over analysis on temperature and cause specific mortality, stratified by UHI , deprovation index.	Humidex and high unemployment rates showed the strongest spatial differences. Combined vulnerability index gave better performance.
Milojevic et al.	2016	Methods to Estimate Acclimatization to Urban Heat Island Effects on Heat- and Cold-Related Mortality.	London, Uk	weather forecast model, 1km resolution	Taused to define UHI anomaly compared to London average	To evaluate local acclimatization to the UHI effect in summer and winter	Case cross over analysis to define whether there was acclimatization to UHI in heat and cold effect in London	Summer acclimatization to UHI effect of heat-related although heat in Lodon limited mortality less clear for winter.
Wong et al.	2016	Spatially Analyzing the Inequity of the Hong Kong Urban Heat Island by Socio-Demographic Characteristics	Hong Kong	LANDSAT	TM	To identify heat vulnerability map combining UHI and socio-demographic characteristics identifying hotspots most at risk	Logistic regression, spatial auto correlation	Disadvantaged socio-demographic groups were more exposed to intense urban heat island effect

Table 4. Percent of daily LST missing values by month and year in the Italian domain (356,432 grid cells) over the study period (2000-2010).

Year	January	February	March	April	May	June	July	August	September	October	November	December	Annual mean
2000	100	100	57.7	64.6	50.9	37.2	34.4	57.4	38.6	63.2	66.0	63.7	**61.0**
2001	76.8	52.8	64.8	52.4	50.1	69.4	33.1	20.8	42.1	39.5	55.6	50.5	**50.6**
2002	42.9	60.0	66.9	57.1	50.2	34.8	36.7	43.1	51.7	52.9	68.0	78.7	**53.5**
2003	60.1	48.9	43.3	54.1	44.4	31.8	24.4	27.0	38.9	64.9	62.5	72.2	**47.7**
2004	65.3	61.7	60.7	62.9	50.9	40.5	26.0	29.7	35.5	62.1	61.1	62.0	**51.5**
2005	47.2	58.2	52.8	52.3	45.6	37.3	26.2	41.7	48.8	53.7	58.6	63.6	**48.7**
2006	58.0	58.5	60.4	53.1	45.8	34.3	31.0	41.9	39.4	41.5	49.0	50.7	**46.9**
2007	54.3	60.6	57.6	40.2	43.7	43.1	16.7	29.4	34.8	52.8	57.0	57.3	**45.5**
2008	62.8	42.2	57.0	54.4	53.1	42.0	26.0	23.3	51.1	48.0	58.5	68.3	**48.9**
2009	65.7	57.7	55.3	62.8	42.2	40.9	22.0	22.7	43.3	44.5	60.1	64.1	**48.3**
2010	68.8	70.6	59.1	49.1	59.2	43.3	27.7	26.0	46.3	59.6	66.0	63.9	**53.2**
Monthly average	**63.8**	**61.0**	**57.8**	**54.8**	**48.7**	**41.3**	**27.7**	**33.0**	**42.8**	**53.0**	**60.2**	**63.2**	